2019-10-17

Bifunctional Helical Peptide Catalysts for Enzyme-like Reactivity and Selectivity and Selective Stapling of Natural Amino Acid Residues with Hydrophilic Squaric Acid Derivatives

Michael James Kinghorn
Brigham Young University

Bifunctional Helical Peptide Catalysts for Enzyme-like Reactivity and Selectivity

AND

Selective Stapling of Natural Amino Acid Residues with Hydrophilic Squaric Acid Derivatives

Michael James Kinghorn

A dissertation submitted to the faculty of
Brigham Young University
in partial fulfillment of the requirements for the degree of

Doctor of Philosophy

David Michaelis, Chair
Joshua Price
Steven Castle
Joshua Andersen

Department of Chemistry and Biochemistry

Brigham Young University

ABSTRACT

Bifunctional Helical Peptide Catalysts for Enzyme-like Reactivity and Selectivity
AND
Selective Stapling of Natural Amino Acid Residues with
Hydrophilic Squaric Acid Derivatives

Michael James Kinghorn
Department of Chemistry and Biochemistry, BYU
Doctor of Philosophy

Peptide secondary structure provides an exceptional scaffold on which to design highly reactive and selective enzyme-like catalysts. This work describes the rational design and synthesis of a suite of helical peptide catalysts that are capable of achieving proximity-induced rate enhancement in Diels-Alder cycloadditions and indole alkylations. Microwave assisted synthesis of resin-supported polypeptides enables incorporation of non-natural amino acid residues that induce helicity (Aib) or provide functional handles on which organic catalytic residues can be attached. These small peptide catalysts exhibit binding-Driven selectivity rather than relying on the inherent reactivity of substrates, which allows access to products that are not obtainable with traditional catalysts in solution. Catalyst efficiency reached up to 28,000 turn overs, which mimics natural enzymatic systems.

Studies were also conducted into the stabilization of peptide secondary structure via covalent linking of nucleophilic amino acid side chains with squaric acid residues. Under mild conditions, stapling of nitrogen, sulfur and oxygen residues can readily be achieved in either organic or aqueous media. Squaric acid staples display pH selectivity for specific side chains and selective removal of diester staples (diserine staple) is demonstrated with methylamine. This new method for peptide stapling is shown to dramatically increase the proteolytic stability of eIF4E cancer inhibitor proteins, which typically are prone to quick degradation. Tyrosidine and RGD peptide analogues were synthesized and cyclized on resin in order to provide a new pathway to macrocyclization of antibacterial and integrin binding cyclic peptides.

Keywords: bifunctional catalysis, peptide catalysis, enzyme-like catalysis, peptide stapling

ACKNOWLEDGEMENTS

I would like to express my appreciation for the many people that have made this work a possibility. First and foremost, my loving and supportive wife Nadia Kinghorn, without whom I never would have made it past my first day in graduate school. Special thanks to my parents for their support and encouragement.

David Michaelis has been an exceptional friend and mentor and I owe so much of my growth as a scientist and individual to his efforts. Thank you to my committee and the department staff who work tirelessly to provide an exceptional research environment.

Table of Contents

List of Figures

List of Tables

Chapter 1 Bifunctional and Enzyme-inspired Catalysis

1.1 Introduction

Catalysis has one key goal: to increase the rates of chemical reactions. This is accomplished by lowering the transition state energy required for a given transformation. A catalyst may use any number of methods to increase reaction rate, such as pre-organizing reactive partners in order to reduce the entropy cost of a reaction, activating starting materials to increase their initial energy, or providing a pathway to lower energy intermediates. Given the large variety of catalytic pathways, the development of selective and efficient catalysts has become an area of significant research in the chemical and biological communities. Two key areas of research at the forefront of chemical catalysis are bifunctional catalysis and enzyme-inspired catalysis.

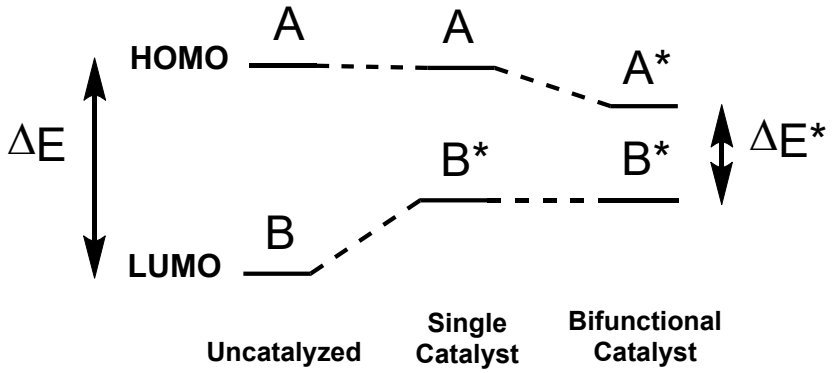

Figure 1.1 Activation pathways for individual and bifunctional catalysts

Bifunctional catalysis, which uses two or more catalytic centers to activate substrates, has seen significant progress over the last decade. Traditional catalysts only activate one molecule at a time, which limits activity for certain reactions that may have particularly unreactive substrates, and makes it difficult to control selectivity (enantioselectivity, diastereoselectivity) at more than one substrate at a time. MacMillan describes in his 2012 review a general method for dual

activation of substrates which leads to unique reactivity and selectivity (Figure 1.1)[1]. This concept of synergistic catalysis presents multiple pathways through which catalysts can work in tandem to promote novel reactivity and selectivity.

1.2 Palladium/enamine Bifunctional Catalysis

One area of particular interest is the combination of a traditional organic catalyst with a palladium transition metal catalyst (Figure 1.2). In this example a simple ketone **1** condenses with a pyrrolidine organocatalyst in order to generate an activated enamine nucleophile. The unactivated allyl acetate, however, is too poor of an electrophile to undergo the desired alkylation reaction. Therefore, the palladium catalyst forms the highly electrophilic palladium-allyl complex that is sufficiently activated to react with the enamine. With both catalysts working in tandem, the desired alkylation product **2** can be achieved in high yield. This dual catalytic approach offers unique advantages such as the ability to easily screen potentially compatible catalyst pairs and provides access to a larger potential scope of reactive partners. Significant research has been conducted confirming the utility of this type of bifunctional catalysis.

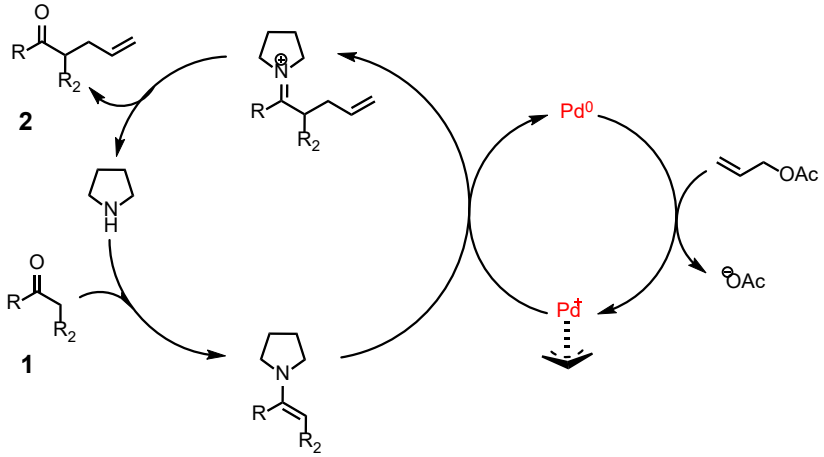

Figure 1.2 Cooperative enamine/palladium allyl catalysis

1.3 Bifunctional Photoredox Catalysis

Using two catalysts cooperatively has had significant impact in the field of photoredox catalysis. The coupling of aryl halides with alcohols to form ethers is commonly accomplished using palladium and copper. Nickel, however, would serve as a more ideal catalyst to do these transformations due to its low cost and the ability of Ni^0 to readily undergo oxidative addition into carbon-halogen bonds. Unfortunately, the resulting Ni^{II} complex has a very endothermic barrier for reductive elimination of C-O bonds, unlike oxidized Pd^{II}. For this reason, Ni^{II} was viewed as a poor transition metal catalyst for C–O bond formation due to its inability to reductively eliminate the product and return to Ni^0. The MacMillan group calculated that the reductive elimination of Ni^{III} to Ni^I was highly exothermic and postulated that using an iridium photocatalyst as a one electron shuttle would allow access to this oxidation state and potentially facilitate the easy Ni(III) to Ni(I) reductive elimination (Figure 1.3 a)[2].

In the catalytic cycle seen in Figure 1.3 b, when the nickel complex oxidatively adds into the C-Br bond the nickel is oxidized to the inactive Ni^{II} state. At this point the oxidized Ir^{III} catalyst is excited using a blue LED and, through single electron transfer (SET), oxidizes the nickel complex to Ni^{III}. The complex then readily undergoes reductive elimination to give Ni^I and the desired product. Ni^I complexes are very poor for oxidative additions, so the catalyst is unable to turn over on its own. However, the iridium catalyst that accepted one electron from nickel previously is now Ir^{II} and through SET can donate that electron back to nickel reforming both catalysts in their ground state (Ni^0, Ir^{III}). This unprecedented use of an iridium photocatalyst as an electron shuttle for nickel creates exceptionally low barriers for both oxidative addition and reductive elimination. Due to this dual catalytic process, previously inaccessible aryl bromides with electron donating groups readily form ethers in high yields. The electron rich rings raise the

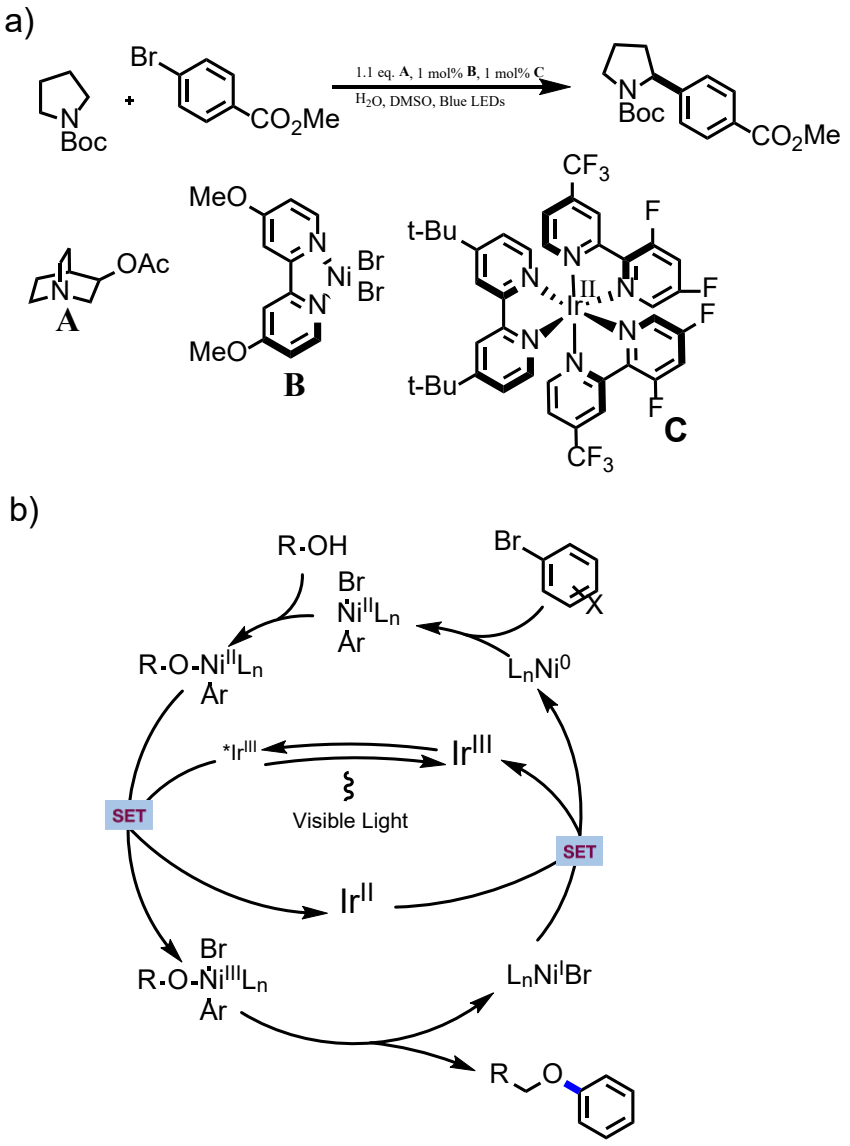

Figure 1.3 a) C-C bond formation via activation of sp^3 C-H bonds.

b) Bifunctional photocatlytic mechanism with Ir and Ni catalysts.

barrier for reductive elimination, which prevents other transition metals, such as palladium and copper from reacting. Only the highly active Ni^{III} complexes have strong enough reductive potential to overcome the reduced reactivity.

In order to confirm the proposed dual catalytic mechanism, several control ether formation reactions were attempted. Without the iridium catalyst, only the Ni^{II} complex was isolated, as there was no way for the catalyst to reductively eliminate the product. Also, when both catalysts

were added, but not in the presence of light, the Ni^{II} complex was again isolated. Only when both catalysts were present in the reaction under visible light conditions was the ether product isolated in over 50% yield. Based on calculations and experimental results, the MacMillan group confirmed that the reaction proceeds to completion via a transient Ni^{III} complex that readily reductively eliminates to form the product. With a much larger substrate scope than previous catalysts, this bifunctional approach shows significant advances in the ability to activate transient transition metal complexes capable of reactivity far superior to previously studied single catalyst systems.

1.4 Dual Activated Diels-Alder Catalysis

The use of two catalysts in tandem can suffer from limitations due to catalyst incompatibility or inherently unreactive starting materials. The development of a single molecule that contains two or more catalytic centers provides a good pathway to overcome these limitations. Jacobsen et. al.[3] provided an exceptional example of this type of catalysis in 2013 (Figure 1.4). Using cyclohexane as a scaffold, a thiourea hydrogen bonding catalytic residue was placed adjacent to an amine active site.

The combination of these two catalysts on a single backbone creates an environment in which an amine and an α,β unsaturated ketone can be simultaneously activated. The thiourea generates an electron deficient iminium dienophile (blue) and the amine condenses with the ketone in order to generate and electron rich diene (red). This push-pull relationship greatly accelerates the rate at which the Diels-Alder cycloaddition can occur and is further increased by both catalytic residues being on the same molecule. Once both substrates are bound to the catalyst, the

cyclization becomes more of an intramolecular reaction, which increases the rate of reactivity by several orders of magnitude.

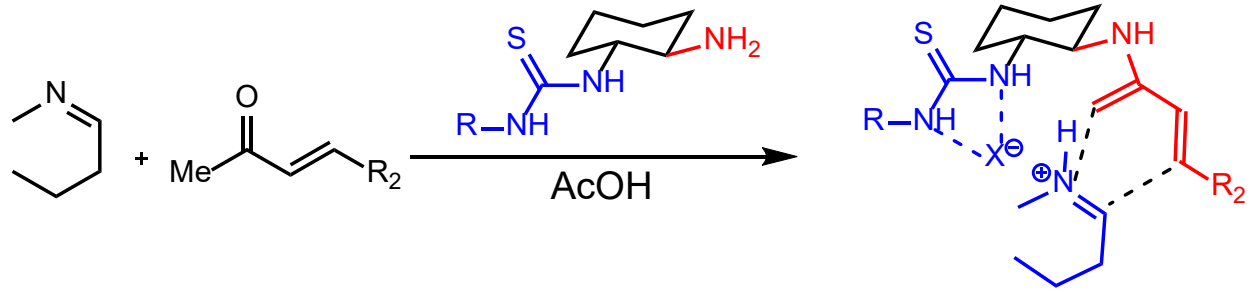

Figure 1.4 Bifunctional thiourea catalyzed Diels Alder cycloadditions

Such examples of bifunctional catalysis, where catalysts are covalently linked, have opened a new area of research that takes advantage of the cooperativity of catalysts as well the ability to tune inter-catalyst distance to optimize catalyst interactions. The Jacobsen group has remained at the forefront of this effort by developing an extensive library of bifunctional thiourea catalysts[4].

1.5 Enzyme-like Catalysis

Enzymes are capable of performing reactions with high turn overs, selectivity and efficiency. This is due to remarkable ability of enzymes to bring substrates into close proximity and to control transition states in the active site. The stable secondary structure of these polypeptides is what grants enzymes such unique reactivity. However, creating enzyme analogues that are capable of catalyzing different reactions or that expand the substrate scope of a reaction is a difficult endeavor. Organic catalysts, on the other hand, are easily tunable and provide access to chemical transformations not observed in nature. For this reason, an area of research has developed in recent years to develop enzyme-inspired organic catalysts. Such catalysts can take

advantage of the efficiency and selectivity of natural enzymes while simultaneously enhancing and broadening the substrate scope of enzyme-mediated reactions.

One of the earliest examples of developing enzyme-inspired approaches to catalysis was demonstrated by the Liu group at Harvard[5] (Figure 1.5). In this study, cross-coupling partners were placed at the terminal ends of complementary strands of DNA. When the strands anneal, it brings the two reactive functional groups into close proximity and constrains their freedom of movement. This essentially pays some of the entropy cost of reacting up front, which leads to proximity-induced rate enhancements of up to ten-fold and enables reactivity at micromolar concentrations. This groundbreaking work demonstrated that small biomolecules could be used to dramatically impact the rates of reactivity. However, this approach is limited in that the reactive substrates are covalently linked to the DNA molecules, which requires stoichiometric amounts of DNA and makes this proof of concept intriguing, but not synthetically useful.

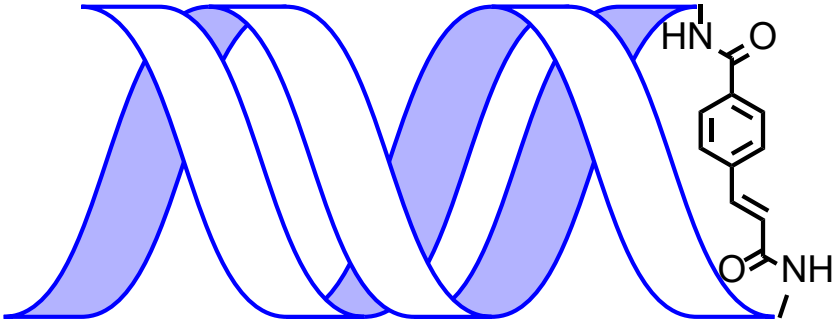

Figure 1.5 DNA-Templated Synthesis-David Liu

Peptides have been shown to be more versatile and stable as a scaffold for enzyme inspired catalysis. The Ball group showed a unique use for peptides to provide enantioselectivity to a catalytic system that previously had none (Figure 1.6). The dirhodium catalyst had previously been shown to be highly efficient at C-Si insertion reactions but was not enantioselective. By covalently linking a short α-helical polypeptide to the catalyst, the catalytic efficiency was retained as well as providing high product enantioselectivity. This approach showcases the efforts of this

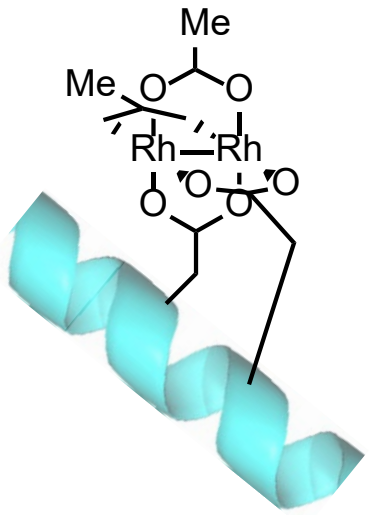

Figure 1.6 Peptide Tethered Dirhodium Catalyst-Zachary Ball

field of study. The dirhodium catalyst species is capable of catalyzing a transformation not observed by any natural system, however the chiral nature of the peptide backbone provided enantioselectivity that would be difficult to achieve using traditional catalytic methods.

Another significant area of enzyme inspired catalysis relies solely on peptide secondary structure. Miller and Wennemers (Figure 1.7) have developed a new class of β-turn peptides that are capable of catalyzing new reactions due to their ability to incorporate unnatural amino acids into the peptide sequence. This allows for greater spatial control, while still maintaining the basic structure found in nature. With the turn as a general template, there are a wide variety of side

chains that can be incorporated into the peptide structure to tune reactivity. This greatly increases the variability that is available from the twenty naturally occurring amino acids.

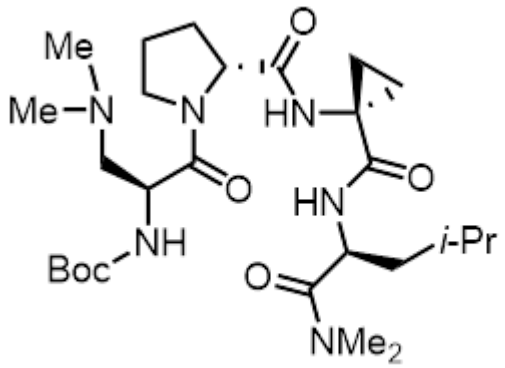

Figure 1.7 Beta Turn Catalyst – Scott Miller/Helma Wenamers

In the same vein of research, Ghadiri[6] has developed helix bundle peptide catalysts which mimic the active site of a natural enzyme, but again are capable of being tuned to maximize catalyst reactivity. Gellman and coworkers (Figure 1.8) designed a catalytic foldamer that places cyclic amines in the backbone of a 12 helix at the *i* and *i*+3 positions. This provides a rigid environment in which the two catalytic amines are held in close proximity to each other. When hydrocinnamaldehyde and acetone condense on the amines, the resulting enamine/iminium condensation achieves a several-fold rate enhancement. This specific spatial control provides the potential to increase the efficiency of known reactions as well as develop new reaction pathways altogether.

In conclusion, cooperative and enzyme-like catalysts have created a new frontier for reaction development. Increased reactivity can be achieved through various pathways such as the combination of multiple catalytic residues in a single reaction or the incorporation of peptide secondary structure into a catalysts structure. In the succeeding chapters, we describe our efforts

to understand how to use peptide catalysts as a platform for developing enzyme-like and cooperative catalyst systems to enhance organic synthesis.

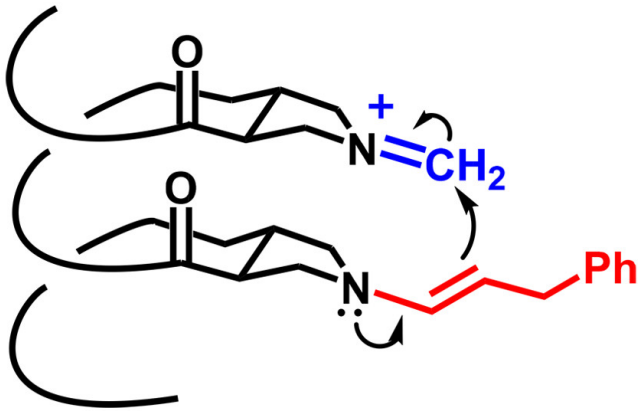

Figure 1.8 Catalytic Foldamer-Sam Gellman

1.6 References

1. Shibasaki, M.; Kanai M.; Matsunaga S.; Kumagai N. Recent progress in asymmetric bifunctional catalysis using multimetallic systems. *Acc Chem Res.* **2009** 42(8):1117-27.

2. Peterson, E. A.; Jacobsen, E. N. Enantioselective, Thiourea-Catalyzed Intermolecular Addition of Indoles to Cyclic N-Acyl Iminium Ions. *Angew. Chem,; Int. Ed.* **2009**, *48*, 6328–6331.

3. Raheem, I. T.; Thiara, P. V.; Jacobsen, E. N. Regio- and Enantioselective Cyclization of Pyrroles onto N-Acyliminium Ions. *Org. Lett.* **2008**, *10*, 1577–1580

4. Allen, A. E.; MacMillan, D. W. C. Synergistic catalysis: A powerful synthetic strategy for new reaction development. *Chem. Sci.* **2012**, *3*, 633.

5. Skubi, K. L.; Blum, T. R.; Yoon, T. P. Dual Catalysis Strategies in Photochemical Synthesis. *Chem. Rev.* **2016**, 116, 10035.

6. Kiss, G.; Celebi-Oelcuem, N.; Moretti, R.; Baker, D.; Houk, K. N. Computational Enzyme Design. *Angew. Chem,; Int. Ed.* **2013**, *52*, 5700.

7. Hilvert, D. Design of Protein Catalysts. *Annu. Rev. Biochem.* **2013**, *82*, 447.

8. Leman, L. J.; Weinberger, D. A.; Huang, Z.-Z.; Wilcoxen, K. M.; Ghadiri, M. R. Synthesis of Functional Amino Acids Bearing 1%2C3-Dithiane Modification. *J. Am. Chem. Soc.* **2007**, *129,* 2959

9. Mayer, C,; Müller, M. M,; Gellman, S. H,; Hilvert, D. Building proficient enzymes with foldamer prostheses. *Angew. Chem. Int. Ed.* **2014***, 53,* 6978.

10. Gilbertson, S. R.; Collibee, S. E.; Agarkov, A. *J. Am. Chem. Soc.* **2000**, *122*, 6522.

11. Austin, J. F.; Kim, S. G.; Sinz, C. J.; Xiao, W. J.; MacMillan, D. W. C. Enantioselective organocatalytic construction of pyrroloindolines by a cascade addition-cyclization strategy: synthesis of (-)-flustramine B. *Proc. Nat. Acad. Sci.* **2004**, *101*, 5482.

12. Yeung, C.; Jacobsen, E. N. Thiourea-Catalyzed Enantioselective Addition of Indoles to Pyrones: Alkaloid Cores with Quaternary Carbons. *J. Am. Chem. Soc*. 2014, 136, 13614−13617

13. Li, X; Liu, D. DNA-templated organic synthesis: nature's strategy for controlling chemical reactivity applied to synthetic molecules. *Angew. Chem. Int. Ed.* **2004**, 43, 4848

14. Ball, Z. T. Designing Enzyme-like Catalysts: A Rhodium(II) Metallopeptide Case Study. *Acc. Chem. Res.* **2013**, 46*,* 560

15. Miller, S. J. In Search of Peptide-Based Catalysts for Asymmetric Organic Synthesis. *Acc. Chem. Res.***2004**, 37, 601 (2004)

16. Colby Davie, E. A,; Mennen, S. M,; Xu, Y,; Miller, S. Asymmetric Catalysis Mediated by Synthetic Peptides. J. *Chem. Rev.* **2007**, 107, 5759.

17. Revell, J. D,; Wennemers, H. Peptidic catalysts developed by combinatorial screening methods. *Curr. Opin. Chem. Biol.* **2007**, 11, 269.

18. J. Duschmalé, Y. Arakawa, H. Wennemers, in *Science of Synthesis: Asymmetric Organocatalysis, Vol. 2* (Ed. Maruoka, K.), Georg Thieme Verlag, **2012**, p. 741.

19. Reisman, S. E.; Doyle, A. G.; Jacobsen, E. N. Enantioselective Thiourea-Catalyzed Additions to Oxocarbenium Ions. *J. Am. Chem. Soc.* **2008**, *130*, 7198–7199.

20. Park, Y.; Harper, K.C.; Kuhl, N.; Kwan, E.E.; Liu, R.Y.; Jacobsen, E.N. Macrocyclic Bis-Thioureas Catalyze Stereospecific Glycosylation Reactions. *Science* **2017**, *Vol. 355, Issue 6321*, 162-166.

21. Kennedy, C.R.; Lehnherr, D.; Rajapaksa, N.S.; Ford, D.D.; Park, Y.; Jacobsen, E.N. Mechanism-Guided Development of a Highly Active, Dimeric Thiourea Catalyst for Anion-Abstraction Catalysis. *J. Am. Chem. Soc.* **2016**, *138*, 13525-13528.

22. Sammakia, T.; Smith, R. S. Evidence for an Oxocarbenium Ion Intermediate in Lewis Acid Mediated Reactions of Acyclic Acetals. *J. Am. Chem. Soc.***1994**, 116, 17, 7915-7916

23. Xu, H.; Zuend, S. J.; Woll, M. G.; Tao, Y.; Jacobsen, E. N. Asymmetric Cooperative Catalysis of Strong Brønsted Acid-promoted Reactions Using Chiral Ureas. *Science*, **2010**, 327, 986

Chapter 2 Proximity-Induced Reactivity and Product Selectivity with a Rationally Designed Bifunctional Peptide Catalyst

2.1 Introduction

Employing multiple catalysts to simultaneously activate substrates in an enzyme-like manner has become a significant focus of research over the past decade. This approach provides access to the large substrate scope available to traditional catalysts, but with the added spatial control and selectivity that enzymes provide. Peptide secondary structure provides the necessary rigidity to constrain transition states, which improves catalytic efficiency. The design of small organic catalysts that are capable of binding and activating multiple substrates simultaneously provides access to chemical reactions that are not observed with monofunctional catalysts in solution. Enzyme-inspired catalysts are capable of taking advantage of the benefits of natural systems while at the same time providing the tunability and substrate scope offered by traditional organic catalysts.[1-5]

2.2 Bifunctional Helical Peptide Catalyst Design and Synthesis

Certain short polypeptides are able to consistently fold into well-defined secondary structures and provide a good scaffold for the design and development of enzyme-like catalysts. Balaram and coworkers developed a small peptide that is able to maintain helicity with as few as seven amino acids. This was accomplished by the incorporation of aminoisobutyric acid (Aib) as a helix-inducing residue into the repeating sequence of Leu-Ala-Val-Aib. Thus, polypeptides as short as 7 residues have been shown to fold into a well defined helical structure., which provides a unique and easily accessed peptide scaffold to explore proximity-induced reactivity. Grubbs

demonstrated that when two terminal olefins were placed adjacent each other at the *i* and *i*+4 position on this short, 7-amino acid peptide helix, the rate of ring closing metathesis increased significantly. This proximity-induced effect relies on the helix backbone, which restricts the freedom of movement of the olefins and holds them within 7 Angstroms of each other. While this rate enhancement is not catalytic with respect to the helix scaffold, the pre-organizing of molecules in this fashion is a hallmark in how natural enzymes lower the activation barrier for reactions.

We endeavored to design a system in which we could use these short helical peptides as a scaffold to bind organic catalysts in close proximity, thus allowing enzymatic rate enhancement. In our standard peptide, a catalytic residue and a binding site were placed at the *i* and *i*+4 positions on the helix in order to explore rate enhancement and selectivity of Diels-Alder cycloadditions (Figure 2.1). As there are very few examples of organic catalysts being covalently linked to polypeptides, this approach offered a unique system to explore enzyme-like activity. Using solid-phase peptide synthesis tools, a short organic-soluble 11 residue amino acid sequence was readily synthesized. Modification of azidolysine with an alkyne-functionalized MacMillan imidazolidinone catalyst via the copper-catalyzed azide/alkyne cycloaddition (CuI) was used to install a 1st generation MacMillan imidazolidinone catalyst (**Figure 2.1** Red). Nucleophilic addition of a lysine residue one turn further on the helix onto an arylisothiocyanate was used to install a thiourea hydrogen bonding catalyst (**Figure 2.1** Blue). Importantly, both of these side chain modifications to introduce our desired active catalysts were performed on resin, making the multistep synthesis of our catalytic peptide much easier. This streamlined catalyst synthesis also allowed for only one purification step of the finished peptide catalyst. As other thiourea-amine

bifunctional catalysts had previously shown utility, we believed this was a good catalyst system for a proof-of-concept study into the utility of short helices as catalyst scaffolds.

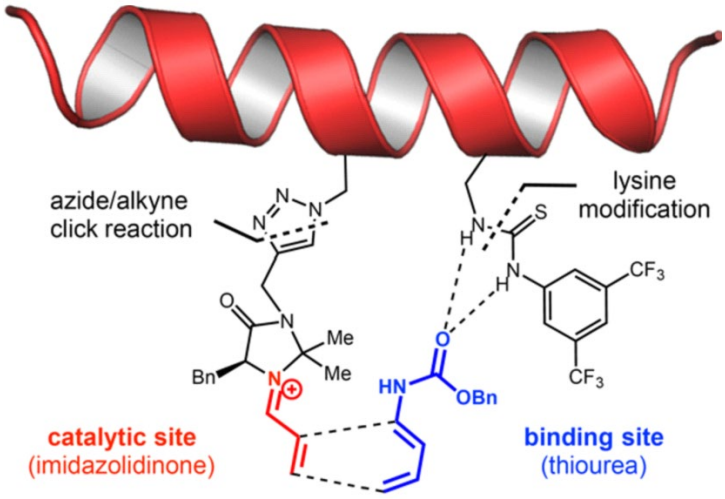

Figure 2.1 Rationally designed bifunctional helical peptide catalyst.

Our initial efforts began with a seven amino acid sequence AcNH-VZLBVXL-HNMe, where imidazolidinone (**Z**) and thiourea (**X**) catalysts were coupled with a single helix inducing Aib (**B**) residue between them (see Figure 2.2). This proved problematic, as after initial synthesis of the bifunctional peptide catalyst the circular dichroism (CD) spectrum indicated that the catalyst was not helical in solution. We hypothesized that the bulk of the catalytic residues and shortness of the peptide sequence prevented proper folding of the peptide backbone. For this reason, the catalyst backbone was expanded to an 11 amino acid (11-mer) sequence AcNH-VZLBVXLBVAL-HNMe **p2**, which placed an additional turn into the helix and two Aib residues at the 4 at 8 positions. CD studies confirmed that the 11-mer sequence remained helical in solution after functionalization and so it was selected for synthesis of all catalysts.

A suite of control catalysts were also synthesized in order to test the importance of our helical catalyst backbone (Figure 2.2). We synthesized two catalysts containing only **X** or **Z** (**p3** and **p4** respectively) and the non-peptide bound catalysts **1** and **2**. A second bifunctional control

peptide (**p5**) was also synthesized with helix disrupting proline residues in place of Aib. This latter peptide represents a bifunctional control that had the same through-bond inter-catalyst distances, but with a disrupted secondary structure that would no longer hold the catalysts adjacent to each other. We were pleased to confirm by CD in trifluoroethanol that all peptides maintained their helicity with the exception of the **p5** proline catalyst, which adopted a random coil conformation. 2D NMR studies were also conducted on **p2** in order to confirm the α-helical secondary structure of the catalyst in solution through nonsequential NOEs. Even more importantly, the NOEs confirmed that the thiourea and imidazolidinone catalytic residues maintain close proximity in solution. This final result was encouraging that we might indeed be able to use helical peptide to bind multiple substrates in close proximity for enzyme-like catalysis.

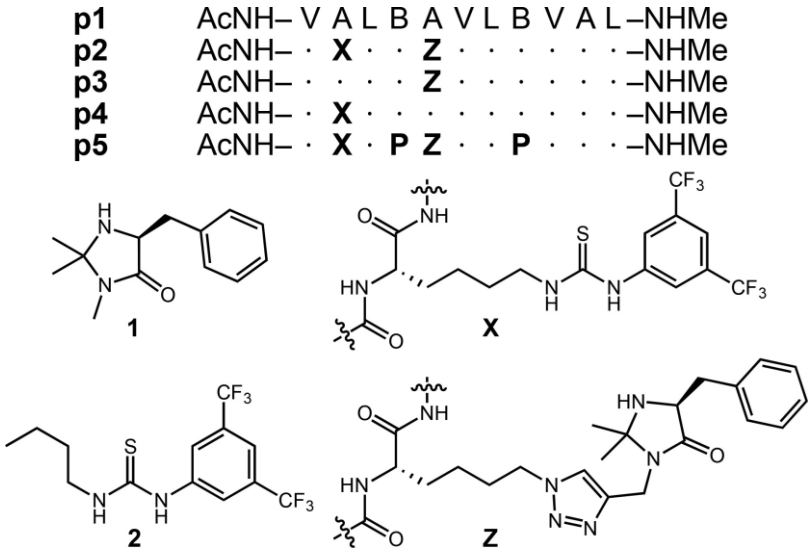

Figure 2.2 Peptide sequences and catalyst structures.

2.3 Mass Spectrum Calibration for Percent Conversion of Diels-Alder Products

Our initial studies explored the ability of the peptide catalysts to perform a well-documented Diels -Alder cycloaddition between α,β-unsaturated crotonaldehyde and an electron-rich carbamate-protected diene **3** (Figure 2.3). As we wanted to explore the reactivity that occurs in the regime of natural enzymes (<10 mmol), we needed a quantitative method for determining conversion of our Diels-Alder product. Since NMR is not sensitive enough for low concentration studies, we looked to develop an LCMS method that could accurately determine our product conversion.

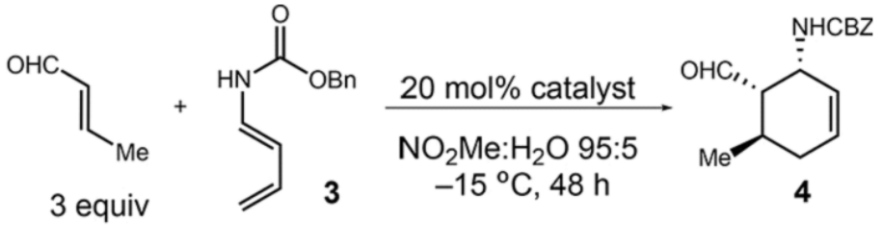

Figure 2.3 Reactivity of bifunctional peptide catalyst p2

In order to accurately observe quantitative yields of Diels-Alder reactions, even at low diene concentrations, the following calibration experiment was performed on the LCMS (Figure 2.4): A stock solution of reactant was prepared by dissolving 20.3 mg of benzyl (E)-buta-1,3-dien-1-ylcarbamate (0.1 mmol, 10 mM) in 10 mL nitromethane. A second stock solution of product was prepared by dissolving 27.3 mg of benzyl (6-formyl-5-methylcyclohex-2-en-1-yl)carbamate (0.1 mmol, 10 mM) in 10 mL nitromethane. These two stock solutions were used to calibrate the mass spectrometer by adding them in 100 μL equivalents to a vial according to the ratios shown in the table below and the final volume of each sample being diluted to 1 mL with nitromethane.

The calibrated P/R ionization efficiency ratio was used in all subsequent reactions to determine product conversion in diene concentration and catalyst loading studies (Table 2.1).

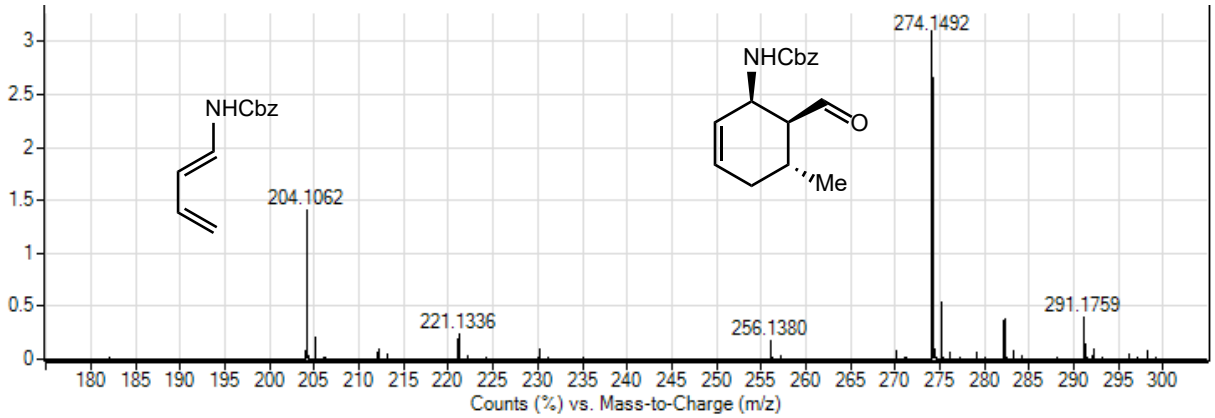

Figure 2.4 Mass spectrometer calibration curve based on 1:2 reactant:product ratio.

Table 2.1 *Calibration data for comparison of product (M = 274.1492) and starting material (M = 204.1062) relative concentrations.*

Equivalents Diene (3)	Equivalents Product(4)	Diene Abundance	Product Abundance	3/4 Ratio	4/3 Ratio
10	1	1308	139	1.062691	0.941007
5	1	694	142	1.023055	0.977465
3	1	182	68	1.120879	0.892157
2	1	323	163	1.009288	0.990798
1	1	124	131	1.056452	0.946565
1	2	144	308	1.069444	0.935065
1	3	109	345	1.055046	0.947826
1	5	137	786	1.147445	0.871501
1	10	96	1026	1.06875	0.935673
			Total Ratio	1.07	0.938

2.4 Catalyst Loading and Diene Concentration Studies

Using the calibrated mass spectral data, we were able to explore the utility of our catalysts at varying concentrations. Initial reactions at 100 mmol diene **3** produced 88% yield for **4** using catalyst **p2**, compared to only 3.4% conversion for the uncatalyzed reaction (Figure 2.5). Even more interestingly the monofunctional imidazolidinone catalyst **p3** gave only 7.1% yield under the same conditions and even after the addition of monofunctional thiourea peptide **p4** the reaction only reached 7.6% conversion. The standard, nonpeptide imidazolidinone **1** achieved 46% conversion on its own, and 35% conversion in conjunction with the butyl thiourea **2**. This suggests that binding a single catalyst to the peptide backbone is detrimental to catalyst activity in comparison with the free catalysts in solution. Only when both catalytic residues are present on the same helix is there an increase in catalytic activity. This effect becomes more pronounced at lower concentrations, where conversion of all control catalysts drops to less than 10% conversion while the **p2** maintains high reactivity. This supports our initial hypothesis that enzyme-like reactivity could be achieved through proximity-induced bifunctional catalysis (Figure 2.5).

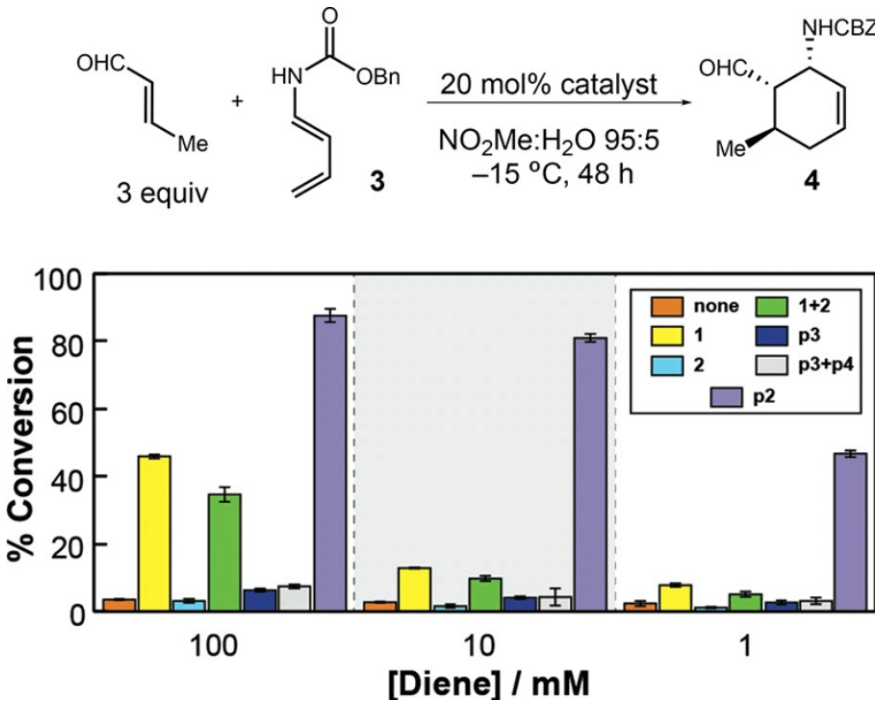

Figure 2.5 Reactivity of bifunctional peptide catalyst p2 vs monofunctional counterparts as a function of diene concentration.

Catalyst loading studies of **p2** and **p3** were conducted at 100 mM with respect to benzyl (E)-buta-1,3-dien-1-ylcarbamate. All experiments were performed in triplicate. A representative reaction procedure with 10% catalyst loading of **1** is provided here: Benzyl (E)-buta-1,3-dien-1-ylcarbamate (20.3 mg, 100 mmol, 1 eq) and freshly distilled crotonaldehyde (31 µL, 300 mmol, 3 eq) were added to a 1 mL solution of 95:5 v/v nitromethane/water. (S)-5-benzyl-2,2,3-trimethylimidazolidin-4-one hydrochloride (**1**) (2.54 mg, 10 mmol, 0.1eq) was then added to the reaction mixture by vortexing. The reactions were stirred at -15 ˚C for 48 h at which time a small aliquot of the reaction was diluted in 1 mL ethyl acetate and conversion determined via HRMS (ESI). Conversions for all other catalysts and catalyst loadings are listed below in table 2.2.

Table 2.2 *Catalyst loading studies.*

Catalyst Loading	20%	2%	0.20%	0.02%	0.002%
1	46.0	31.5	5.7	3.3	0.1
p2	87.5	70.8	49.0	8.8	0

%Conversion of Diels-Alder product (4) at 48 hours

2.5 Maximum Turn over for **p2**

One remaining question about the reactivity or our peptide was whether it could achieve enzyme-like reactivity in terms of catalyst turnover. To explore this point, we dropped the catalyst loading dramatically. For example, benzyl (E)-buta-1,3-dien-1-ylcarbamate (40.6mg, 200 mmol, 1 eq) and freshly distilled crotonaldehyde (104 μL, 500 mmol, 5 eq) were added to a 200 μL solution of 95:5 v/v nitromethane/water. Catalyst **p2** (0.35mg, 0.01mmol, 0.001 mol%) was then added to the reaction mixture by vortexing. The reaction was stirred at 4 ˚C for 48 h at which time the solvent was removed under vacuum and the product isolated over silica as a yellow oil 7:1 Hexanes:EtOAc. 15.3 mg (28%, 28,000 turn overs) was isolated in the presence of catalyst **p2**, while <1% was isolated in the absence of catalyst.

2.6 Effect of Nonbinding Dienes on Reactivity

While catalyst **p2** displayed exceptional reactivity with the carbamate diene, the role of the thiourea catalytic residue **X** was not fully understood. In order for catalysis to occur, the crotonaldehyde dienophile must condense with the imidazolidinone residue **Y** to form an activated

iminium (Figure 2.1). We hypothesized that the carbamate **3** would hydrogen bond with the adjacent thiourea **X,** which would facilitate proximity-induced reactivity. In order to further explore this possibility, a control Diels-Alder reaction was performed where cyclopentadiene **5** was used (Figure 2.6). Since **5** is significantly more reactive than the carbamate diene **3**, catalyst **1** achieved 70% conversion of the cyclized product **6**. However, catalyst **p2** and **p3** only reached 32% and 34% conversion, respectively. Cyclopentadiene lacks the necessary carbonyl binding site that would allow it to hydrogen bond with the thiourea residue on **p2**, thus preventing the catalyst from bringing both reactive partners in close proximity. For this reason, **p2** and **p3** have essentially the same reactivity, which reinforces the need for a binding site on the diene in order to achieve bifunctional activity.

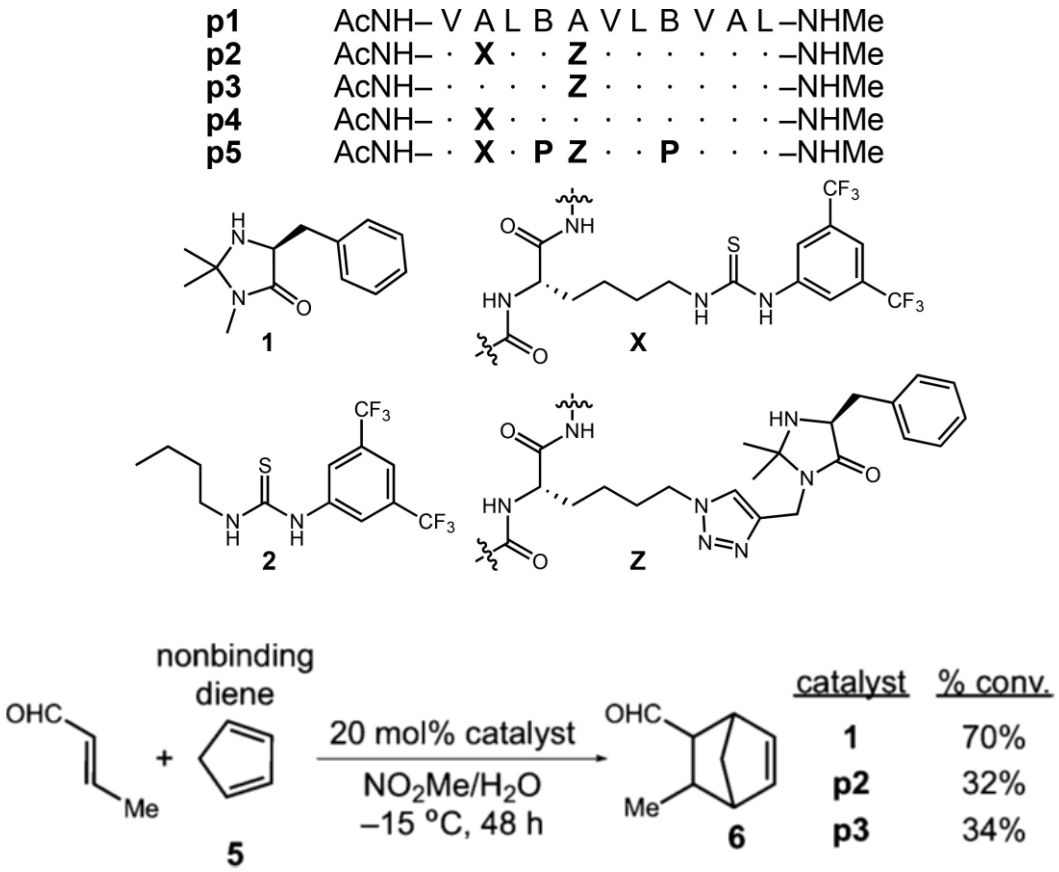

Figure 2.6 Nonbinding diene reactivity with 1, p2, and p3.

2.7 Binding-Driven Selectivity for Diels-Alder Products

Since natural enzymes are capable of discriminating between a large amount of potentially reactive molecules, a study was conducted to determine if bifunctional catalyst **p2** was capable of selecting between two dienes based on binding affinity to the thiourea residue **X**. Of particular interest was if our catalyst was capable of overcoming the inherent reactivity of a system. Cyclopentadiene **5** (16.8 μL, 2mmol, 2eq) and benzyl (E)-buta-1,3-dien-1-ylcarbamate **3** (40.6 mg, 0.2 mmol, 2 eq) were added to 10 mL of 95:5 v/v nitromethane/water at 4 ˚C. Distilled crotonaldehyde (10.3 μL, 0.1 mmol, 1 eq) and 0.01 eq of catalysts **p2** or 0.1 eq of **1** were then added to the reaction mixture and the reaction was stirred at 4 ˚C for 48 hours (Figure 2.7). 1,3-Bis(trifluoromethyl)-5-bromobenzene (17.2 μL, 0.1 mmol, 1 eq) was then added to the reaction as an internal standard and an aliquot of the reaction was taken and diluted in 1 mL deuterated chloroform into an NMR tube. Conversion to the product 3-methylbicyclo[2.2.1]hept-5-ene-2-carbaldehyde **6** was determined by integration of the aldehyde peak in reference to the internal standard due to high volatility of the product. The benzyl (6-formylcyclohex-2-en-1-yl) carbonate **4** product was purified by removing the solvent on a rotary evaporator and flashed over silica gel with 9:1 Hexanes/Ethyl Acetate. $R_f = 0.28$. The ratio of products determined in this manner was 16:1 for **p2** (Yield: 48% for **4** and 3% for **6)** and 1:1.4 for **1** (Yield: 19% for **4** and 27% for **6**). Thus, not only does our catalyst allow us to select for the binding diene **3** (16:1), it also overcomes the inherent reactivity displayed by catalyst **1** for the more reactive diene **5** (1:1.4), in favor of binding-induced selectivity.

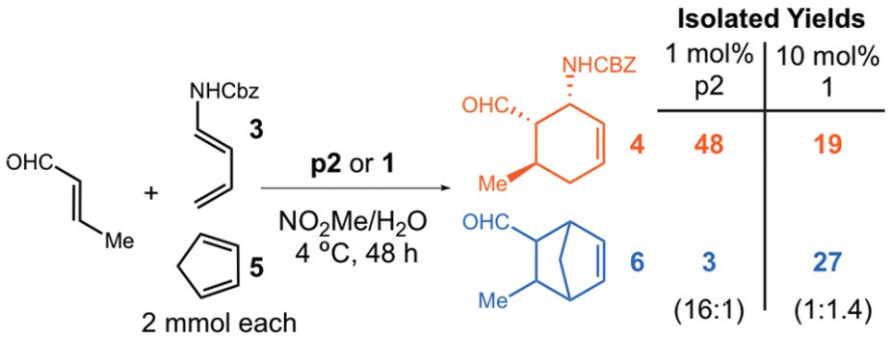

Figure 2.7 Thiourea binding group scope

2.8 Thiourea Binding Site Substrate Scope

As the presence of a binding site on the diene was determined to be essential for reactivity, we explored the substrate scope of **p2** for various Lewis-basic carbonyl binding groups. Diels-Alder reactions were conducted with 1 mol% **p2** to form the standard carbamate product (**4**), as well as carbonate (**7**), urea (**8**) and acetyl (**9**) products (Figure 2.8). All binding groups gave good yields, with the exception of the urea (**8**) which degraded on silica and formed multiple polymerization products. Even at lower catalyst concentrations, **p2** maintained reactivity across several binding partners, while very little reactivity was observed with imidazolidinone **1** at the same catalyst loading. This opens the door for a large scope of potential substrates that can be catalyzed by and take advantage of the spatial control of **p2**.

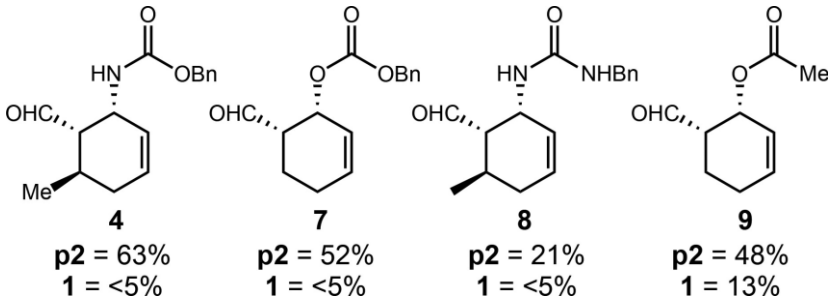

Figure 2.8 Substrate scope of various H-bonding sites in proximity-induced Diels-Alder reactions catalyzed by p2.

2.9 Alkylation of Indoles with Variable Binding Site Locations

Our next goal in this study was to determine if the proximity-induced reactivity and selectivity of **p2** was exclusive for Diels-Alder cycloadditions, or if these effects could be extended to other reactions that are accelerated by catalytic iminium formation. In order to investigate this, a previously reported indole alkylation using a carbamate protected *N*-methyltryptamine (**10**) and acrolein was preformed using 1 mol % **p2** or **1** (**Figure 2.9**). Catalyst **p2** achieved 100% conversion at 48 hours with a 76% isolated yield of the cyclized indole product **11**. However, catalyst **1** never went to full conversion and only provided a 21% isolated yield. Not only did the bifunctional peptide catalyst **p2** give a several-fold rate enhancement, but enantioselectivity was increased from 8% ee (**1**) to 42% ee (**p2**). This increase in enantioselectivity suggests that the peptide backbone is not only facilitating faster reaction rates but forming an environment similar to an enzyme active site, which favors the formation of one enantiomer over another. By placing the carbamate binding group at another position on the indole **12**, similar increases in rate and enantioselectivity were observed with **p2** in an indole alkylation reaction, giving 84% yield and 61% ee of **13**, while **1** only achieved 31% yield and 33% ee under the same reaction conditions. These results suggest that this form of helical peptide catalysis can be expanded to incorporate a broad range of potential bifunctional reaction mechanisms.

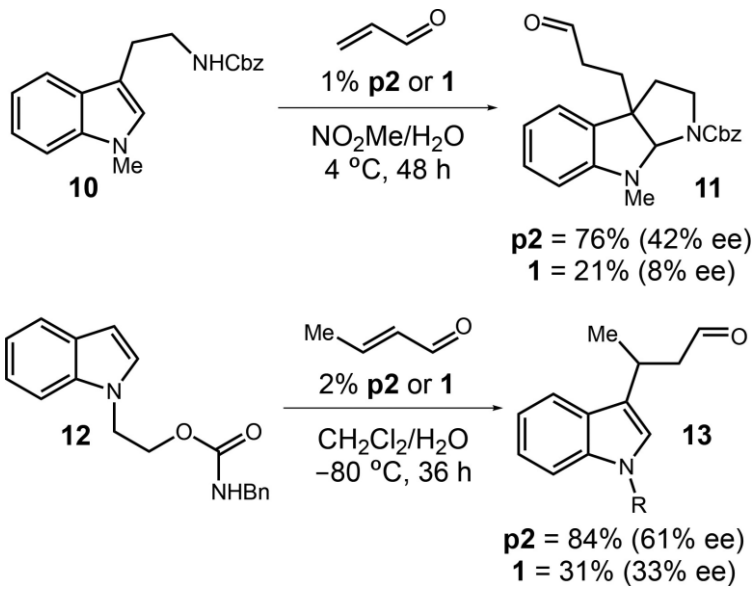

Figure 2.9 Alkylation of two different carbamate protected indoles with p2 and 1.

2.10 Binding-Driven Selectivity for Indole Alkylation Products

A competition study was conducted to determine if **p2** would select for a binding indole **12** in the presence of a non-binding indole **14** (Figure 2.10). What made this system unique from the previous Diels-Alder competition studies was that both indoles have essentially the same inherent reactivity with imidazolidinone catalyst **1**, which gave an 84% yield overall with a product ratio of **13**:**15** of 1:1.05. Catalyst **p2** again exceeded expectations giving an 83% yield overall and a ratio of **13**:**15** of 4.9:1. This increased selectivity again indicates this templated catalyst systems ability to provide rate enhancement across different reaction mechanisms and demonstrates a general strategy for achieving enzyme-like bifunctional catalysis

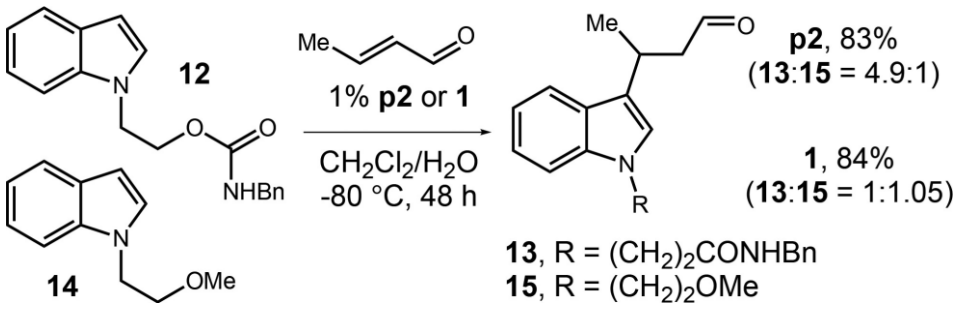

Figure 2.10 Competition study between binding and non-binding indole substrates.

2.11 Site Selectivity via Substrate Recognition

One of the most powerful tools that enzymes have is their ability to selectively modify one functional group on a target molecule. This is a difficult problem to solve in traditional organic synthesis, often requiring the use of several protecting groups. A helical peptide template provides the potential for site selective functionalization based on proximity to a binding site. To test for site selectivity with our peptide catalysts, a substrate was synthesized containing two nearly equivalent indole functional groups (**16**), but with one proximal to a carbamate binding site (**B ring**, Figure 2.11).

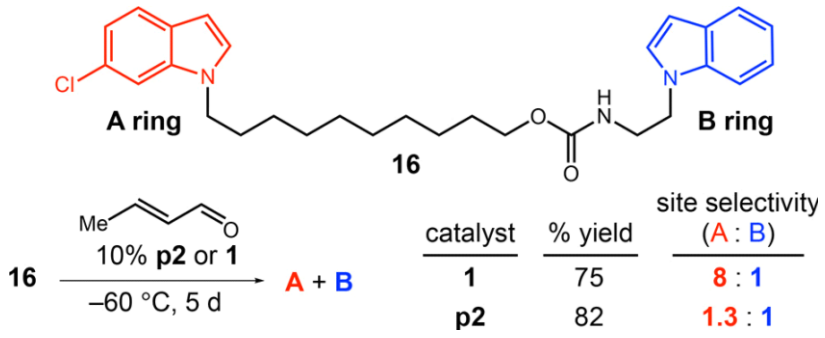

Figure 2.11 Single molecule site selectivity via substrate recognition.

This substrate provided a template on which to explore the ability of **p2** to selectively target a specific site on a molecule by recognizing a nearby binding group. With 10 mol % **p2** or **1**, acrolein was reactive with **16** over 5 days at low temperature to give the product in 82% and 75% yield, respectively. As with previous studies, imidazolidinone **1** reacted based on the inherent reactivity of the system, providing an 8:1 ratio of A:B ring products. It was not expected that the chloroindole A ring would have such higher reactivity. While **p2** was able to select for more B ring product, rather than reversing the selectivity as in previous studies, the selectivity moved to a 1.1:1 ratio of A:B ring products. However, this did provide a nearly 40% yield of B ring product, which is enough to be synthetically useful, and could not be achieved with the use of catalyst **1**.

In conclusion, the utility of bifunctional helical peptide catalysts has been clearly demonstrated by this work. Peptide scaffolds provide effective structural support to promote synergistic interactions between thiourea and imidazolidinone catalytic groups. The resulting rate enhancement and product selectivity in Diels-Alder cycloadditions and indole alkylations serve as a proof-of-concept. We expect this method to be readily applied to other bifunctional peptide catalyst systems as well. Of particular interest will be the future development of bifunctional helical peptide catalysts that are able to perform site selective modification of natural products or active drug molecules.

2.12 General Procedures and Methods

All reactions were carried out in oven-dried glassware with magnetic stirring, unless otherwise indicated. All the reagents were used as obtained from commercial sources unless otherwise noted. Analytical thin-layer chromatography was performed with 0.25 mm coated commercial silica gel plates (E. Merck, DC-Plastikfolien, silicagel 60 F_{254}). Flash Chromatography

was performed with EM Science silica gel (0.040-0.063μm grade). Proton nuclear magnetic resonance (^{1}H-NMR) data were acquired on an Inova 300 MHz, an Inova 500 MHz, or an NMR-S 500 MHz spectrometer. Chemical shifts are reported in ppm units relative to the ^{1}H signal of the $CDCl_3$ solvent. Signals are reported as follows: s (singlet), d (doublet), t (triplet), q (quartet), dd (doublet of doublets), qd (quartet of doublets), brs (broad singlet), m (multiplet). Coupling constants are reported in hertz (Hz). Carbon-13 nuclear magnetic resonance (^{13}C-NMR) data were acquired on an Inova or NMR-S spectrometer at 125 MHz. All NMR spectra were collected at 298 K. Mass spectral data were obtained using ESI techniques (Agilent, 6210 TOF). Microwave-assisted solid phase peptide synthesis was conducted on a CEM Mars 6 microwave. Analytical HPLC traces were conducted on a Shimadzu LCAD semi-preparative HPLC system on a C18 column using a linear gradient of water in acetonitrile with 0.1% v/v TFA.

Peptides **p1, p2, p3, p4, p5** were synthesized as C-terminal amides by microwave-assisted solid-phase peptide synthesis (SPPS), using a standard Fmoc Nα protection strategy as described previously.[1] Fmoc protected amino acids were activated by 2-(1H-benzotriazole-1-yl)-1,1,3,3-tetramethyluronium hexafluorophosphate (HBTU) and N-hydroxybenzotriazole hydrate (HOBt), all purchased from Advanced ChemTech. Hydroxymethyl Benzoic Acid Resin (HMBA) was synthesized using aminomethylated resin purchased from Advanced ChemTech (1.6 mmol/g, SA5003).

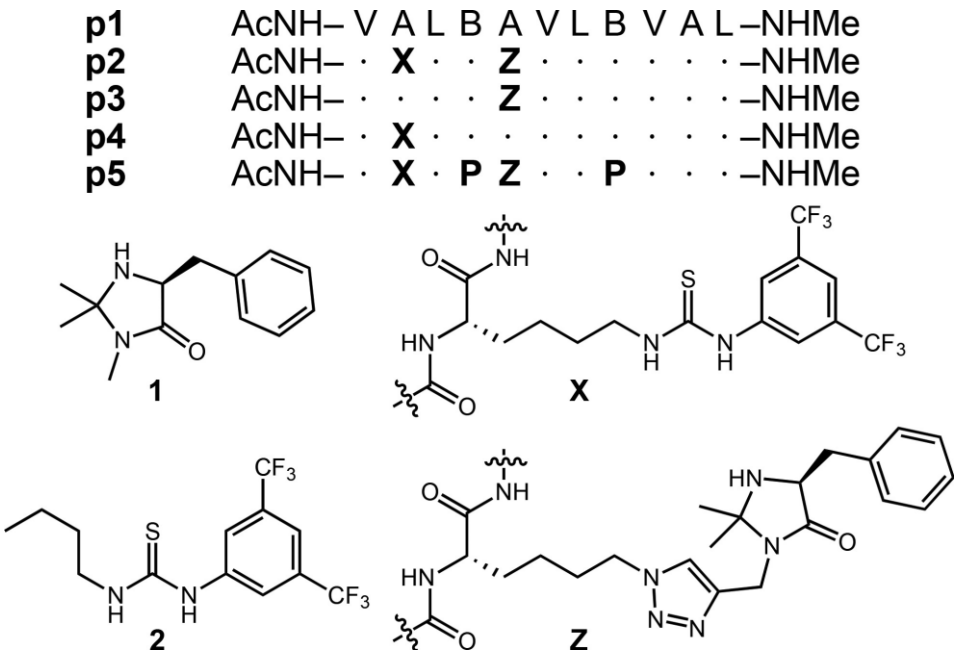

Figure 2.12 Representative synthesis of polypeptide scaffolds on 200 uMol scale via microwave assisted peptide synthesis.

All peptides were synthesized on a 200 μmol scale using the following general procedure. Hydroxymethylbenzoic acid (HMBA) resin (0.5 g; 200 μmol at 0.4 mmol/g loading; 1eq) was placed in a fritted polypropylene syringe (20 ml volume) and allowed to swell in CH_2Cl_2 for 10 minutes. The solvent was then removed using a vacuum manifold and N,N-dimethylformamide (DMF) was added to further swell the resin for 5 minutes. In order to perform activated amino acid couplings, a stock *coupling solution* was prepared by adding HBTU (15.85 g, 0.05 mol, 0.1 M) and HOBt (7.65 g, 0.05 mol, 0.1 M) to 500 mL N-methyl-2-pyrrolidone (NMP). The desired Fmoc-protected amino acid (1 mmol, 5 eq) was dissolved by vortexing in 10 mL of *coupling solution*. Diisopropylethylamine (DIEA) (352 μL, 2 mmol, 10 eq) was added to the amino acid solution; after vortexing, the activated solution was allowed to rest at room temperature for at least 60 seconds. The activated amino acid solution was then added to the resin and the syringe was placed

in the microwave. The coupling method consisted of a 2-minute ramp from room temperature to 70 ˚C, followed by stirring at 70 °C for 4 minutes. The syringe was then removed from the microwave, the amino acid solution was removed on the vacuum manifold and the resin was rinsed 5 times with DMF.

A stock solution of 20% v/v piperidine in DMF was prepared by adding 100 mL piperidine to 400 mL dry DMF under an argon balloon (note: dry DMF was used because adventitious water can lead to cleavage of the peptide from the HMBA resin under basic conditions). Fmoc was removed from resin-bound amino acids by adding the deprotection solution (10 mL) to the resin and allowing the resulting mixture to rest at room temperature for at least 60 seconds. The solution was then removed on the vacuum manifold; an additional 10 mL of deprotection solution was added to the resin, and the syringe was placed in the microwave. The deprotection method consisted of a 2-minute ramp from room temperature to 80 ˚C, followed by stirring at 80 °C for an additional 2 minutes. The syringe was then removed from the microwave and the deprotection solution removed on the vacuum manifold before rinsing the resin 5 times in DMF. The resin was then ready for subsequent coupling and deprotection steps to yield the completed 11-residue polypeptide.

After deprotecting the final amino acid in the sequence and rinsing the resin, the peptide was capped at the N-terminus with an acetyl group. The capping solution was prepared by adding 400 μL acetic anhydride (1mmol, 5eq), 400 μL triethyl amine (1mmol, 5eq) and 4-dimethylaminopyridine (DMAP) (1.36mg, 1mmol, 10 eq) to 5 mL of DCM. The capping solution was then added to the syringe containing the resin and the reaction was stirred for 30 minutes at room temperature. The solution was removed on the vacuum manifold and the resin was rinsed 5 times in DMF.

Cleavage of the finished peptide was performed after the appropriate residues were functionalized with the necessary catalysts. The cleavage reaction was performed on a 200 μmol scale by suspending the resin in 2 mL DCM, adding 2 mL of methylamine solution (31% by weight in absolute ethanol) and stirring under argon for 18 hours. The cleaved peptide was then filtered into a recovery flask, the resin washed 3 times with 10 ml of DCM and the combined solvent was removed under reduced pressure on a rotary evaporator. The crude peptide was loaded onto a column of silica gel (2 cm x 25 cm) and eluted with 10% v/v methanol in DCM with 1% v/v ammonium hydroxide. The fractions containing pure peptide (as determined by mass spec analysis) were dried under vacuum and then dissolved in 2:1 MeCN:Water with 0.1% trifluoroacetic acid. The solution was then frozen with liquid nitrogen and placed on the lyophilizer overnight to yield a fine, white powder. Proteins were identified using electrospray ionization time of flight mass spectrometry (ESI-TOF). Mass spectra values are shown below and peptide purity was determined via Analytical HPLC. Yields for each peptide synthesized are provided in the figure captions.

2.13 Substrate Synthesis Methods

HMBA Resin Synthesis

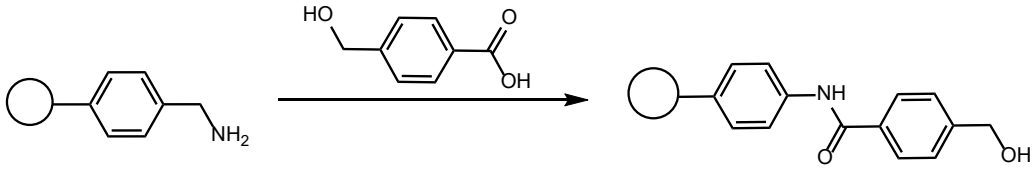

Aminomethylated resin (200 mesh, 10.1 g, 8 mmol, 1 eq) was added to a flame dried, 500 mL round bottom flask under and argon balloon. In a separate flask was mixed: 200 mL dry DMF, PyBop (16.65 g, 32 mmol, 4 eq), 4-hydroxymethylbenzoic acid (4.87g, 32 mmol, 4eq) and diisopropylethylamine (DIEA, 13.93 mL, 80 mmol, 10 eq). This activated acid solution was then added to the resin flask and the mixture was stirred (slowly) under argon at room temperature for 2 hours. Completion of the reaction was determined via a Kaiser test by treating a small amount of resin with ninhydrin solution until no purple color is observed after 1-2 minutes (ninhydrin solution: 1.5 g ninhydrin dissolved in 100 ml *n*-butanol with 3 ml AcOH). The reaction solution containing the resin was then filtered through a fritted syringe and the resin was rinsed 3 times with DMF and three times with DCM. The resin was then dried overnight on high vacuum.

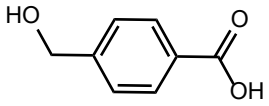

4-Hydroxymethyl Benzoic Acid was synthesized according to the following procedure: A solution of sodium borohydride ($NaBH_4$) was prepared by adding 370 mg (10mmol, 10eq) to 10 ml of methanol chilled in an ice bath. 4-Formyl benzoic acid (150mg, 1mmol, 1eq) was then added

to the solution, and allowed to warm to room temperature. The mixture was stirred for 4 hours after which the solvent was removed on the rotary evaporator. 30 mL of water was added and the solution was extracted 3 times with 20 mL of ethyl acetate. The organic layer was then dried over sodium sulfate and the solvent removed via rotary evaporation to yield a white powder. (109mg, 71% yield). Reaction readily conducted on large scale (up to 50 g 4-formylbenzoic acid with slow addition of 4-formylbenzoic acid to the methanol solution) in similar yield. See: Okada, Y.; Tsuda, Y.; Tada, M.; Wanaka, K.; Okamoto, U.; Hijikata-Okunomiya, A.; Okamoto, S,; *Chem. Pharm. Bull.* **2000**, *48*, 1964–1972.

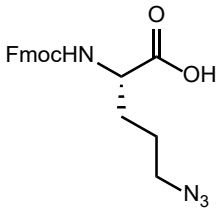

Fmoc-L-Lys(Azide)-OH was synthesized according to the following procedure: Fmoc-L-Lys-OH (4.5 g, 12 mmol, 1 eq), K_2CO_3 (3.55 g, 25 mmol, 2 eq), Imadazole-sulfonyl azide HCl (4.5 g, 18 mmol, 1.5 eq) and Copper (II) sulfate pentahydrate (30 mg, 0.12 mmol, 0.01 eq) were dissolved in 100 mL of an 80:20 mixture of MeOH:Water. The reaction was then stirred at room temperature for 5 hours. Ethyl acetate (100 mL) and water (100 mL) were then added to the reaction and the mixture was acidified to pH 4 with 10% HCl. The aqueous layer was removed and the organic layer was washed with water and brine, dryed over sodium sulfate and the solvent removed under reduced pressure to yield a yellow oil, which was dried overnight under high vacuum. Spectra matched that of previously reported material. (2.9 g, 65% yield). Böse, D.; Frey, W.; Pietruszka, J. *Synthesis* **2014**, *46*, 2524–2532.

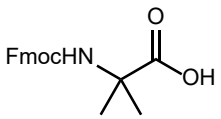

Fmoc-Aib-OH was synthesized according to the following procedure: H-Aib-OH (10.3 g, 100 mmol, 1 eq) and sodium carbonate (20.6 g, 200 mmol, 2 eq) were added to 100 mL water and the mixture was cooled to 0 °C in an ice bath. Fmoc-Cl (37.6 g, 150 mmol, 1.5eq) in 100 mL 1,4-dioxane was then added and the reaction was stirred at room temperature overnight. Water (100 ml) was then added and the reaction was extracted with ethyl acetate (2 x 50 mL). The organic layer was then back extracted with saturated sodium bicarbonate solution and the combined water layers were acidified to pH 1 with 10% HCl. The acidified aqueous phase was then extracted with ethyl acetate (3 x 50 mL) and the combined EtOAc extracts dried over sodium sulfate. After the solvent was remove under reduced pressure the white solid was placed under high vacuum overnight. (18.3 g, 56% yield)

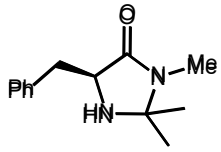

(S)-5-benzyl-2,2,3-trimethylimidazolidin-4-one (1) was synthesized as previously reported. Spectra matched that of previously reported material. See: Pagoti, S.; Dutta, D.; Dash, J. *Adv. Synth. Catal.* **2013**, *355*, 3532–3538.

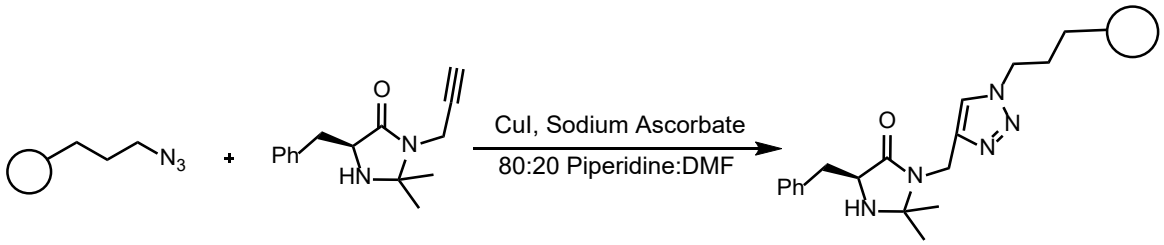

On Resin Click Reaction between Lys(azide) and (S)-5-benzyl-2,2-dimethyl-3-(prop-2-yn-1-yl)imidazolidin-4-one was performed according to the following procedure: to 160 mL of 20% piperidine in dry DMF (160mL) were added (1) resin-bound 11-residue peptide containing Lys(azide) (200 umol scale, 1 eq); (2) sodium ascorbate (200 mg, 1 mmol, 5 eq); (3) CuI (190 mg, 1 mmol, 5 eq); and (4) (S)-5-benzyl-2,2-dimethyl-3-(prop-2-yn-1-yl)imidazolidin-4-one (48 mg, 400 μmol, 2 eq). The solution was allowed to stir under a balloon of argon at room temperature for 18 hours, after which solvent was removed via filtration on a sintered glass filter funnel and the resin washed 5 times with DCM.

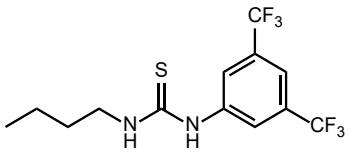

1-(3,5-bis(trifluoromethyl)phenyl)-3-butylthiourea (2) was synthesized according to the following procedure: 3,5-Bistriflouromethyl(phenyl) isothiocyanate (2 ml, 10 mmol, 2.7 g, 1 eq) was added to 1.5 mL butylamine (15 mmol, 1.1 g, 1.5 eq) and the reaction was stirred neat at room temperature overnight. The excess butylamine was removed under vacuum and the product was purified on a column of silica gel with 3:1 hexanes:ethyl acetate as eluent. The purified product was a pale, yellow oil. (3.1 g, 90% yield). Spectra matched previously reported values: Lu, A.; Wang, Z.; Zhou, Z.; Chen, J.; Wang, Q.; *J. Agric. Food Chem,;* **2015**, *63*, 1378–1384.

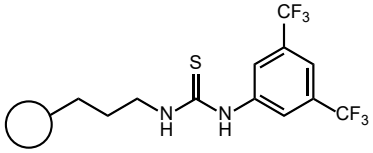

On-Resin Thiourea Catalyst was synthesized according to the following procedure: resin-bound peptide containing Lys(Boc) (200 μM, 1 eq) was treated with 10 mL of 20% v/v trifluoroacetic acid in dichloromethane and allowed to stir for 5 minutes. The acid solution was then drained into a glass flask and anther 10mL of acid solution was added and allowed to stir for 15 minutes. The acid solution was again drained and the resin was rinsed 3 times with dichloromethane and 3 times with 5% v/v diisopropyl ethylamine in dichloromethane and dried on the vacuum manifold. The resin was then suspended in 2 mL of DMF and 3,5-bistriflouromethyl(phenyl) isothiocyanate (260 μL, 1 mmol, 5 eq) was added to the resin suspension. The reaction was capped tightly and heated to 60 ˚C for 48 hours. The reaction solution was then drained on the vacuum manifold and the resin was rinsed three times with 10 mL DMF and three times with 10 mL DCM.

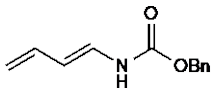

Benzyl (E)-buta-1,3-dien-1-ylcarbamate (3): Synthesized as previously reported from (E)-penta-2,4-dienoic acid: *Org. Synth.* **1979**, *59*, 1.

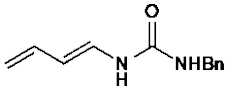

(E)-1-benzyl-3-(buta-1,3-dien-1-yl)urea: Synthesized following the same procedure as reported for benzyl (E)-buta-1,3-dien-1-ylcarbamate using 4.75 g trans-2,4-pentanedienoic acid (De Cusati,

P. F.; Olofson, R. A. *Tetrahedron Lett*. **1990**, *31*, 1405–1408) with the exception that N-benzylamine was substituted for benzyl alcohol. Purified via silica gel chromatography using using 2:1 hexanes:EtOAc. Isolated as an orange solid as a 13:1 mixture of E and Z isomers (0.51 g product). Rf = 0.35 (2:1 Hexanes:EtOAc). IR (film): 3286, 3084, 1655, 1619, 1550, 1453, 1265, 1004; ^{1}H NMR ($CDCl_3$, 500 MHz) 7.21–7.38 (m, 5H), 6.43 (dt, J = 10.61, 16.76 Hz, 1H), 5.97 (bs, 1H), 5.91 (d, J = 15.2 Hz, 1H), 5.57 (d, J = 16.8 Hz, 1H), 5.44 (d, J = 10.37 Hz, 1H),4.52 (d, J = 5.95 Hz, 2H); ^{13}C NMR ($CDCl_3$, 125 MHz): 165.8, 141.5, 138.1, 134.7, 128.7, 127.9, 127.6, 124.6, 124.3, 43.8; HRMS (ESI): $C_{12}H_{15}N_2O$ (M+H) calculated: 203.1184, found 203.1186.

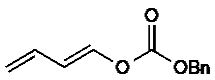

(E)-benzyl buta-1,3-dien-1-yl carbonate: Synthesized according to the same procedure as reported for (E)-ethyl buta-1,3-dien-1-yl carbonate (De Cusati, P. F.; Olofson, R. A. *Tetrahedron Lett*. **1990**, *31*, 1405–1408) using 5.0 g (71.3 mmol) crotonaldehyde, 15.21 g benzyl chloroformate (89.2 mmol, 1.25 equiv), and 9.34 g (83.2 mmol, 1.15 equiv) potassium tert-butoxide. Isolated after flash chromatography on silica gel (15:1 hexanes:EtOAc) as a colorless oil (3.8 g, 26%). Rf = 0.55 (12:1 hexanes:EtOAc). IR(film): 3091, 3035, 2691, 1762, 1663, 1290, 1246; ^{1}H NMR ($CDCl_3$, 300 MHz) 7.35–7.48 (m, 5H), 7.25 (d, J = 12.04 Hz, 1H), 6.30 (dt, J = 10.80, 16.67 Hz, 1H), 6.10 (t, J =11.88 Hz, 1H), 5.27 (s, 2H), 5.26 (d, J = 16.54 Hz, 1H), 5.14 (d, J = 10.34 Hz, 1H); ^{13}C NMR ($CDCl_3$, 75 MHz): 152.6, 140.1, 131.1, 128.8, 128.7, 128.7, 128.6, 128.5, 128.4, 117.6, 116.3, 70.4; HRMS (ESI): $C_{12}H_{16}NO_3$ (M+NH_4) calculated: 222.1130, found 222.1168.

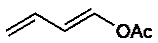

(E)-buta-1,3-dien-1-yl acetate: Synthesized as previously reported. Spectra matched that of previously reported material: Böse, D.; Frey, W.; Pietruszka, J. *Synthesis* **2014**, *46*, 2524–2532.

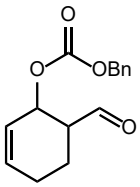

Benzyl (6-formylcyclohex-2-en-1-yl) carbonate (7) was synthesized according to the following procedure. (E)-Benzyl buta-1,3-dien-1-yl carbonate (20.4 mg, 0.1 mmol, 10 mM, 1eq) and 25.7 μL of distilled acrolein (0.5 mmol, 50 mM, 5eq) were dissolved in 10mL of 95:5 nitromethane/water at 4˚ C. Catalyst **p2** (1.7 mg, 1 μmol, 1 mM, 0.01 eq) was added to the reaction mixture and the reaction was kept at -4˚ C for 48 hours. The solvent was then removed under vacuum and product was purified over silica gel with 9:1 Hexanes/Ethyl Acetate. Yield: 142.5mg, 52%; 65% ee for **p2**. Chiral HPLC on IB column, Methanol at 0.4 mL/min, major peak: 10.2 minutes, minor peak: 11.2 minutes. Rf = 0.28 (12:1 hexanes:EtOAc). IR(film): 3583, 3033, 2923, 1728, 1250, 1312, 1290, 843 ; ^{1}H NMR ($CDCl_3$, 500 MHz) 9.794 (s, 1H), 7.372 (m, 5H), 6.070 (m, 1H), 5.975 (m, 1H), 5.559(t, J = 4.34, 2H), 5.161 (d, 1H), 2.637 (dt, J = 10.9, 3.15 Hz, 1H), 2.267 (m, 1H), 2.086 (m, 1H), 1.964 (m, 1H), 1.567 (s, 3H); ^{13}C NMR ($CDCl_3$, 75 MHz): 201.7, 154.6, 135.0, 134.5, 128.6, 128.5, 128.3, 123.4, 69.8, 49.8, 29.7, 24.0, 17.9; HRMS (ESI): $C_{15}H_{16}O_4$ (M+H) calculated: 274.1205, found 274.1210.

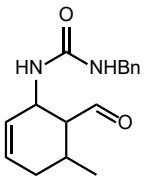

1-benzyl-3-(6-formylcyclohex-2-en-1-yl)urea (8) was synthesized according to the following procedure. (E)-1-Benzyl-3-(buta-1,3-dien-1-yl)urea (20.2 mg, 0.1mmol, 10mM, 1eq) and crotonaldehyde (51.5 μL, 0.5 mmol, 50 mM, 5 eq) were dissolved in 10mL of 95:5 nitromethane/water at 4˚ C. Catalyst **p2** (1.7 mg, 1 μmol, 0.1 mM, 0.01 eq) was added to the reaction mixture and the reaction was kept at -4˚ C for 48 hours. The solvent was then removed under vacuum and an internal standard (4-bromo-3,5-bistriflouromethylbenzene, 0.2 eq) was added and the yield of the reaction calculated by comparison of the ratios in ^{1}H NMR. 21% yield by internal standard, 48 h. Rf = 0.47 (1:1 hexanes:EtOAc). IR(film): 3288, 2927, 1720, 1548, 1271, 1008, 699; ^{1}H NMR ($CDCl_3$, 500 MHz) 9.78 (s, 1H), 7.34 (m, 5H), 6.89 (m,1H), 5.84 (m, 2H), 5.36 (m, 1H), 4.38 (m, 3H), 2.86 (m, 1H), 2.53 (m, 2H), 1.97 (m, 1H), 0.96 (d, J = 6.95 Hz, 3H); ^{13}C NMR ($CDCl_3$, 75 MHz): 204.3, 167.2, 130.6, 128.3, 125.3, 123.0, 121.9, 64.1, 47.5, 29.3, 19.9; HRMS (ESI): $C_{16}H_{20}N_2O_2$ (M+H) calculated: 273.1558, found 273.1927.

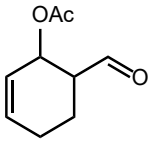

6-formyl-5-methylcyclohex-2-en-1-yl acetate (9) was synthesized according to the following procedure. 11.2 mg of (E)-buta-1,3-dien-1-yl acetate (0.1 mmol, 10 mM, 1 eq) and 25.7 μL of distilled acrolein (0.5 mmol, 50 mM, 5 eq) were dissolved in 10 mL of 95:5 nitromethane/water at 4 ˚C. 1.7 mg of catalyst **p2** (1 μmol, 0.1 mM, 0.01 eq) was added to the reaction mixture and the reaction was kept at -4 ˚C for 48 hours. The solvent was then removed under vacuum and product

was purified over silica gel with 9:1 Hexanes/Ethyl Acetate. Yield: 80.6 mg, 48%; Spectra match previously reported data: Gouesnard, J.P. et al,; *Tetrahedron* **1974** , *30*, 151–157.

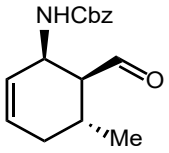

Benzyl ((1R,5R,6S)-6-formyl-5-methylcyclohex-2-en-1-yl)carbamate (4) was synthesized according to the following procedure. Benzyl (E)-buta-1,3-dien-1-ylcarbamate (20.3 mg, 0.1 mmol, 10 mM, 1 eq) and crotonaldehyde (51.5 μL, 0.5 mmol, 50 mM, 5 eq) were dissolved in 10 mL of 95:5 nitromethane/water at 4 ˚C. Catalyst **p2** (0.17 mg, 1 μmol, 0.1 mM, 0.001 eq) was added to the reaction mixture and the reaction was kept at -4 ˚C for 48 hours. The solvent was then removed under vacuum and product was purified over silica gel with 4:1 Hexanes/Ethyl Acetate as a yellow oil. Yield: 17.2 mg, 63%, (89% ee).

Alternatively, Benzyl (E)-buta-1,3-dien-1-ylcarbamate (20.3mg, 0.1mmol, 10mM, 1 eq) and crotonaldehyde (51.5 μL, 0.5mmol, 50mM, 5eq) were dissolved in 10 mL of 95:5 nitromethane/water at 4˚ C. Catalyst **1** (2.45 mg, 0.01 mmol, 1 mM, 0.1 eq) was added to the reaction mixture and the reaction was kept at -4˚ C for 48 hours and worked up as shown above. Yield: 15.56mg, 57%, (77% ee).

In both cases, spectra matched previously reported data (Overman, L.E.; Jessup, Peter J. *J. Am. Chem. Soc*. **1978**, 100 (16), pp 5179–5185). The absolute stereochemistry of the products was inferred based on previous reports of catalytic Diels-Alder reactions with catalyst **1** and diene **3** and by comparing the HPLC traces of products generated with catalyst **1** and peptide catalyst **p2**.

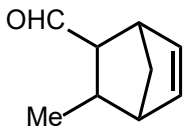

3-methylbicyclo[2.2.1]hept-5-ene-2-carbaldehyde (6) was synthesized by adding distilled cyclopentadiene (84 μL, 1 mmol, 1 eq) and 0.1 eq of catalyst (**1**, **p3** or **p2**) to 10 mL of 95:5 v/v nitromethane/water at -15 ˚C. Distilled crotonaldehyde (309 μL, 3 mmol, 3 eq) was then added to the reaction mixture and the reaction was stirred at -15 ˚C for 48 hours. Due to the volatility of the product, and in order to obtain accurate yield information, 1,3-bis(trifluoromethyl)-5-bromobenzene (172 μL, 1 mmol, 1 eq) was then added to the reaction as an internal standard and an aliquot of the reaction was taken and diluted in 1 mL deuterated chloroform into an NMR tube. By integration of the product aldehyde peak in reference to the internal standard, yield by internal standard was determined to be 70% for catalyst **1**, 34% for catalyst **p3** and 32% for catalyst **p2**. Spectra matched the previously reported data. (Northrup, A.B.; MacMillan, D.W.C. *J. Am. Chem. Soc*. **2002**, 124, 2458-2460).

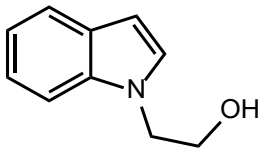

2-(1H-indol-1-yl)ethan-1-ol: Synthesized as previously reported from indole: Nguyen, T.M.; Duong, H.A.; Richard, J.-A.; Johannes, C.W.; Pincheng, F.; Ye, D.K.J.; Shuying, E.L. *Chem. Commun.* **2013**, *49*, 10602–10604.

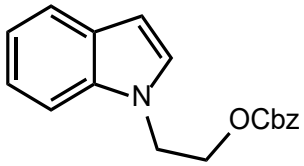

2-(1H-indol-1-yl)ethyl benzyl carbonate (12) was synthesized by dissolving 2-(1H-indol-1-yl)ethan-1-ol (161 mg, 1 mmol, 1 eq) in 40 mL THF at 0 ˚C. Benzylchloroformate (171 µL, 1.2 mmol, 1.2 eq) and pyridine (80.6 µL, 1 mmol, 1 eq) were then added drop-wise and the reaction was stirred at 50 ˚C for 24 hours. The solvent was then removed under vacuum and product was purified over silica gel with 4:1 Hexanes/Ethyl Acetate. Product was isolated as amber oil (257 mg, 87%) R_f = 0.29; ^{1}H NMR ($CDCl_3$, 500 MHz) 7.68 (d, J = 13.04 Hz, 1H), 7.38 (m, 6H), 7.22 (m, 4H), 6.55 (d, J = 4.95 Hz, 1H), 5.14 (m, 2H), 4.47 (m, 5H); ^{13}C NMR ($CDCl_3$, 75 MHz): 154.8, 136.0, 135.0, 128.7, 128.7, 128.4, 128.1, 121.9, 121.1, 119.7, 109.0, 102.0, 77.3, 69.9, 66.3, 44.9; HRMS (ESI): $C_{18}H_{17}NO_3$ (M+H) calculated: 296.1242, found 296.1421.

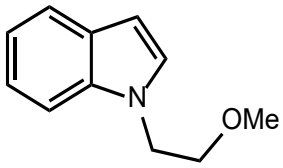

1-(2-methoxyethyl)-1H-indole (14) was synthesized by dissolving 2-(1H-indol-1-yl)ethan-1-ol (161 mg, 1 mmol, 1 eq) in 40 mL THF at 0 ˚C. Sodium Hydride, 60% dispersion in mineral oil, (40 mg, 1 mmol, 1 eq) was added and the solution stirred for 10 minutes at 0 ˚C. Iodomethane (184.5 mg, 1.3 mmol, 1.3 eq) was then added and the reaction was stirred at room temperature for 3 hours. The solvent was then removed under vacuum and product was purified over silica gel with 7:1 Hexanes/Ethyl Acetate. (154mg, 90%) R_f = 0.29; ^{1}H NMR ($CDCl_3$, 500 MHz) 7.68 (d, J = 8.04 Hz, 1H), 7.40 (d, J = 8.04 Hz, 1H), 7.26 (t, J = 7.54 Hz, 1H), 7.20 (d, J = 3.11 Hz, 1H), 7.15 (t, J = 7.54 Hz, 1H), 6.55 (d, J = 30.52 Hz, 1H), 4.32 (t, J = 5.51 Hz, 2H), 3.74 (t, J = 5.51 Hz, 2H),

3.35 (s, 3H); ^{13}C NMR ($CDCl_3$, 75 MHz): 136.1, 128.7, 128.4, 121.5, 121.0, 119.4, 109.2, 101.3, 71.6, 59.4, 46.2; HRMS (ESI): $C_{11}H_{13}NO$ (M+H) calculated: 176.1031, found 176.0842.

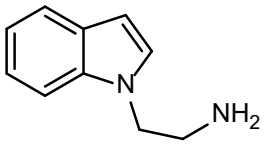

2-(1*H*-indol-1-yl)ethan-1-amine: Prepared as previously reported from indole: Wu, F.; Zhu, H.; Sun, L.; Rajendran, C.; Wang, M.; Ren, X.; Panjikar, S.; Cherkasov, A.; Zou, H.; Stoeckigt, J. *J. Am. Chem. Soc.* **2012**, *134*, 1498–1500.

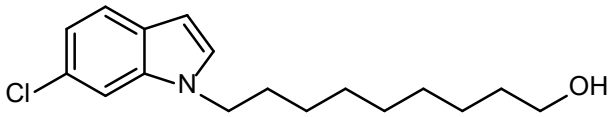

9-(6-chloro-1H-indol-1-yl)nonan-1-ol was synthesized as follows: Into a 50 mL round bottom flask was placed 9-bromo-1-nonanol (2.2 g, 9.9 mmol, 1.5 eq), 1.02 g indole (6.59 mmol, 1 eq), 1.85 g KOH (33 mmol, 5 eq), 0.121 g tetrabutylammonium iodide (0.05 eq), and finally DMF (13 mL). The mixture was heated under nitrogen to 70 °C overnight (14 h). The reaction was then cooled to ambient temperature and 50 mL water was added. The mixture was extracted 3 times with 60 mL Et_2O and the combined organic layers were then back washed three times with 50 mL H_2O. The organic layer was then dried over $MgSO_4$, and the solvent was removed. Purification of the resulting oil on a column of silica gel and eluting with 2.5:1 Hexanes:EtOAc provided the desired product as a slightly orange oil (1.97 g, 99% yield). R_f = 0.3 (2.5:1 hexanes:EtOAc). IR(film): 3292,2855, 1762, 1609, 1506, 1467, 1404, 1374, 1317, 1290, 1240; ^{1}H NMR ($CDCl_3$, 500 MHz) 7.53 (d, J = 8.52 Hz, 1H), 7.34 (s, 1H), 7.08 (m, 2H), 6.47 (d, J = 3.07 Hz, 1H), 4.07 (t, J = 7.08 Hz, 2H), 3.64 (t, J = 7.08 Hz, 2H), 1.82 (m, 2H), 1.56 (m, 2H), 1.31 (m, 11H); ^{13}C NMR

($CDCl_3$, 75 MHz): 136.4, 128.5, 127.3, 127.1, 121.7, 119.9, 109.4, 101.1, 63.0, 46.5, 32.7, 30.1, 29.4, 29.3, 29.1, 26.9, 25.7; HRMS (ESI): $C_{28}H_{34}ClN_3O_2$ (M+H) calculated: 295.1517, found: 295.1612 .

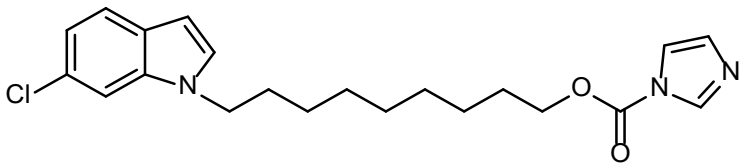

N-(9-(6-chloro-1H-indol-1-yl)nonyl)-1H-imidazole-1-carboxamide was synthesized as follows: Into a 50 mL round bottom flask was placed 1,1'-carbonyldiimidazole (0.83 g, 5.12 mmol, 1.5 eq) and 12 mL THF. The solution was cooled to 0 °C and **9-(6-chloro-1H-indol-1-yl)nonan-1-ol** (1.0 g, 3.41 mmol, 1 eq) was added dropwise as a solution in 4 mL CH_2Cl_2. The reaction was stirred at 0 °C for 1 h, when allowed to warm to room temperature and stirred an additional 2 h. The solvent was then removed and the residue loaded directly onto a column of silica gel and eluted with 2:3 hexanes:EtOAc to provide a slightly orange oil (1.205 g, 91% yield). R_f = 0.65 (1:2 Hexanes:EtOAc). IR(film): 3131, 2930, 2855, 1762, 1609, 1506, 1467, 1404, 1374, 1317, 1290, 1240, 1176, 1095, 1003, 901, 804, 770; ^{1}H NMR ($CDCl_3$, 500 MHz) 8.15 (s, 1H), 7.53 (d, J = 8.54 Hz), 7.43 (s, 1H), 7.33 (s, 1H), 7.07 (m, 3H), 6.46 (d, J = 3.52 Hz, 1H), 4.40 (t, J = 7.01 Hz, 2H), 4.07 (t, J = 7.01 Hz, 2H), 1.79 (m, 4H), 1.33 (m, 11H); ^{13}C NMR ($CDCl_3$, 75 MHz): 148.8, 137.1, 136.3, 130.6, 128.5, 127.3, 127.1, 121.8, 119.9, 117.1, 109.4, 101.1, 69.9, 68.4, 46.5, 30.1, 29.3, 29.1, 29.0, 28.4, 26.8, 25.7; HRMS (ESI): $C_{21}H_{27}ClN_4O$ (M+H) calculated: 388.1844, found 388.1891.

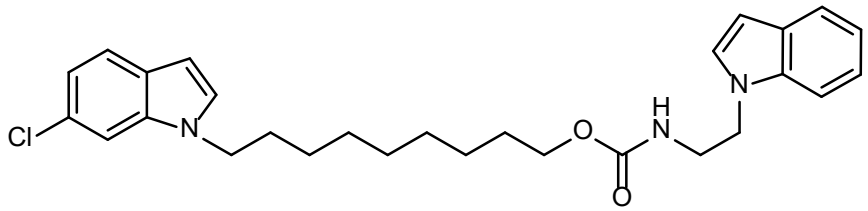

2-(1H-indol-1-yl)ethyl (9-(6-chloro-1H-indol-1-yl)nonyl)carbamate (16) was synthesized as follows: Into a 10 mL round bottom was placed N-(9-(6-chloro-1H-indol-1-yl)nonyl)-1H-imidazole-1-carboxamide (0.35 g, 0.9 mmol, 1.2 eq) in 1.5 mL of dry MeCN. Under a nitrogen atmosphere, Iodomethane (2.56 g, 18 mmol, 20 eq) was then added, the flask was sealed, and the reaction was heated to 60 °C for 5 h. The volatiles were then removed on the hi-vacuum and 2-(1*H*-indol-1-yl)ethan-1-amine was added as a solution in 10 mL CH_2Cl_2. The reaction was stirred overnight, the volatiles removed, and the resulting product purified on a column of silica gel (2:1 Hexanes:EtOAc) to provide the title compound as a colorless oil (0.105 g, 24% yield). R_f = 0.7 (3:2 Hexanes:EtOAc). IR(film): 3339, 3054, 2929, 2854, 1714, 1610, 1512, 1463, 1316, 1241, 1197, 901, 741, 717; ^{1}H NMR ($CDCl_3$, 500 MHz) 7.68 (d, J = 8.05 Hz, 1H), 7.56 (d, J = 8.015 Hz), 7.38 (m, 2H), 7.25 (t, J = 8.16 Hz, 1H), 7.16 (t, J = 8.16 Hz, 1H), 7.10 (m, 4H), 6.55 (d, J = 2.02 Hz, 1H), 6.50 (d, J = 2.02 Hz, 1H), 4.72 (bs, 1H), 4.29 (m, 2H), 4.08 (m, 4H), 3.55 (m, 2H), 1.84 (m, 2H), 1.60 (m, 2H), 1.32 (m, 11H); ^{13}C NMR ($CDCl_3$, 75 MHz): 156.8, 136.4, 136.0, 128.7, 128.6, 127.9, 127.4, 127.0, 121.8, 121.1, 119.9, 119.6, 109.4, 109.3, 101.7, 101.2, 65.2, 46.5, 45.9, 41.1, 30.2, 29.3, 29.2, 29.2, 29.0, 26.9, 25.8; HRMS (ESI): $C_{28}H_{34}ClN_3O_2$ (M+H) calculated: 481.2310, found 481.2193.

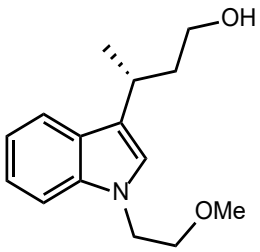

(R)-3-(1-(2-methoxyethyl)-1H-indol-3-yl)butanol (15) was synthesized by dissolving 1-(2-methoxyethyl)-1H-indole (17.5 mg, 100 mmol, 1 eq) in 1 mL DCM and the solution was cooled to -80 ˚C. **Catalyst 2** (3.49 mg, 2 mmol, 0.02 eq) and then crotonaldehyde (21 mg, 300 mmol, 3 eq) were added and the reaction was stirred for 36 h. Sodium borohydride (37.8 mg, 1 M, 10 eq) in 1 mL cold methanol was then added and the reaction stirred an additional 4 hours. The reaction was then quenched with 10 mL water, washed 3 times with 10 mL of ethyl acetate and dried over sodium sulfate. The product was purified over silica 4:1 Hexanes:EtOAc to yield a clear oil. **Yield**: 12.1 mg, 49%; R_f =0.47; IR(film): 3642, 3610, 3348, 2894, 2140, 1656, 1572, 723 ;^{1}H NMR ($CDCl_3$, 500 MHz) 7.53 (m, 1H), 7.27 (m, 1H), 7.27 (s, 1H), 7.16 (m, 1H), 7.08 (m, 1H), 6.49 (d, J = 3.56 Hz, 1H), 4.28 (t, J = 5.52 Hz, 2H), 3.81 (t, J = 5.52 Hz, 2H), 3.65 (m, 2H), 3.49 (m, 3H); ^{13}C NMR ($CDCl_3$, 75 MHz): 136.6, 129.1, 127.6, 127.2, 121.9, 120.3, 120.2, 109.4, 101.8, 101.7, 72.4, 70.0, 61.7, 48.7, 46.5; HRMS (ESI): $C_{15}H_{21}NO_2$ (M+H) calculated: 248.1606, found 248.1643.

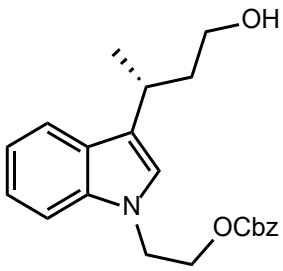

(R)-benzyl (2-(3-(4-oxobutan-2-yl)-1H-indol-1-yl)ethyl) carbonate (13) was synthesized by dissolving 2-(1H-indol-1-yl)ethyl benzyl carbonate (29.5 mg, 100 mmol, 1 eq) in 1 mL DCM and

the solution was cooled to -80 ˚C. **Catalyst 2** (3.49 mg, 2 mmol, 0.02 eq) and then crotonaldehyde (21 mg, 300 mmol, 3 eq) were added and the reaction was stirred for 36 hours. Sodium borohydride (37.8 mg, 1 M, 10 eq) in 1 mL cold methanol was then added and the reaction stirred an additional 4 h. The reaction was then quenched with 10 mL water, washed 3 times with 10 mL of ethyl acetate and dried over sodium sulfate. The product was purified over silica 4:1 Hexanes:EtOAc to yield a pail red oil. Yield: 25.8 mg, 70%; 61% ee for **p2** and 33% ee for **1**. Chiral HPLC on IB column, 96:4 Hexanes:Isopropanol, major peak: 7.6 minutes, minor peak: 8.2 minutes. R_f =0.31; IR(film): 3642, 3610, 3348, 2894, 2140, 1656, 1572, 723; ^{1}H NMR ($CDCl_3$, 500 MHz) 7.66 (d, J = 8.10 Hz, 1H), 7.35 (m, 5H), 7.27 (m, 3H), 7.22 (t, J = 8.10 Hz, 1H), 7.11 (t, J = 8.10 Hz, 1H), 5.12 (s, 2H), 4.40 (dt, J = 42.06, 5.51 Hz, 4H), 3.65 (m, 2H), 3.20 (m, 1H), 2.00 (m, 2H); ^{13}C NMR ($CDCl_3$, 75 MHz): 154.8, 136.6, 135.0, 128.6, 128.4, 127.4, 124.2, 121.9, 121.1, 119.6, 119.0, 109.1, 69.9, 66.3, 61.5, 44.7, 40.3, 29.7, 27.6, 21.8; HRMS (ESI): $C_{22}H_{25}NO_4$ (M+H) calculated: 368.1817, found 368.1798.

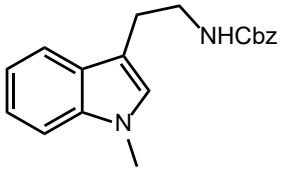

Benzyl (2-(1-methyl-1H-indol-3-yl)ethyl)carbamate (10) Prepared as previously reported from tryptamine. Lozano, O,; Blessley, G,; Martinez del Campo, T,; Thompson, A. L,; Giuffredi, G. T,; Bettati, M,; Walker, M,; Borman, R. and Gouverneur, V. (**2011**), *Angew. Chem. Int. Ed*,; 50: 8105–8109. doi:10.1002/anie.201103151

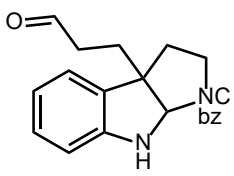

Benzyl 3a-(3-oxopropyl)-3,3a,8,8a-tetrahydropyrrolo[2,3-b]indole-1(2H)-carboxylate (11) was synthesized by adding benzyl (2-(indolin-3-yl)ethyl)carbamate (30.8 mg, 0.1 mmol, 1 eq) and catalyst **p2** (1.7 mg, 1 μmol, 0.01 eq) to 1 mL of 95:5 v/v nitromethane/water at -4 ˚C. Distilled acrolein (24 μL, 0.3 mmol, 3 eq) was then added to the reaction mixture and the reaction was stirred at -4 ˚C for 48 h. The solvent was then removed on a rotary evaporator and the product was purified via flash chromatography on silica gel (5:1 hexanes:EtOAc) as a colorless oil (27.7 mg, 76%). 42% ee for **p2** and 8% ee for **1**. Chiral HPLC on IA column, 96:4 Hexanes:Isopropanol, major peak: 15.0 minutes, minor peak: 16.6 minutes. R_f =0.59; IR(film): 3642, 3610, 3348, 2894, 2140, 1656, 1572, 723 ; ^{1}H NMR ($CDCl_3$, 500 MHz) 9.63 (s, 1H), 7.35 (m, 5H), 7.17 (m, 1H), 6.98 (m, 2H), 6.69 (m, 2H), 6.38 (m, 2H) 6.38 (dd, J = 36.28, 21.09 Hz, 2H), 5.32 (s, 1H), 5.27 (s, 2H), 3.91 (dt, J = 47.07, 21.59 Hz, 2H), 2.42 (m, 1H), 2.19 (m, 2H), 2.01 (m, 1H); ^{13}C NMR ($CDCl_3$, 75 MHz): 203.4, 132.9, 131.3, 129.5, 125.8, 119.8, 107.3, 89.4, 68.1, 67.5, 55.0, 46.4, 45.3, 40.1, 38.4, 37.9, 33.5, 32.5, 29.1, 7.5; HRMS (ESI): $C_{21}H_{22}N_2O_3$ (M+H) calculated: 351.1664, found 351.1698

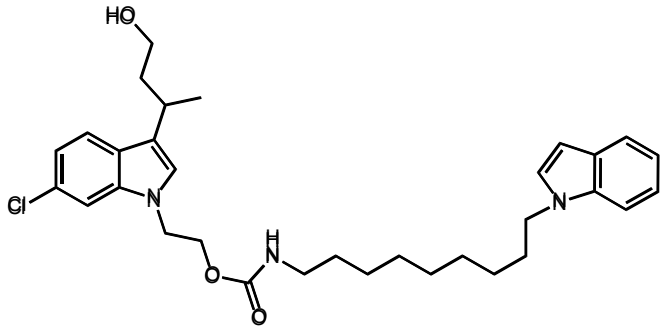

2-(6-chloro-3-(4-hydroxybutan-2-yl)-1H-indol-1-yl)ethyl (9-(1H-indol-1-yl)nonyl)carbamate (A) was synthesized by dissolving 2-(1H-indol-1-yl)ethyl (9-(6-chloro-1H-indol-1-yl)nonyl)carbamate (24mg, 50 mmol, 1 eq) in 5 mL wet DCM at -60 ˚C. Catalyst **1** (1.25mg, 5mmol, 0.1 eq) and distilled crotonaldehyde (16µL, 150mmol, 3 eq) were then added and the reaction was stirred for 48 h. Sodium borohydride (37.8 mg, 1 M, 10 eq) in 1 mL cold methanol was then added and the reaction stirred an additional 30 minutes at room temperature. The reaction was then quenched with 10 mL water, washed 3 times with 10 mL of ethyl acetate and dried over sodium sulfate. The product was purified over silica 1:1 Hexanes:EtOAc to yield a yellow oil. Yield: 20.6 mg, 75% (8:1 ratio of **A** to **B**); R_f =0.27; IR(film): 3341, 3059, 2854, 2359, 1714, 1610, 1512, 1463, 1316, 1241, 1197, 901, 741, 717; ^{1}H NMR ($CDCl_3$, 500 MHz) 7.68 (d, J = 7.91 Hz, 1H), 7.56 (d, J = 7.91 Hz, 2H), 7.33 (m, 1H), 7.25 (t, J = 8.02 Hz, 1H), 7.08 (m, 5H), 6.87 (s, 1H), 6.46 (d, J = 2.63 Hz, 1H), 4.64 (bs, 1H), 4.23 (m, 2H), 4.13 (q, J = 7.15 Hz, 4H), 3.62 (m, 2H), 3.55 (m, 2H), 1.84 (m, 2H), 1.60 (m, 2H), 1.32 (m, 8H), 1.16 (d, J = 7.15 Hz, 3H), 0.90 (m, 4H); ^{13}C NMR ($CDCl_3$, 75 MHz): 156.7, 148.3, 146.0, 136.3, 136.0, 128.7, 128.5, 127.9, 127.4, 127.1, 121.8, 121.1, 119.6, 109.4, 113.6, 109.4, 109.2, 101.1, 65.2, 46.5, 46.0, 43.6, 41.1, 32.7, 30.1, 29.7, 29.4, 29.1, 28.9, 26.9, 25.8, 14.2; HRMS (ESI): $C_{32}H_{42}ClN_3O_3$ (M+H) calculated: 552.2915, found 552.3005.

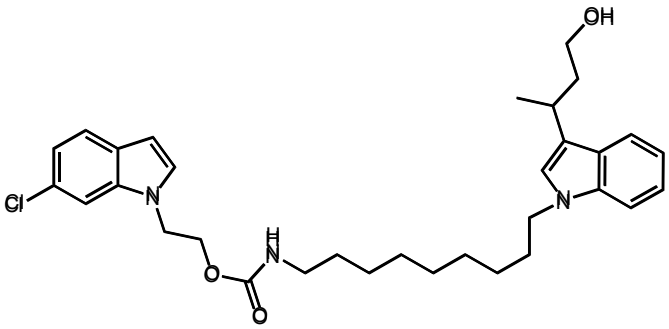

2-(6-chloro-1H-indol-1-yl)ethyl (9-(3-(4-hydroxybutan-2-yl)-1H-indol-1-yl)nonyl)carbamate (B) was synthesized by dissolving 2-(1H-indol-1-yl)ethyl (9-(6-chloro-1H-indol-1-yl)nonyl)carbamate (24mg, 50 mmol, 1 eq) in 5 mL wet DCM at -60 ˚C. Catalyst **p1** (8.73mg, 5mmol, 0.1 eq) and distilled crotonaldehyde (16μL, 150mmol, 3 eq) were then added and the reaction was stirred for 5 days. Sodium borohydride (37.8 mg, 1 M, 10 eq) in 1 mL cold methanol was then added and the reaction stirred an additional 30 minutes at room temperature. The reaction was then quenched with 10 mL water, washed 3 times with 10 mL of ethyl acetate and dried over sodium sulfate. The product was purified over silica 1:1 Hexanes:EtOAc to yield a yellow oil as a 1.3:1 mixture of **A** to **B**. Yield: 22.6 mg, 82%; R_f =0.27; IR(film): 3341, 3059, 2854, 2359, 1714, 1610, 1512, 1463, 1316, 1241, 1197, 901, 741, 717; ^{1}H NMR ($CDCl_3$, 500 MHz) 7.68 (d, J = 7.91 Hz, 1H), 7.56 (d, J = 7.91 Hz, 2H), 7.33 (m, 1H), 7.25 (t, J = 8.02 Hz, 1H), 7.08 (m, 5H), 6.87 (s, 1H), 6.52 (d, J = 2.54 Hz, 1H), 4.64 (bs, 1H), 4.23 (m, 2H), 4.13 (q, J = 7.15 Hz, 4H), 3.62 (m, 2H), 3.55 (m, 2H), 1.84 (m, 2H), 1.60 (m, 2H), 1.32 (m, 8H), 1.16 (d, J = 7.15 Hz, 3H), 0.90 (m, 4H); ^{13}C NMR ($CDCl_3$, 75 MHz): 156.7, 148.3, 146.0, 136.3, 136.0, 128.7, 128.5, 127.9, 127.4, 127.1, 121.8, 121.1, 119.6, 109.4, 113.6, 109.4, 109.2, 101.7, 65.2, 46.5, 46.0, 43.6, 41.1, 32.7, 30.1, 29.7, 29.4, 29.1, 28.9, 26.9, 25.8, 14.2; HRMS (ESI): $C_{32}H_{42}ClN_3O_3$ (M+H) calculated: 552.2915, found 552.3005.

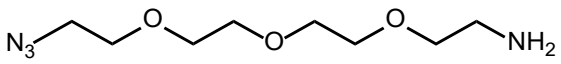

2-(2-(2-(2-azidoethoxy)ethoxy)ethoxy)ethan-1-amine: prepared as previously reported from tetraethylene glycol: Okoth, R.; Basu, A.; *J. Org. Chem.* **2013**, 9:608-12

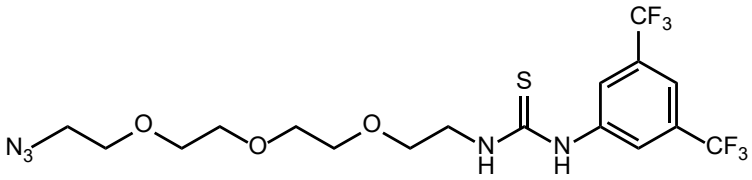

1-(2-(2-(2-(2-azidoethoxy)ethoxy)ethoxy)ethyl)-3-(3,5-bis(trifluoromethyl)phenyl)thiourea was synthesized as follows: Into a 100 ml round bottom flask was placed 2-(2-(2-(2-azidoethoxy)ethoxy)ethoxy)ethan-1-amine (438 mg, 2 mmol, 1 eq) and 3,5-Bis(trifluoromethyl)phenyl isothiocyanate (596 mg, 2.2 mmol, 1.1 eq). The reaction was stirred for 18 hours under nitrogen and the excess starting material was removed under vacuum. The resulting amber oil was taken on to the next step crude. Rf = 0.69 (9:1 hexanes:EtOAc). IR(film): 3275, 3182, 2911, 1784, 1520, 1397, 1256; ^{1}H NMR ($CDCl_3$, 500 MHz) 8.08 (s, 1H), 7.77 (s, 1H), 7.65 (m, 3H), 3.69 (m, 10H), 3.41 (m, 2H), 1.72 (m, 4H), ^{13}C NMR ($CDCl_3$, 75 MHz): 182.1, 132.0, 131.9, 128.8, 128.7, 124.2, 123.2, 122.0, 117.5, 72.4, 70.7, 70.6, 70.5, 70.4, 70.0, 69.7, 50.6; HRMS (ESI): $C_{17}H_{21}N_5O_3S$(M+1) calculated: 490.1303, found 490.1766

.

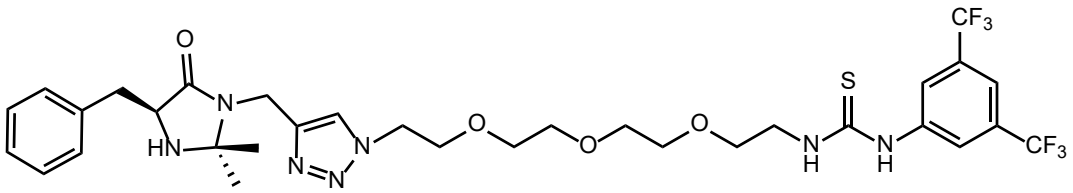

(S)-1-(2-(2-(2-(2-(4-((4-benzyl-2,2-dimethyl-5-oxoimidazolidin-1-yl)methyl)-1H-1,2,3-triazol-1-yl)ethoxy)ethoxy)ethoxy)ethyl)-3-(3,5-bis(trifluoromethyl)phenyl)thiourea was synthesized as follows: 1-(2-(2-(2-(2-azidoethoxy)ethoxy)ethoxy)ethyl)-3-(3,5-bis(trifluoromethyl)phenyl)thiourea (48 mg, 0.1 mmol, 1eq) was added to 20 mL of 20% piperidine in dry DCM. Sodium ascorbate (100 mg, 0.5 mmol, 5 eq), CuI (80 mg, 0.5 mmol, 5 eq); and (S)-5-benzyl-2,2-dimethyl-3-(prop-2-yn-1-yl)imidazolidin-4-one (48 mg, 0.2 mmol, 2 eq) were then added and the reaction was stirred at room temperature under inert atmosphere for 18 hours. The solvent was removed under reduced pressure and the crude product was purified over silica (9:1 DCM:MeOH with 1% ammonium hydroxide) to yield a clear oil. Rf = 0.43 (9:1 hexanes:EtOAc). IR(film): 3261, 3217, 2901, 1759, 1592, 1407, 1362; ^{1}H NMR ($CDCl_3$, 500 MHz) 8.04 (s, 1H), 7.75 (s, 1H), 7.62 (m, 6H), 7.48 (t, J=5.12 Hz, 1H), 7.34 (m, 4H), 4.41(s , 1H), 3.73 (m, 10H), 3.47 (m 3H) 3.31 (m, 5H), 1.69 (m, 5H), 1.42 (s, 3H), ^{13}C NMR ($CDCl_3$, 75 MHz): 182.2, 166.0, 141.7, 140.3, 134.1, 132.4, 131.9, 128.9, 128.8, 128.7, 127.7, 124.2, 123.2, 122.0, 117.5, 76.8, 72.4, 70.7, 70.6, 70.5, 70.4, 70.0, 69.9, 69.8, 69.7, 50.6, 25.1, 24.5, 24.2; HRMS (ESI): $C_{32}H_{39}F_6N_7O_4S$ ($M+NH_4$) calculated: 750.3060, found 750.3148.

2.14 Catalyst Loading and Low Diene Concentration Studies

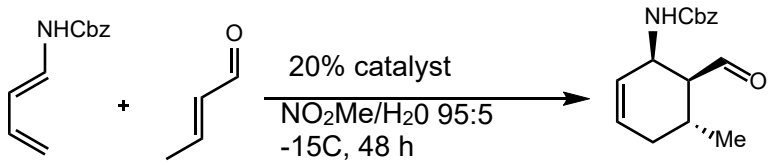

Diene concentration studies were performed according to the following procedure. All experiments were conducted in triplicate. As an example: benzyl (E)-buta-1,3-dien-1-ylcarbamate (2.03 mg, 10 mmol, 1 eq) and freshly distilled crotonaldehyde (3.1 μL, 30 mmol, 3 eq) were added to 1 mL 95:5 v/v nitromethane/water. **p2** (3.5 mg, 2 mmol, 0.2 eq) was added and dissolved by vortexing. The reactions were stirred at -15 ˚C for 48 h at which time a small aliquot of the reaction was diluted in 1 mL ethyl acetate and conversion determined via HRMS (ESI). Conversions for all other diene concentrations and catalysts are listed below in Table S2. Conversions in Table 2.3 represent the average of three independent runs.

Table 2.3 *Percent conversion at 48 hours*

mM diene	**1000**	**100**	**10**	**1**	**0.1**	**0.01**
No Catalyst	4.2	3.4	2.9	2.5	2.5	1.2
2	3.4	3.4	1.5	1.3	1.5	0.1
1	70.6	46.0	13.0	7.7	6.8	0.0
1 + p4	64.8	34.5	9.7	5.1	2.8	1.5
P3	16.7	6.7	4.4	3.8	0.5	0.5
p3 + 2	14.7	7.1	8.3	5.6	1.8	0.7
p3 + p4	17.1	7.6	4.5	3.3	2.9	0.6
p2	96.4	87.5	80.9	46.8	8.1	5.2

Table 2.4 *Concentration studies with peptide and non-peptide catalysts. % conversion at 48 hours.*

		1000	100	10	1	0.1	0.01	0.001
No Catalyst	**Reaction #**	**mM**	**mM**	**mM**	**mM**	**mM**	**mM**	**mM**
	1	4.9	3.3	2.7	4.2	2.6	1.9	0
	2	3.5	3.8	2.6	1.7	3.4	0.6	3.7
	3	4.2	3.1	3.4	1.5	1.4	1.2	5.8
	Average % Conversion	4.2	3.4	2.9	2.47	2.467	1.23333	3.166667
	Standard Error	0.7	0.3606	0.436	1.5	1.007	0.65064	2.936551

		1000	100	10	1	0.1	0.01	0.001
Catalyst 1	**Reaction #**	**mM**	**mM**	**mM**	**mM**	**mM**	**mM**	**mM**
	1	67.3	46.9	13	7.1	4.6	0	1.3
	2	72.2	45.3	13.2	7.4	8.2	0	1.6
	3	72.3	45.9	12.8	8.5	7.7	0	3.5
	Average % Conversion	70.6	46.033	13	7.67	6.833	0	2.133333
	Standard Error	2.85832	0.8083	0.2	0.74	1.95	0	1.193035

		1000	100	10	1	0.1	0.01	0.001
Catalyst 2	**Reaction #**	**mM**	**mM**	**mM**	**mM**	**mM**	**mM**	**mM**
	1	4.3	2.1	0.7	1.5	1	0	4.4
	2	2.6	3.8	2.3	1.6	3.5	0.2	2.6
	3	3.3	4.2	1.4	0.9	0	0	3.1
	Average % Conversion	3.4	3.3667	1.467	1.33	1.5	0.06667	3.366667
	Standard Error	0.8544	1.115	0.802	0.38	1.803	0.11547	0.929157

		1000	100	10	1	0.1	0.01	0.001
Catalyst p2	**Reaction #**	**mM**	**mM**	**mM**	**mM**	**mM**	**mM**	**mM**
	1	96.9	83.4	79.3	45.4	7.5	5.7	10.8

	2	95.3	89.9	83.4	48.7	10.3	4.7	9.7
	3	97.1	89.3	80.1	46.2	6.5	5.2	12.7
Average % Conversion		96.4333	87.533	80.93	46.8	8.1	5.2	11.06667
Standard Error		0.98658	3.5921	2.173	1.72	1.97	0.5	1.517674

Catalyst		**1000**	**100**	**10**	**1**	**0.1**	**0.01**	**0.001**
p3+2	**Reaction #**	**mM**	**mM**	**mM**	**mM**	**mM**	**mM**	**mM**
	1	16.4	7.4	7.7	5.6	0	0	3.9
	2	14.7	7.9	8.1	4.8	2.1	0.7	2.3
	3	13.1	6	9.2	6.5	3.3	1.4	0.6
Average % Conversion		14.7333	7.1	8.333	5.63	1.8	0.7	2.266667
Standard Error		1.65025	0.9849	0.777	0.85	1.67	0.7	1.650253

		1000	**100**	**10**	**1**	**0.1**	**0.01**	**0.001**
Catalyst 1+2	**Reaction #**	**mM**	**mM**	**mM**	**mM**	**mM**	**mM**	**mM**
	1	62.5	37.4	10.9	4.6	2.7	0.4	1.1
	2	66.6	36	8.6	4.2	3.4	0.8	3.1
	3	65.3	30.1	9.6	6.5	2.2	3.4	0
Average % Conversion		64.8	34.5	9.7	5.1	2.767	1.53333	1.4
Standard Deviation		2.09523	3.8743	1.153	1.23	0.603	1.62891	1.571623

Catalyst		**1000**	**100**	**10**	**1**	**0.1**	**0.01**	**0.001**
p3+p4	**Reaction #**	**mM**	**mM**	**mM**	**mM**	**mM**	**mM**	**mM**
	1	18.5	6.4	2.4	1.4	3.7	0.1	3.7
	2	17.2	7.9	1.4	4.2	2.6	0	2.9
	3	15.6	8.4	9.7	4.3	2.5	1.6	2.1
Average % Conversion		17.1	7.5667	4.5	3.3	2.933	0.56667	2.9
Standard Error		1.45258	1.0408	4.531	1.65	0.666	0.89629	0.8

Catalyst p3	Reaction #	1000 mM	100 mM	10 mM	1 mM	0.1 mM	0.01 mM	0.001 mM
	1	15.2	5.4	4.8	2.1	2.3	0.9	2.3
	2	14.5	6.9	3.2	2.3	1.7	1.4	3
	3	16.7	6.7	4.4	3.8	0.5	0.5	1.3
Average % Conversion		15.4667	6.3333	4.133	2.73	1.5	0.93333	2.2
Standard Error		1.12398	0.8145	0.833	0.93	0.917	0.45092	0.8544

2.15 Analytical HPLC Traces and Mass Spectra of 11-mer Catalysts

All analytical HPLC experiments were performed with a Vydac C18 monomeric analytical column. Traces were run on a reverse phase gradient in H_2O/MeCN with 0.1% v/v TFA. Each run had a 40 minute ramp from 90:10 H_2O/MeCN to 5:95 H_2O/MeCN. The raw data was exported to excel for graphing and analysis.

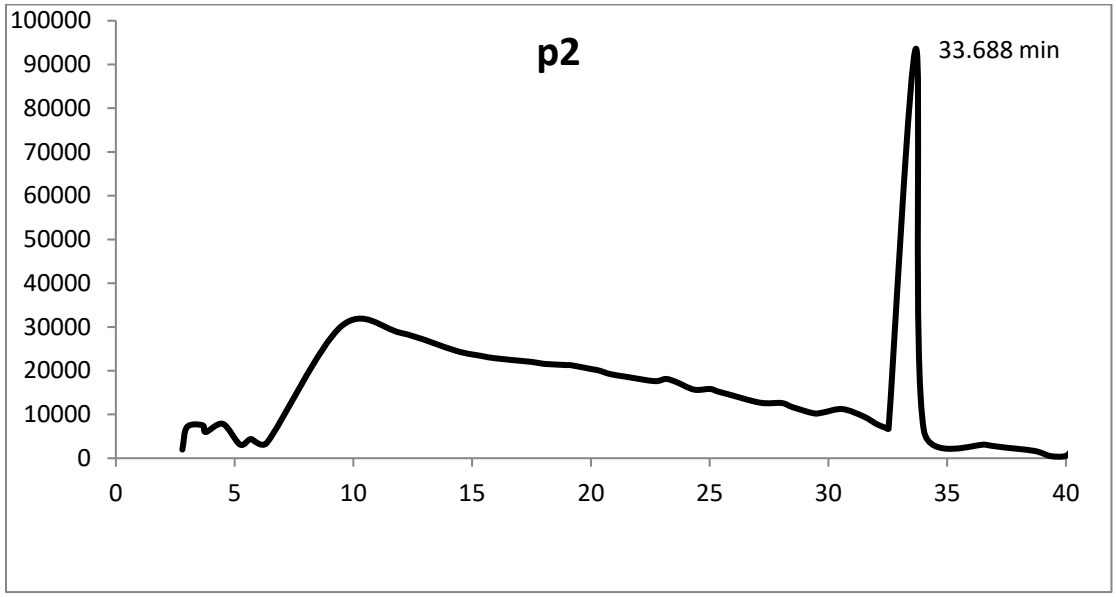

HRMS (ESI): $C_{84}H_{130}F_6N_{18}O_{15}$ (M+NH_4+Na)/2 calculated: 900.0510, found 900.0547.

Yield: 254mg, 72%

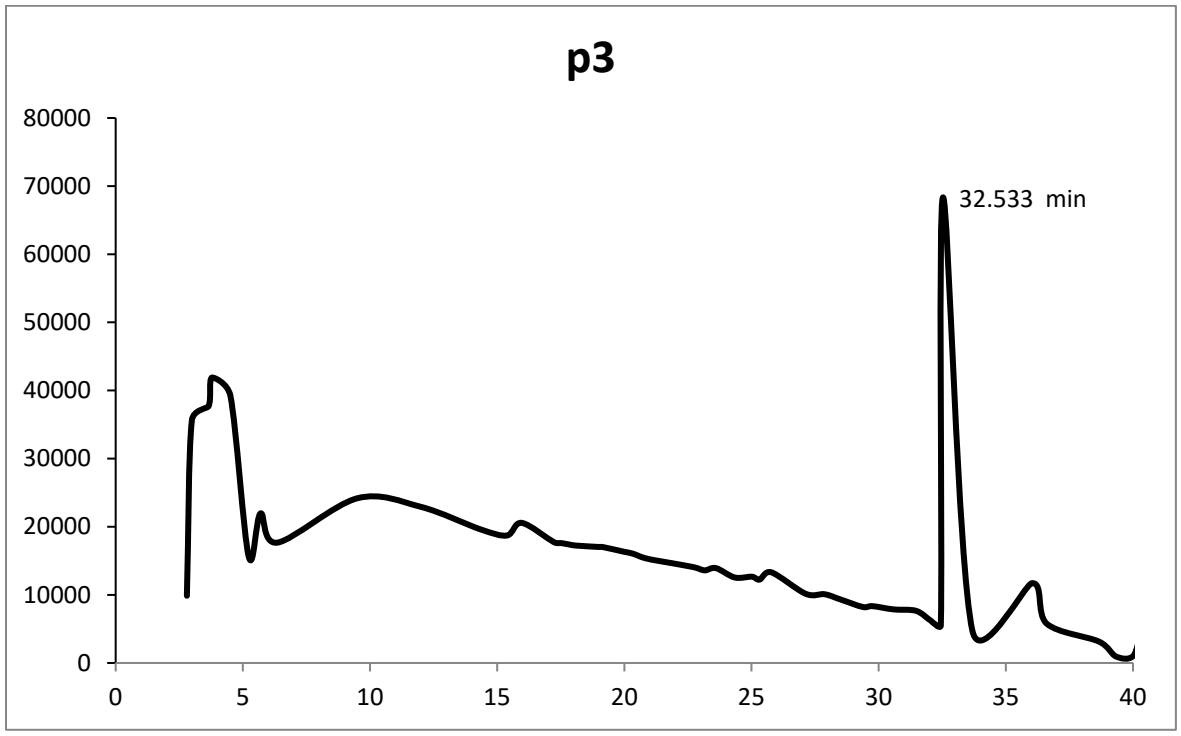

HRMS (ESI): $C_{72}H_{120}N_{16}O_{14}$ (M+NH_4+Na)/2 calculated: 744.4784, found 744.4771.

Yield: 225mg, 77%

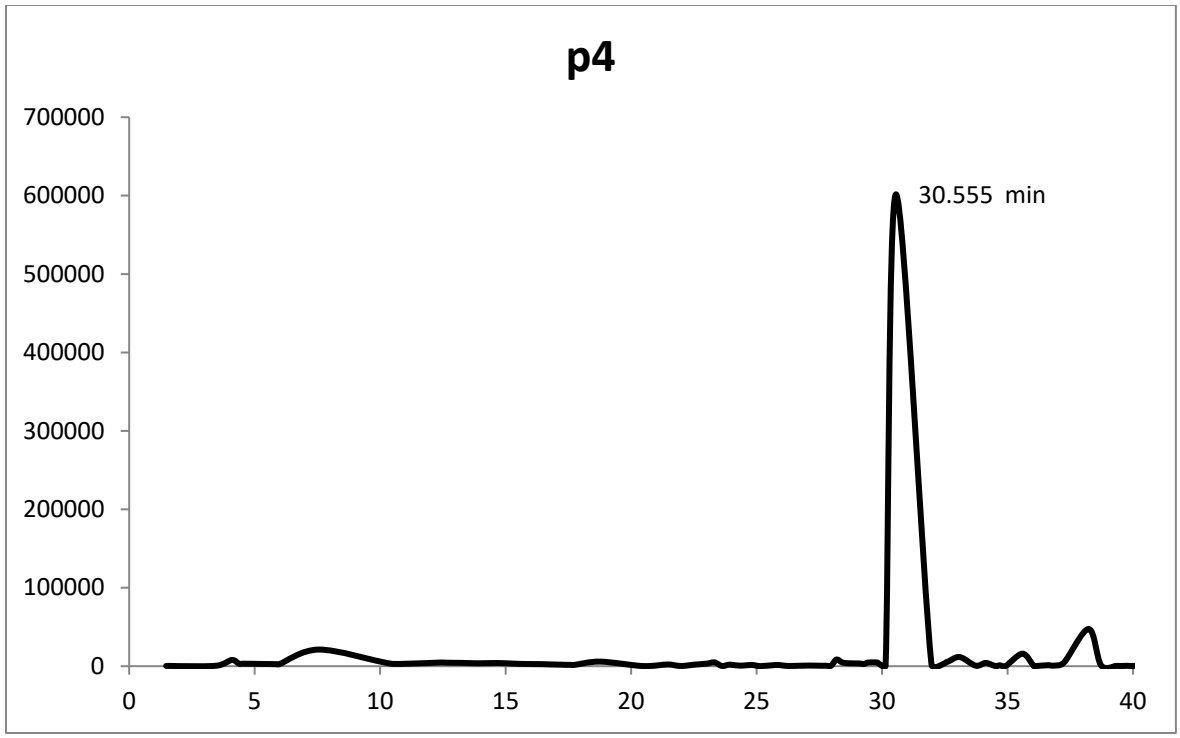

HRMS (ESI): $C_{65}H_{106}F_6N_{14}O_{13}$ (M+1) calculated: 1405.7968, found 1404.7915.

Yield: 120mg, 43%

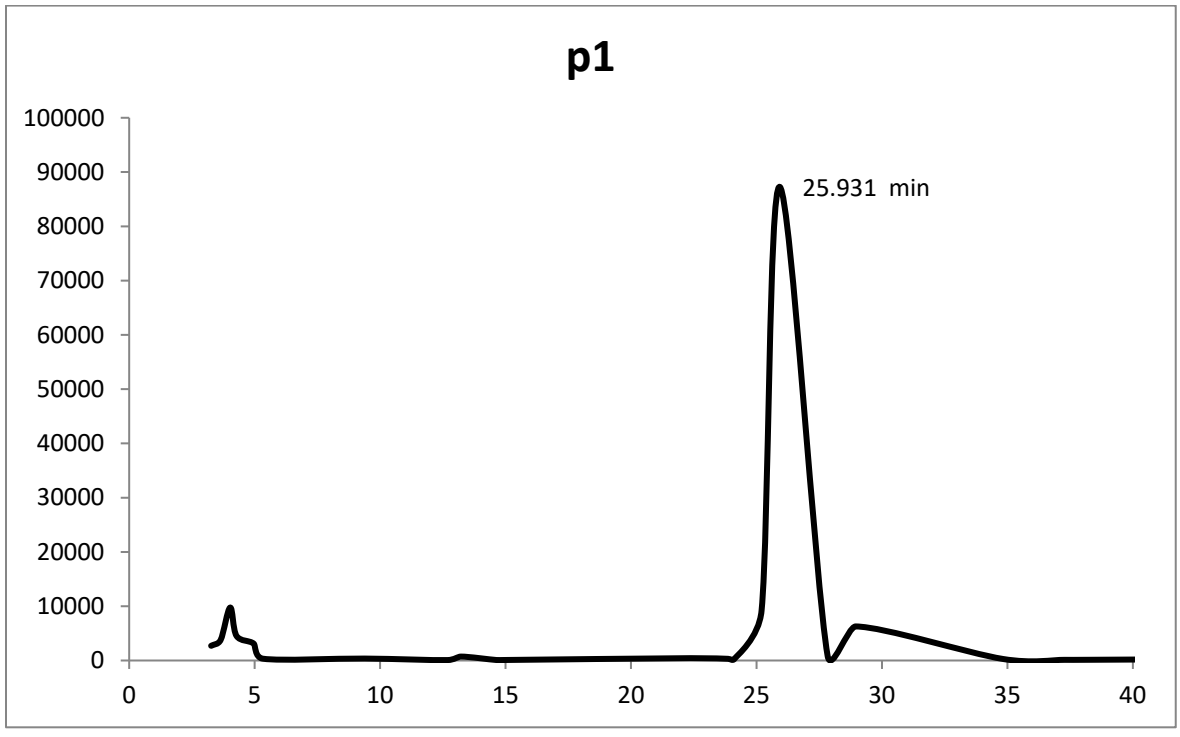

HRMS (ESI): $C_{53}H_{96}N_{12}O_{12}$ (M+1) calculated: 1093.7304, found 1093.7296.

Yield: 137mg, 63%

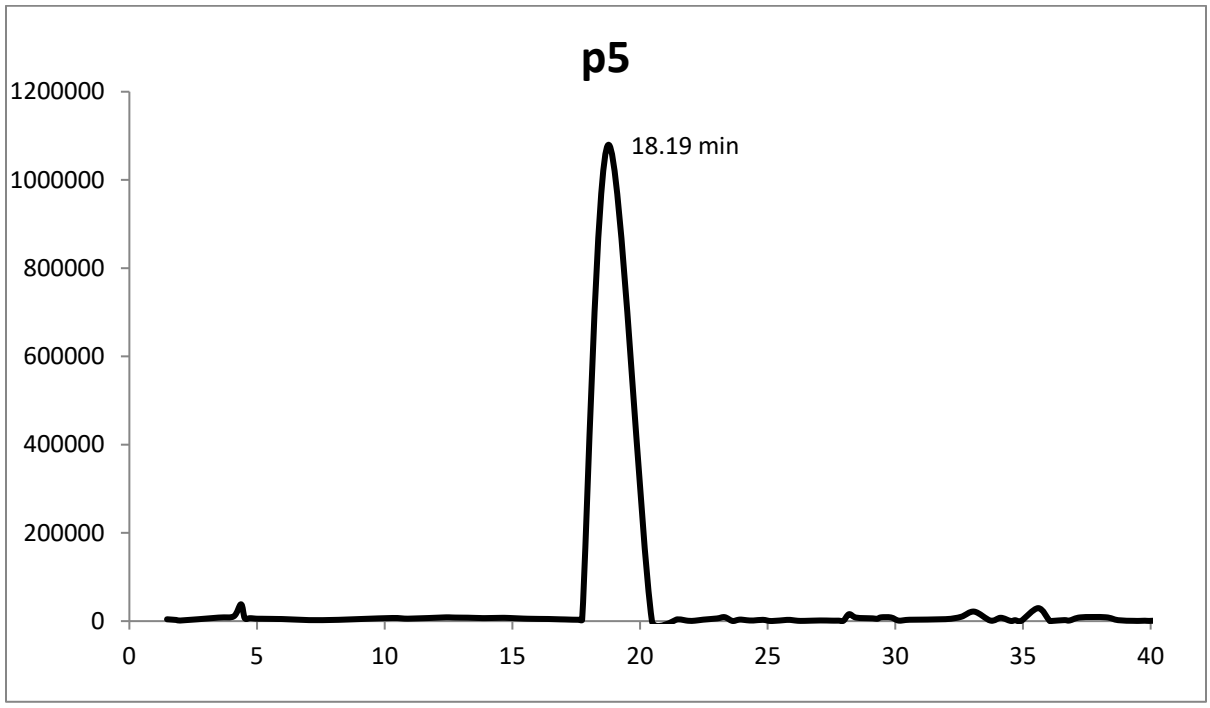

HRMS (ESI): $C_{86}H_{130}F_6N_{18}O_{15}$ ($M+NH_4+MeNH_4$)/2 calculated: 908.5356, found 908.5631.

Yield: 74mg, 21%

2.16 Chiral Separation and ee Determination

Catalytic reaction with 0.1 mol% p2

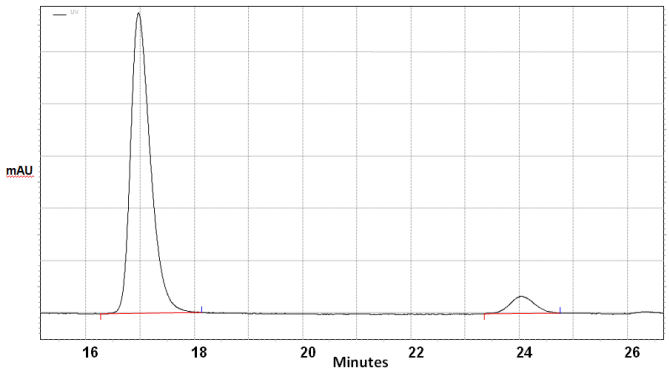

UV Results λ256nm

Retention Time	**Peak Area**	**Peak Height**
16.97	584106	23005
24.03	42600	1312
Totals	607626	71342
ee	**89.12**	

Catalyst 1 ee

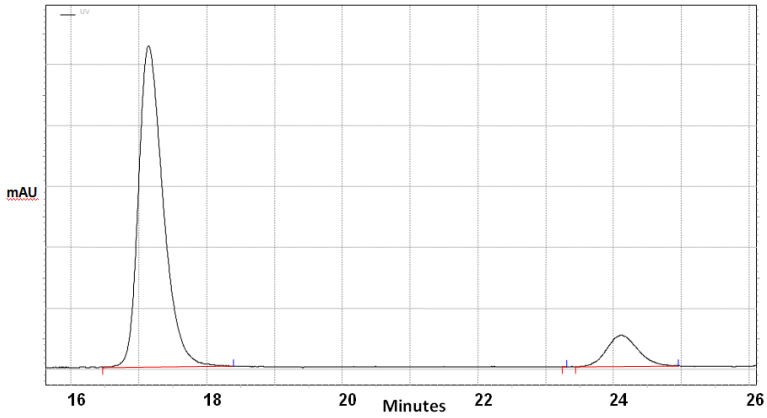

UV Results λ256nm

Retention Time	Peak Area	Peak Height
17.14	531647	21080
24.10	66484	2058
Totals	598131	23138
ee	**77.77**	

Racemic

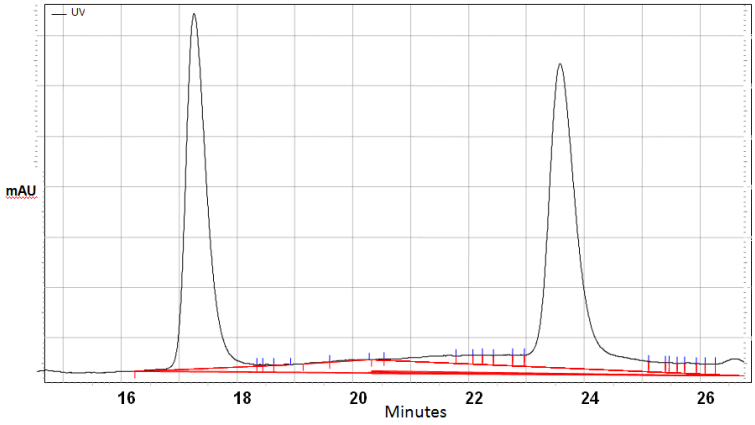

UV Results λ256nm

Retention Time	Peak Area	Peak Height
17.393	710438	375936
23.717	735766	347213
Totals	1436204	723149
ee	**1.7**	

2.17 Circular Dichroism

Samples were prepared by dissolving 10 mmol of catalyst in 1 mL of trifluoroethanol (TFE). The instrument was unable to tolerate samples dissolved in nitromethane, however 2D NMR studies were conducted in deuterated nitromethane to confirm that the peptide scaffold remains helical. Scans were taken from 195-260nm. A blank sample of HPLC grade TFE was taken in the same sample cuvette in order to determine background absorbance of the solvent and cuvette. After running each sample, the raw data was extracted to Excel for data analysis. The following equation was used to give the values at each wavelength shown below in Figure 2.13:

((sample-blank)/(1000*5E-07dmole cm^{-3}*path length (0.1cm)*# of amino acid residues))/1000

Units: **[θ] / deg·cm2·dmol-1 × 10-3**

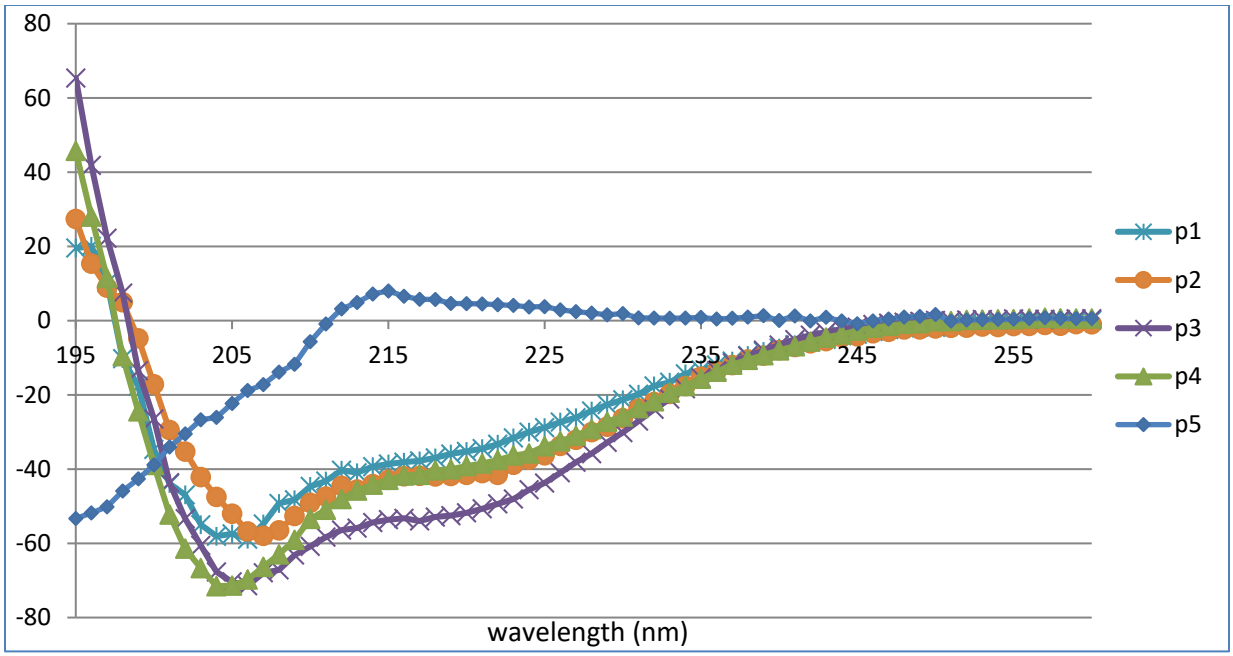

Figure 2.13 Cicular Dichoism Graphs for 11-mer Peptide Catalysts

2.18 NOE NMR Experiments

The NMR sample for **p2** was prepared at 4 mM peptide concentration in 700 µL deuterated nitromethane. One drop of TFA was added to enhance resolution. The sample was transferred to a Varian 500 MHz magnet and data was collected using vnmrJ software. 2D TOCSY experiments were collected with 8 scans, 400 t1 increments, and 80 ms mixing time. 2D adiabatic ROESY experiments were collected with 64 scans, 256 t1 increments, and 400 ms mixing time. Data was processed using vnmrJ followed by ccpNMR software. The 2D TOCSY and ROESY spectra for **p2** are shown in Figure 2.18. Summaries of assignments and correlations are shown in tables 2.5-2.7 according to the residue and proton descriptions presented in Figure 2.19. A summary of the observed non-sequential and sequential NOEs for **p2** appears in Figures 2.16–2.17.

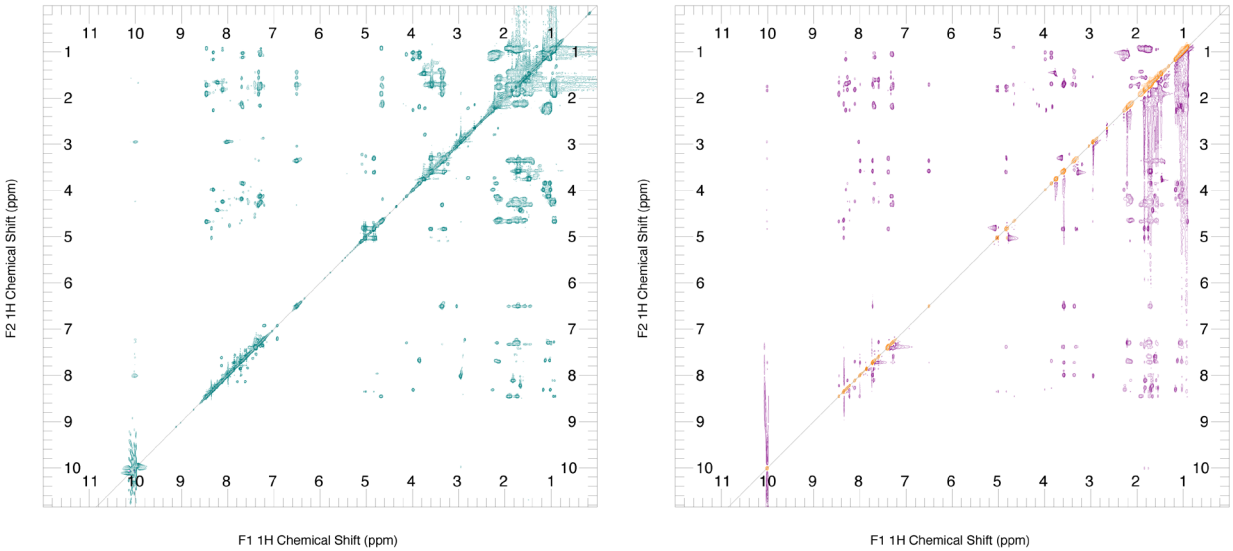

Figure 2.14. NMR Data for **p2**. 2D TOCSY data (left), 2D ROESY data (right).

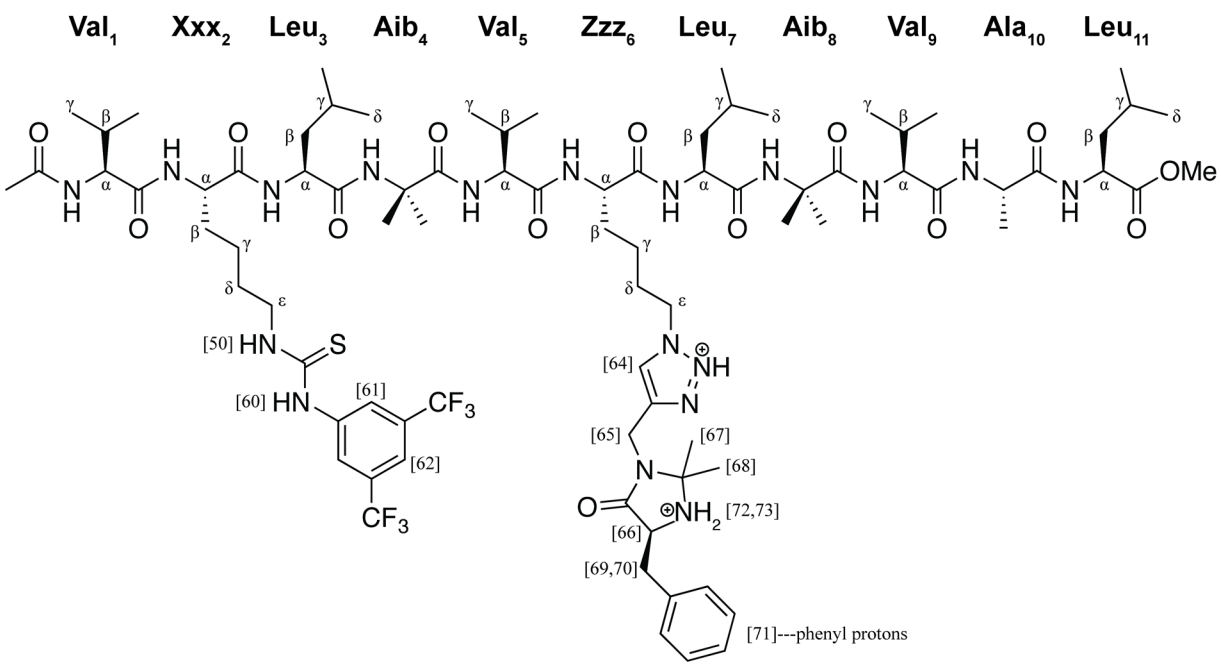

Figure 2.15 Protons within 4 mM solution of **p2** in nitromethane.

Table 2.5. *TOCSY correlations for p2.*[a]

δ (ppm) F1	Assignment F1	δ (ppm) F2	Assignment F2	δ (ppm) F1	Assignment F1	δ (ppm) F2	Assignment F2
7.29983	1ValH	4.12716	1ValHα	7.70237	6ZzzH	4.18333	6ZzzHα
7.29995	1ValH	2.16689	1ValHβ	7.70254	6ZzzH	2.13285	6ZzzHβa
7.29862	1ValH	1.05221	1ValHγa	7.70288	6ZzzH	1.7598	6ZzzHδa
4.13477	1ValHα	1.05724	1ValHγa	7.70253	6ZzzH	4.64595	6ZzzHεa
6.50267	2Xxx[50]	3.04197	2Xxx[51]	7.70183	6ZzzH	1.57322	6ZzzHγa
6.50195	2Xxx[50]	1.79929	2XxxHβa	4.64562	6ZzzHεa	2.13156	6ZzzHβa
6.50728	2Xxx[50]	1.91405	2XxxHβb	4.64844	6ZzzHεa	1.57751	6ZzzHγa
6.50596	2Xxx[50]	1.71676	2XxxHδa	8.11467	7LeuH	1.82389	7Leu(Hγ/Hβa)
6.50552	2Xxx[50]	3.35922	2XxxHεa	8.1142	7LeuH	4.24162	7LeuHα
6.50627	2Xxx[50]	1.44268	2XxxHγa	8.11636	7LeuH	0.9204	7LeuHδa
6.50676	2Xxx[50]	1.56154	2XxxHγb	8.11531	7LeuH	0.97236	7LeuHδb
7.72525	2Xxx[61]	7.72378	2Xxx[61]	8.31499	9ValH	3.98603	9ValHα
7.72529	2Xxx[61]	7.85772	2Xxx[62]	8.31478	9ValH	2.26691	9ValHβ
7.85899	2Xxx[62]	7.72415	2Xxx[61]	8.31555	9ValH	1.01617	9ValHγa
7.85919	2Xxx[62]	7.85821	2Xxx[62]	8.31552	9ValH	1.16594	9ValHγb
7.33002	2XxxH	4.31386	2XxxHα	3.99295	9ValHα	2.25917	9ValHβ
7.33033	2XxxH	1.79948	2XxxHβa	8.22403	10AlaH	4.42771	10AlaHα
7.33081	2XxxH	1.91127	2XxxHβb	8.22405	10AlaH	1.66793	10AlaHβ
7.32919	2XxxH	1.71624	2XxxHδa	8.45885	11LeuH	4.67746	11LeuHα
7.32892	2XxxH	3.35595	2XxxHεa	8.45894	11LeuH	1.91046	11LeuHβa
7.33112	2XxxH	1.44295	2XxxHγa	8.45874	11LeuH	0.91045	11LeuHδa
7.33034	2XxxH	1.55794	2XxxHγb	8.45876	11LeuH	0.94202	11LeuHδb
3.35852	2XxxHεa	4.31529	2XxxHα	8.45936	11LeuH	1.72381	11LeuHγ
3.35766	2XxxHεa	1.79765	2XxxHβa	4.67931	11LeuHα	1.91164	11LeuHβa
3.35724	2XxxHεa	1.90908	2XxxHβb	4.67704	11LeuHα	0.90781	11LeuHδa
3.35776	2XxxHεa	1.71186	2XxxHδa	4.6783	11LeuHα	0.93583	11LeuHδb
3.35744	2XxxHεa	1.4409	2XxxHγa	4.6653	11LeuHα	1.72736	11LeuHγ
3.35751	2XxxHεa	1.55665	2XxxHγb				
7.28349	3LeuH	1.71884	3Leu(Hβa/Hγ)				
7.28331	3LeuH	4.25183	3LeuHα				
7.28271	3LeuH	0.9298	3LeuHδa				
7.2829	3LeuH	0.99941	3LeuHδb				
7.6798	5ValH	3.85183	5ValHα				
7.68127	5ValH	2.1915	5ValHβ				
7.67963	5ValH	1.0283	5ValHγa				
7.68002	5ValH	1.12333	5ValHγb				
3.85506	5ValHα	2.18786	5ValHβ				
8.35251	6Zzz[64]	8.35128	6Zzz[64]				
8.35215	6Zzz[64]	5.01496	6Zzz[65]				
8.35291	6Zzz[64]	4.82636	6Zzz[66]				
3.61988	6Zzz[69]	4.82759	6Zzz[66]				
3.58766	6Zzz[69]	4.83017	6Zzz[66]				
3.33425	6Zzz[70]	4.83427	6Zzz[66]				
3.31485	6Zzz[70]	4.83044	6Zzz[66]				
7.38736	6Zzz[71]	7.386	6Zzz[71]				

[a]Assignments made based on 2D ^{1}H NMR TOCSY and ROESY experiments on a 4mM solution of **p2** in nitromethane at room temperature using a 500 MHz Varian INOVA spectrometer.

Table 2.6. *Intra-residue NOE assignments for p2.*[a]

δ (ppm) F1	Assign. F1	δ (ppm) F2	Assign. F2	Volume	δ (ppm) F1	Assign. F1	δ (ppm) F2	Assign. F2	Volume
7.29408	1ValH	4.12633	1ValHa	1.4E+05	4.83696	6Zzz[66]	1.75438	6Zzz[67]	3.0E+05
7.29319	1ValH	1.05843	1ValHγa	2.8E+05	4.80134	6Zzz[66]	1.75374	6Zzz[67]	8.6E+04
4.11893	1ValHα	2.16263	1ValHβ	1.0E+05	4.83596	6Zzz[66]	1.84493	6Zzz[68]	1.2E+05
2.1638	1ValHβ	7.29822	1ValH	1.3E+05	4.79937	6Zzz[66]	1.84493	6Zzz[68]	5.0E+04
6.50503	2Xxx[50]	1.70985	2XxxHδa	1.3E+05	4.84734	6Zzz[66]	3.59666	6Zzz[69]	1.4E+05
6.507	2Xxx[50]	3.3585	2XxxHεa	2.2E+05	4.82967	6Zzz[66]	3.30341	6Zzz[70]	2.5E+05
7.99611	2Xxx[60]	7.72392	2Xxx61]	1.8E+05	4.83828	6Zzz[66]	7.385	6Zzz[71]	9.0E+04
7.99491	2Xxx[60]	1.70647	2XxxHδa	5.8E+04	1.75352	6Zzz[67]	8.35283	6Zzz[64]	5.2E+04
7.99453	2Xxx[60]	3.35886	2XxxHεa	2.3E+05	1.75476	6Zzz[67]	5.01606	6Zzz[65]	1.3E+05
7.72539	2Xxx[61]	6.49952	2Xxx[50]	8.0E+04	1.75488	6Zzz[67]	4.82512	6Zzz[66]	5.6E+05
7.72546	2Xxx[61]	7.9917	2Xxx[60]	4.3E+05	1.84	6Zzz[68]	8.34818	6Zzz[64]	6.4E+04
7.72477	2Xxx[61]	1.70492	2XxxHδa	2.6E+05	1.84147	6Zzz[68]	5.01998	6Zzz[65]	1.9E+05
7.72506	2Xxx[61]	3.35727	2XxxHεa	2.2E+05	1.84192	6Zzz[68]	4.81959	6Zzz[66]	2.6E+05
7.72365	2Xxx[61]	1.44886	2XxxHγa	2.4E+04	3.61984	6Zzz[69]	7.38386	6Zzz[71]	8.5E+04
7.32824	2XxxH	4.30805	2XxxHα	1.2E+05	3.58462	6Zzz[69]	7.38439	6Zzz[71]	1.1E+05
7.327	2XxxH	1.79673	2XxxHβa	1.7E+05	3.33415	6Zzz[70]	7.38346	6Zzz[71]	7.9E+04
7.32688	2XxxH	1.44483	2XxxHγa	6.2E+04	7.38463	6Zzz[71]	4.83078	6Zzz[66]	1.7E+05
7.32729	2XxxH	1.55536	2XxxHγb	9.7E+04	7.39388	6Zzz[71]	1.8386	6Zzz[68]	4.2E+04
1.69774	2XxxHδa	7.99616	2Xxx[60]	7.1E+04	7.38462	6Zzz[71]	3.59894	6Zzz[69]	1.9E+05
1.7119	2XxxHδa	7.71721	2Xxx[61]	1.3E+05	7.38428	6Zzz[71]	3.30757	6Zzz[70]	2.3E+05
3.36016	2XxxHεa	7.99307	2Xxx[60]	1.4E+05	10.01005	6Zzz[72]	1.7505	6Zzz[67]	8.9E+04
3.36059	2XxxHεa	7.72496	2Xxx[61]	7.3E+04	10.00985	6Zzz[72]	1.84156	6Zzz[68]	1.0E+05
3.36372	2XxxHεa	1.43282	2XxxHγa	1.2E+05	10.06708	6Zzz[73]	7.38618	6Zzz[71]	5.9E+04
3.34385	2XxxHεa	1.56061	2XxxHγb	7.8E+04	7.70406	6ZzzH	4.18115	6ZzzHα	9.6E+04
7.59536	4AibH	1.61234	4AibHβ	5.0E+05	7.70212	6ZzzH	2.13611	6ZzzHβa	3.1E+05
1.61856	4AibHβ	7.59728	4AibH	3.9E+05	7.70346	6ZzzH	1.75873	6ZzzHδa	7.7E+04
7.68648	5ValH	3.84989	5ValHα	9.6E+04	4.17157	6ZzzHα	2.12749	6ZzzHβa	5.4E+04
7.68046	5ValH	2.18356	5ValHβ	2.6E+05	2.13858	6ZzzHβa	8.34907	6Zzz[64]	4.4E+04
7.68041	5ValH	1.02864	5ValHγa	8.5E+04	2.13806	6ZzzHβa	7.69887	6ZzzH	1.7E+05
7.67738	5ValH	1.12109	5ValHγb	2.2E+05	8.11015	7LeuH	1.82083	7Leu(Hβa/Hγ)	3.1E+05
3.85497	5ValHα	1.02583	5ValHγa	2.2E+05	8.10855	7LeuH	4.24103	7LeuHα	9.1E+04
3.85422	5ValHα	1.12151	5ValHγb	2.4E+05	4.2455	7LeuHα	1.81818	7Leu(Hβa/Hγ)	5.6E+04
2.18633	5ValHβ	7.68501	5ValH	1.6E+05	8.01067	8AibH	1.54207	8AibHβ	3.8E+04
1.12548	5ValHγb	7.67939	5ValH	2.1E+05	1.54329	8AibHβ	8.01084	8AibH	4.7E+04
8.3495	6Zzz[64]	5.0217	6Zzz[65]	1.0E+05	8.30769	9ValH	2.2611	9ValHβ	2.1E+05
8.35027	6Zzz[64]	4.81915	6Zzz[66]	1.1E+05	8.30742	9ValH	1.01536	9ValHγa	5.1E+04
8.35023	6Zzz[64]	1.74643	6Zzz[67]	5.7E+04	8.30778	9ValH	1.16345	9ValHγb	2.1E+05
8.34922	6Zzz[64]	1.84248	6Zzz[68]	6.2E+04	3.99717	9ValHα	8.30738	9ValH	4.3E+04
8.34934	6Zzz[64]	2.13079	6ZzzHba	1.2E+05	3.99292	9ValHα	1.01315	9ValHγa	1.1E+05
8.34954	6Zzz[64]	4.64278	6ZzzHea	3.2E+05	3.99149	9ValHα	1.16234	9ValHγb	1.2E+05
5.04529	6Zzz[65]	8.35021	6Zzz[64]	3.9E+04	1.16774	9ValHγb	8.30487	9ValH	2.1E+05
5.00867	6Zzz[65]	8.34895	6Zzz[64]	5.5E+04	8.22353	10AlaH	4.42448	10AlaHα	8.5E+04
5.04123	6Zzz[65]	1.75214	6Zzz[67]	7.1E+04	8.22433	10AlaH	1.66439	10AlaHγ	2.7E+05
5.00926	6Zzz[65]	1.75295	6Zzz[67]	1.1E+05	8.46066	11LeuH	4.67046	11LeuHα	1.1E+05
5.04414	6Zzz[65]	1.8431	6Zzz[68]	8.6E+04	8.4552	11LeuH	1.91266	11LeuHβa	2.6E+05
5.00877	6Zzz[65]	1.84165	6Zzz[68]	1.3E+05	4.67677	11LeuHα	0.90441	11LeuHδa	9.7E+04
4.83326	6Zzz[66]	8.34715	6Zzz[64]	4.0E+04	1.90463	11LeuHβa	8.45179	11LeuH	1.2E+05

[a]Assignments made based on 2D ^{1}H NMR TOCSY and ROESY experiments on 4mM solution of **p2** in nitromethane at room temperature using a 500 MHz Varian INOVA spectrometer.

Table 2.7. *Sequential NOE assignments for p2.*

δ (ppm) F1	Assign. F1	δ (ppm) F2	Assign. F2	Volume
7.32665	2LysH	4.12517	1ValHα	1.8E+05
7.28271	3LeuH	4.30579	2LysHα	1.4E+05
7.28246	3LeuH	7.59553	4AibH	1.7E+05
1.71929	3LeuHγ	7.59642	4AibH	8.3E+04
7.59568	4AibH	7.27975	3LeuH	1.4E+05
7.59565	4AibH	4.24789	3LeuHα	6.4E+04
1.61882	4AibHβ	7.67683	5ValH	2.4E+05
7.67697	5ValH	1.61408	4AibHβ	2.5E+05
7.70564	6ZzzH	8.10589	7LeuH	1.0E+05
2.13783	6ZzzHβa	8.10748	7LeuH	5.9E+04
1.58714	6ZzzHγa	8.10185	7LeuH	7.1E+04
8.11025	7LeuH	7.69968	6ZzzH	9.3E+04
8.11	7LeuH	2.13037	6ZzzHβa	9.8E+04
8.11155	7LeuH	1.58503	6ZzzHγa	5.4E+04
2.26147	9ValHβ	8.2194	10AlaH	5.5E+04
8.22746	10AlaH	8.45409	11LeuH	1.2E+05
8.23103	10AlaH	8.30418	9ValH	1.6E+05
8.22193	10AlaH	3.9826	9ValHα	2.5E+04
8.22373	10AlaH	2.26235	9ValHβ	8.8E+04
1.66519	10AlaHβ	8.45469	11LeuH	1.1E+05
8.45642	11LeuH	8.22497	10AlaH	8.8E+04
8.45492	11LeuH	4.4211	10AlaHα	2.7E+04
8.45525	11LeuH	1.66337	10AlaHβ	1.1E+05

[a]Assignments made based on 2D ^{1}H NMR TOCSY and ROESY experiments on a 4mM solution of **p2** in nitromethane at room temperature using a 500 MHz Varian INOVA spectrometer.

Table 2.8 *Non-sequential NOE assignments for p2.*

δ (ppm) F1	Assign. F1	δ (ppm) F2	Assign. F2	Volume	contact
7.29324	1ValH	2.20254	5ValHβ	3.2E+05	*i* to *i*+4
6.50493	2Xxx[50]	3.58111	6Zzz[69]	3.9E+05	*i* to *i*+4
7.99441	2Xxx[60]	3.58001	6Zzz[69]	3.3E+05	*i* to *i*+4
7.72476	2Xxx[61]	3.58153	6Zzz[69]	3.5E+05	*i* to *i*+4
1.69696	2XxxHδa	3.84819	5ValHα	4.2E+05	*i* to *i*+3
7.27317	3LeuH	1.587	6ZzzHγa	4.5E+04	*i* to *i*+3
0.93165	3LeuHδa	8.35426	6Zzz[64]	5.3E+04	*i* to *i*+3
7.595	4AibH	4.13023	1ValHα	3.6E+04	*i* to *i*+4
7.59386	4AibH	1.76189	6ZzzHδa	9.7E+04	*i* to *i*+2
1.61836	4AibHβ	4.12554	1ValHα	2.4E+05	*i* to *i*+
3.85306	5ValHα	1.69549	2XxxHδa	2.5E+05	*i* to *i*+3
1.02547	5ValHγa	8.30347	9ValH	7.4E+04	*i* to *i*+4
1.1244	5ValHγb	4.3107	2XxxHα	6.9E+04	*i* to *i*+3
3.58285	6Zzz[69]	6.50367	2Xxx[50]	5.2E+05	*i* to *i*+4
3.5826	6Zzz[69]	7.99268	2Xxx[60]	3.0E+05	*i* to *i*+4
3.58267	6Zzz[69]	7.72467	2Xxx[61]	1.6E+05	*i* to *i*+4
8.00347	8AibH	8.45397	11LeuH	8.4E+04	*i* to *i*+3
8.01058	8AibH	4.67036	11LeuHα	3.4E+04	*i* to *i*+3
8.01406	8AibH	1.90124	11LeuHβa	2.1E+04	*i* to *i*+3
1.54585	8AibHβ	8.45191	11LeuH	6.1E+04	*i* to *i*+3
1.16776	9ValHγb	4.17714	6ZzzHα	9.1E+04	*i* to *i*+3
8.22758	10AlaH	4.65127	6ZzzHεa	4.4E+04	*i* to *i*+4
8.22343	10AlaH	4.24217	7LeuHα	4.8E+04	*i* to *i*+3
8.45683	11LeuH	8.00942	8AlaH	5.0E+04	*i* to *i*+3
8.45438	11LeuH	1.54523	8AlaHβ	5.3E+04	*i* to *i*+3
4.66857	11LeuHα	2.13592	6ZzzHβa	6.0E+04	*i* to *i*+5

[a]Assignments made based on 2D ^{1}H NMR TOCSY and ROESY experiments on a 4mM solution of **p2** in nitromethane at room temperature using a 500 MHz Varian INOVA spectrometer.

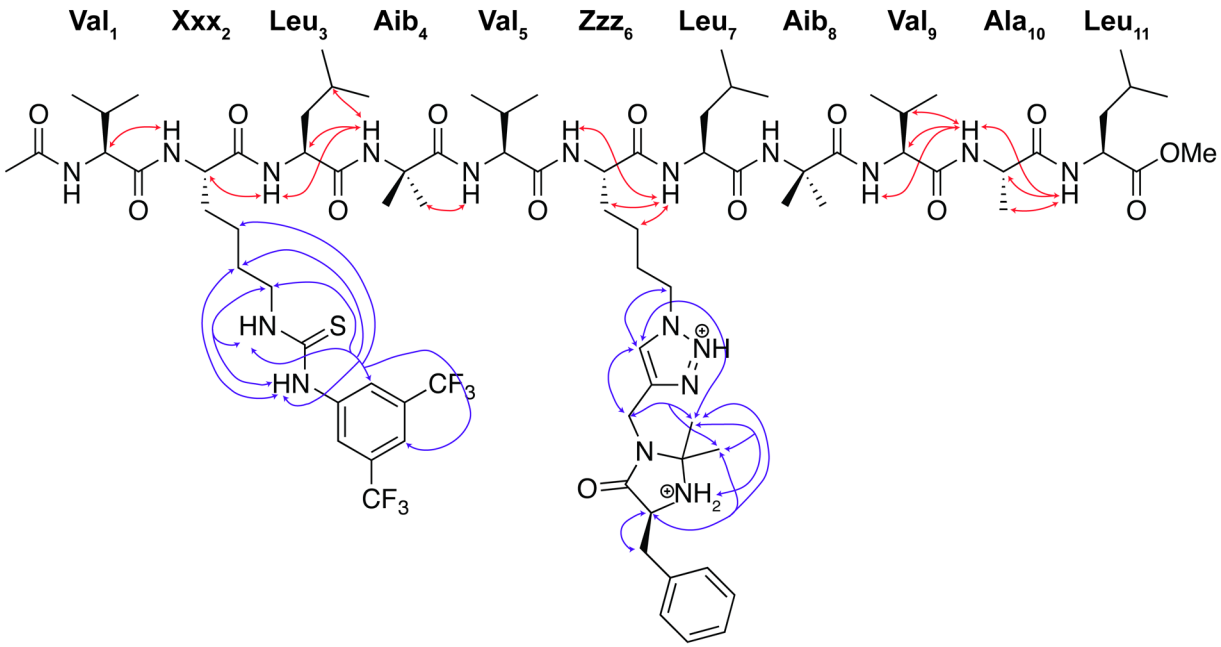

Figure 2.16. Observed sequential NOEs for 4 mM solution of **p2** in nitromethane.

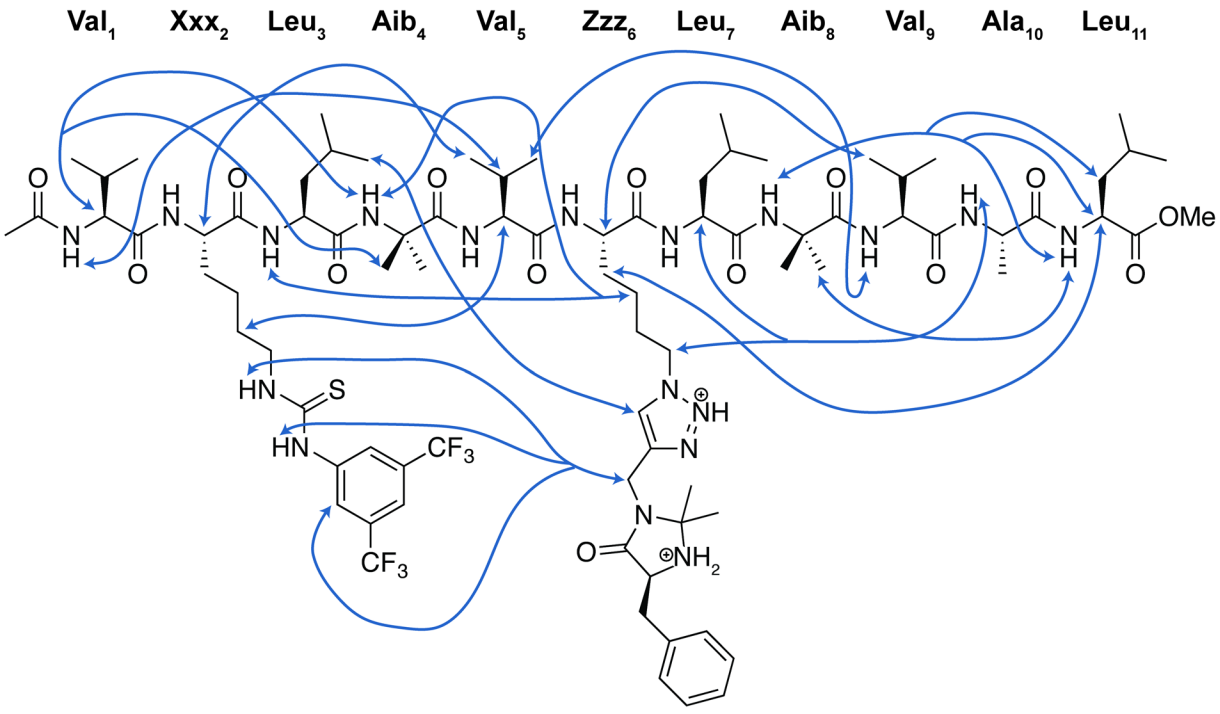

Figure 2.17. Observed non-sequential NOEs for 4 mM solution of **p2** in nitromethane.

2.19 References

1. Allen, A. E,; MacMillan, D. W. C. Synergistic catalysis: A powerful synthetic strategy for new reaction development. *Chem. Sci.* **2012** 3, 633

2. Inamdar, S. M,; Shinde, V. S,; Patil, N. T. Enantioselective cooperative catalysis. *Org. Biomol. Chem.* **2015** 13, 8116

3. Skubi, K. L,; Blum, T. R,; Yoon, T. P. Dual Catalysis Strategies in Photochemical Synthesis. *Chem. Rev.* **2016**, 116, 10035

4. Kaniraj, P. J,; Maayan, G. Metallopeptoids as efficient biomimetic catalysts. *Chem Commun.* **2015**, 51, 11096

5. Liu, Y.-L,; Zhou, J. Catalytic Asymmetric Strecker Reaction: Bifunctional Chiral Tertiary Amine/Hydrogen-Bond Donor Catalysis Joins the Field. *Synthesis* **2015**, 47, 1210

6. Alemán, J,; Parra, A,; Jiang, H,; Jørgensen, K. A. Squaramides: Bridging from Molecular Recognition to Bifunctional Organocatalysis. *Chem. Eur. J.* **2011**, 17, 6890

7. Mo, F,; Dong, G. C-H bond activation. Regioselective ketone α-alkylation with simple olefins via dual activation. *Science* **2014**, 345, 6

8. Goldys, A. M,; Dixon, D. J. Organocatalytic Ring-Opening Polymerization of Cyclic Esters Mediated by Highly Active Bifunctional Iminophosphorane Catalysts. *Macromolecules* **2014**, 47*,* 1277

9. Trost, B. M,; Bartlett, M. J. ProPhenol-Catalyzed Asymmetric Additions by Spontaneously Assembled Dinuclear Main Group Metal Complexes. *Acc. Chem. Res.* **2014**, 48, 68

10. Shibasaki, M,; Kanai, M,; Matsunaga, S,; Kumagai, N. Recent Progress in Asymmetric Bifunctional Catalysis Using Multimetallic Systems. *Acc. Chem. Res.* **2009**, 42, 1117

11. Huang, H,; Jacobsen, E. N. Highly Enantioselective Direct Conjugate Addition of Ketones to Nitroalkenes Promoted by A Chiral Primary Amine−Thiourea Catalyst. *J. Am. Chem. Soc.* **2006**, 128, 7170

12. Pleiss, J. in *Enzyme Catalysts in Organic Synthesis, 3rd Ed.* **2012**, (Eds. Drauz, K,; Gröger, H,; May, O.), Wiley-VCH Verlag GmbH & Co. pp. 89

13. Kiss, G,; Celebi-Oelcuem, N,; Moretti, R,; Baker, D,; Houk, K. N. Computational enzyme design. *Angew. Chem,; Int. Ed.* **2013**, 52, 5700

14. Hilvert, D. Design of protein catalysts. *Annu. Rev. Biochem.* **2013**, 82, 447

15 Renata, H,; Wang, Z. J,; Arnold, F. H. Expanding the Enzyme Universe: Accessing Non-Natural Reactions by Mechanism-Guided Directed Evolution. *Angew. Chem. Int. Ed.* **2015**, 54, 3351

16. Nair, N. U,; Denard, C. A,; Zhao, H. Engineering of enzymes for selective catalysis. *Curr. Org. Chem.* **2010**, 14, 1870

17. Tebo, A. G,; Pecoraro, V. L. Artificial metalloenzymes derived from three-helix bundles. *Curr. Opin. Chem. Biol.* **2015**, *25*, 65

18. Zastrow, M. L,; Pecoraro, V. L. Influence of Active Site Location on Catalytic Activity in de Novo-Designed Zinc Metalloenzymes. *J. Am. Chem. Soc.* **2013**, 135, 5895

19. Huang, Z.-Z,; Leman, L. J,; Ghadiri, M. R. Biomimetic Catalysis of Diketopiperazine and Dipeptide Syntheses. *Angew. Chem. Int. Ed.* **2008**, 47, 1758

20. Leman, L. J,; Weinberger, D. A,; Huang, Z.-Z,; Wilcoxen, K. M,; Ghadiri, M. R. Biomimetic Catalysis of Intermodular Aminoacyl Transfer. *J. Am. Chem. Soc*. **2007**, 129, 2959

21. Miller, S. J. In Search of Peptide-Based Catalysts for Asymmetric Organic Synthesis. *Acc. Chem. Res.* **2004**, 37, 601

22. Colby Davie, E. A,; Mennen, S. M,; Xu, Y,; Miller, S. Asymmetric Catalysis Mediated by Synthetic Peptides. J. *Chem. Rev.* **2007**, 107, 5759

23. Revell, J. D,; Wennemers, H. Peptidic catalysts developed by combinatorial screening methods. *Curr. Opin. Chem. Biol.* **2007** 11, 269

24. J. Duschmalé, Y. Arakawa, H. Wennemers, in *Science of Synthesis: Asymmetric Organocatalysis, Vol. 2* (Ed. Maruoka, K.), Georg Thieme Verlag, p. 741, **2012**

25. Müller, M. M,; Windsor, M. A,; Pomerantz, W. C,; Gellman, S. H,; Hilvert, D. A rationally designed aldolase foldamer. *Angew. Chem. Int. Ed.* **2009**, 48, 922

26. Mayer, C,; Müller, M. M,; Gellman, S. H,; Hilvert, D. Building proficient enzymes with foldamer prostheses. *Angew. Chem. Int. Ed.* **2014**, 53, 6978

27. Johnsson, K,; Allemann, R. K,; Widmer, H,; Benner, S. A. Synthesis, structure and activity of artificial, rationally designed catalytic polypeptides. *Nature* **1993**, 365, 530

28. Wang, P. S. P,; Schepartz, A. β-Peptide bundles: Design. Build. Analyze. Biosynthesize. *Chem. Commun.* **2016**, 52, 7420

29. Bezer, S,; Matsumoto, M,; Lodewyk, M. W,; Lee, S. J,; Tantillo, D. J,; Gagné, M. R,; Waters, M. L. Identification and optimization of short helical peptides with novel reactive functionality as catalysts for acyl transfer by reactive tagging. *Org. Biomol. Chem*. **2014**, 12, 1488

30. Razkin, J,; Nilsson, H,; Baltzer, L. Catalysis of the Cleavage of Uridine 3‘-2,2,2-Trichloroethylphosphate by a Designed Helix−Loop−Helix Motif Peptide. *J. Am. Chem. Soc.* **2007**, 129, 14752

31. Matsumoto, M,; Lee, S. J,; Waters, M. L,; Gagné, M. R. A Catalyst Selection Protocol That Identifies Biomimetic Motifs from β-Hairpin Libraries. *J. Am. Chem. Soc.* **2014**, 136, 15817

32. Blank, J. T,; Miller, S. J. Studies of folded peptide-based catalysts for asymmetric organic synthesis. *Biopolymers* **2006**, 84, 38

33. Agarkov, A,; Greenfield, S. J,; Ohishi, T,; Collibee, S. E,; Gilbertson, S. R. Catalysis with Phosphine-Containing Amino Acids in Various "Turn" Motifs. *J. Org. Chem.* **2004**, 69, 8077

34. Ball, Z. T. Designing Enzyme-like Catalysts: A Rhodium(II) Metallopeptide Case Study. *Acc. Chem. Res.* **2013**, 46*,* 560

35. Gilbertson, S. R,; Collibee, S. E,; Agarkov, A. Asymmetric Catalysis with Libraries of Palladium β-Turn Phosphine Complexes. *J. Am. Chem. Soc.* **2000**, 122, 6522

36. Lu, Y,; Yeung, N,; Sieracki, N,; Marshall, N. M. Design of functional metalloproteins. *Nature* **2009**, 460, 855

37. For computational design of a Diels-Alderase, see: Siegel, J. B,; Zanghellini, A,; Lovick, H. M,; Kiss, G,; Lambert, A. R,; St. Clair, J. L,; Gallaher, J. L,; Hilvert, D,; Gelb, M. H,; Stoddard, B. L,; Houk, K. N,; Michael, F. E,; Baker, D. Computational design of an enzyme catalyst for a stereoselective bimolecular Diels-Alder reaction. *Science* **2010**, 329, 309

38. Karle, I. L,; Flippen-Anderson, J. L,; Uma, K,; Balaram, P. Unfolding of an α-helix in peptide crystals by solvation: Conformational fragility in a heptapeptide. *Biopolymers* **1993**, 33, 827

39. Blackwell, H. E,; Grubbs, R. H. Ring-closing olefin metathesis as a highly efficient method for the synthesis of covalently cross-bridged peptides. *Angew. Chem. Int. Ed.* **1998**, 37, 3281

40. Pace, C. N,; Scholtz, J. M. A helix propensity scale based on experimental studies of peptides and proteins. *Biophys. J.* **1998**, 75, 422

41. Ahrendt, K. A,; Borths, C. J,; MacMillan, D. W. C. New Strategies for Organic Catalysis: The First Highly Enantioselective Organocatalytic Diels−Alder Reaction. *J. Am. Chem. Soc.* **2000**, 122, 4243–4244

42. Momiyama, N,; Funayama, K,; Noda, H,; Yamanaka, M,; Akasaka, N,; Ishida, S,; Iwamoto, T,; Terada, M. Hydrogen Bonds-Enabled Design of a C1-Symmetric Chiral Brønsted Acid Catalyst. *ACS Catal.* **2016**, 6, 94

43. Austin, J. F.; Kim, S. G.; Sinz, C. J,; Xiao, W. J,; MacMillan, D. W. C. Enantioselective organocatalytic construction of pyrroloindolines by a cascade addition–cyclization strategy: Synthesis of (–)-flustramine B. *Proc. Nat. Acad. Sci.* **2004**, 101, 5482

Chapter 3 Structure Optimization and Reaction Screening for Helical Peptide Catalysts

3.1 Introduction

Natural enzymes provide excellent spatial control for the specific placement of reactive functional groups, which can be tuned by altering side chains in or near the active site. We endeavored to apply this principle to bifunctional peptide catalysts by altering the inter-catalyst distance via side chain length optimization in order to optimize the rate of Diels-Alder cycloadditions and indole alkylations.[1,4] Thiourea and squaramide catalysts are also capable of generating a variety of electrophiles such as oxocarbenium and n-acyliminium cations via activation of acetal starting materials (Figure 3.1).[5] One of the principle limitations of these catalysts is that they require strong nucleophiles that often must be prepared beforehand. Silyl ketene acetals and TBS enol ethers are commonly used, however there are few examples of unactivated nucleophiles reacting with thiourea-activated substrates.

One question we desired to ask was whether placement of a MacMillan imidazolidinone catalyst near a thiourea catalyst on a peptide backbone could enable generation of a strong nucleophile in close proximity to the reactive thiourea-generated oxocarbenium intermediate. MacMillan imidazolidinones are efficient at activating aldehyde substrates to generate strongly nucleophilic enamine species. Placing both a thiourea and imidazolidinone catalyst at the *i* and *i+4* position on a helical peptide as in catalyst **p2** offers the potential to generate both an electrophile and nucleophile in close proximity. In this chapter, we describe our efforts to screen new bifunctional thiourea reactions as well as test new peptide-bound catalyst combinations.

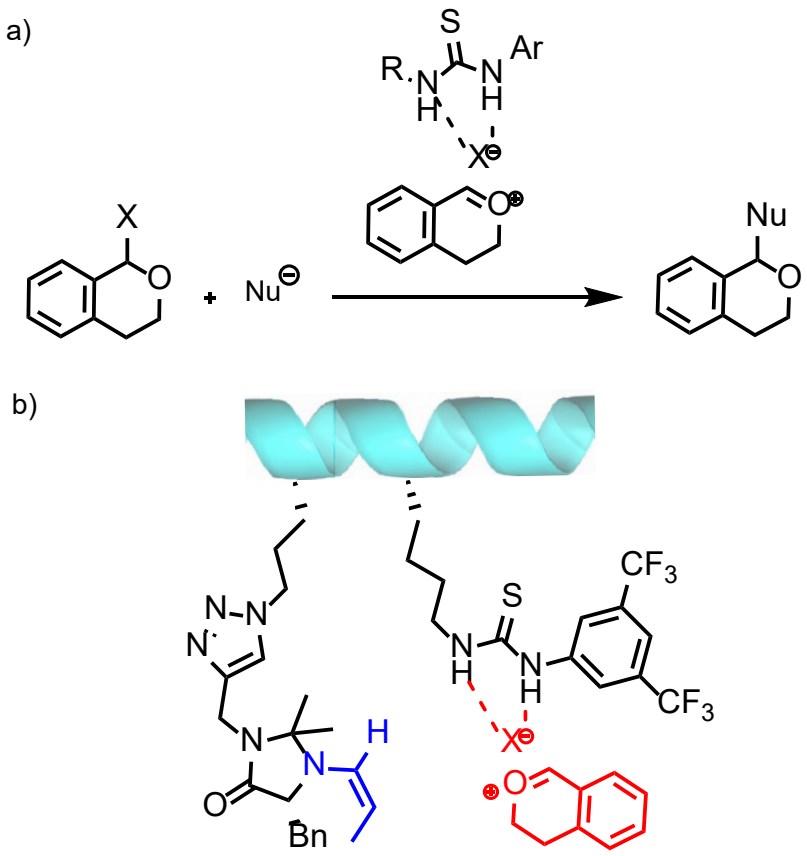

Figure 3.1 a) Thiourea activation to form strongly electrophilic oxocarbenium intermediates. b) Proposed bifunctional thiourea/iminium peptide catalyst.

3.2 Bifunctional Thiourea Reaction Optimization

In our initial efforts, it was important to demonstrate that the thiourea in our bifunctional catalyst **p2** was capable of catalyzing known reactions. In previous studies it was shown that a monofunctional MacMillan peptide was significantly slower at catalyzing Diels-Alder reactions than its counterpart in solution. We investigated the efficiency of butyl thiourea **2**, monofunctional thiourea 11-mer **p4** and bifunctional 11-mer **p2** catalysts in reactions with isochroman, isoquinoline and pyrone substrates (Figure 3.2). Unlike the Diels-Alder reactions, in all cases **2** and **p4** performed almost identically, but there was a significant drop in reactivity with the **p2**.

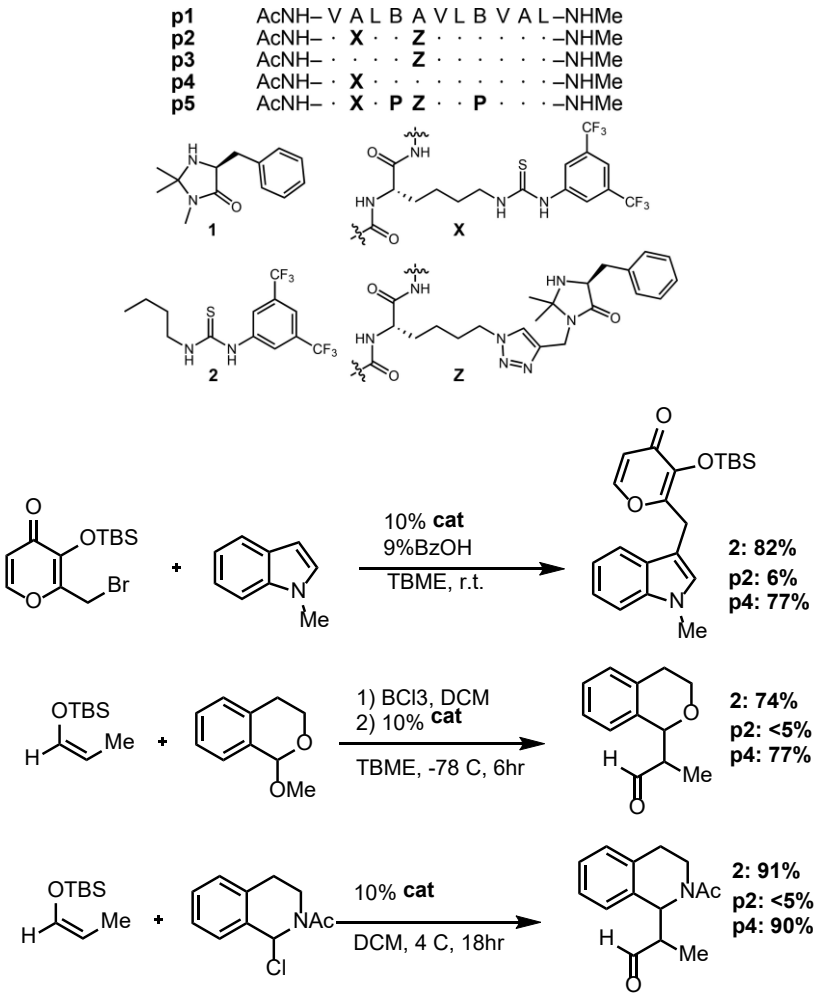

Figure 3.2 Thiourea reactions with bifunctional peptide catalyst. Isolated yields listed.

This decrease in reactivity could be due to the imidazolidinone residue on the peptide preventing the silyl ethers from reaching the thiourea residue due to sterics.

After confirming that a monofunctional thiourea on the helical peptide backbone is able to catalyze the desired reactions, we set about optimizing conditions under which both catalysts could engage their substrates and generate both the nucleophilic (enamine) and electrophilic (oxocarbenium) partners. Nine solvents were screened: MeOH, MeCN, NO_2Me, TBME, Et_2O, chloroform, dichloromethane, toluene, and THF. Concentrations from 1mM to 1M and catalyst concentrations from 2-20% were also screened. In all cases no product was observed from

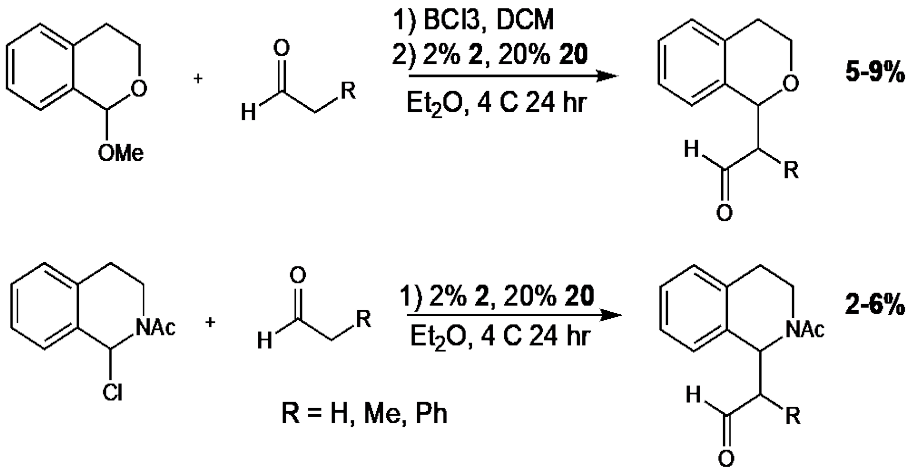

Figure 3.3 Optimized In-solution Bifunctional Reactions.

bifunctional catalysts **p2, p7**, or **p8**. Further screens were done with two catalysts not on the peptide backbone (MacMillan **1** and butyl thiourea **2**) to give meager yields when imidazolidinone catalyst **1** was 10x more concentrated than the butyl thiourea **2** (Figure 3.3). These disappointing results highlight one of the principal difficulties in bifunctional catalysis, which is that catalyst pairs may not be compatible for a desired reaction.

3.3 Solvent, Substrate and Resin Screening

In addition to screening our bifunctional peptide catalyst (**p2**) in new bifunctional reactions, we also continued studies in the Diels-Alder reaction to maximize the cooperativity between the two catalysts. First, screening reactions were conducted in order to determine which solvent and aldehydes gave the most ideal reactivity in the Diels-Alder reaction. To establish a baseline of reactivity for imidazolidinone catalysts, a solvent screen was conducted using catalyst **1** in a Diels-Alder cycloaddition with crotonaldehyde and diene **3** (Table 3.1). Toluene, THF and nitromethane gave modest yields, while MeCN and chloroform provided the least amount of product. Further

Table 3.1 *Percent yield in various solvents for 4 in using catalyst 1 with crotonaldehyde.*

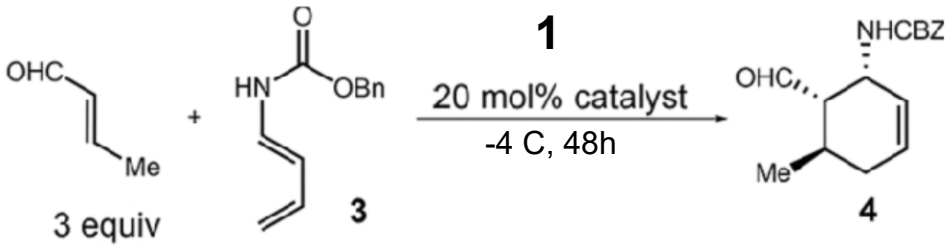

	Crotonaldehyde		
[mMol]	**100**	**10**	**1**
NO_2Me	41	36	17
CHCl3	18	5	0
DCM	24	11	0
THF	44	20	9
MeCN	13	<5	0
DMF	25	16	<5
EtOH	21	18	0
Tol.	33	24	8

Table 3.2 *Aldehyde and solvent screening yields for catalyst p2*

	Crotonaldehyde			Acrolein			Cinnamaldehyde		
NO_2Me	59	55	42	40	41	35	15	5	0
$CHCl_3$	38	33	27	35	35	20	10	0	0
DCM	35	30	19	25	20	20	<5	0	0
THF	52	43	38	65	50	45	40	10	0
MeCN	22	14	<5	15	20	10	0	0	0
DMF	48	46	37	70	40	30	30	15	5
EtOH	12	0	0	0	0	0	5	0	0
Tol.	18	9	0	30	10	0	20	15	5
[mMol]	**100**	**10**	**1**	**100**	**10**	**1**	**100**	**10**	**1**

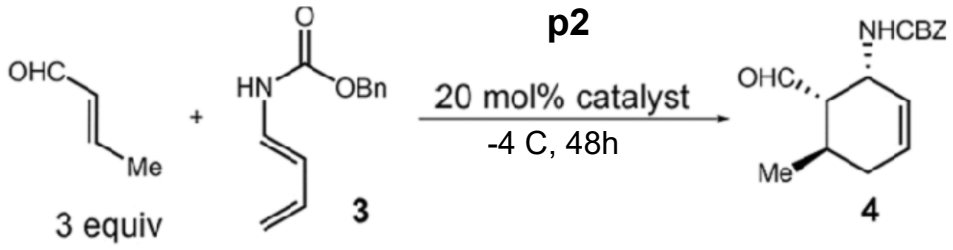

screening reactions were conducted for catalyst **p2** in various solvents, as well as with acrolein, crotonaldehyde and cinnamaldehyde (Table 3.2). Interestingly, solvent was shown to be very substrate dependent. In the case of acrolein, DMF gave the highest reactivity. With crotonaldehyde, nitromethane gave the best yields, although most solvents gave modest yields. Cinnamaldehyde was the most solvent restrictive, only reacting significantly in three solvents with the highest yield in THF. One interesting trend was the lack of reactivity in both the most polar (ethanol) and least polar (toluene) solvents. Lack of solubility of **p2** in both of these solvents is the most likely reason for this diminished reactivity. This data was inconclusive as to which solvent would be ideal for screening a large number of substrates, however, it did

showcase that catalyst **p2** is capable of catalyzing Diels-Alder cycloadditions in a variety of solvents and with multiple different diene and dienophile reactive partners.

3.4 Tether Length Optimization

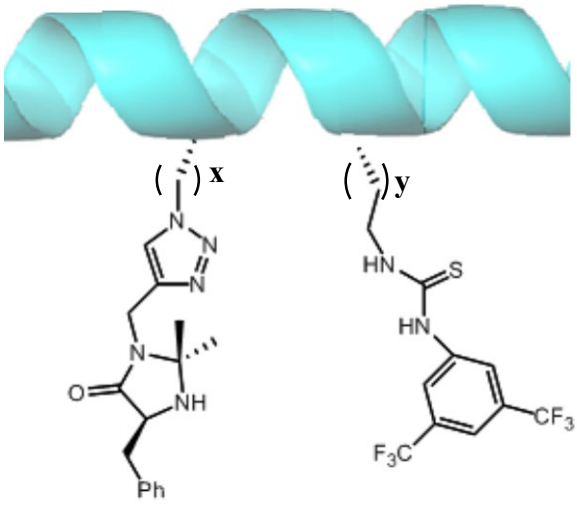

	X	Y
p2	4	4
t3	4	3
t4	4	2
t5	4	1
t6	3	4
t7	2	4
t8	3	3
t9	2	2

Figure 3.4 Suite of tether length bifunctional peptide catalysts.

Our next goal was to determine the impact of inter-catalyst distance on the reactivity of our bifunctional peptide p2. A library of peptides was synthesized with varying tether lengths between the peptide and the catalyst itself (Figure 3.4). Tether lengths ranged from one to four carbons long and all peptides were purified over silica 1-10% MeOH:DCM with 1% ammonium hydroxide. The resulting free base was then dissolved in 2:1 MeCN:Water with 1% TFA and lyophilized to yield the pure powders. We hypothesized that this suite of peptides with varying tether length would allow optimization of the interaction between catalyst pairs and the bound substrates.

Diels-Alder reactions with crotonaldehyde and **3** were conducted in order to probe the reactivity of the varying tether length catalysts (Figure 3.5). Catalyst **p2** performed the best, yielding 89% of the product **4**. As a general trend, the shorter the tether became, such as in **t8**, the lower the yield of the reaction. Reactivity also seemed to suffer as the difference in tether lengths between the two catalytic residues increase, as with **t4**. This approach provided good insight into the reactivity of the thiourea and imidazolidinone catalyst pair on the peptide, however further computational studies are currently being conducted in order to better predict and optimize the reactivity of bifunctional peptide catalysts. In particular, the reaction seems to be relatively insensitive to the length of the tether between catalysts. While reactivity changes slightly, none of the changes to the tether length reduced or increased reactivity by an order of magnitude. This result suggests that the two catalysts may not achieve a specific conformation, but the important factor may be that the two catalysts bring the catalysts "close enough" or hold them in higher local concentrations to achieve faster reactions.

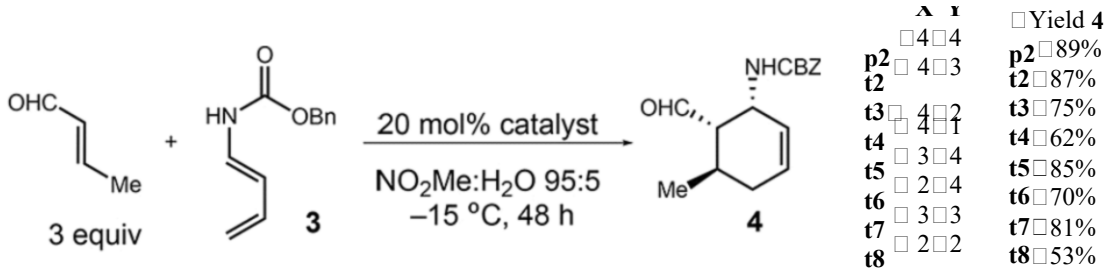

Figure 3.5 Tether length studies for bifunctional catalysts in Diels-Alder cycloadditions. Conversions by mass spectrum

In conclusion, we have demonstrated that peptide-bound thiourea catalysts are capable of forming oxocarbenium, N-acyliminium, and bromopyranone electrophiles. Unfortunately, thiourea activation was not observed in conjunction with enamine formation. A screen of

catalysts with variable tether lengths maintained reactivity in Diels-Alder cycloadditions with reactivity decreasing slightly with shorter tether lengths. Further optimization and catalyst combinations will continue to be screened in the future.

3.5 Experimental Procedures and Substrate Synthesis Methods

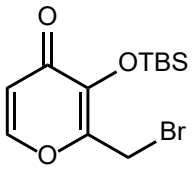

2-(bromomethyl)-3-((tert-butyldimethylsilyl)oxy)-4H-pyran-4-one was synthesized as previously reported. All spectra match reported data.[12]

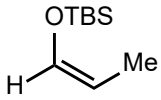

(Z)-tert-butyldimethyl(prop-1-en-1-yloxy)silane was synthesized as previously reported. All spectra match reported data.[1]

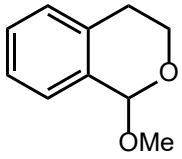

1-methoxyisochromane was synthesized as previously reported. All spectra match reported data.[1]

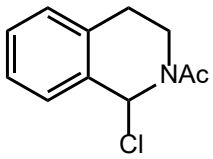

1-(1-chloro-3,4-dihydroisoquinolin-2(1H)-yl)ethan-1-one was synthesized as previously reported. All spectra match reported data.[1]

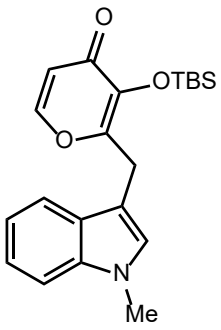

3-((tert-butyldimethylsilyl)oxy)-2-((1-methyl-1H-indol-3-yl)methyl)-4H-pyran-4-one was synthesized according to the following procedure. 2-(bromomethyl)-3-((tert-butyldimethylsilyl)oxy)-4H-pyran-4-one (31.2 mg, 0.1 mmol, 10 mM, 1eq) and 1-methyl-1H-indole (14.4 mg, 0.11 mmol, 11 mM, 1.1eq) were dissolved in 10 mL of dry TBME under Argon. Benzyl alcohol (1.8mg, 0.01 mmol, 1 mM, 0.1 eq) and 10% thiourea catalyst **4**, **p2**, or **p4** was added and the reaction was stirred overnight and purified over silica, Hex:EtOAc 2:1. All spectra match previously reported data.[12]

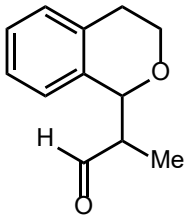

2-(isochroman-1-yl)propanal was synthesized according to the following procedure. 1-methyoxyisochroman (16.4 mg, 0.1 mmol, 10 mM, 1eq) was dissolved in 10 mL dry DCM under Argon at -78 ℃. Boron trichloride (11.4 mg, 0.1 mmol, 10 mM, 1eq) was added and the reaction was stirred for 30 minutes. Z)-tert-butyldimethyl(prop-1-en-1-yloxy)silane (20mg, 0.11 mmol, 11mM, 1.1eq) and 10% thiourea catalyst **4**, **p2**, or **p4** was added were then added and the reaction stirred for 6 hours. The solvent was removed under vacuum and the product purified over silica, Hex:EtOAc 5:1. . All spectra matched previously reported data.[1]

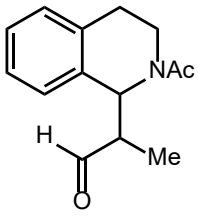

2-(2-acetyl-1,2,3,4-tetrahydroisoquinolin-1-yl)propanal was synthesized according to the following procedure. 1-(1-chloro-3,4-dihydroisoquinolin-2(1H)-yl)ethan-1-one (32mg, 0.1 mmol, 10mM, 1 eq) and (Z)-tert-butyldimethyl(prop-1-en-1-yloxy)silane (20mg, 0.11 mmol, 11mM, 1.1eq) were dissolved in 10mL DCM at 4 ℃. 10% thiourea catalyst **4**, **p2**, or **p4** was added and the reaction was stirred overnight and purified over silica, Hex:EtOAc 4:1. All spectra reported data.[1]

3.6 Analytical HPLC Traces and Mass Spectra

t2. Rf=0.54; $C_{83}H_{128}F_6N_{18}O_{15}S$ (M+NH_4+Na)/2 calculated: 891.51, found 891.70. Yield: 37mg, 51%; HPLC retention time: 34.23 min.

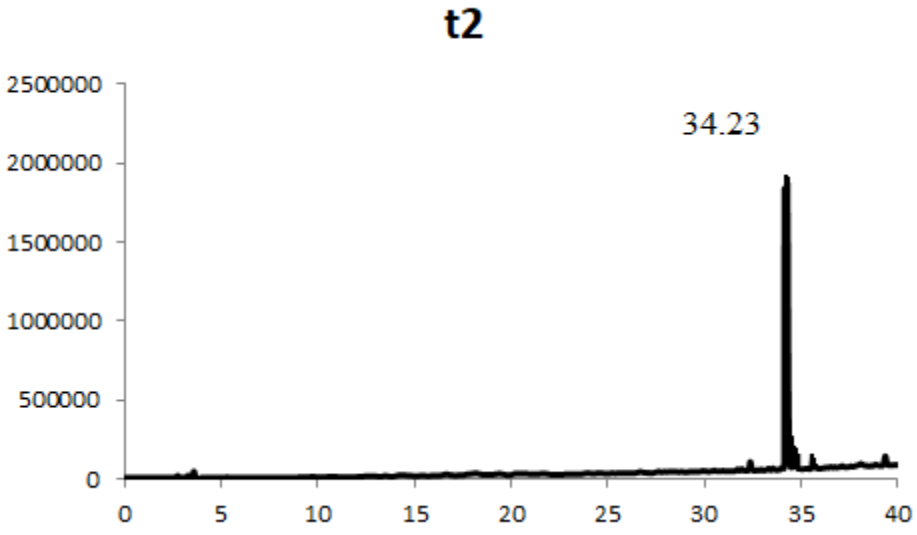

t3. Rf=0.51; $C_{82}H_{126}F_6N_{18}O_{15}S$ (M+NH_4+Na)/2 calculated: 884.99, found 884.87. Yield: 30mg, 42%; HPLC retention time: 33.80 min

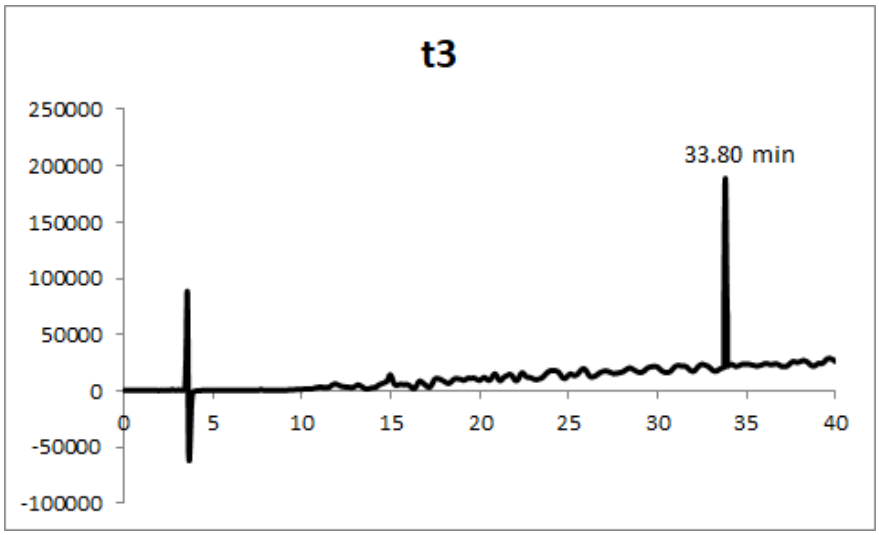

t4. Rf=0.47; $C_{81}H_{124}F_6N_{18}O_{15}S$ (M+NH_4+Na)/2 calculated: 877.98, found 877.74. Yield: 13mg, 28%; HPLC retention time: 33.521 min

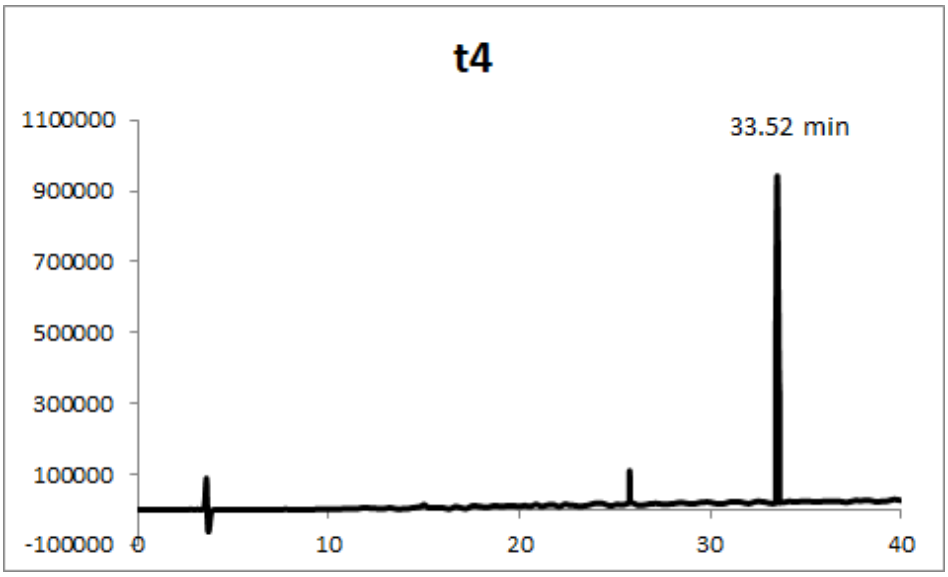

t5. Rf=0.49; $C_{83}H_{128}F_6N_{18}O_{15}S$ $(M+NH_4+Na)/2$ calculated: 891.51, found 891.63. Yield: 32mg, 45%; HPLC retention time: 33.598 min.

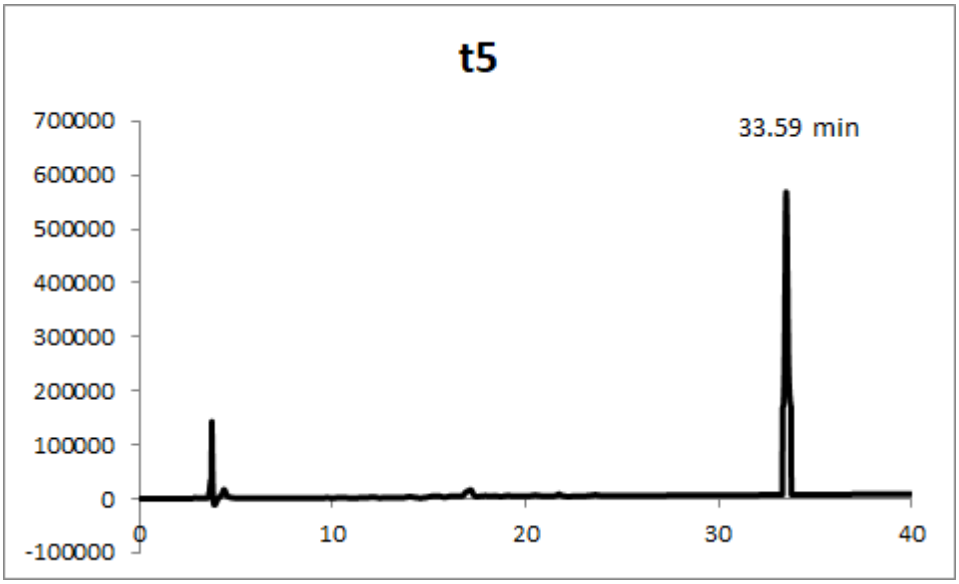

t6. Rf=0.48; $C_{81}H_{122}F_6N_{18}O_{15}S$ $(M+NH_4+Na)/2$ calculated: 884.99, found 884.95. Yield: 26mg, 53%; HPLC retention time: 34.12 min

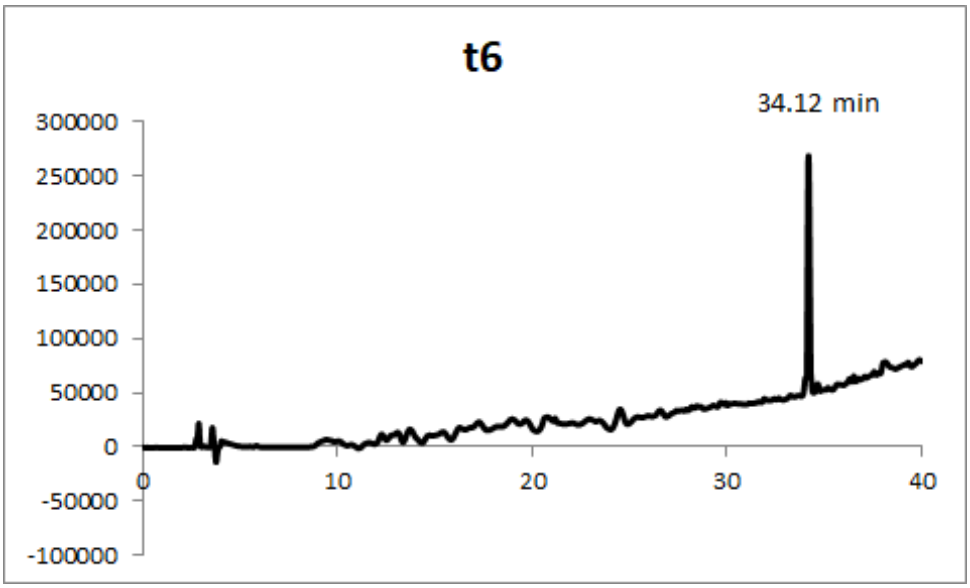

t7. Rf=0.47; $C_{81}H_{122}F_6N_{18}O_{15}S$ (M+NH_4+Na)/2 calculated: 884.99, found 884.82. Yield: 49mg, 92%; HPLC retention time: 36.594 min

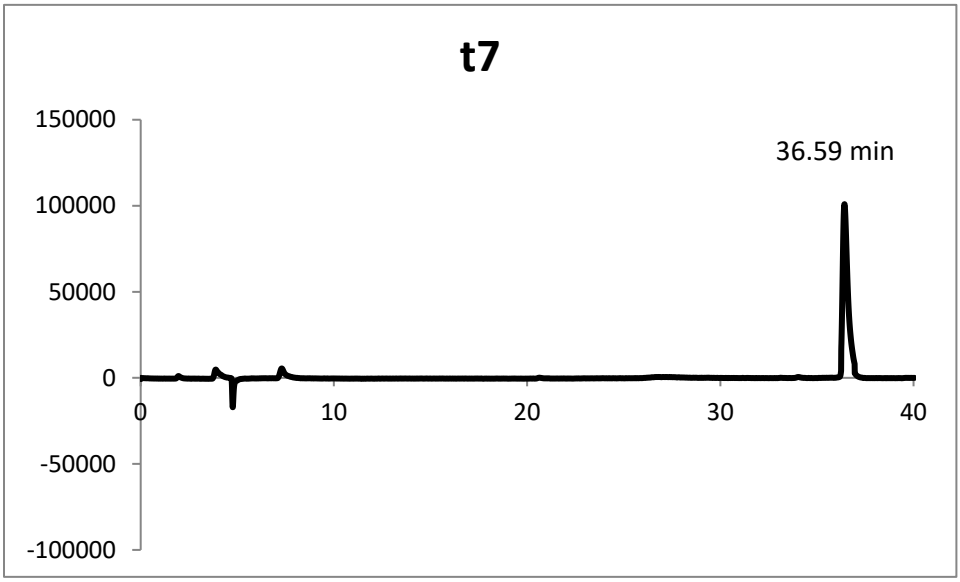

t8. Rf=0.47; $C_{79}H_{121}F_6N_{18}O_{15}S$ (M+NH_4+Na)/2 calculated: 870.98, found 870.86. Yield: 22mg, 51%; HPLC retention time: 36.601 min

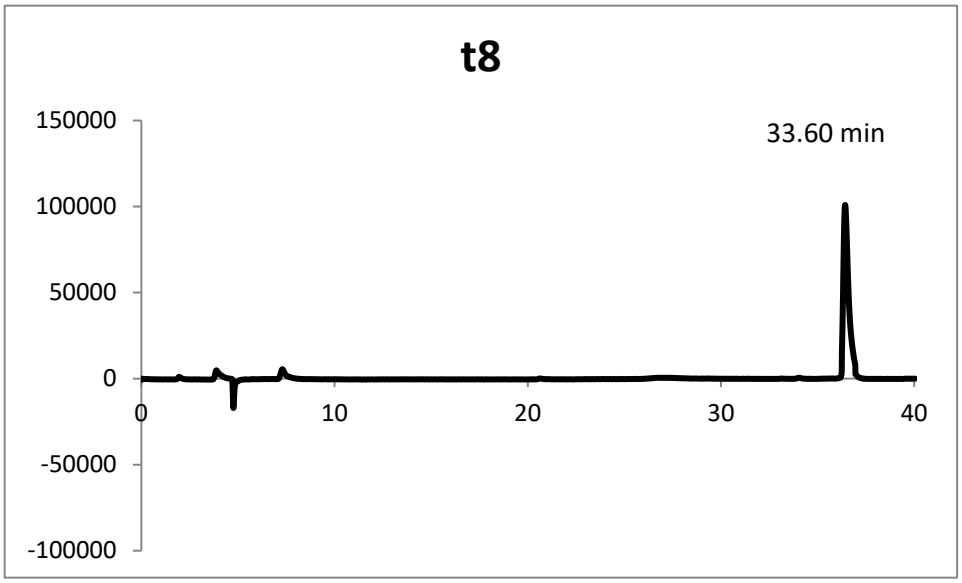

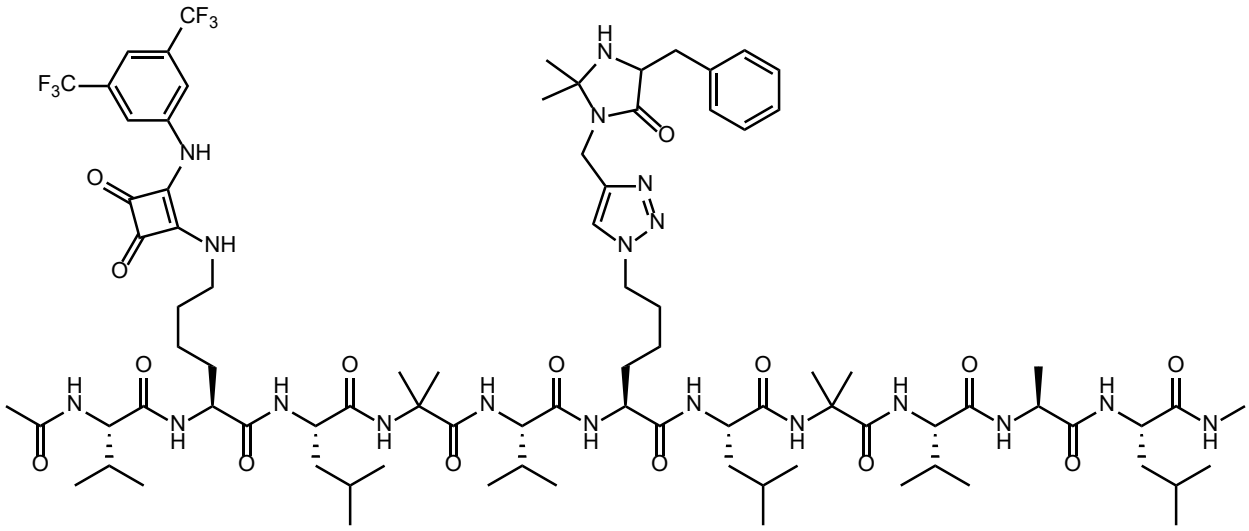

p7. Squaramide/1st Generation MacMillan 11-mer. Rf=0.36; $C_{86}H_{129}F_6N_{19}O_{15}$ $(M+NH_4)/2$ calculated: 917.02, found 917.14. Yield: 41mg, 36%; HPLC retention time: 31.978 min

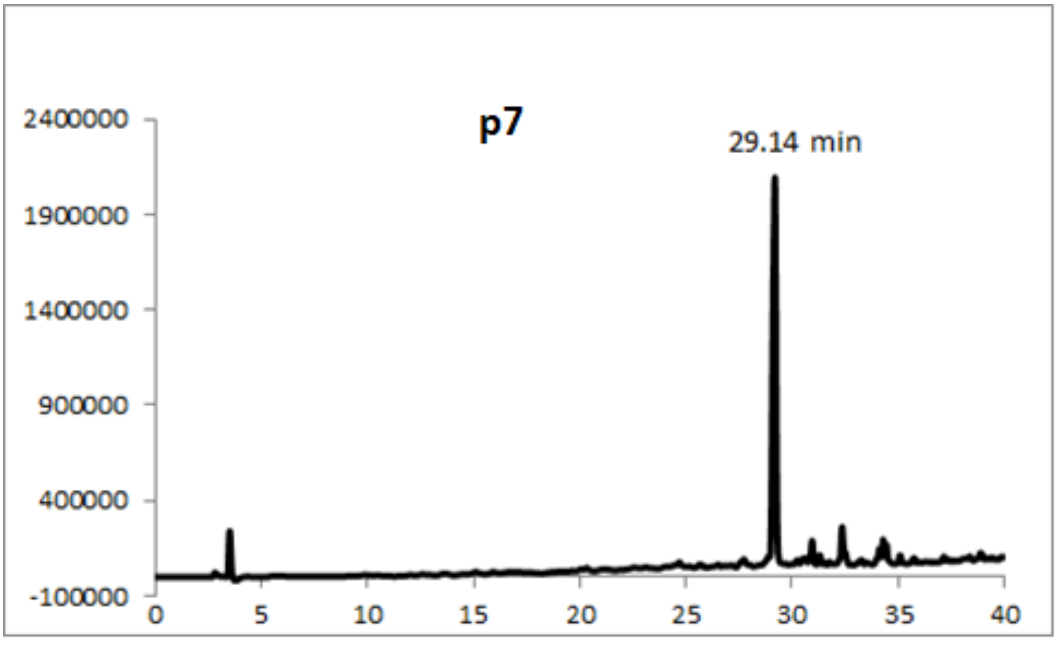

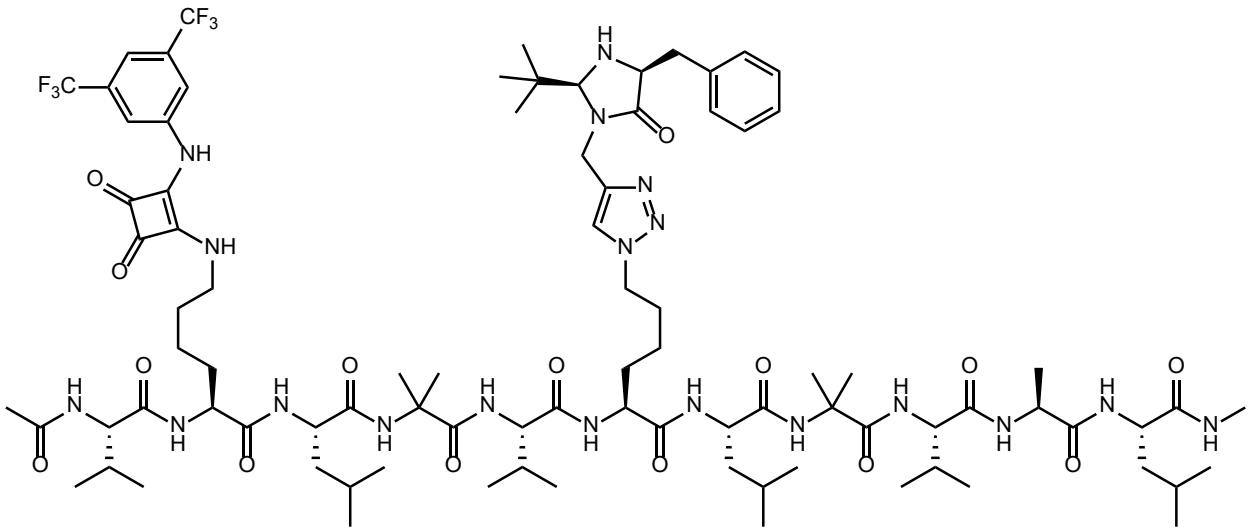

p8. Squaramide/2nd Generation MacMillan 11-mer. Rf=0.39; $C_{88}H_{134}F_6N_{19}O_{15}$ $(M+NH_4)/2$ calculated: 931.03, found 931.08. Yield: 31mg, 27%; HPLC retention time: 39.14 min

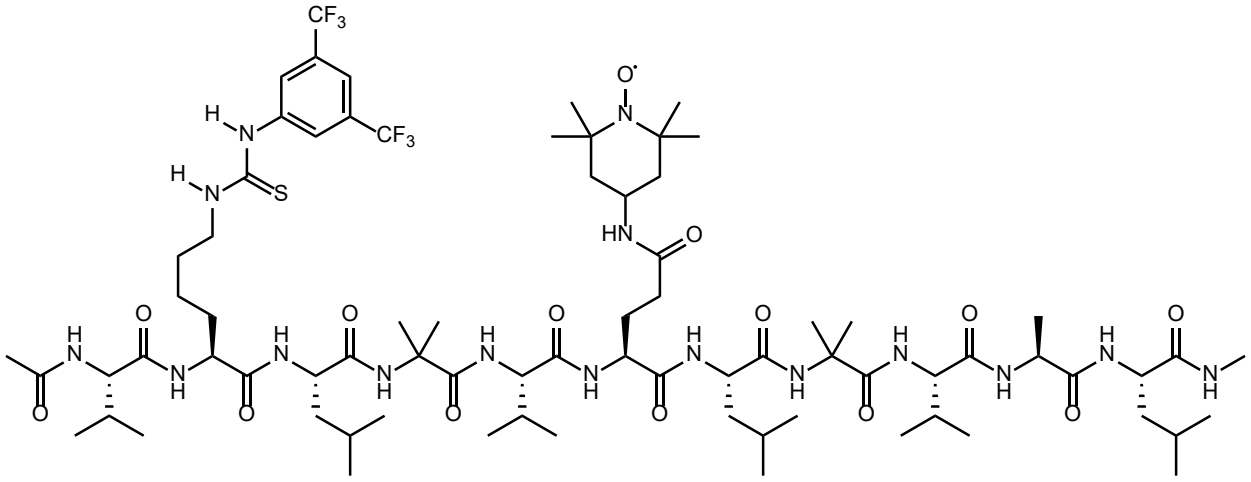

p9. Thiourea/TEMPO 11-mer. Rf=0.35; $C_{76}H_{125}F_6N_{16}O_{14}S$ $(M+NH_4)/2$ calculated: 841.99, found 842.17. Yield: 106mg, 58%; HPLC retention time: 22.13 min

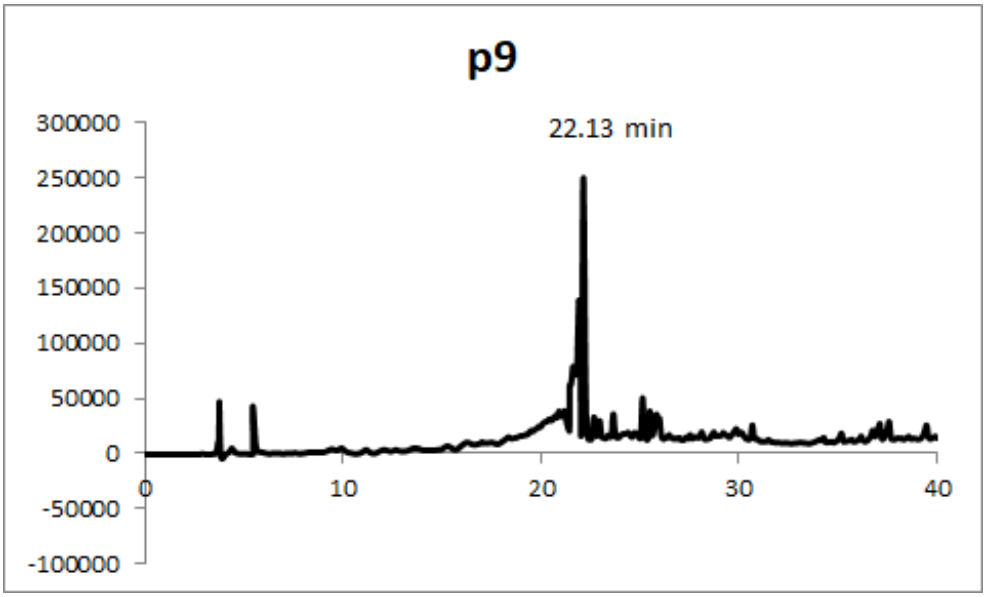
p9
22.13 min
300000
250000
200000
150000
100000
50000
0
-50000
-100000
0
10
20
30
40

3.7 References

1. Peterson, E. A.; Jacobsen, E. N. Enantioselective, Thiourea-Catalyzed Intermolecular Addition of Indoles to Cyclic N-Acyl Iminium Ions *Angew. Chem, Int. Ed*. **2009**, 48, 6328–6331.

2. Raheem, I. T.; Thiara, P. V.; Jacobsen, E. N. Regio- and Enantioselective Cyclization of Pyrroles onto N-Acyliminium Ions *Org. Lett.* **2008**, 10, 1577–1580.

3. Chen, Ying; Crockett, Richard D.; Wang, Xin; Larsen, Robert D.; Cui, Sheng; Faul, Margaret M. Development of a Scalable Synthesis of a VEGFR Inhibitor Synlett **2013**, 24(3): 301-304

4. Allen, A. E.; MacMillan, D. W. C. Synergistic catalysis: A powerful synthetic strategy for new reaction development *Chem. Sci.* **2012**, *3*, 633.

5. Skubi, K. L.; Blum, T. R.; Yoon, T. P. Dual Catalysis Strategies in Photochemical Synthesis *Chem. Rev.* **2016**, 116, 10035.

6. Kiss, G.; Celebi-Oelcuem, N.; Moretti, R.; Baker, D.; Houk, K. N. Computational Enzyme Design *Angew. Chem,; Int. Ed.* **2013**, *52*, 5700.

7. Hilvert, D. Design of protein catalysts *Annu. Rev. Biochem.* **2013**, *82*, 447.

8. Leman, L. J,; Weinberger, D. A,; Huang, Z.-Z,; Wilcoxen, K. M,; and Ghadiri, M. R. Functional and mechanistic analyses of biomimetic aminoacyl transfer reactions in de novo designed coiled coil peptides via rational active site engineering. *J. Am. Chem. Soc.* **2007**, 129, 2959-2966.

9. Mayer, C,; Müller, M. M,; Gellman, S. H,; Hilvert, D. Building proficient enzymes with foldamer prostheses *Angew. Chem. Int. Ed.* **2014***, 53,* 6978.

10. Gilbertson, S. R.; Collibee, S. E.; Agarkov, A. Cu−Catalyzed Enantioselective Conjugate Addition of Alkylzincs to Cyclic Nitroalkenes: Catalytic Asymmetric Synthesis of Cyclic α-Substituted Ketones *J. Am. Chem. Soc.* **2000**, *122*, 6522.

11. Austin, J. F.; Kim, S. G.; Sinz, C. J.; Xiao, W. J.; MacMillan, D. W. C. Enantioselective organocatalytic construction of pyrroloindolines by a cascade addition-cyclization strategy: synthesis of (-)-flustramine B *Proc. Nat. Acad. Sci.* **2004**, *101*, 5482.

12. Yeung, C; Jacobsen, E. Thiourea-Catalyzed Enantioselective Addition of Indoles to Pyrones: Alkaloid Cores with Quaternary Carbons *J. Am. Chem. Soc*. **2014**, 136, 13614−13617

13. Taylor M.S.; Jacobsen E. N. Highly Enantioselective Catalytic Acyl-Pictet−Spengler Reactions *J. Am. Chem. Soc.* **2004**;126:10558–10559.

14. Case, M. A,; Ghadiri, M. R,; Mutz, M. W,; and McLendon, G. L. Stereoselection in designed three-helix bundle metalloproteins *Chirality* **1998**, 10, 35-40.

15. Allen, A. E,; MacMillan, D. W. C. Synergistic catalysis: A powerful synthetic strategy for new reaction development. *Chem. Sci.* **2012** 3, 633

16. Reisman, S. E.; Doyle, A. G.; Jacobsen, E. N. Enantioselective Thiourea-Catalyzed Additions to Oxocarbenium Ions. *J. Am. Chem. Soc.* **2008**, *130*, 7198–7199.

17. Park, Y.; Harper, K.C.; Kuhl, N.; Kwan, E.E.; Liu, R.Y.; Jacobsen, E.N. Macrocyclic Bis-Thioureas Catalyze Stereospecific Glycosylation Reactions. *Science* **2017**, *Vol. 355, Issue 6321*, 162-166.

18. Kennedy, C.R.; Lehnherr, D.; Rajapaksa, N.S.; Ford, D.D.; Park, Y.; Jacobsen, E.N. Mechanism-Guided Development of a Highly Active, Dimeric Thiourea Catalyst for Anion-Abstraction Catalysis. *J. Am. Chem. Soc.* **2016**, *138*, 13525-13528.

19. Sammakia, T.; Smith, R. S. Evidence for an Oxocarbenium Ion Intermediate in Lewis Acid Mediated Reactions of Acyclic Acetals. *J. Am. Chem. Soc.***1994**, 116, 17, 7915-7916

20. Xu, H.; Zuend, S. J.; Woll, M. G.; Tao, Y.; Jacobsen, E. N. Asymmetric Cooperative Catalysis of Strong Brønsted Acid-promoted Reactions Using Chiral Ureas. *Science*, **2010**, 327, 986

Chapter 4 Selective Stapling of Natural Amino Acids with Hydrophilic Squaric Acid Derivatives

4.1 Introduction

Peptide and protein-based pharmaceuticals are an important and emerging class of drugs that continue each year to capture a larger percentage of the market. These polypeptide-based drugs, however, are often easily recognized by the body and degraded to their individual amino acids. Thus, various strategies have emerged to stabilize the structure of polypeptides and increase their lifetime in the body. One approach involves the covalent modification of peptide side chains to link them together and form a bridge or "staple" between residue. (peptide stapling). This covalent modification approach can greatly increase the efficiency of peptide drug candidates, as well as prevent degradation by increasing proteolytic stability. In this chapter, we report the development of a robust and selective stapling method of natural nucleophilic amino acid side chains. Under mild conditions and in both organic and aqueous media, nitrogen-, sulfur-, and oxygen-based side chains are readily stapled in various combinations using a squaric acid-based bifunctional staple. pH selectivity for specific functional groups and the selective removal of the staple demonstrate the utility of this method. Our results also demonstrate that squaric acid staples help increase the thermodynamic stability of peptide secondary structure in the WW domain by -0.75 $\pm$ 0.04 kcal/mol. An eIF4E cancer inhibitor protein was also stapled and shown to have significantly increased proteolytic stability, which suggests that this method could be applied to developing longer lasting and more effective drugs.

In recent years, the number of protein-based pharmaceuticals has increased significantly due to the myriad targets that involve protein-protein interactions. Protein-protein interactions (PPIs) are responsible for regulating most biological interactions and signaling and so offer a large range

of potential drug targets. Protein drugs offer unique selectivity that in many cases are the only viable treatments for diseases such as cancer and immunodeficiency diseases. It is estimated that protein-based drug treatments now account for nearly 10% of all pharmaceuticals on the market. However, development of protein-based drugs that are stable to proteolysis, that don't elicit a negative immune response, and that are able to reach the target receptor is a difficult challenge.

The relatively rigid secondary structure of folded proteins allows specific interactions with target cells, which can greatly decrease the frequency of side effects from protein-based drug treatments. Small peptides are particularly useful because they bridge the gap between traditional, small molecule and large protein treatments. Unlike larger macromolecules, small peptides have some flexibility that allows them to interact with a variety of receptors while still participating in protein-protein interactions. Covalent peptide staples have been shown to be capable of not only stabilizing peptide secondary structure, but can also induce helicity in random coil peptide chains. Many drug targets have become viable treatments though covalently linking their amino acid side chains through peptide staples.[1-3] The most common stapling method, developed by Grubbs et. al.[4], is the use of non-natural olefin containing amino acids to cyclize a peptide via ring closing metathesis (Figure 4.1 **a**). This is an efficient method which provides good selectivity and high yield. However, the use of non-natural amino acids complicates the synthesis and the hydrophobic tether could potentially decrease the solubility of the protein in vitro. Due to these limitations, a large effort has been to develop new peptide staples that are capable of selectively and covalently linking naturally occurring amino acid side chains. Much of this work has been centered on functionalized lysine side chains, which are a straightforward target for nucleophilic functionalization[5-7] (Figure 4.1 **b**). The work of the Pentelute laboratory[8] is of particular note due

to their bis-aryl staple, which significantly increases the hydrophobicity of modified proteins and enables them to pass through the blood-brain barrier. Multiple other methods have been developed using amide bond formation on lysine or aspartic acid residues or via alkyne/azide click reactions with alkyne and azide-containing side chains. While great progress has been made in the field of peptide stapling, limited examples exist for selective stapling reagents capable of functionalizing natural, nucleophilic amino acid residues other than lysine.

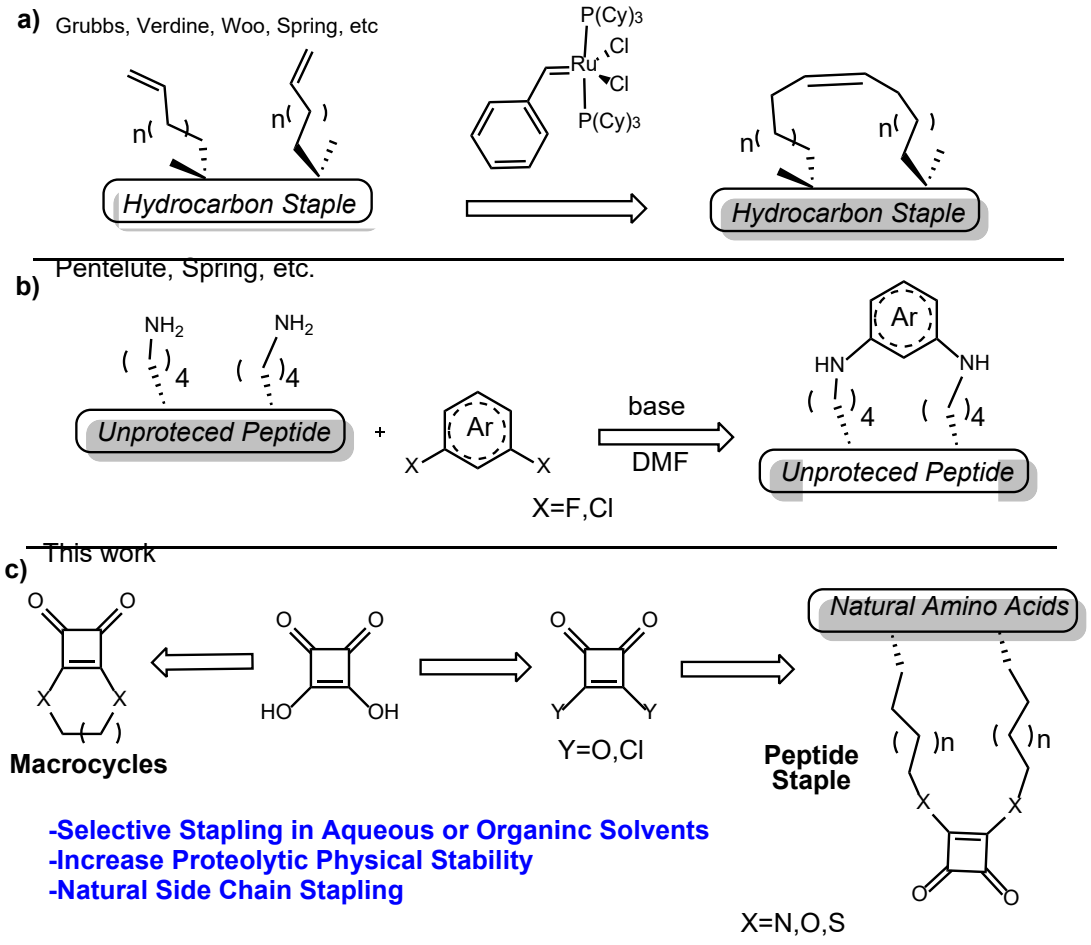

Figure 4.1 Strategies for peptide stapling.

4.2 Squaric Acid as a Hydrophilic Stapling Reagent

Two significant problems remain with current stapling methods. First, the use of unnatural amino acids limits the applicability of many peptide staples to non-natural peptides or proteins (click, metathesis). This limitation prevents stapling on larger, expressed proteins with the exception of labor-intensive tools such as via amber suppression of auxotrophic strains. The second limitation is that the arylation of natural lysine residues decreases the hydrophilicity of the peptide as a whole, which could potentially lead to solubility issues in an aqueous environment. What has not yet been developed is a polar, hydrophilic method for stapling natural amino acids that can increase solubility and provide more potential hydrogen bonding interactions with the drug's target protein. This work describes our efforts to design such a method with the use of a squaric acid-based stapling reagent (Figure 4.1 **c**). In particular, this peptide stapling approach is applied to both polypeptide macrocyclizations and helical peptide stapling via modicifation of nucleophilic amino acid residues (N, O, and S). Commercially available squaric acid can readily be functionalized to the corresponding acid chloride or ester (Figure 4.2) The squaric acid itself has reactivity similar to a carboxylic acid due to conjugation of the oxygens with the two carbonyl groups (vinylogous acid functional groups). These equivalent acids can readily undergo transformation to the bis-methoxy ester **1** via refluxing in MeOH with trimethylorthoformate and the bis acid chloride **2** via refluxing with oxalyl chloride (Figure 4.2). The squaric ester or squaric acid chloride can then react with lysine side chains to form squaramide functional groups. Squaramides are common hydrogen bonding analogs to thioureas that can be used to introduce additional drug-protein interactions with our stapled drugs.[5,9]

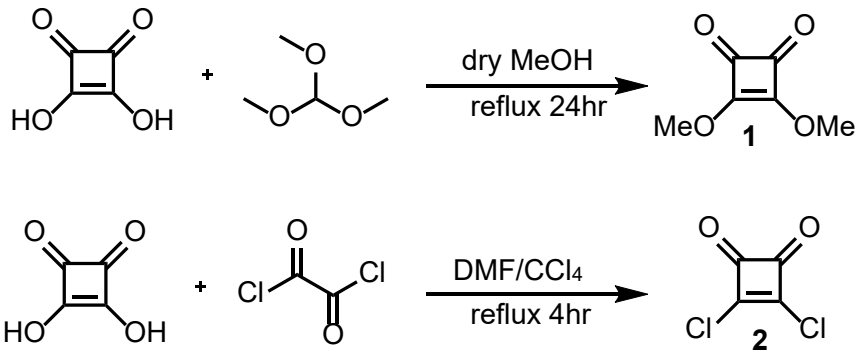

Figure 4.2 Conditions for the preparation of squaric acid derivatives for stapling.

Based on literature precedent, squaric ester **1** is commonly used in order to form squaramides, as the nucleophilic substitution from ester to amide is well established and straightforward. Due to its symmetry, we hypothesized that it would make an ideal reagent for coupling equivalent primary amines in order to perform macrocyclizations and staple native lysine residues. However, **1** is not reactive enough to react with less nucleophilic functional groups such as alcohols and thiols. To overcome this low reactivity, we employed the use of the symmetric bis-acid chloride **2,** which provides the same core structure but with increased electrophilicity to attract less reactive nucleophiles. The acid chloride is reactive enough to undergo substitution with secondary amines, as well as various alcohol and thiol functional groups.

4.3 Macrocyclizations

Our initial studies consisted of screening the reactivity of bis acid chloride **2** in macrocyclization reactions with a suite of diamine, diol and dithiol chains (Figure 4.2) Remarkably, macrocyclizations readily occurred to form various ring sizes in high to moderate yields. Ring size ranged from 6 to as large as 10 with diol and diamine starting materials. Diester

macrocycles (**4a-4e**) can only be accessed with the use of the more reactive stapling reagent **2**, which further suggests that serine residues can be stapled using this same reagent. Diamines macrocycles (5**a-5d**) as well as amino alcohols (**5**) and amino thiols (**6**) formed macrocycles as well, showcasing the scope of this method for stapling reactions. Not only can symmetric staples be formed, but asymmetric with two different nucleophilic amino acid residues.

The next step to explore the utility of squaric acid derivatives was to cyclize short, peptide sequences. Peptide macrocycles have been shown to have increased activity and stability in vivo. This is most likely due to increased proteolytic stability from the more rigid structure of the cyclized vs. linear peptide. Many macrocycles rely on an amide bond formation between the C- and N-terminus or a disulfide linkage. It was not known if a non-natural staple would provide the same activity and stability of the native system. Two tyrosidine analogues and one RGD peptide analogue were selected due to their antibacterial[3] and integrin binding[4] activity, respectively (Figure 4.3). The linear peptides underwent macrocyclization readily with **2** to form the corresponding cyclized peptide. Not only is this the first example of squaric acid being employed to cyclize polypeptides (blue), but the reaction readily occurs on resin after the synthesis of the peptide sequence. Thus, this approach to macrocyclization greatly streamlines the synthesis of macrocyclic peptides and minimizes purification steps to a single, final workup of the finished product.

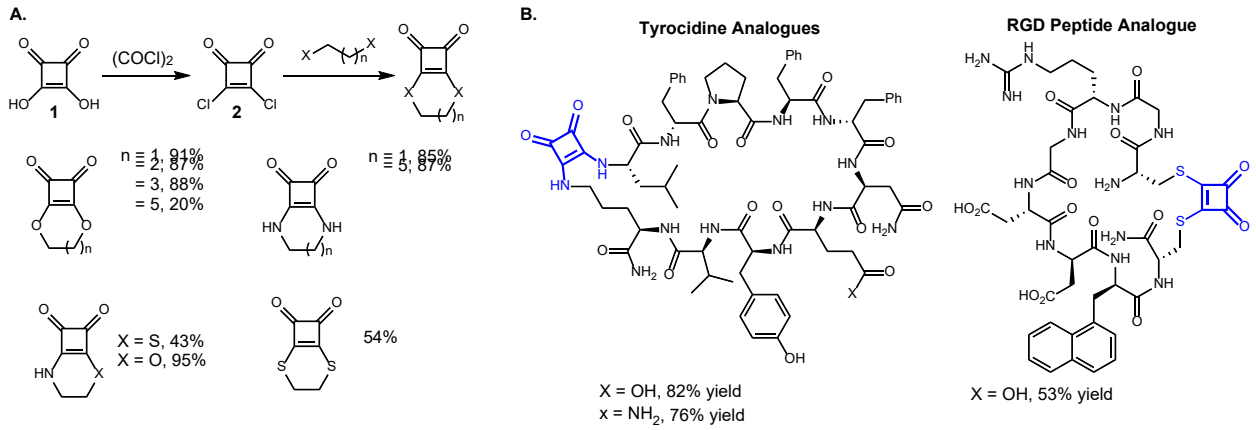

Figure 4.3 Macrocyclization and formation of macrocyclic peptides with a squaric acid-based bifunctional linker. a) conditions: squaric chloride (5 mmol), bifunctional linker (5.1 mmol), CH2Cl2 (0.005M), Et3N. b) Synthesized via solid phase synthesis, including macrocyclization on resin prior to peptide cleavage.

4.4 Stapling of Helical Peptides

Grubbs initial work in developing hydrocarbon-based peptide staples was on a short, seven amino acid helical peptide developed by Balaram.[11] This work in selective peptide stapling not only benefited from the proximity-induced rate enhancement discussed in previous chapters, but also significantly increased the stability of the helix secondary structure by covalently linking one turn of the helix at the i and i+4 positions. Our goal was to determine if squaric acid staples were capable of providing the same helix stabilizing effects at different positions on the helix and with various amino acid side chain combinations. First, the ability of **2** to staple varying side chain lengths by was investigated by stapling 7-amino acid helical peptides containing the primary amine side chains from either lysine, ornithine, Dab or Dap (**Pa**–**Pd**, Figure 4.4). The reactions proceeded efficiently with each of the bifunctional peptides, showing high selectivity for the cyclized stapled product in as little as 30 minutes. The efficiency of stapling is of particular note because other methods require significant reaction times (4 hours required for squaramide formation using **2** and

simple amines (i.e. butylamine). This illustrates the ability of this staple to form various ring sizes on a peptide at the i and i+4 positions of the helix, while also taking advantage of the rate enhancement provided by the peptide helical structure. Other side chains were then investigated to determine the ability of **2** to react with serine and cysteine side chains. Both 7- and 11-amino acid peptides were made containing two serine or cysteine residues (**Pe-Ph**). In all cases the stapling occurred in high yield, which is significant due to previous methods inability to form a serine-serine staple. This opens the door to new stapling substrates for structural studies and

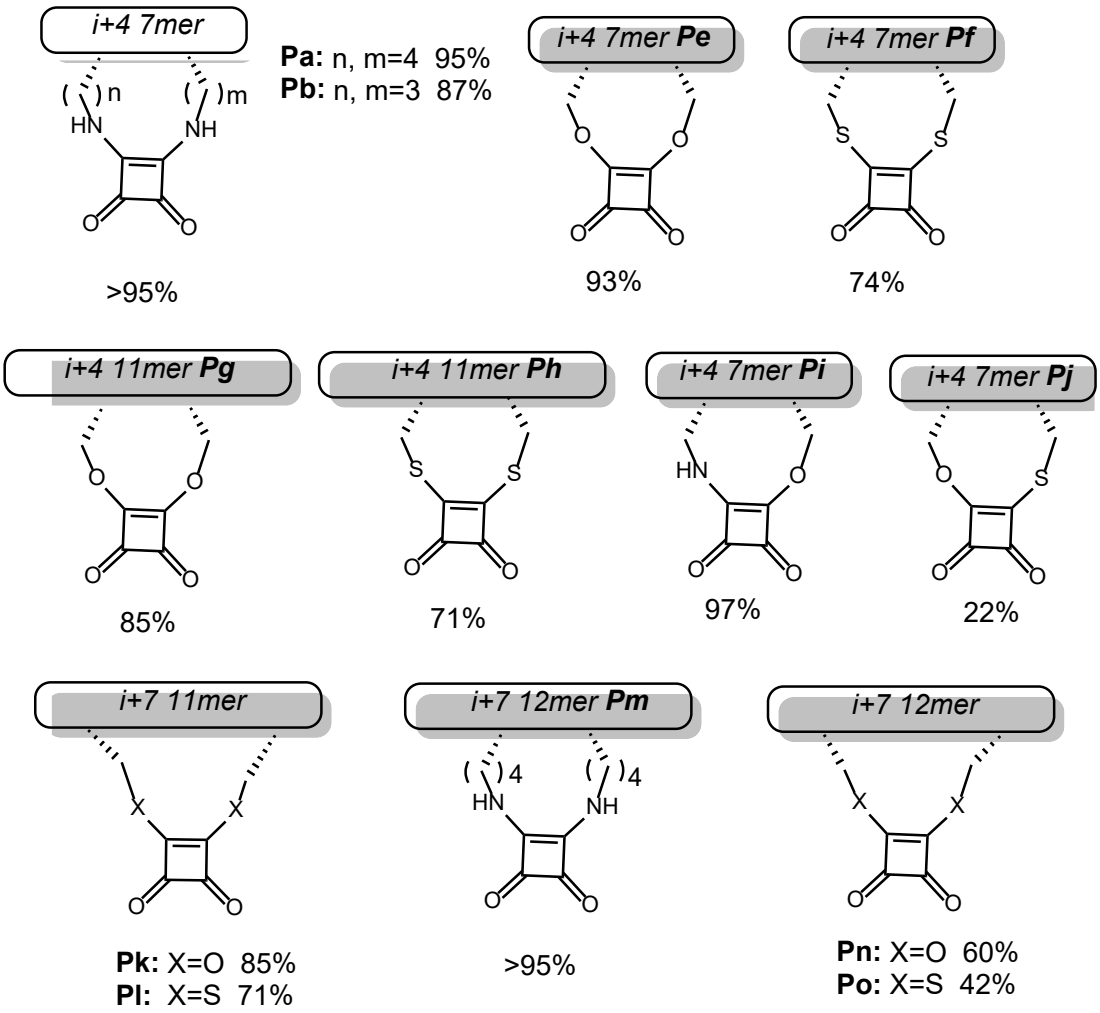

Figure 4.4 Side chain scope for squaric acid staples.

pharmaceutical development. Next, non-equivalent amino acid stapling reactions were investigated and it was shown that lysine-serine (**Pi**), lysine-cysteine (**Pi**), and cysteine-serine (**Pj**) peptides could all be stapled. This novel asymmetric stapling of two non-equivalent natural amino acid residues is something that has not been previously reported and presents the potential for stabilization of systems that could not previously be accessed. Position on the helix is also not a limiting factor, by increasing the side chain distance to the i and i+7 positions, which is two turns of the helix (**Pk-Po**), stapling reactions still readily occurred. With the ability to mix and match different side chains for stapling and to target various regions on a peptide, this method offers a wide scope of potential stapled peptides.

4.5 Stapling *i*+*x* Peptides

We further investigated the importance of positioning on the helix backbone in order for stapling to occur. Stapling reaction were conducted between lysine residues at the *i+1*, *i+2*, *i+3*, *i+5* and *i+6* positions of standard 7-mer and 11-mer peptides and provided excellent stapling activity in all positions including *i+3*, and *i+5* (Figure 4.5). This later result was unexpected as in both cases the residues are on opposite ends of the helix backbone, however the lysine residues likely provide enough flexibility for the stapling to occur at any position on the helix. For this reason, it is unlikely that a shorter amino acid side chain would be capable of stapling at the *i+3*, and *i+5* positions without significantly disrupting the peptide secondary structure.

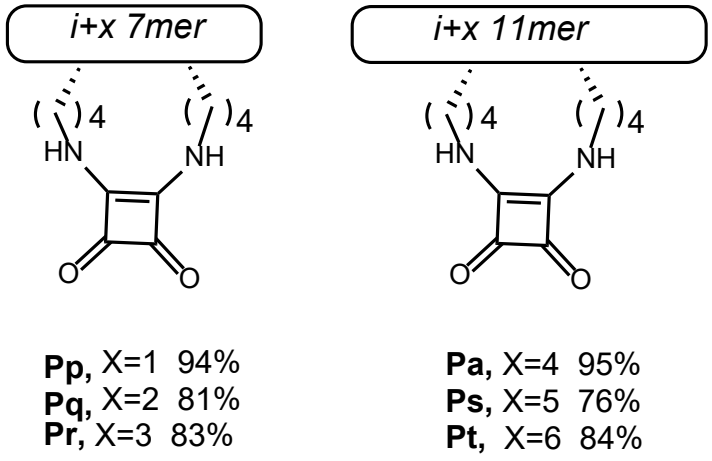

Figure 4.5 Peptide stapling of varying distance between residues from i+1 to i+6.

4.6 Stapling Under Aqueous Conditions

Up to this point, all stapling reactions had been conducted in organic solvents, either on resin in DMF or in solution in DCM or THF. This was made possible due to the hydrophobic nature of the Balaram peptide template. Many peptides, however, are significantly more hydrophilic, which limits solubility in organic solvents. For this reason, we endeavored to develop conditions under which the squaric acid staple could be used in aqueous media. Unfortunately, bis acid chloride **2** was not a viable stapling reagent under these conditions due to its high sensitivity to water, which readily degrades it to the inert squaric acid **1**. For this reason, the less reactive bis methyl ester **3** was selected and, when placed in a phosphate buffered saline solution at pH 10, was able to produce the hydrophilic peptide staple reported by Pentelute[10] **Pm** in 71% conversion by HPLC (Figure 4.6). Unfortunately, this method can only be used for lysine containing peptides as serine and cysteine lack the nucleophilicity to react with **3**. Regardless, the

ability to form the squaramide staples in both aqueous and organic solvents provides access to a wide variety of potential peptides that could be stabilized through this method.

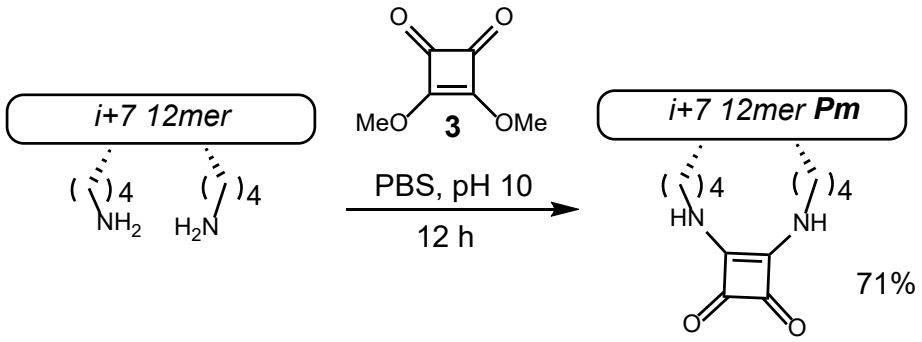

Figure 4.6 Peptide stapling in aqueous media with stapling reagent 3.

4.7 Deprotection of Squaric Acid Staples

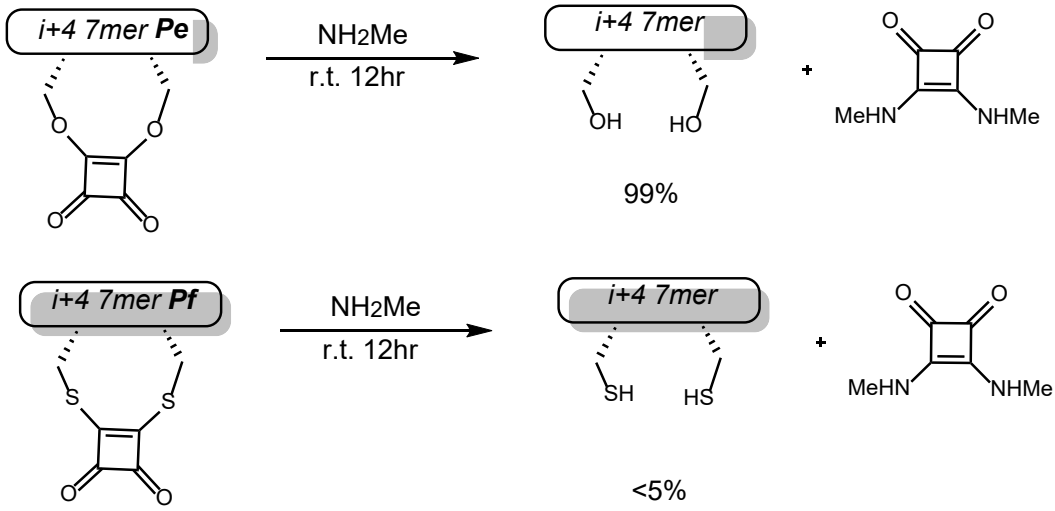

Figure 4.7 Deprotection of stapled peptides with methylamine.

Disulfide bridges serve as Nature's natural stapling method, which can covalently link two cysteine residues reversibly. Disulfide bond formation provides the needed structural stabilization from a covalent bond, but can be selectively removed to alter the activity of the bridged protein.

As the bis methoxy squaramide **3** readily undergoes conversion to a squaramide in the presence of nucleophilic amine functional groups, we hypothesized that methylamine could be used as a reagent to remove staples under mild conditions from serine or cysteine residues. In reactions with **Pe** and **Pf** with methylamine at room temperature the staples were removed at 99% and <5% respectively after 12 h (Figure 4.7). Such mild conditions proved sufficient to selectively remove serine-based staples, but were unable to remove the more stable cysteine- and lysine-based staples.

4.8 pH-Selective Stapling of Multifunctional Peptides

Since our stapling method is capable of reacting with various amines, as well as serine and cysteine residues, selectivity became an issue. One solution, which has already been demonstrated, is the use of the bis-methoxy squaric acid **3** to selectively react with amine functional groups as alcohols and thiols lack the reactivity necessary to form a staple from this reagent. Selecting for less reactive serine residues in the presence of more reactive lysine residues presents a more difficult challenge. In order to address this, we took advantage of the inherent basicity of amines. In all previous examples of squaramide formation from the bis-acid chloride **2**, a secondary base such as triethylamine or DIEA is necessary for the reaction to proceed to completion. This is due to the formation of HCl as a biproduct of condensation with **2**, which protonates remaining amines and deactivates it as a nucleophile. A complete shutdown in reactivity occurs when TFA is added in place of a base to a reaction containing **2** and lysine residues. Serine, on the other hand, doesn't require a base to react completely with **2** and is not deactivated under acidic conditions due to its lower propensity to become protonated. Taking advantage of these trends, we designed a helical peptide sequence in which there were two adjacent lysine residues and two adjacent serine residues on the same backbone (Figure 4.8). When this peptide is reacted with **2** under basic conditions,

only the lysine staple product **a** is formed. However, under acidic conditions the reactivity of the lysine residues completely shuts down and the less reactive serine product **b** is the only product formed. Conversions for these reactions were determined by HPLC, as both products are isomers of each other and therefore had the same mass. Under reverse-phase conditions on a C-18 column, the two peaks could be isolated. It was hypothesized that the earlier peak represented **b** due to protonated lysine, while the later peak represented **a**. This was confirmed when after purification of the two major peaks, a Kaizer test was conducted on both products indicating that the first peak had free amines present (**b**) and the later peak had none (**a**). Our novel approach allows for the selective stapling of nucleophilic residues based on pH rather than the inherent reactivity of the nucleophiles, which could provide access to site selective stapling on a large protein containing several nucleophilic side chains.

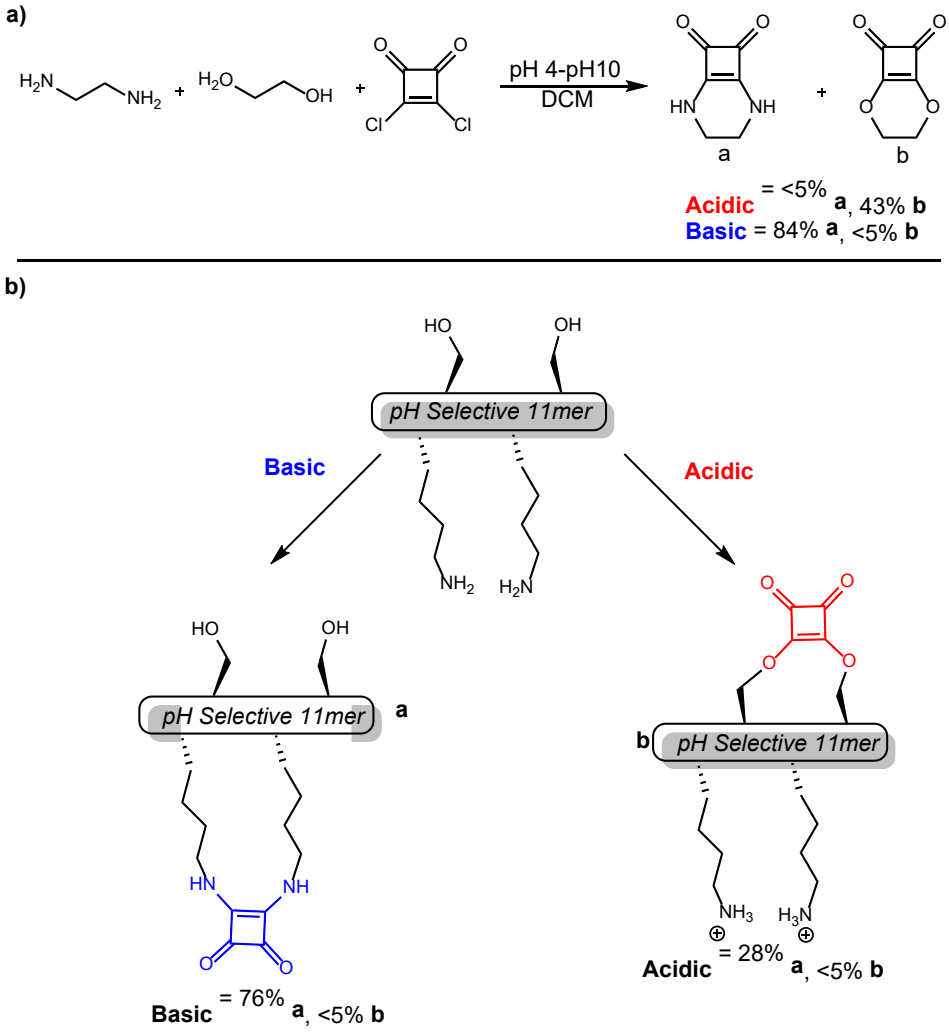

Figure 4.8 Acid/Base selective stapling of multifunction helical peptides

4.9 Proteolytic and Physical Stability Studies

Squaric acid peptide staples have been shown up to this point to be exceptional at reacting with a variety of side chains, in a number of locations, and with high selectively. However, the most important factors in this methods utility is its ability to stabilize peptide secondary structure under thermal or proteolytic conditions. Pentelute synthesized a 12mer peptide sequence with two lysine residues at the *i* and *i+7* positions that when stapled with their bis-aryl staple, saw a significant increase in proteolytic stability.[34] We synthesized and stapled this bis-lysine peptide analogue (Pm) with our squaric acid reagent **3,** and also synthesized and stapled the corresponding bis-serine (Pn) and bis-cysteine (Po) analogues with **2** (Figure 4.9). The lysine analogue **Pm** increased proteolytic stability significantly over the unstapled peptide and nearly as well as the reported stability for the Pentelute staple. Serine **Pn** provided no increase in stability while Cysteine **Po** gave a modest increase. This data shows that squaric acid staples could increase the lifetime of potential drug candidates in vitro by increasing their resistance to proteolysis.

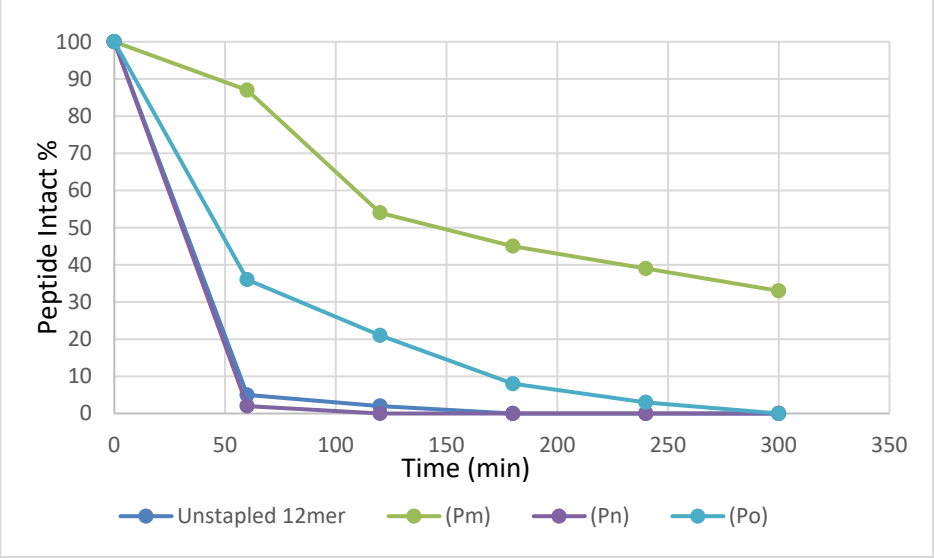

Figure 4.9 Proteolysis studies on *i+7* stapled 12mers with protease K and measured by HPLC 0-300 minutes. Sequence NH2-SXLQAWYHXFTL-Ac, X = K, S, C.

Recent work in the Price laboratory at BYU has show that stapling PEGylated side chains in the WW domain protein via Grubbs metathesis leads to increased confomational stability as determined by circular dichroism.[33] The WW domain offers a good platform to study the effects of peptide stapling since the secondary structure is well understood and conducting melting temperature studies is relatively straightforward. We selected a staple site by placing lysine residues in the 16 and 19 positions on opposite ends of a beta turn **W0** (Figure 4.10). Studies from the Price group showed that PEGylated stapling was able to decrease the total energy of the system by 1 kcal/mol. We envisioned that this would be a good location to preform the stapling test for our study. When **W0** was stapled with **3**, the resulting squaramide staple **W1** decreased the total energy by -0.75 $\pm$ 0.04 kcal/mol. This stabilization confirms that squaric acid staples are able to promote more efficient folding of peptide secondary structures.

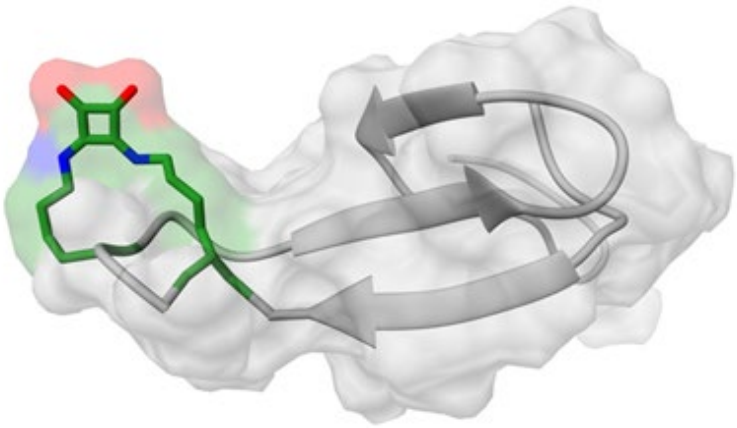

Figure 4.10 WW domain squaramide staple W1, Ac-KLPPGWEKRMKRSKGRVYYFNHITNASQFERPSG-NH2 . Melting temperature studies were conducted by CD.

In conclusion, squaric acid has been shown to be an exceptional reagent for stapling peptides and promoting stability. The broad side chain tolerance as well as the ability to selectively target specific nucleophilic functional groups highlights the synthetic utility of this method. Mild reaction conditions on or off resin in either aqueous or organic solvent systems gives the flexibility

to staple a large variety of potential peptide targets. Selective removal of staples from serine residues also suggests that this method could be used as new protecting group. CD and proteolytic studies have shown that squaric acid staples provide increased stability of peptide secondary structure, particularly for amine side chains.

4.10 Experimental Procedures and Substrate Synthesis Methods

Peptides **Pa-Po**, **W0** and **W1** were synthesized as C-terminal amides by microwave-assisted solid-phase peptide synthesis (SPPS), using a standard Fmoc Nα protection strategy as described previously.[1] Fmoc protected amino acids were activated by 2-(1H-benzotriazole-1-yl)-1,1,3,3-tetramethyluronium hexafluorophosphate (HBTU) and N-hydroxybenzotriazole hydrate (HOBt), all purchased from Advanced ChemTech.

All peptides were synthesized on a 50-200 μmol scale using the following general procedure. Rink amide resin (0.5 g; 200 μmol at 0.4-0.6 mmol/g loading; 1eq) was placed in a fritted polypropylene syringe (20 ml volume) and allowed to swell in CH_2Cl_2 for 10 minutes. The solvent was then removed using a vacuum manifold and N,N-dimethylformamide (DMF) was added to further swell the resin for 5 minutes. In order to perform activated amino acid couplings, a stock *coupling solution* was prepared by adding HBTU (15.85 g, 0.05 mol, 0.1 M) and HOBt (7.65 g, 0.05 mol, 0.1 M) to 500 mL N-methyl-2-pyrrolidone (NMP). The desired Fmoc-protected amino acid (1 mmol, 5 eq) was dissolved by vortexing in 10 mL of *coupling solution*. Diisopropylethylamine (DIEA) (352 μL, 2 mmol, 10 eq) was added to the amino acid solution; after vortexing, the activated solution was allowed to rest at room temperature for at least 60 seconds. The activated amino acid solution was then added to the resin and the syringe was placed in the microwave. The coupling method consisted of a 2-minute ramp from room temperature to 70 ˚C, followed by stirring at 70 °C for 4 minutes. The syringe was then removed from the microwave, the amino acid solution was removed on the vacuum manifold and the resin was rinsed 5 times with DMF.

A stock solution of 20% v/v piperidine in DMF was prepared by adding 100 mL piperidine to 400 mL dry DMF under an argon. Fmoc protecting groups were removed from resin-bound amino acids by adding the deprotection solution (10 mL) to the resin and allowing the resulting mixture to rest at room temperature for at least 60 seconds. The solution was then removed on the vacuum manifold; an additional 10 mL of deprotection solution was added to the resin, and the syringe was placed in the microwave. The deprotection method consisted of a 2-minute ramp from room temperature to 80 ˚C, followed by stirring at 80 °C for an additional 2 minutes. The syringe was then removed from the microwave and the deprotection solution removed on the vacuum manifold before rinsing the resin 5 times in DMF. The resin was then ready for subsequent coupling and deprotection steps to yield the completed 11-residue polypeptide.

After deprotecting the final amino acid in the sequence and rinsing the resin, the peptide was capped at the N-terminus with an acetyl group. The capping solution was prepared by adding 400 μL acetic anhydride (1mmol, 5eq), 400 μL triethyl amine (1mmol, 5eq) and 4-dimethylaminopyridine (DMAP) (1.36mg, 1mmol, 10 eq) to 5 mL of DCM. The capping solution was then added to the syringe containing the resin and the reaction was stirred for 30 minutes at room temperature. The solution was removed on the vacuum manifold and the resin was rinsed 5 times in DMF.

Cleavage of the finished peptide was performed after the appropriate residues were functionalized with the necessary catalysts. The cleavage reaction was performed on a 200 μmol scale by suspending the resin in a 5 mL TFA solution containing triisopropyl silane, water, ethane dithiol, phenol and thioanisol. The cleaved peptide was then filtered into a recovery flask, the resin rinsed with 1mL TFA and the cleaving solution was blown off with air. The dried, crude peptide was loaded onto a column of silica gel (2 cm x 25 cm) and eluted with 10% v/v methanol in DCM

with 1% v/v ammonium hydroxide or purified by HPLC. The fractions containing pure peptide (as determined by mass spec analysis) were dried under vacuum and then dissolved in 2:1 MeCN:Water with 0.1% trifluoroacetic acid. The solution was then frozen with liquid nitrogen and placed on the lyophilizer overnight to yield a fine, white powder. Proteins were identified using electrospray ionization time of flight mass spectrometry (ESI-TOF). Mass spectra values are shown below and peptide purity was determined via Analytical HPLC. Yields for each peptide synthesized are provided in the figure captions.

W1 Ac-KLPPGWEKRMKRSKGRVYYFNHITNASQFERPSG-NH_2 was synthesized on a 100 μmol scale, with alloc protected lysine side chains at the 16 and 19 positions. After the completion of the synthesis of the peptide backbone, the last amino acid in the sequence was left with the N-terminus Fmoc protected. This allowed for removal of the alloc protecting groups to be removed on resin according to the following procedure. The peptide was rinsed 8 times with dry DCM under inert atmosphere. Phenylsilane (5eq) was added to a fritted syringe containing the peptide and stirred for 1 minute under argon. Palladium tetrakis triphenylphosphine (0.05eq) was then added and stirred for 10 minutes. The reaction was drained and rinsed 8 times with dry DCM and the entire process repeated. The complete removal of the alloc protecting group was confirmed by mass spectrometry. The now deprotected resin bound WW domain mutant was then suspended in dry DMF with triethylamine (25mg, 0.25mmol, 2.5eq.) and 3,4-dimethoxycyclobut-3-ene-1,2-dione **3** (14.2mg, 0.1mmol, 1eq.) were then added and the reaction mixture was stirred under argon overnight. The final Fmoc group was deprotected in the microwave, the peptide cleaved from the resin and the crude peptide was purified by reverse-phase HPLC and lyophilized to yield a clean, white powder.

Acid/Base selectivity studies on **KSKS Free**, **NH_2-LAVSLKVSLKV-Ac** were conducted in solution.

Base selectivity was achieved by dissolving KSKS Free (12mg, 10 µmol, 10mM, 1eq.) in 1mL dry DCM in an ice bath. **2** (1.6mg, 10.5 µmol, 10.5mM, 1.05eq.) and triethylamine (2.5mg, 2.5 µmol, 2.5mM, 2.5eq.) Were added and the reaction was allowed to warm to room temperature and stirred for 4 hours. The reaction was quenched with saturated $NaHCO_3$, extracted with DCM and dried under vacuum. The crude product was purified over silica, DCM:MeOH, 2:1 with 1% ammonium hydroxide to yield the clean product as a yellow oil. 9.34mg (74%) A Kaizer test was negative, confirming that basic conditions were selective for the amide staple. Acid selectivity was achieved by dissolving KSKS Free (12mg, 10 µmol, 10mM, 1eq.) in 1mL dry DCM in an ice bath. **2** (1.6mg, 10.5 µmol, 10.5mM, 1.05eq.) and trifluoroacetic acid (3.4mg, 2.5 µmol, 2.5mM, 2.5eq.) Were added and the reaction was allowed to warm to room temperature and stirred for 4 hours. The reaction was quenched with saturated $NaHCO_3$, extracted with DCM and dried under vacuum. The crude product was purified over silica, DCM:MeOH 2:1 with 1% ammonium hydroxide to yield the clean product as a yellow oil. 2.8 mg (23%) A Kaizer test was positive, confirming that acidic conditions were selective for the ester staple. Overall yield was low due to some hydrolysis that the ester staples are prone to and substitution products by the free lysine residues on the peptide.

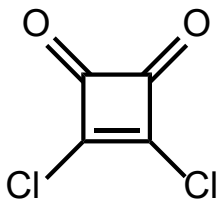

3,4-dichlorocyclobut-3-ene-1,2-dione (2) was synthesized as previously reported by B. Lunelli.[30] All spectra matched the reported data.

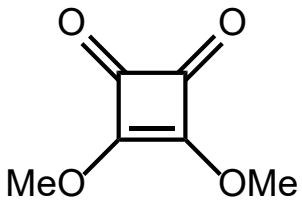

3,4-dimethoxycyclobut-3-ene-1,2-dione (3) was synthesized as previously reported by Liu.[13] All spectra matched the reported data.

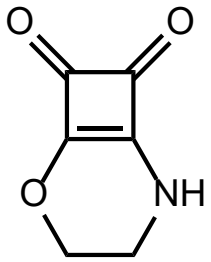

2-oxa-5-azabicyclo[4.2.0]oct-1(6)-ene-7,8-dione was synthesized by dissolving of 3,4-dichlorocyclobut-3-ene-1,2-dione (15mg, 0.1 mmol, 1eq) in 25ml dry DCM under argon. Ethanolamine (6.4mg, 0.105 mmol, 1.05eq) was added dropwise over 30 min and stirred for 2 hours at 0 ˚C. The reaction was warmed to room temperature and the solvent removed under vacuum. The crude residue was purified over silica, 5:1 EtOAc:Hex to yield a yellow solid, 95%.

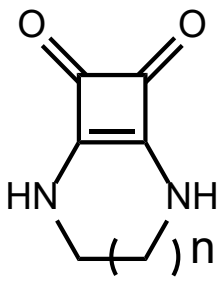

Stapled squaramides were synthesized using the following general procedure: Diamine was dissolved in 10 mL dry dichloromethane under nitrogen. 3,4-dimethoxycyclobut-3-ene-1,2-dione was then added and the reaction was stirred at 30 ℃ overnight. The solvent was removed under vacuum and product recrystallized in DCM or MeOH to yield the pure product as a solid.

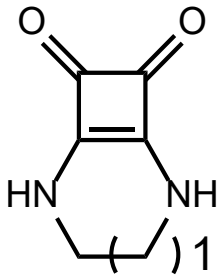

2,5-diazabicyclo[4.2.0]eth-1(6)-ene-7,8-dione was precipitated from DCM and rinsed 3 times with MeOH. Rf = 0.17 (2:1 Hexanes:EtOAc). IR (film): 3217, 1790, 1668; ^{1}H NMR (DMSO-*d6*, 500 MHz); 8.36 (s, 2H), 3.40 (m, 4H) ^{13}C NMR ($CDCl_3$, 125 MHz): 181.4, 167.7, 45.1 ; HRMS (ESI): $C_6H_6N_2O_2$ (M+H) calculated: 138.04. 84% yield. All spectra matched previously reported data.[31]

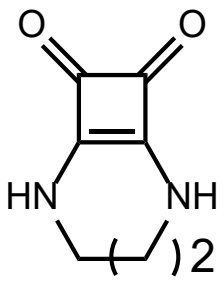

2,5-diazabicyclo[4.2.0]prop-1(6)-ene-7,8-dione was recrystallized from DCM and rinsed 3 times with MeOH. 94% Yield. All spectra matched the previously reported data.[31]

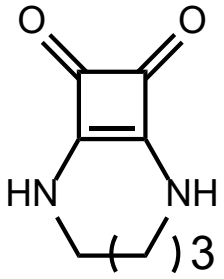

2,5-diazabicyclo[4.2.0]but-1(6)-ene-7,8-dione was recrystallized from DCM and rinsed 3 times with MeOH was recrystallized from DCM and rinsed 3 times with MeOH. 91% Yield. All spectra matched the previously reported data.[31]

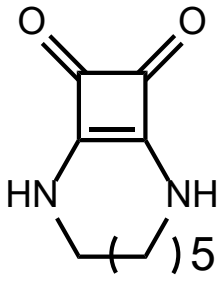

2,5-diazabicyclo[4.2.0]hex-1(6)-ene-7,8-dione was recrystallized from DCM and rinsed 3 times with MeOH was recrystallized from DCM and rinsed 3 times with MeOH. 87% Yield.

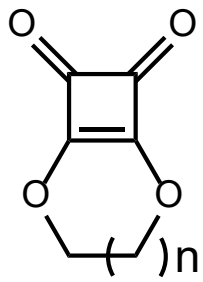

Stapled diesters were synthesized using the following general procedure: Diol (0.5mmol, 5mM, 1eq) was dissolved in 100 mL dry dichloromethane under nitrogen and cooled in an ice bath. 3,4-dimethoxycyclobut-3-ene-1,2-dione was then added and the reaction was stirred at 50 ℃ overnight. The solvent was removed under vacuum and residue purified over silica, Hex:EtOAc.

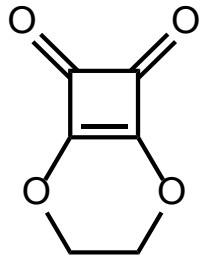

2,5-dioxabicyclo[4.2.0]oct-1(6)-ene-7,8-dione was purified over silica (Hex:EtOAc 1:2) to give white solid, 91% yield. IR (film): 1822, 1744, 1729, 1616; ^{1}H NMR ($CDCl_3$, 500 MHz); 4.68 (s, 4H), ^{13}C NMR ($CDCl_3$, 125 MHz): 186.4, 185.9, 67.2.; HRMS (ESI): $C_6H_4O_4$ (M+H) calculated: 140.01, observed: 140.01, 84% yield. All spectra matched previously reported data.[32]

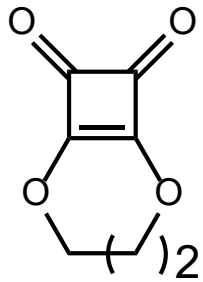

2,6-dioxabicyclo[5.2.0]non-1(7)-ene-8,9-dione was purified over silica (Hex:EtOAc 1:2) to give white solid, 91% yield. ^{1}H NMR ($CDCl_3$, 500 MHz); 4.62 (m, 4H), 2.10 (m, 4H) ^{13}C NMR ($CDCl_3$, 125 MHz): 186.2, 185.8, 65.1, 38.7.; HRMS (ESI): $C_7H_6O_4$ (M+H) calculated: 154.03, observed: 154.03, 84% yield. All spectra matched previously reported data.[32]

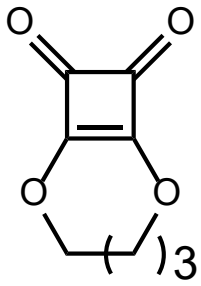

2,7-dioxabicyclo[6.2.0]dec-1(8)-ene-9,10-dione was purified over silica (Hex:EtOAc 1:2) to give white solid, 91% yield. ^{1}H NMR ($CDCl_3$, 500 MHz); 4.60 (m, 4H), 1.61 (m, 4H) ^{13}C NMR ($CDCl_3$, 125 MHz): 186.0, 185.7, 66.3, 34.9.; HRMS (ESI): $C_8H_8O_4$ (M+H) calculated: 168.04, observed: 168.04, 84% yield.

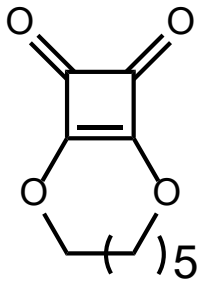

2,9-dioxabicyclo[8.2.0]dodec-1(10)-ene-11,12-dione was purified over silica (Hex:EtOAc 1:2) to give white solid, 91% yield. ^{1}H NMR ($CDCl_3$, 500 MHz); 4.59 (m, 4H), 2.14 (m, 4H), 1.52 (m, 2H) ^{13}C NMR ($CDCl_3$, 125 MHz): 185.1, 184.5, 64.0, 30.4, 26.8; HRMS (ESI): $C_{10}H_{12}O_4$ (M+H) calculated: 196.07, observed: 196.07, 84% yield.

4.11 HPLC Traces and Mass Spectra

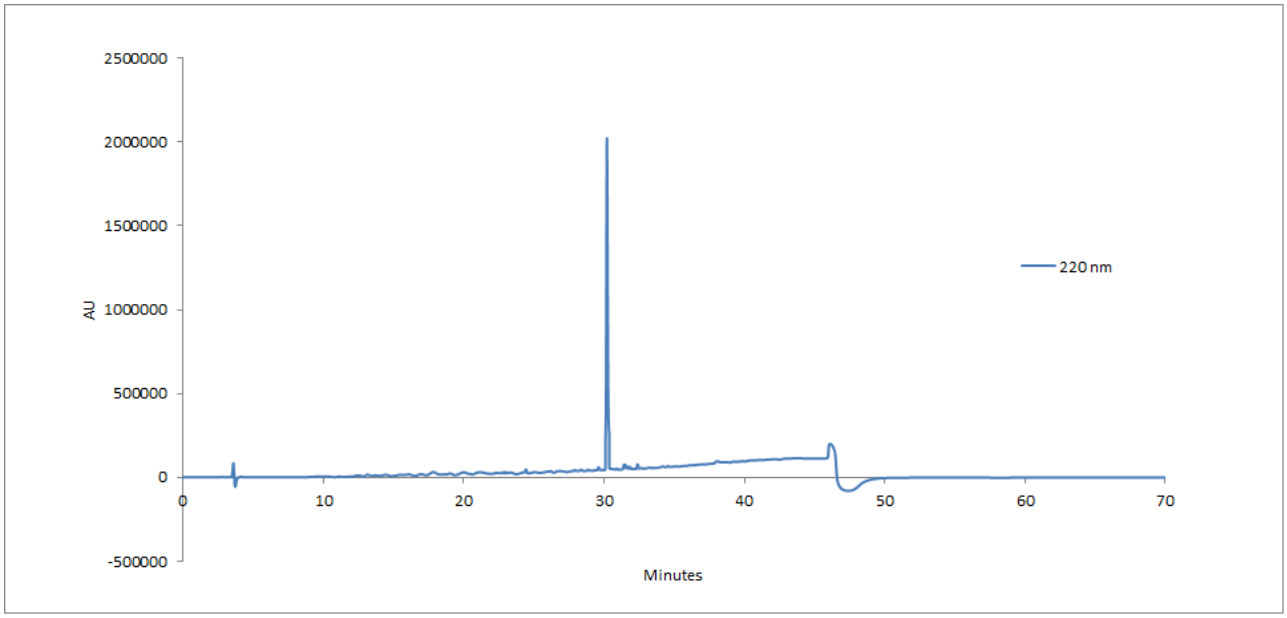

Pa $C_{44}H_{74}N_{10}O_{10}$ (M+H) calculated: 902.56, found 902.57. HPLC retention time: 30.36 min

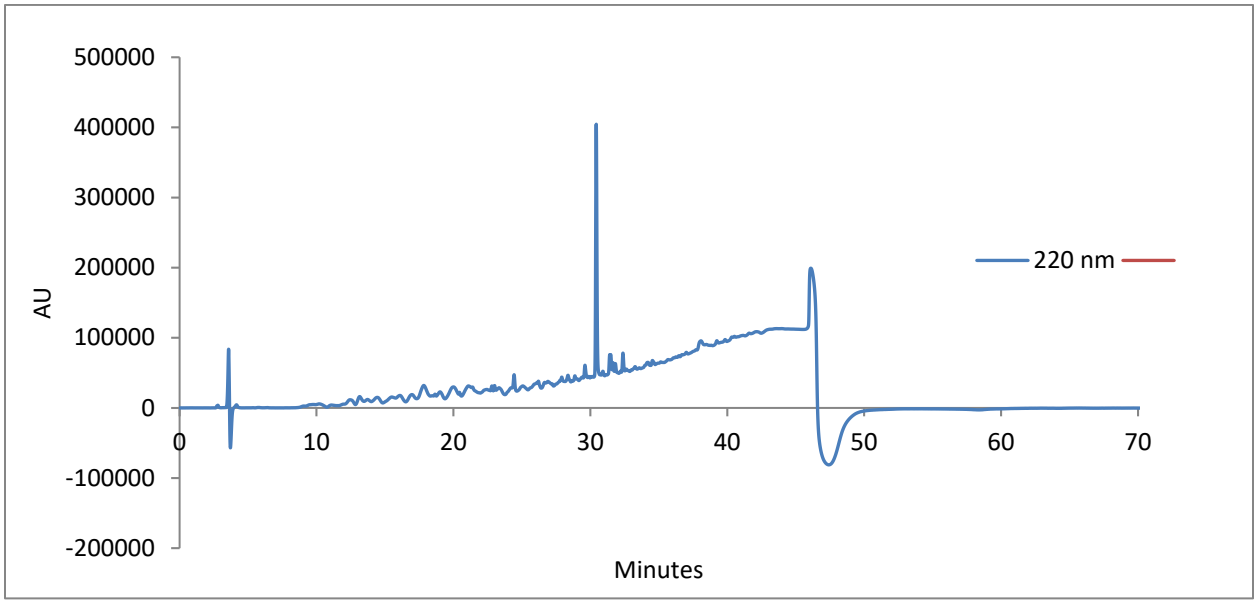

Pb $C_{44}H_{74}N_{10}O_{10}$ (M+H) calculated: 874.53, found 874.54. HPLC retention time: 30.82 min

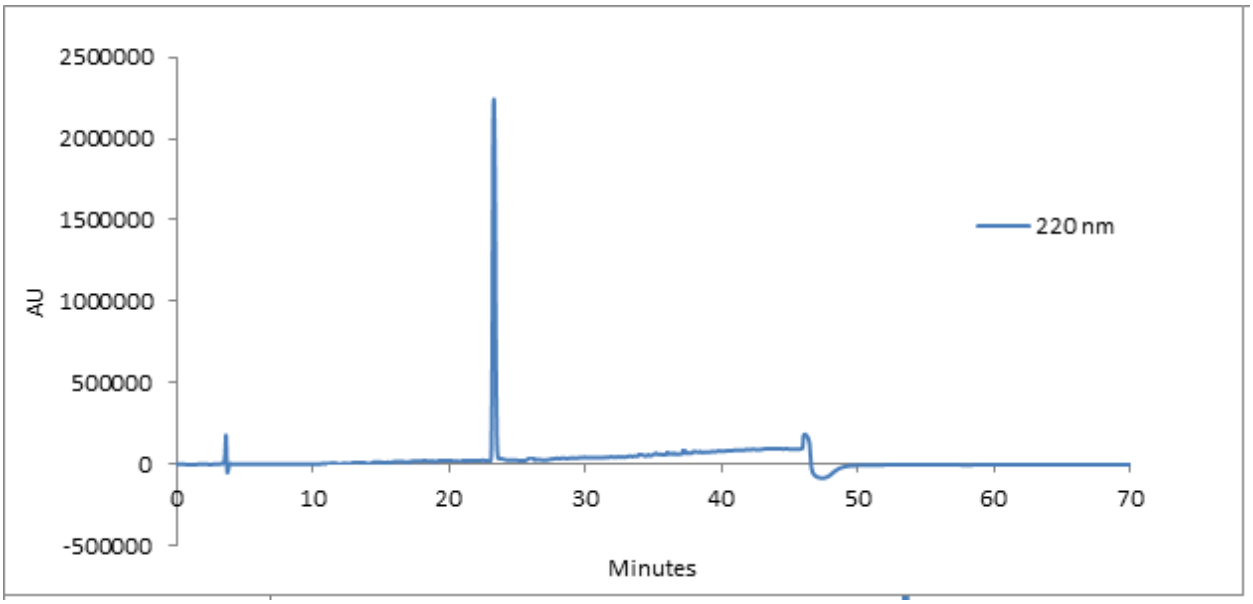

Pe $C_{38}H_{62}N_8O_{12}$ (M+H) calculated: 820.43, found 820.43. HPLC retention time: 24.38 min

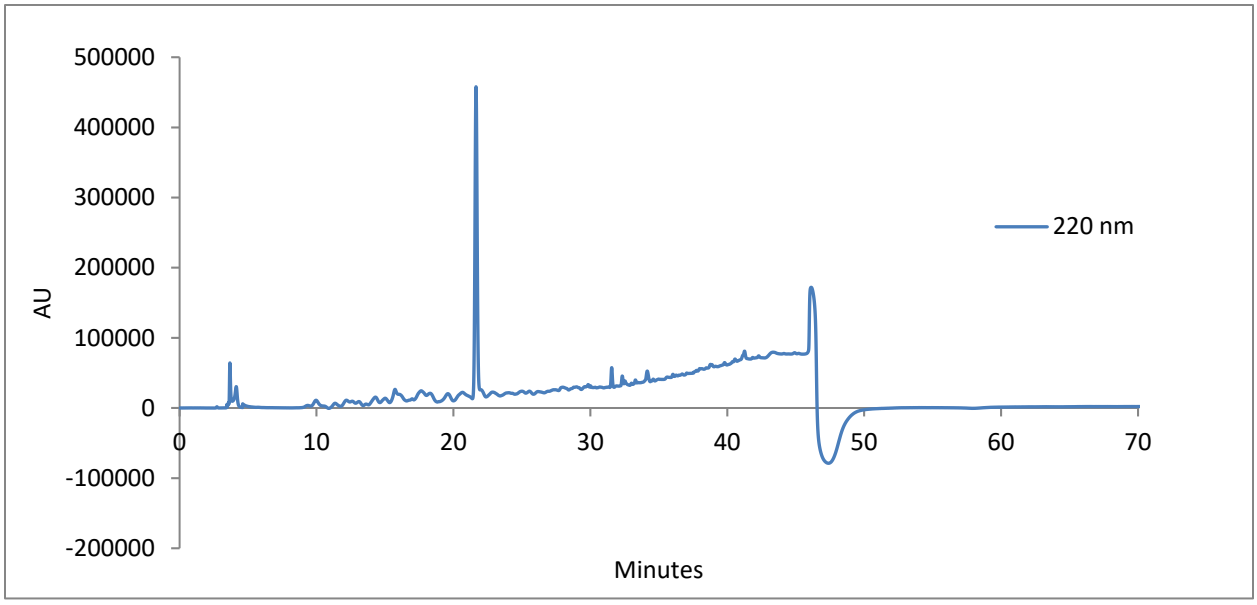

Pf. $C_{38}H_{62}N_8O_{10}S_2$ (M+H) calculated: 853.39, found 853.40. HPLC retention time: 21.66 min

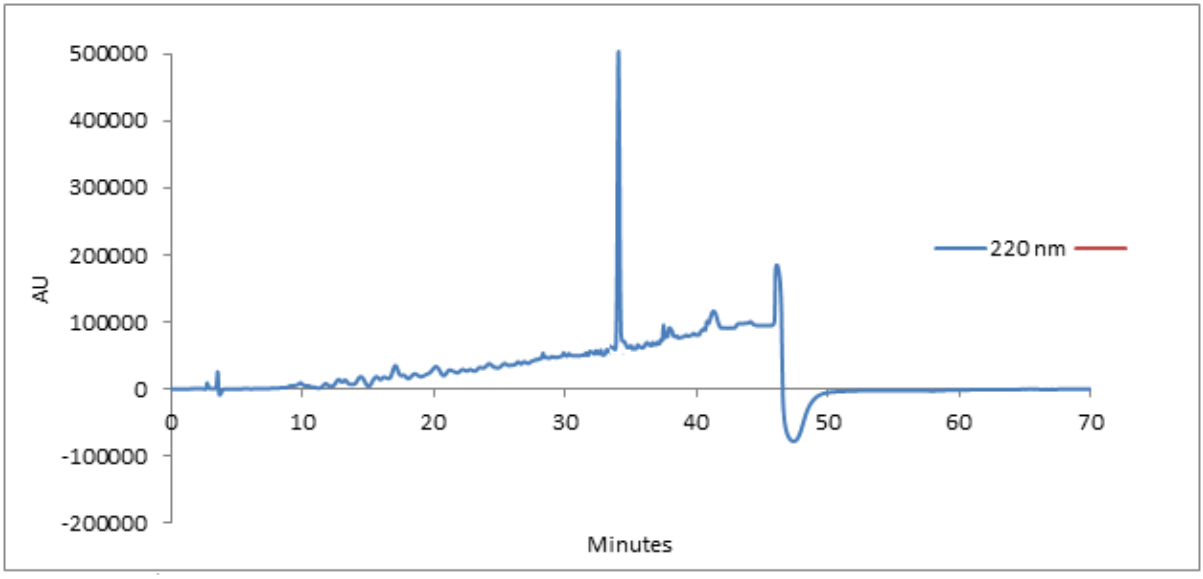

Pg $C_{56}H_{92}N_{12}O_{16}$ (M+H) calculated: 1188.68, found 1188.68. HPLC retention time: 33.99 min

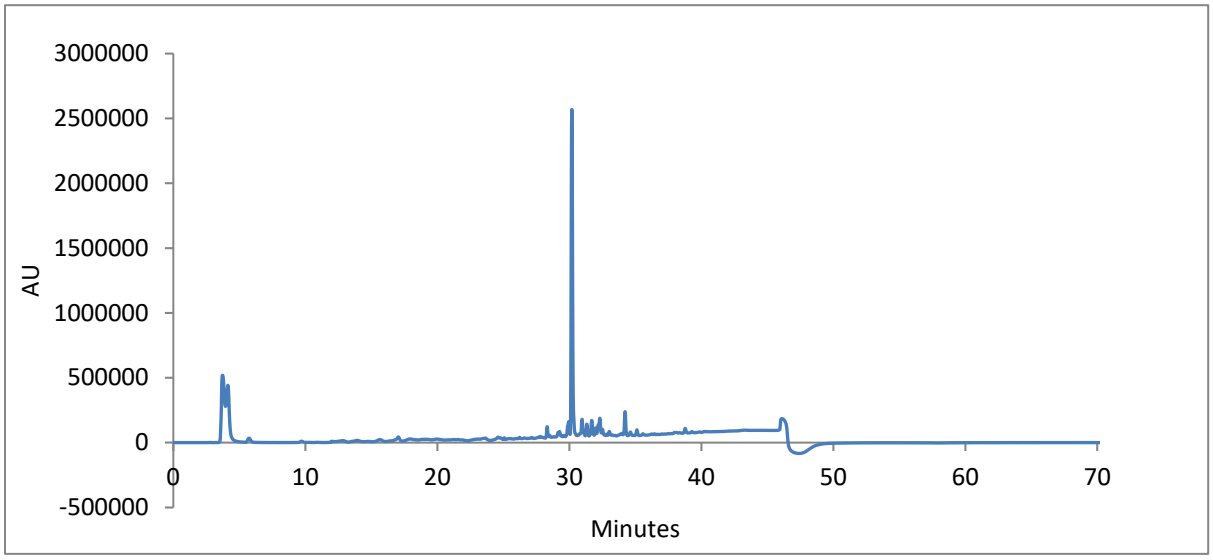

Ph $C_{56}H_{92}N_{12}O_{14}S_2$(M+H) calculated: 1220.63, found 1220.63. HPLC retention time: 30.25 min

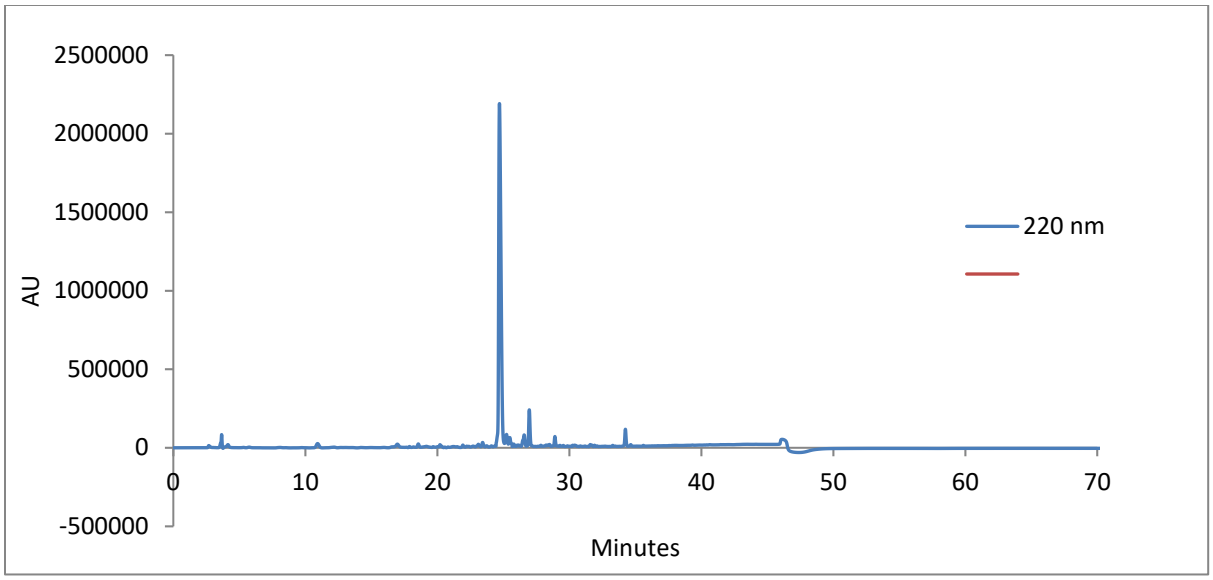

Pi $C_{41}H_{67}N_9O_{11}$ (M+H) calculated: 861.50, found 861.51. HPLC retention time: 24.77 min

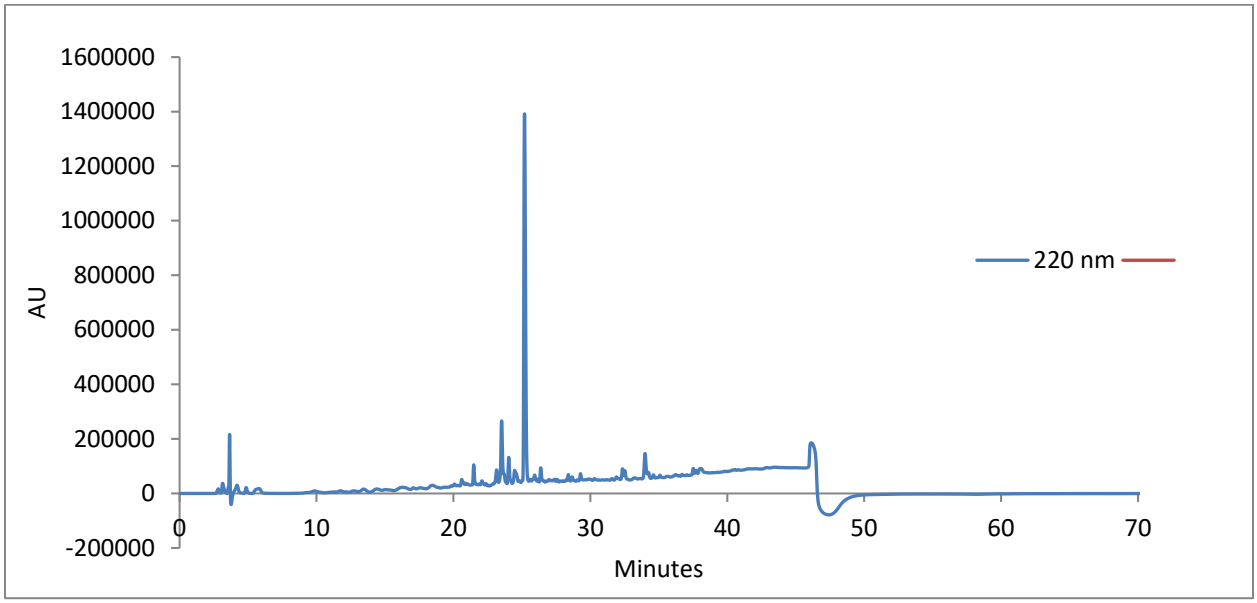

Pj $C_{38}H_{60}N_8O_{11}S$ (M+H) calculated: 836.41, found 836.42. HPLC retention time: 25.21 min

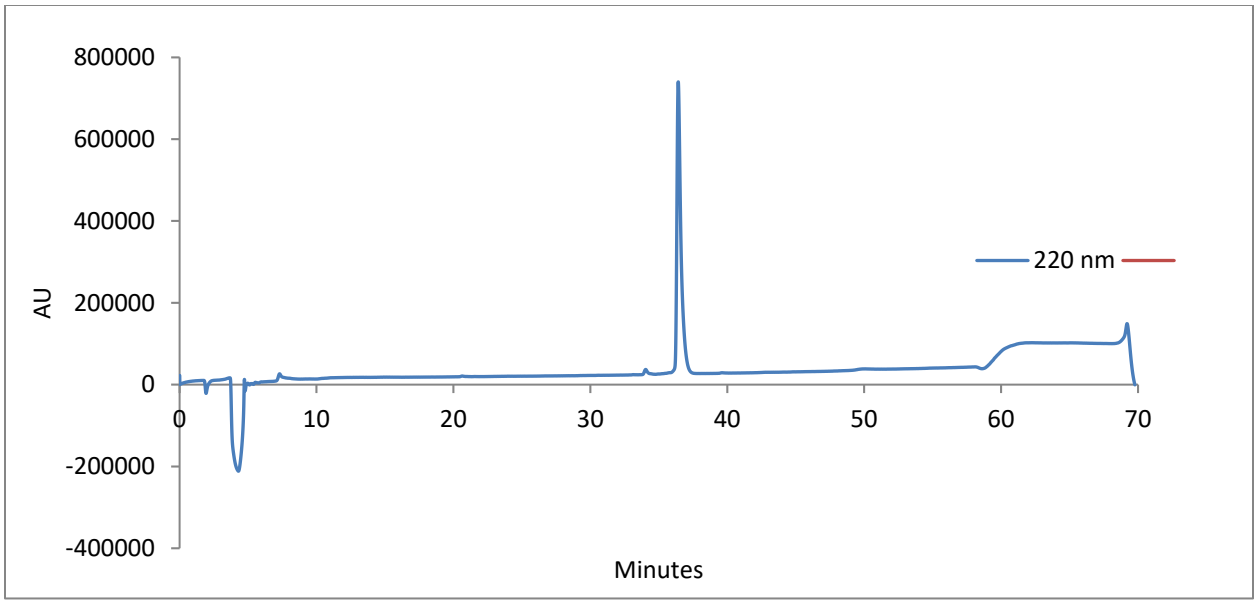

Pk $C_{56}H_{92}N_{12}O_{16}$ (M+H) calculated: 1188.68, found 1188.68. HPLC retention time: 36.41min

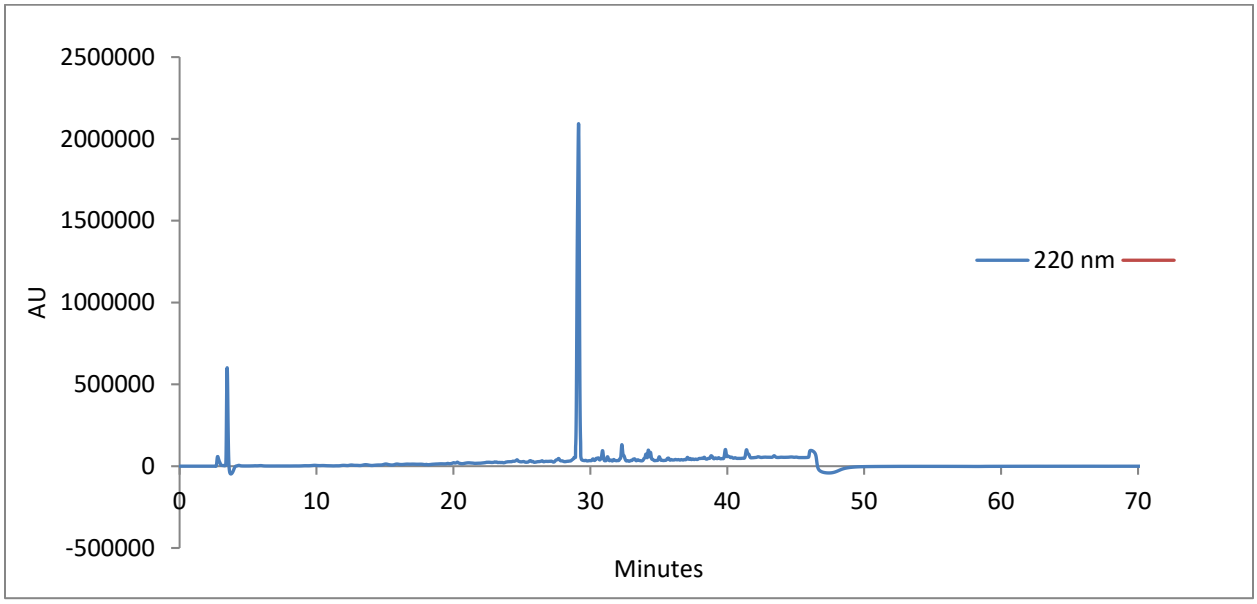

Pl $C_{56}H_{92}N_{12}O_{14}S_2$(M+H) calculated: 1220.63, found 1220.64. HPLC retention time: 29.15 min

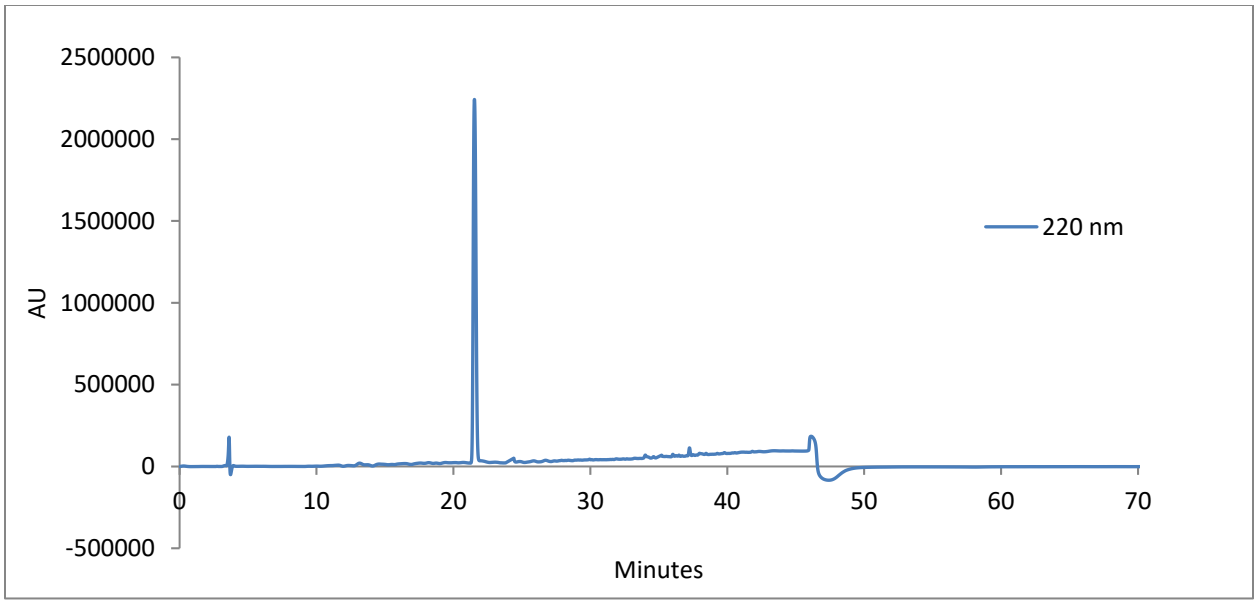

WW Lys/Lys Mutant $C_{198}H_{306}N_{62}O_{55}S$ (M+4H)/4 calculated: 1116.57, found 1116.57. HPLC retention time: 21.56 min

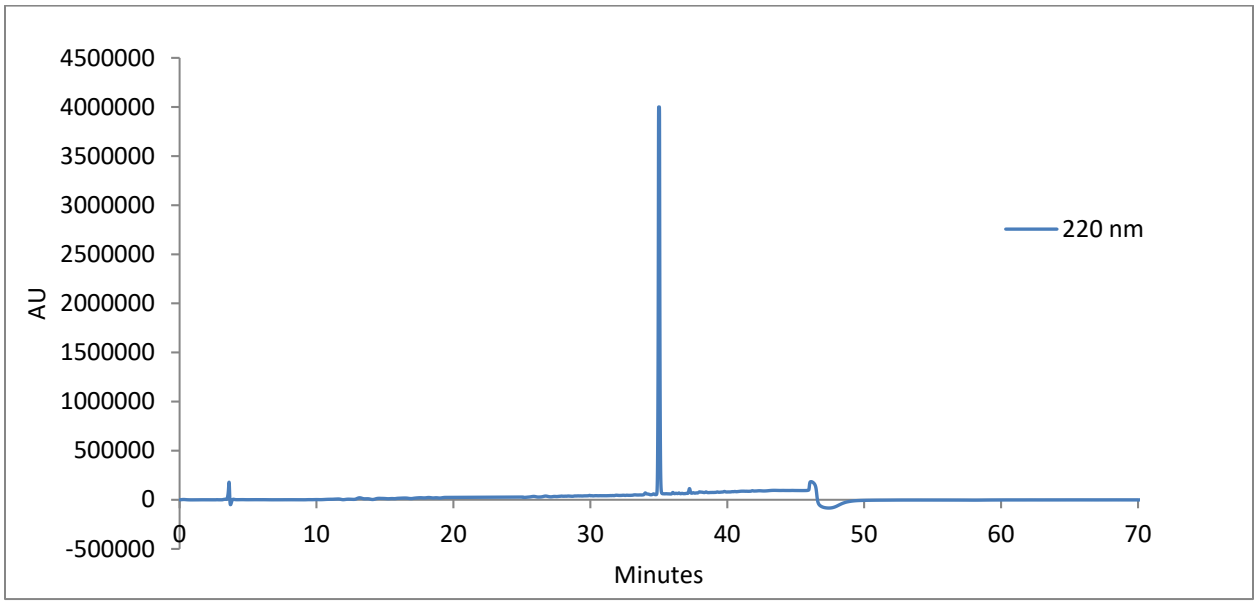

WW Staple $C_{202}H_{304}N_{62}O_{57}S$ (M+4H)/4 calculated: 1136.06, found 1136.06. HPLC retention time: 34.99 min

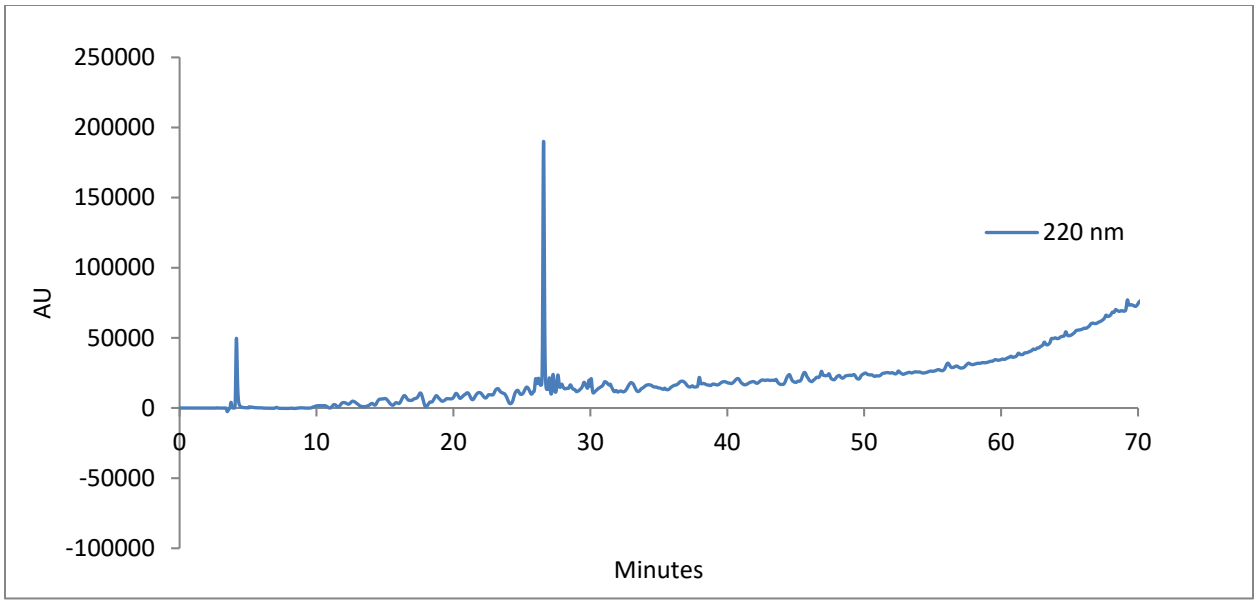

Pm $C_{80}H_{109}N_{19}O_{19}$ (M+H) calculated: 1640.82, found 1640.82. HPLC retention time: 26.58 min

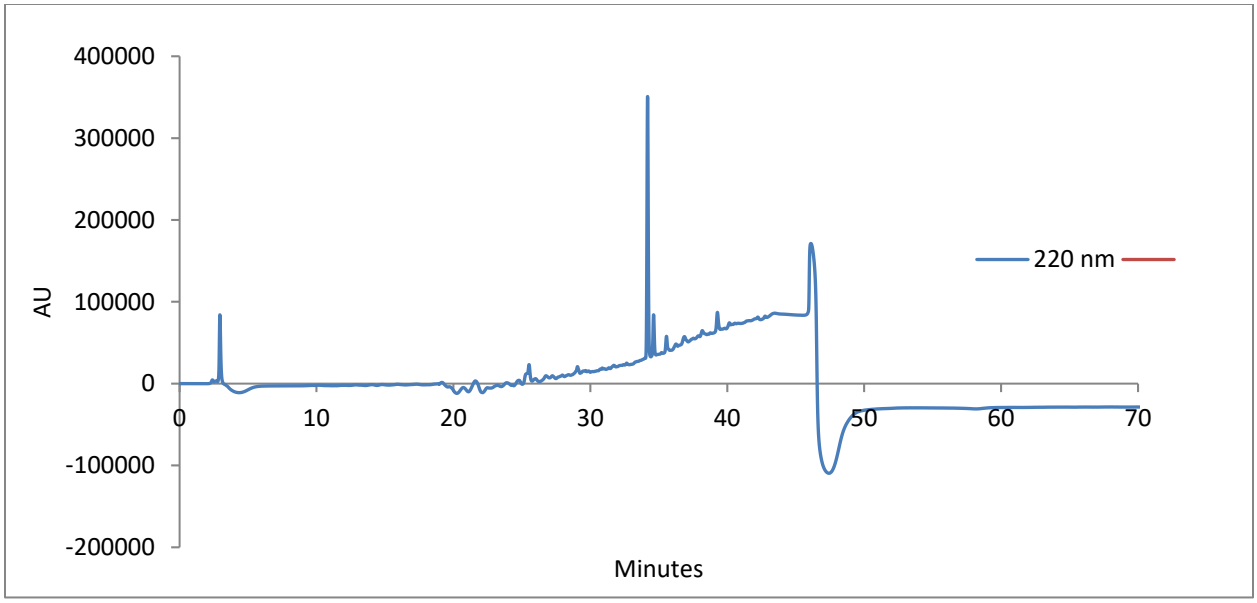

KSKS Free, NH_2-LAVSLKVSLKV-Ac $C_{62}H_{104}N_{14}O_{14}$ (M+H+$NH4^+$)/2 calculated: 607.41, found 607.41.

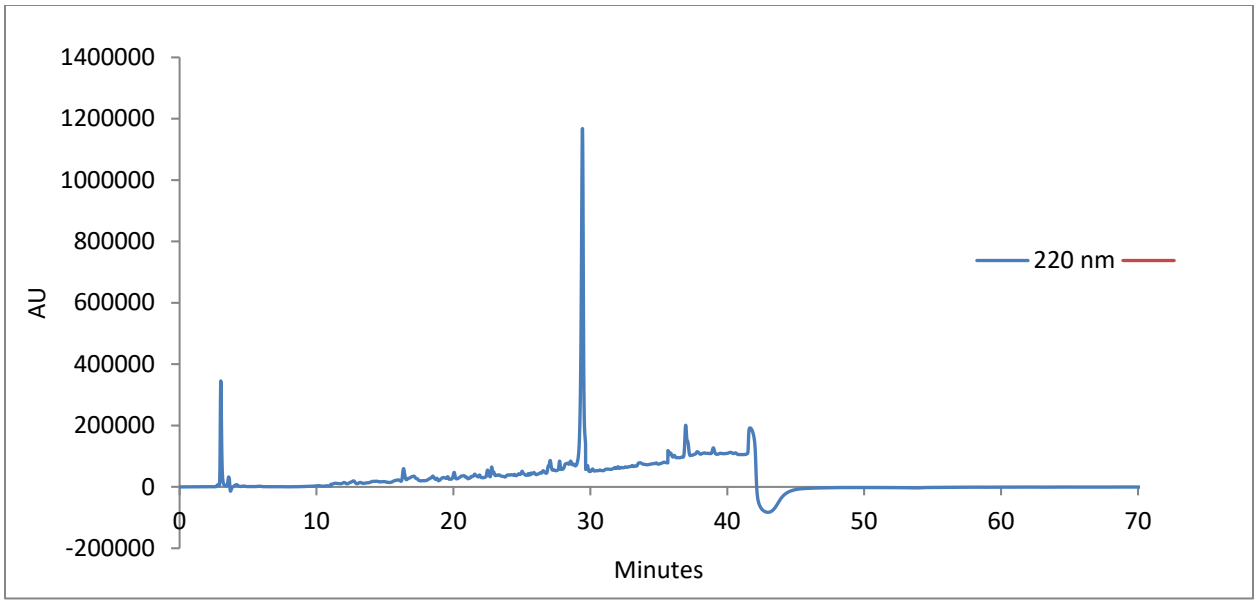

Gln Tyrosidine Analogue $C_{70}H_{88}N_{14}O_{15}$ (M+H) calculated: 1364.67, found 1364.67. HPLC retention time: 29.41 min

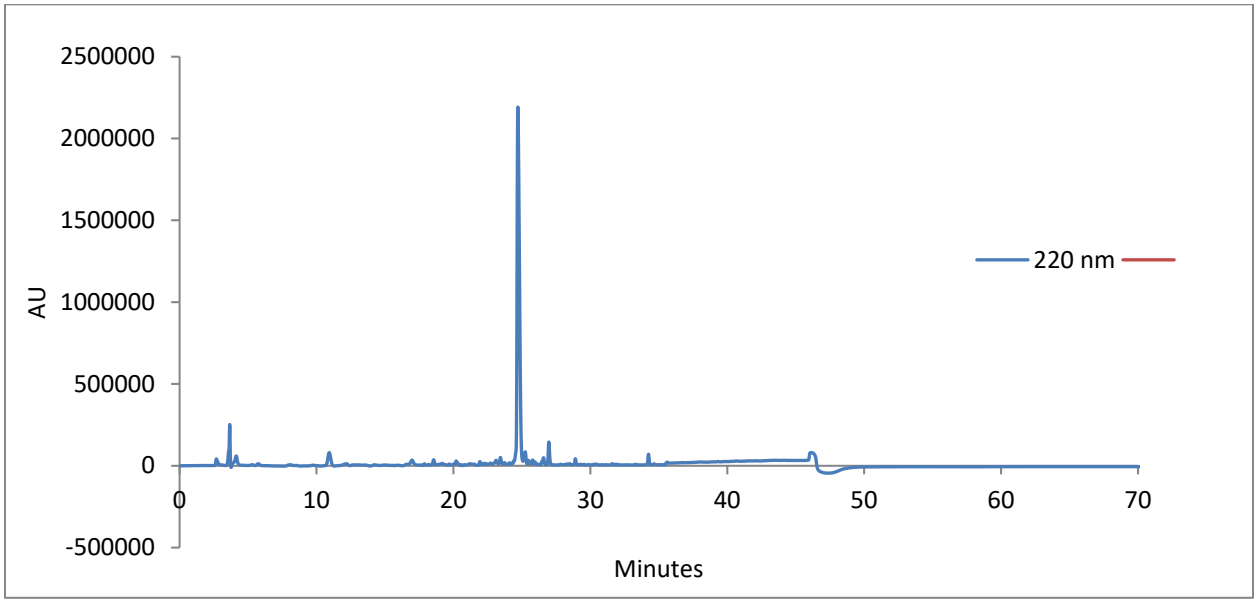

Glu Tyrosidine Analogue $C_{70}H_{87}N_{13}O_{16}$ (M+H) calculated: 1365.66, found 1365.67. HPLC retention time: 24.73 min

4.12 References

1. S. Raina; D. Missiakas, Making and Breaking Disulfide Bonds, *Annual Review of Microbiology* **1997** 51:1, 179-202

2. Lau, Y. H.; de Andrade, P.; Wu, Y.; Spring, D. R. Peptide stapling techniques based on different macrocyclization chemistries *Chem. Soc. Rev.* **2015**, 44, 91.

3. Walensky, L. D.; Kung, A. L.; Escher, I.; Malia, T. J.; Barbuto, Wright, R. D.; Wagner, G.; Verdine, G. L.; Korsmeyer, S. J. Activation of apoptosis in vivo by a hydrocarbon-stapled BH3 helix *Science,* **2004**, 305, 1466.

4. Wang, Y; Xiao, W; Zhang, Y; Meza, L; Tseng, H; Takada, Y; Ames, J. B.; Lam, K. S. Optimization of RGD containing cyclic peptides against αvβ3 integrin *Mol. Cancer Ther.* **2016**, 15(2): 232–240.

5. Walensky, L. D.; Pitter, K.; Morash, J.; Oh, K. J.; Barbuto, S.; Fisher, J.; Smith, E.; Verdine, G. L.; Korsmeyer, S. A stapled BID BH3 helix directly binds and activates BAX *J. Mol.Cell* **2006**, 24, 199.

6. Chang, Y. S.; Graves, B.; Guerlavais, V.; Tovar, C.; Packman, K.; To, K. H.; Olson, K. A.; Kesavan, K.; Gangurde, P.; Mukherjee, A.; Baker, T.; Darlak, K.; Elkin, C.; Filipovic, Z.; Qureshi, F. Z.; Cai, H.; Berry, P.; Feyfant, E.; Shi, X. E.; Horstick, J.; Annis, D. A.; Manning, A. M.; Fotouhi, N.; Nash, H.; Vassilev, L. T.; Sawyer, T. K. Stapled α-helical peptide drug development: a potent dual inhibitor of MDM2 and MDMX for p53-dependent cancer therapy *Proc. Natl. Acad. Sci. U. S. A.* **2013**, 110, E3445.

7. Walensky, L. D.; Bird, G. H. Hydrocarbon-Stapled Peptides: Principles, Practice, and Progress *J. Med. Chem.* **2014**, 57, 6275.

8. Bock J. E.; Gavenonis J.; Kritzer J. A. Getting in shape: controlling peptide bioactivity and bioavailability using conformational constraints. *ACS Chem. Biol.* **2013**, 8, 488–499.

9. Balaram P. Non-standard amino acids in peptide design and protein engineering. *Curr. Opin. Struct. Biol.* **1992**, 2, 845–851.

10. Schafmeister C. E.; Po J.; Verdine G. L. An all-hydrocarbon cross-linking system for enhancing the helicity and metabolic stability of peptides. *J. Am. Chem. Soc.* **2000**, 122, 5891–5892.

11. Blackwell H. E.; Grubbs R. H. Highly efficient synthesis of covalently cross-linked peptide helices by ring-closing metathesis. Angew. Chem,; Int. Ed. 1994, 37, 3281–3284.

12. Whelan J. Stapled peptide induces cancer cell death. *Drug Discovery Today* **2004**, 9, 907.

13. Barthe P.; Rochette S.; Vita C.; Roumestand C. Synthesis and NMR solution structure of an alpha-helical hairpin stapled with two disulfide bridges. *Protein Sci.* **2000**, 9, 942–955.

14. Blackwell H. E.; Sadowsky J. D.; Howard R. J.; Sampson J. N.; Chao J. A.; Steinmetz W. E.; O'Leary D. J.; Grubbs R. H. Ring-closing metathesis of olefinic peptides: design, synthesis, and structural characterization of macrocyclic helical peptides. *J. Org. Chem.* **2001**, 66, 5291–5302.

15. Williams R. M.; Sinclair P. J.; Zhai D.; Chen D. Practical asymmetric syntheses of alpha.-amino acids through carbon–carbon bond constructions on electrophilic glycine templates. *J. Am. Chem. Soc.* **1988**, 110, 1547–1557.

16. Bird G. H.; Bernal F.; Pitter K.; Walensky L. D. Synthesis and biophysical characterization of stabilized alpha-helices of BCL-2 domains. *Methods Enzymol.* **2008**, 446, 369–386.

17. Bird G. H.; Crannell C. W.; Walensky L. D. Chemical synthesis of hydrocarbon-stapled peptides for protein interaction research and therapeutic targeting *Curr. Protoc. Chem. Biol.* **2011**, 3, 99–117.

18. Kim Y. W.; Grossmann T. N.; Verdine G. L. Synthesis of all-hydrocarbon stapled alpha-helical peptides by ring-closing olefin metathesis. *Nat. Protoc.* **2011**, 6, 761–771.

19. Walensky L. D.; Pitter K.; Morash J.; Oh K. J.; Barbuto S.; Fisher J.; Smith E.; Verdine G. L.; Korsmeyer S. J. A stapled BID BH3 helix directly binds and activates BAX. Mol. Cell 2006, 24, 199–210.

20. Bird G. H.; Madani N.; Perry A. F.; Princiotto A. M.; Supko J. G.; He X.; Gavathiotis E.; Sodroski J. G.; Walensky L. D. Hydrocarbon double-stapling remedies the proteolytic instability of a lengthy peptide therapeutic *Proc. Natl. Acad. Sci. U.S.A.* **2010**, 107, 14093–14098.

21. Baek S.; Kutchukian P. S.; Verdine G. L.; Huber R.; Holak T. A.; Lee K. W.; Popowicz G. M. Structure of the stapled p53 peptide bound to Mdm2 *J. Am. Chem. Soc.* **2012**, 134, 103–106.

22. Chang Y. S.; Graves B.; Guerlavais V.; Tovar C.; Packman K.; To K. H.; Olson K. A.; Kesavan K.; Gangurde P.; Mukherjee A.; Baker T.; Darlak K.; Elkin C.; Filipovic Z.; Qureshi F. Z.; Cai H.; Berry P.; Feyfant E.; Shi X. E.; Horstick J.; Annis D. A.; Manning A. M.; Fotouhi N.; Nash H.; Vassilev L. T.; Sawyer T. K. Stapled alpha-helical peptide drug development: a potent dual inhibitor of MDM2 and MDMX for p53-dependent cancer therapy *Proc. Natl. Acad. Sci. U.S.A.* **2013**, 110, E3445–E3454.

23. Kim Y. W.; Kutchukian P. S.; Verdine G. L. Introduction of all-hydrocarbon i,i+3 staples into alpha-helices via ring-closing olefin metathesis *Org. Lett.* **2010**, 12, 3046–3049.

24. Platt R. J.; Han T. S.; Green B. R.; Smith M. D.; Skalicky J.; Gruszczynski P.; White H. S.; Olivera B.; Bulaj G.; Gajewiak J. Stapling mimics noncovalent interactions of gamma-carboxyglutamates in conantokins, peptidic antagonists of N-methyl-d-aspartic acid receptors *J. Biol. Chem.* **2012**, 287, 20727–20736.

25. Long Y. Q.; Huang S. X.; Zawahir Z.; Xu Z. L.; Li H.; Sanchez T. W.; Zhi Y.; De Houwer S.; Christ F.; Debyser Z.; Neamati N. Design of cell-permeable stapled peptides as HIV-1 integrase inhibitors. *J. Med. Chem*. **2013**, 56, 5601–5612.

26. Blackwell, H. E.; Grubbs, R. H. Highly Efficient Synthesis of Covalently Cross-Linked Peptide Helices by Ring-Closing Metathesis *Angew. Chem,; Int. Ed.* **1998**, 37, 3281.

27. Scrima, M.; Le Chevalier-Isaad, A.; Rovero, P.; Papini, A. M.; Chorev, M.; D'Ursi, A. M. Eur. J. Org. Chem. 2010, 2010, 446. (b) Lau, Y.; de Andrade, P.; Quah, S.-T.; Rossmann, M.; Laraia, L.; Skold, N.; Sum, T.; Rowling, P.; Joseph, T.; Verma, C.; Hyvonen, M.; Itzhaki, L.; Venkitaraman, A.; Brown, C.; Lane, D.; Spring, D. Functionalized staple linkages for modulating the cellular activity of stapled peptides *Chem. Sci.* **2014**, 5, 1804.

28. Jo, H.; Meinhardt, N.; Wu, Y.; Kulkarni, S.; Hu, Z.; Low, K. E.; Davies, P. L.; DeGrado, W. F.; Greenbaum, D. C. Stapling peptides using cysteine crosslinking *J. Am. Chem. Soc.* **2012**, 134, 17704.

29. Lai, J.-I,; Leman, L.J,; Ku, S,; Vickers, C.J,; Olsen, C.A,; Montero, A,; Ghadiri, M.R,; and Gottesfeld, J.M. Cyclic tetrapeptide HDAC inhibitors as potential therapeutics for spinal muscular atrophy: Screening with iPSC-derived neuronal cells *Bioorg. Med. Chem. Lett.* **2017**, 27, 3289-3293.

30. Bruno Lunelli. New, optimized preparation of 1,2-dichlorocyclobuten-3,4-dione (C4O2Cl2) from squaric acid and oxalyl chloride. *Tetrahedron Letters* **2007,** *48* (20) , 3595-3597.

31. Ximenis, M,; Pitarch-Jarque, J,; Blasco, S.; Rotger, C,; García-España, E,; Costa, A. Water-Soluble Squaramide Dihydrates: N-Methylation Modulates the Occurrence of One- and Two-Dimensional Water Clusters through Hydrogen Bonding and Dipolar Interactions *Cryst. Growth Des.* **2018,** 18, 8, 4420-4427

32. Nanyan, F.; Allen, A. D.; Kobayashi, S.; Tidwell, T. T.; Vukovic, S.; Matsuoka, T; Mishima, M. Structural Effects on Interconversion of Oxygen-Substituted Bisketenes and Cyclobutenediones *The Journal of Organic Chemistry* **2008** *73* (5), 1768-1773

33. Xiao, Q.; Becar, N. A.; Brown, N. P.; Smith, M. S.; Stern, K. L.; Draper, S. R. E.; Thompson, K. P.; Price, J. L. Stapling of two PEGylated side chains increases the conformational stability of the WW domain via an entropic effect *Org. Biomol. Chem.* **2018**,16, 8933-8939

34. Lautrette, G.; Touti, F.;Lee, H. G.; Dai, P.; Pentelute, B. L. Nitrogen Arylation for Macrocyclization of Unprotected Peptides *J. Am. Chem. Soc.* **2016**, 138, 27, 8340-8343

Appendix A NMR Spectra for Chapters 2,3 and 4.

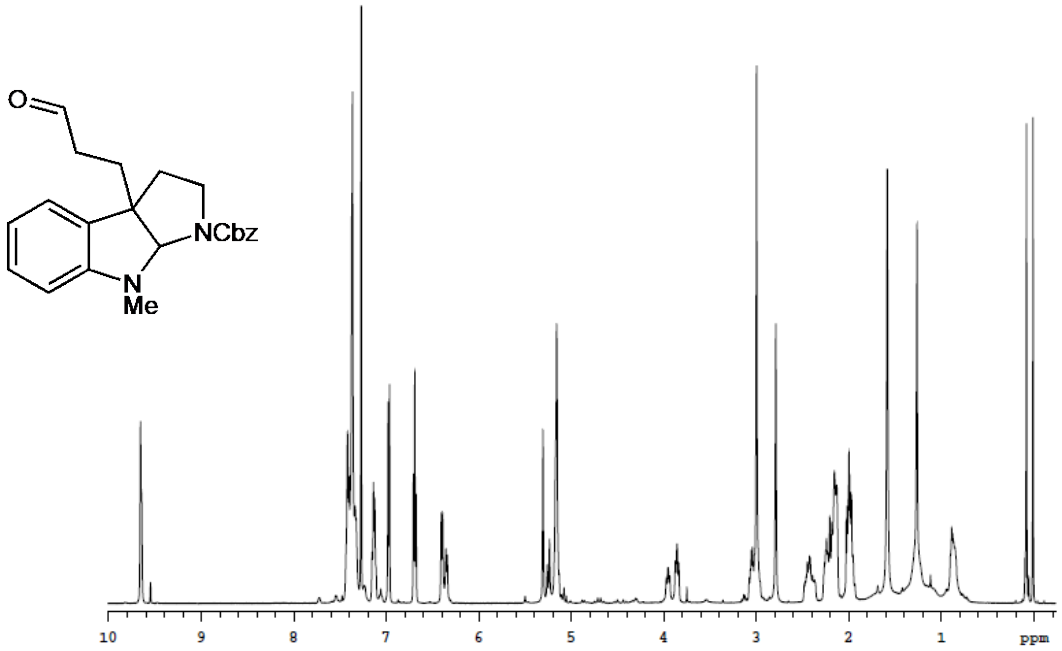

Benzyl 3a-(3-oxopropyl)-3,3a,8,8a-tetrahydropyrrolo[2,3-b]indole-1(2H)-carboxylate, ^{1}H NMR

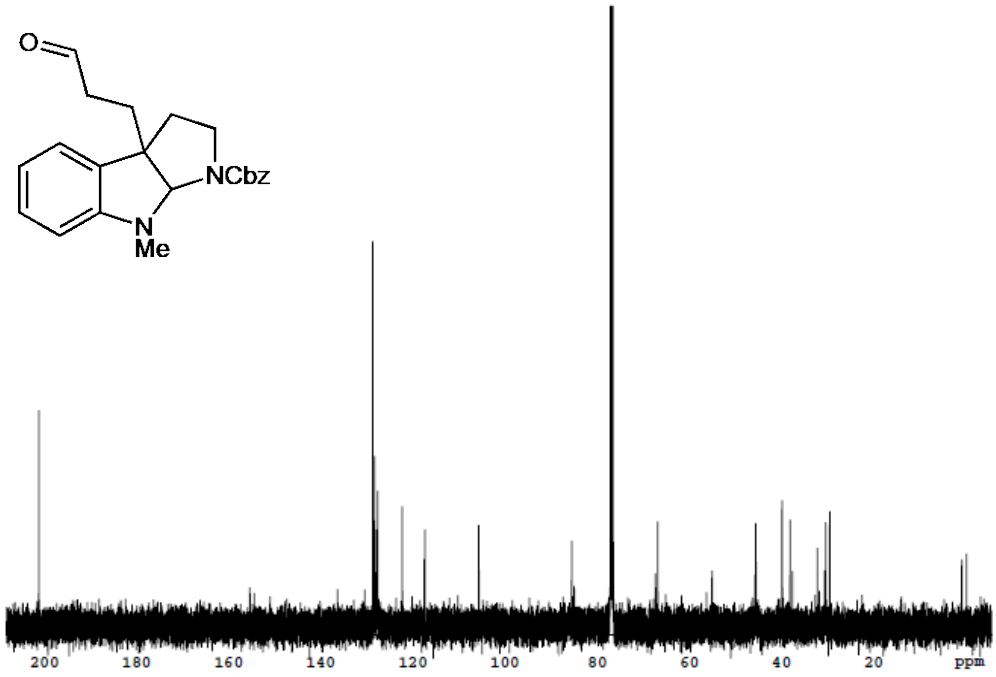

Benzyl 3a-(3-oxopropyl)-3,3a,8,8a-tetrahydropyrrolo[2,3-b]indole-1(2H)-carboxylate, ^{13}C NMR

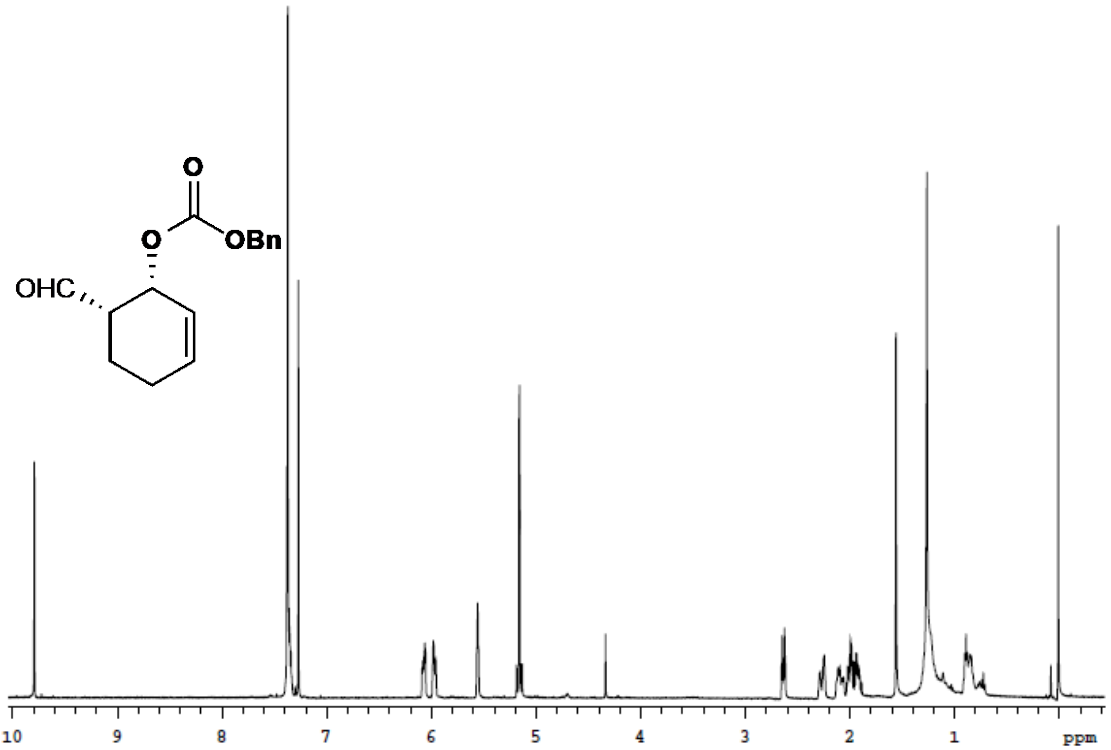

Benzyl (6-formyl-5-methylcyclohex-2-en-1-yl) carbonate, ^{1}H NMR

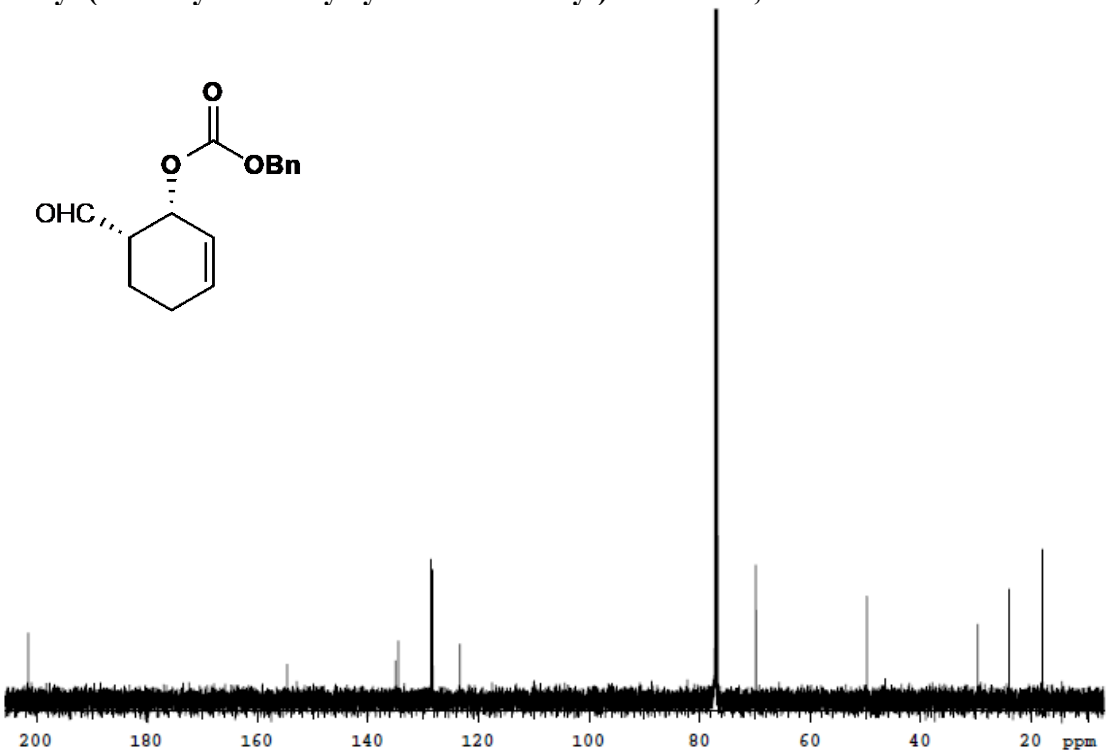

Benzyl (6-formyl-5-methylcyclohex-2-en-1-yl) carbonate, ^{13}C NMR

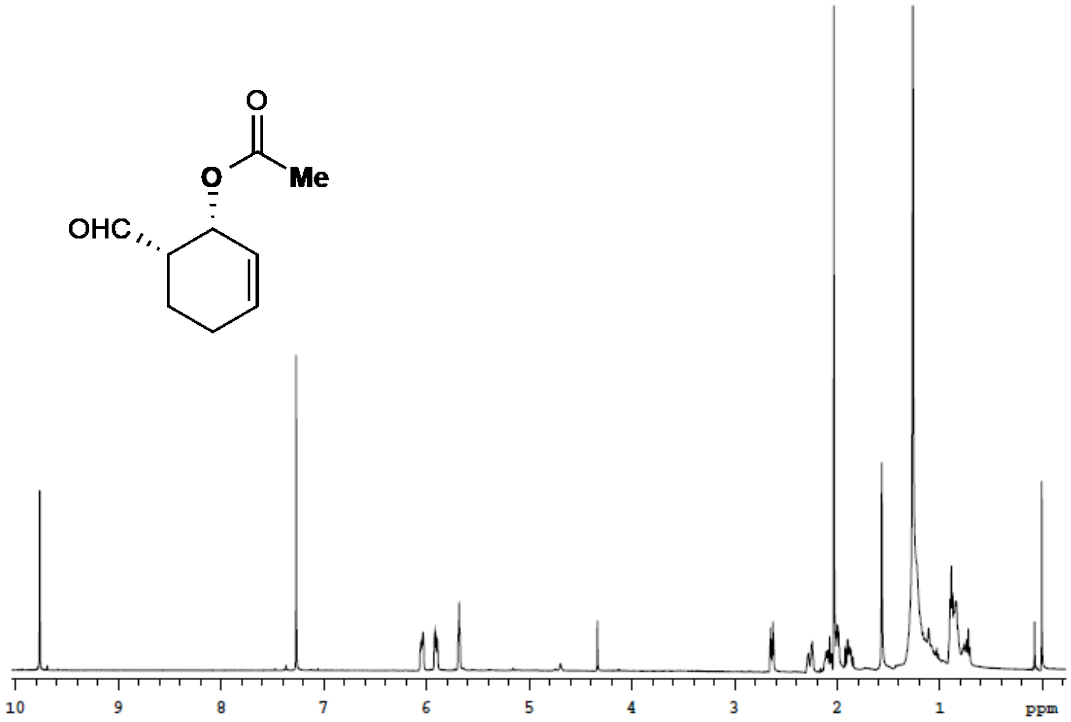

6-formyl-5-methylcyclohex-2-en-1-yl acetate, ^{1}H NMR

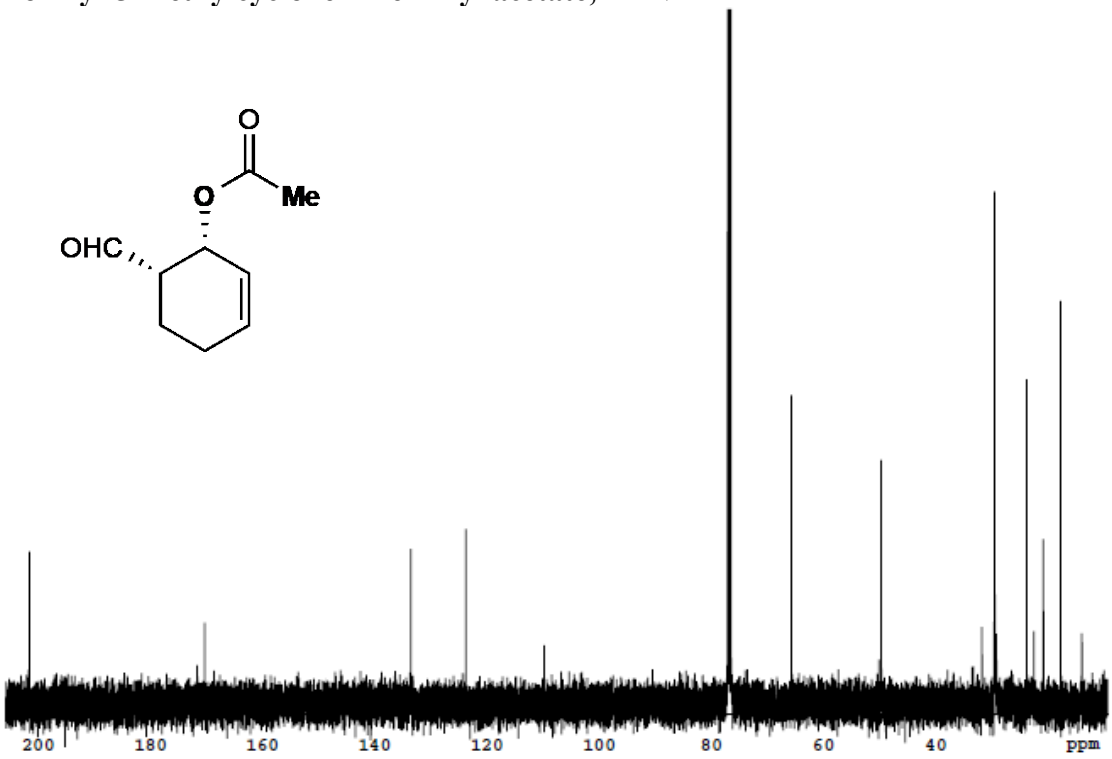

6-formyl-5-methylcyclohex-2-en-1-yl acetate, ^{13}C NMR

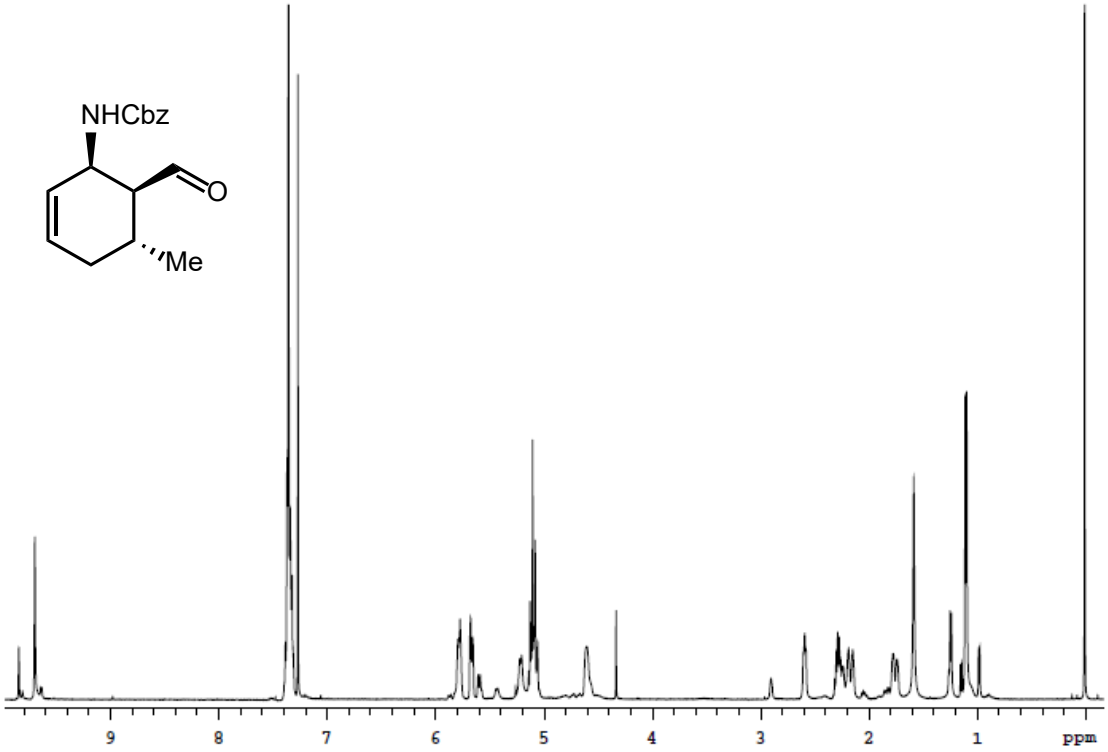

Benzyl ((1R,5R,6S)-6-formyl-5-methylcyclohex-2-en-1-yl)carbamate, ^{1}H NMR

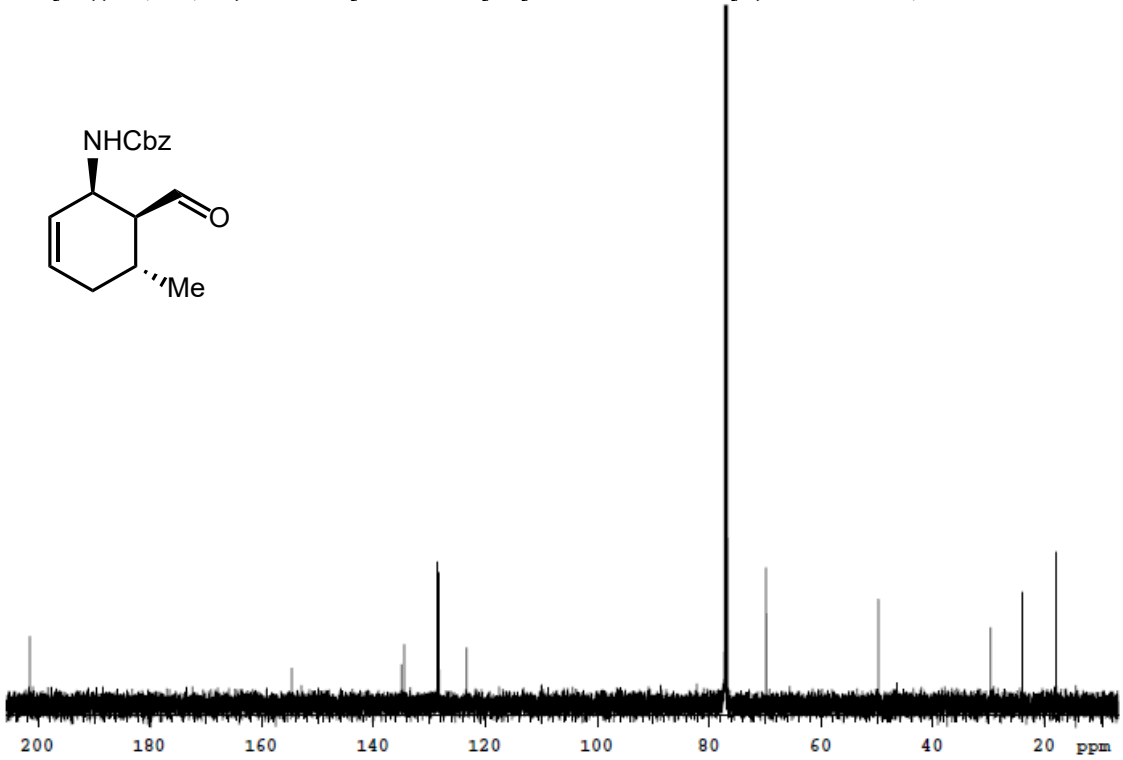

Benzyl ((1R,5R,6S)-6-formyl-5-methylcyclohex-2-en-1-yl)carbamate, ^{13}C NMR

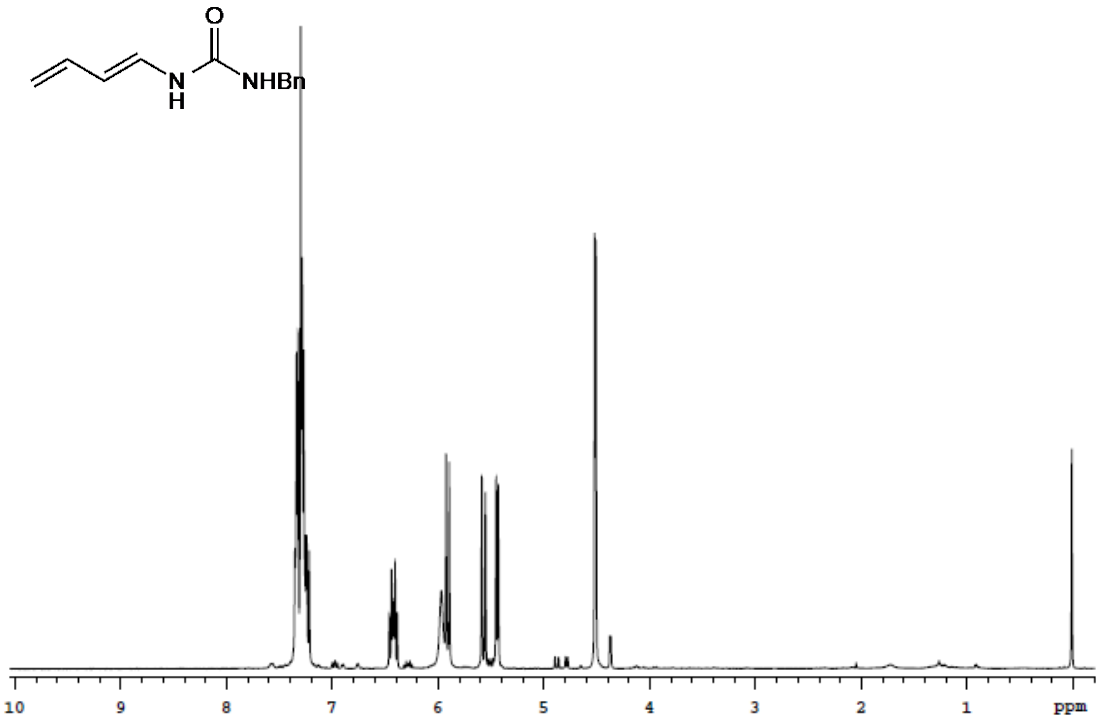

(E)-1-benzyl-3-(buta-1,3-dien-1-yl)urea, ^{1}H NMR

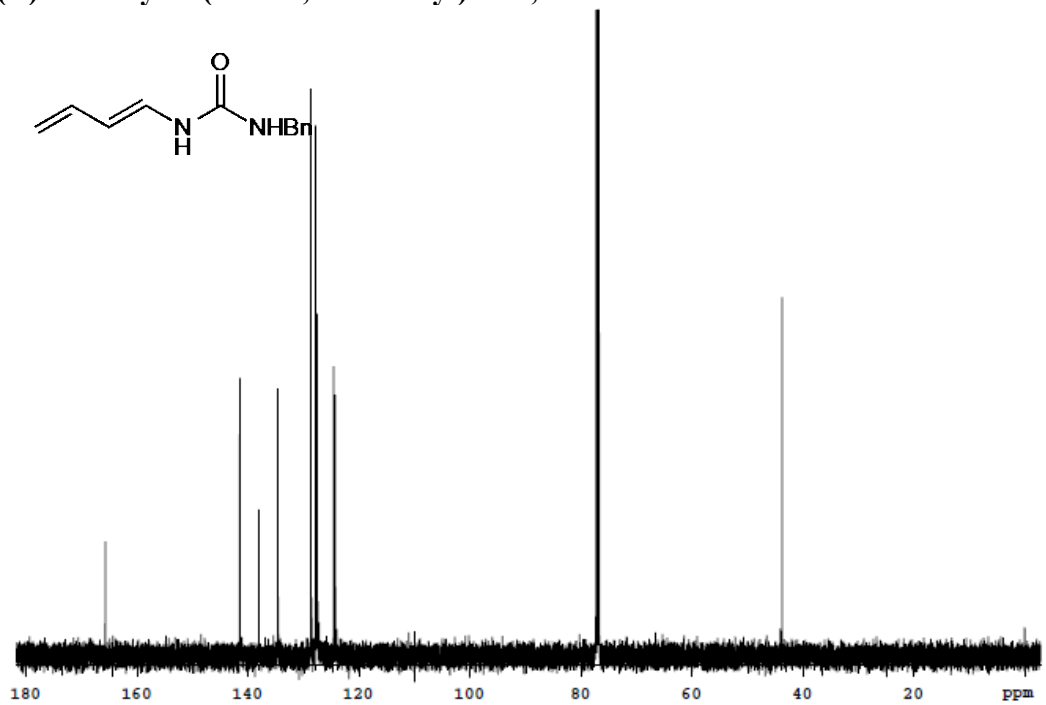

(E)-1-benzyl-3-(buta-1,3-dien-1-yl)urea, ^{13}C NMR

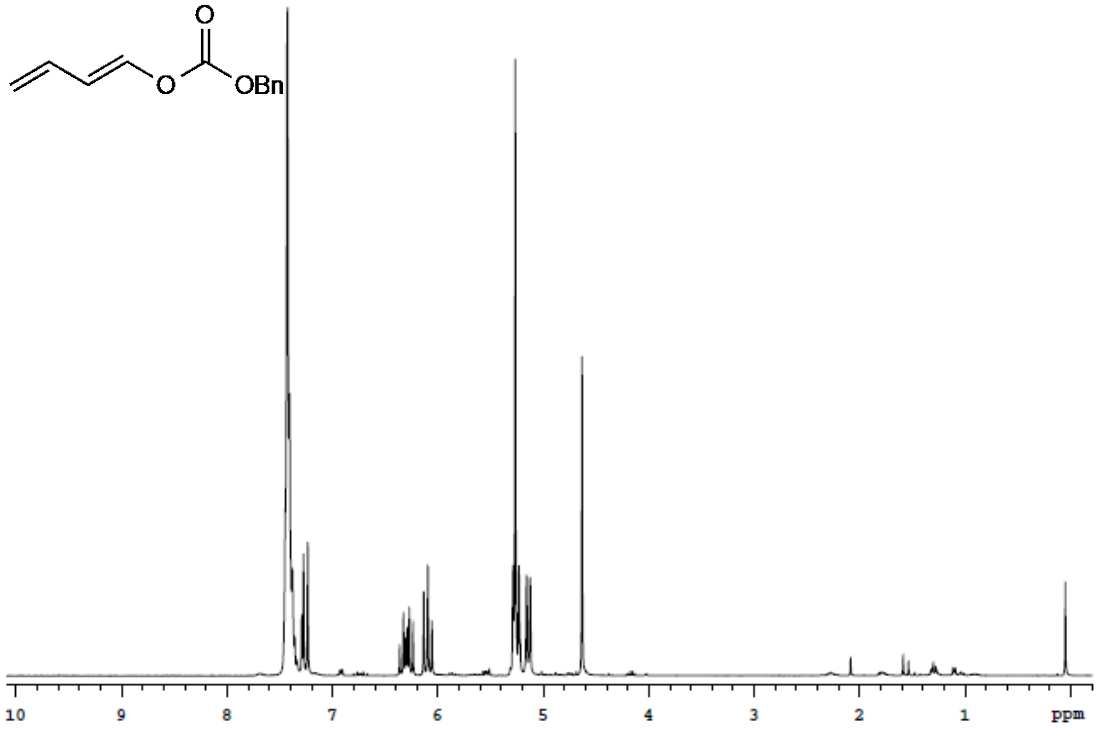

(E)-benzyl buta-1,3-dien-1-yl carbonate, ^{1}H NMR

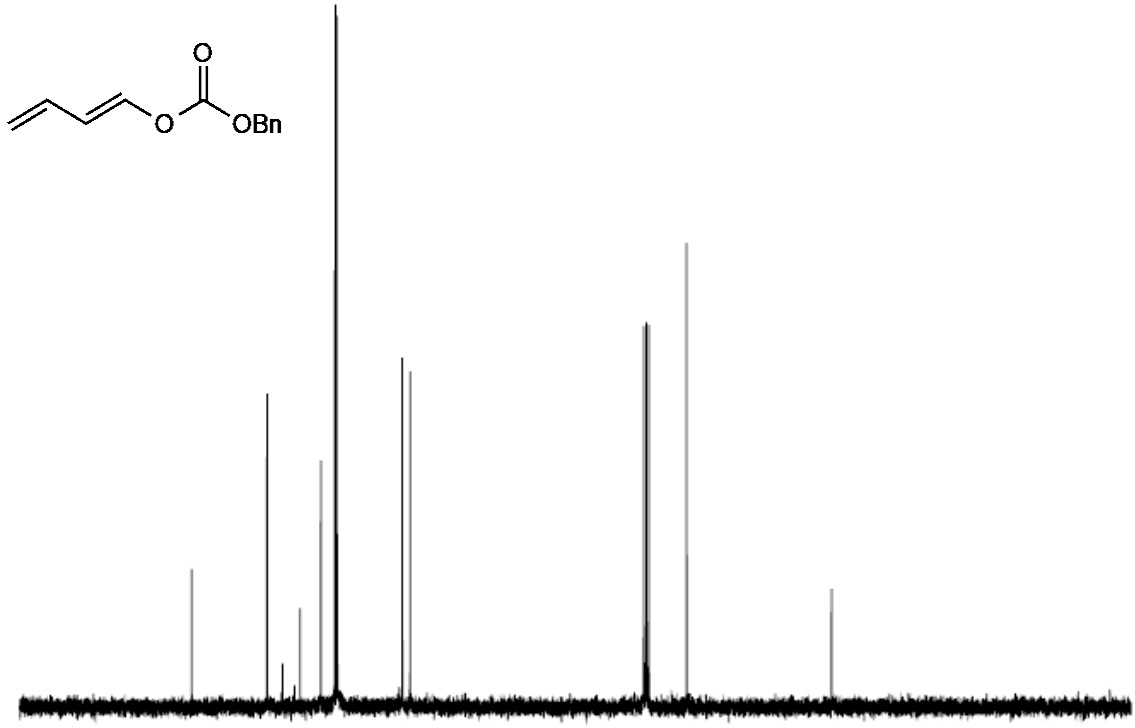

(E)-benzyl buta-1,3-dien-1-yl carbonate, ^{13}C NMR

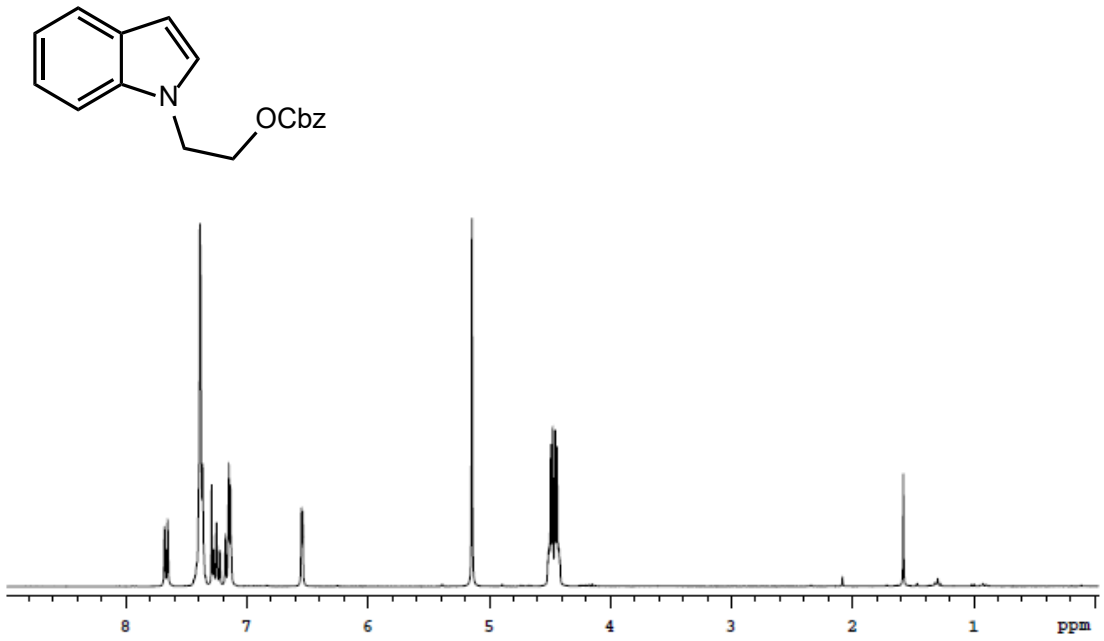

2-(1H-indol-1-yl)ethyl benzyl carbonate, ^{1}H NMR

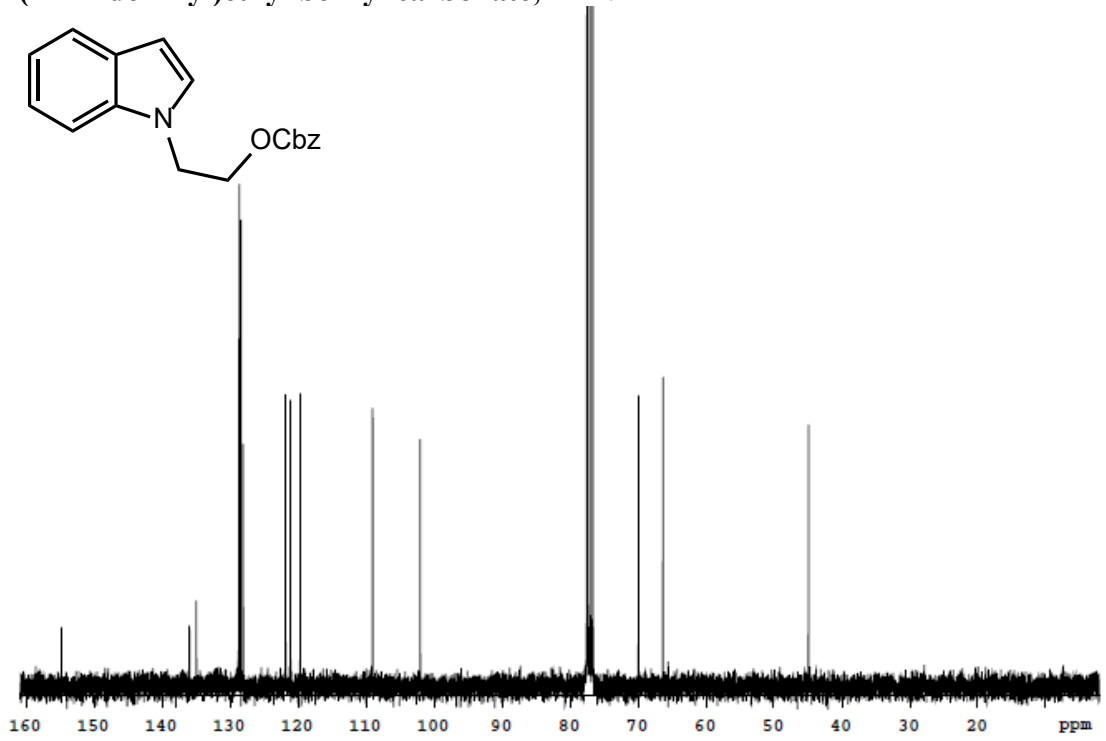

2-(1H-indol-1-yl)ethyl benzyl carbonate, ^{13}C NMR

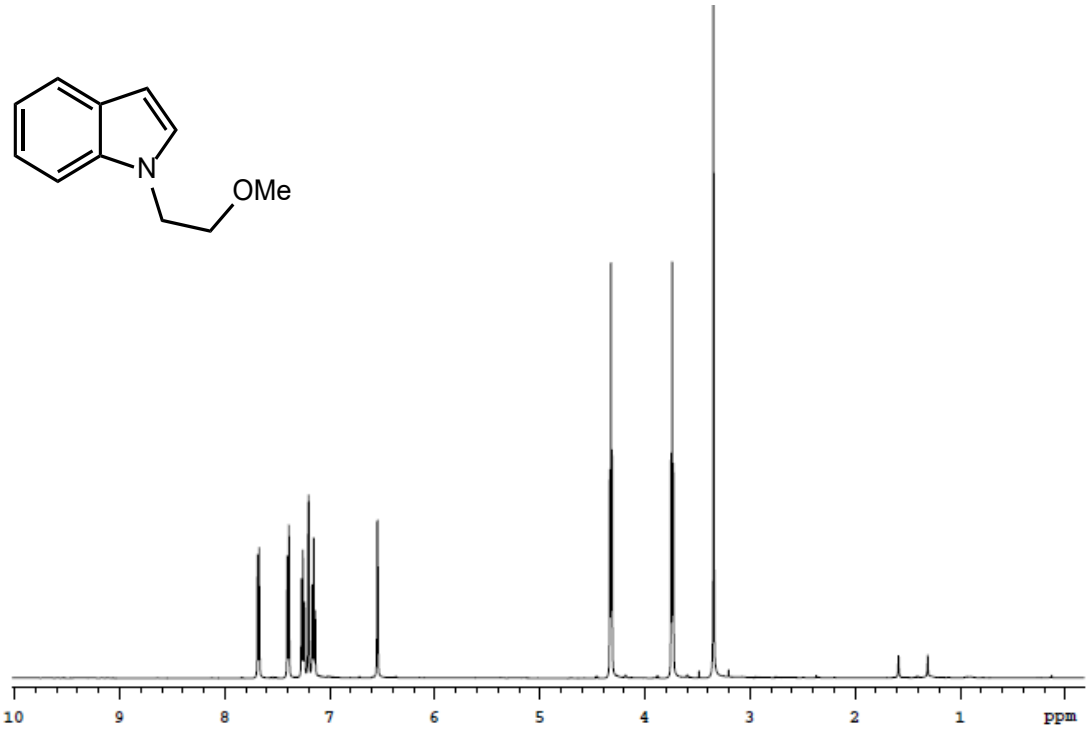

1-(2-methoxyethyl)-1H-indole, ^{1}H NMR

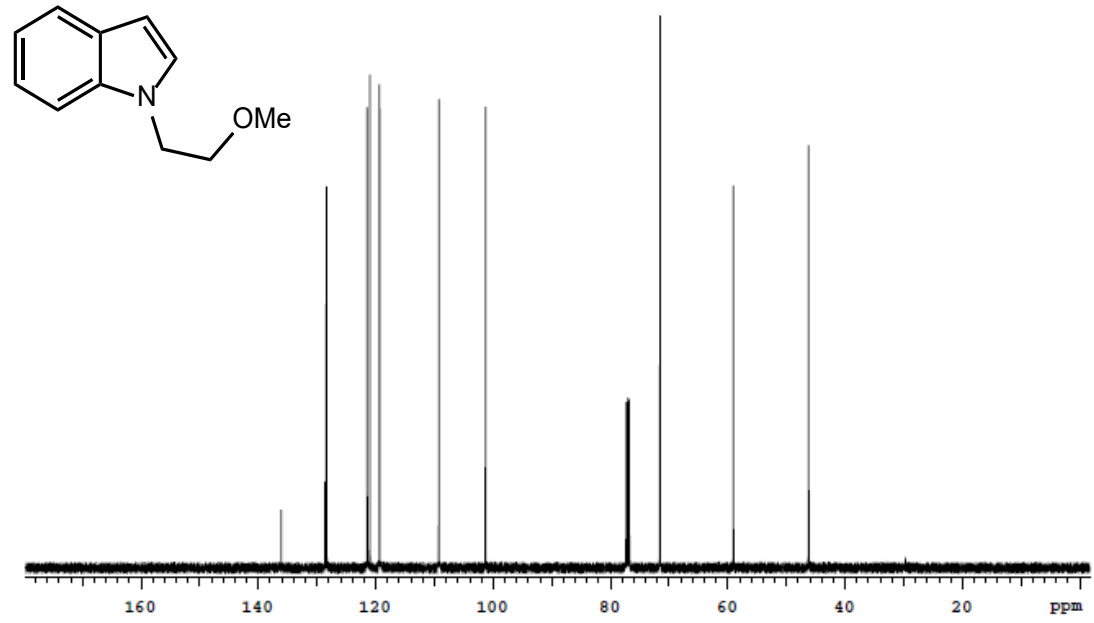

1-(2-methoxyethyl)-1H-indole, ^{13}C NMR

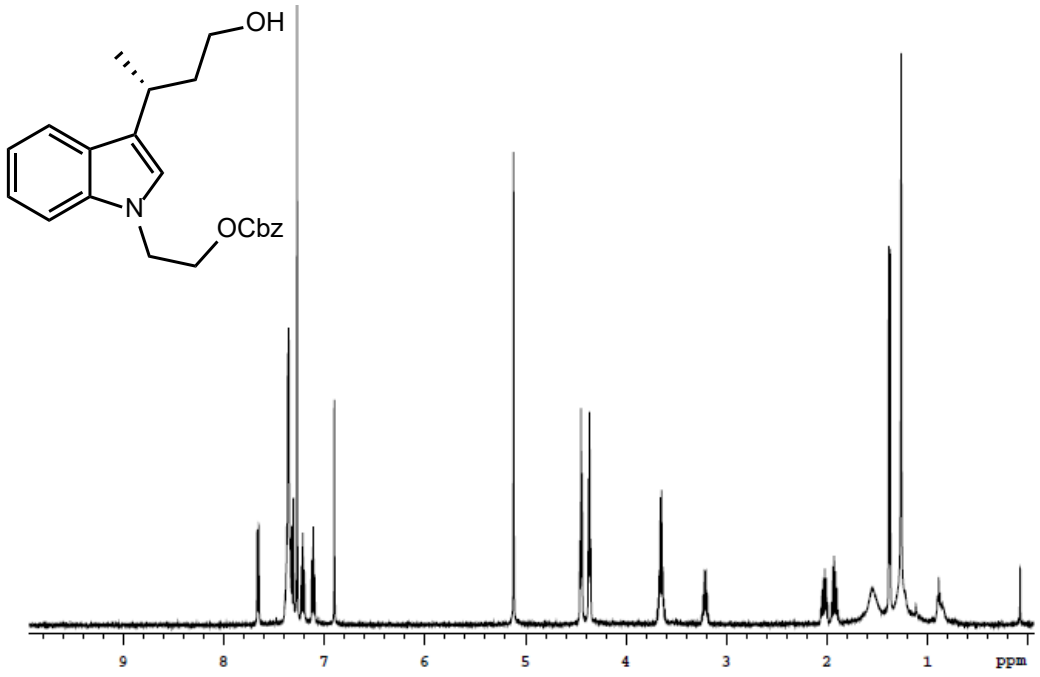

(R)-benzyl (2-(3-(4-oxobutan-2-yl)-1H-indol-1-yl)ethyl) carbonate, ^{1}H NMR

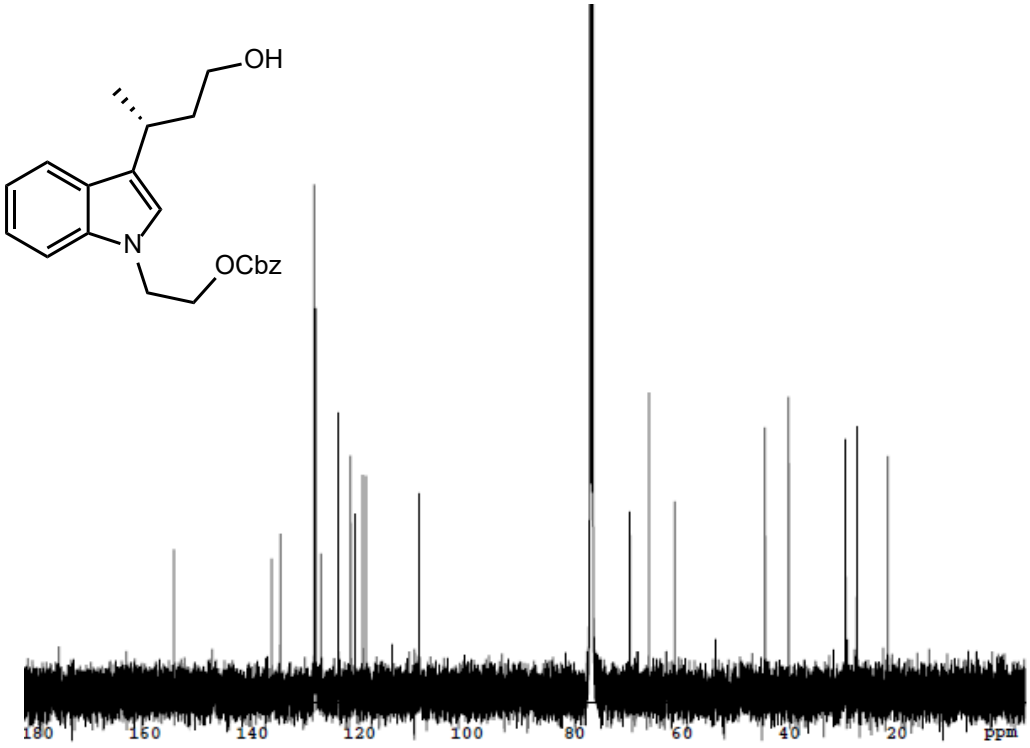

(R)-benzyl (2-(3-(4-oxobutan-2-yl)-1H-indol-1-yl)ethyl) carbonate, ^{13}C NMR

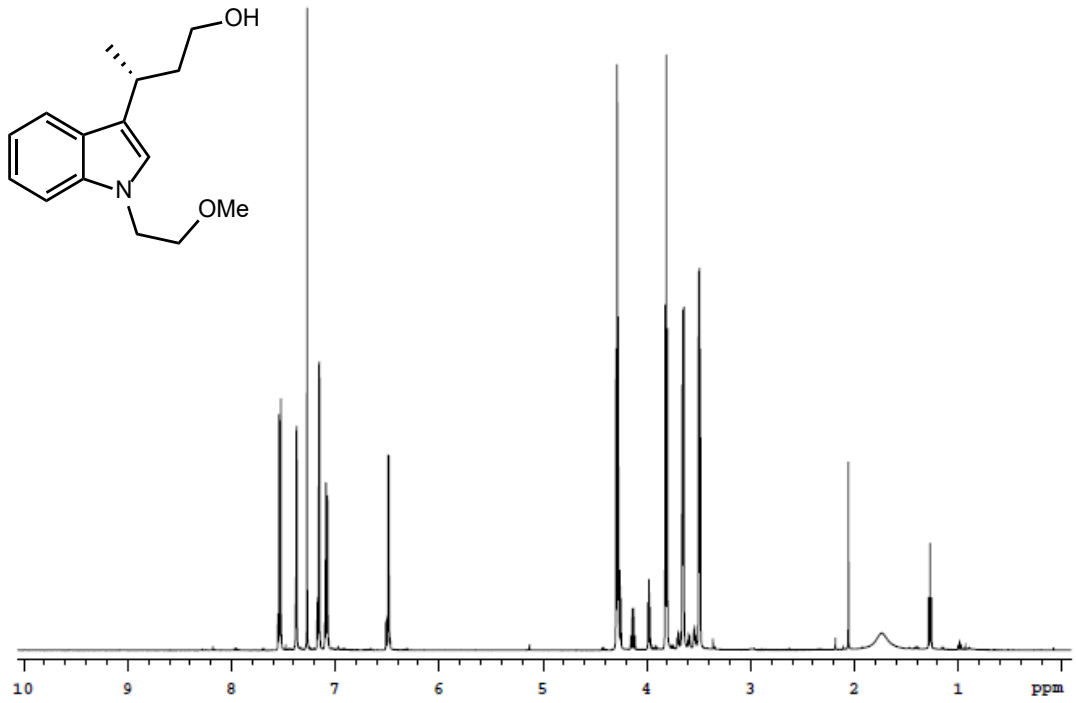

(R)-3-(1-(2-methoxyethyl)-1H-indol-3-yl)butanol, ^{1}H NMR

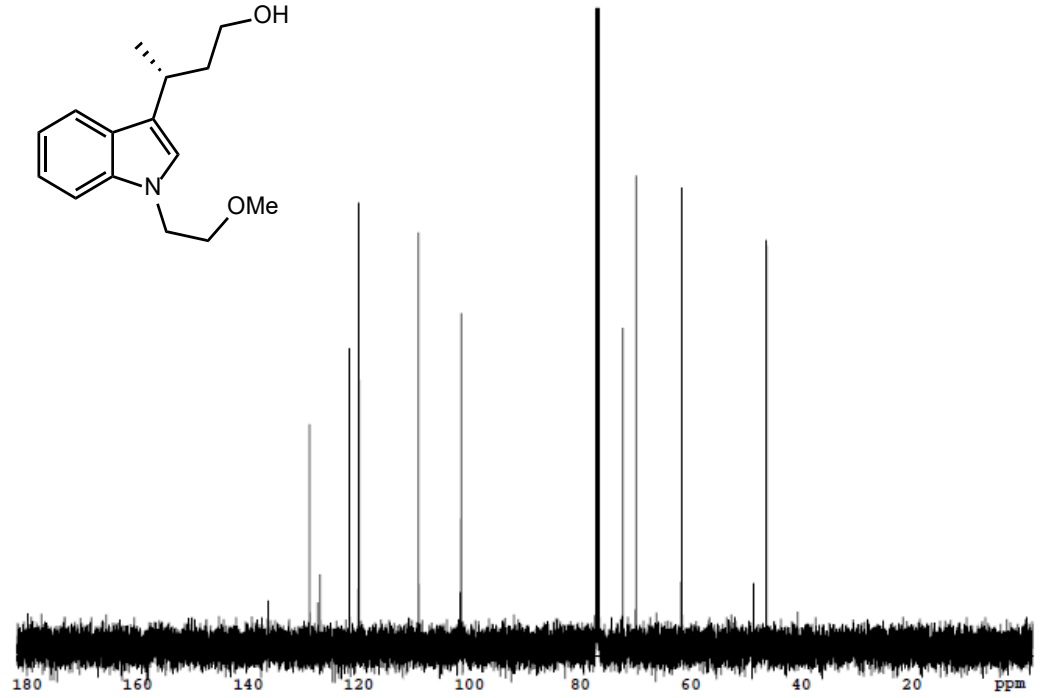

(R)-3-(1-(2-methoxyethyl)-1H-indol-3-yl)butanol, ^{13}C NMR

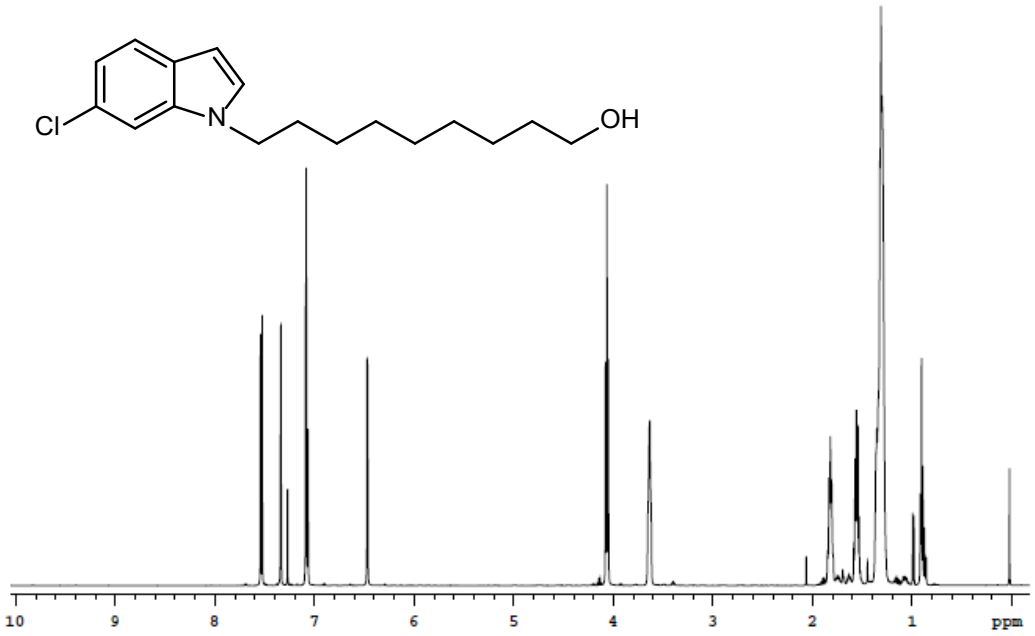

9-(6-chloro-1H-indol-1-yl)nonan-1-ol, ^{1}H NMR

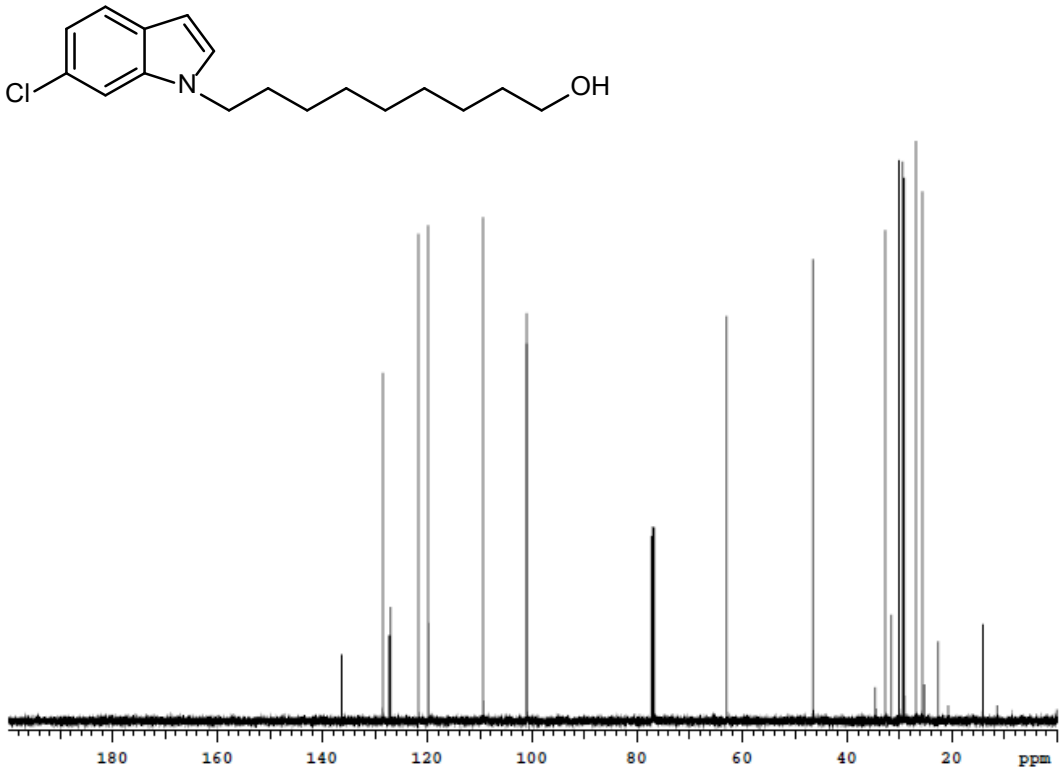

9-(6-chloro-1H-indol-1-yl)nonan-1-ol, ^{13}C NMR

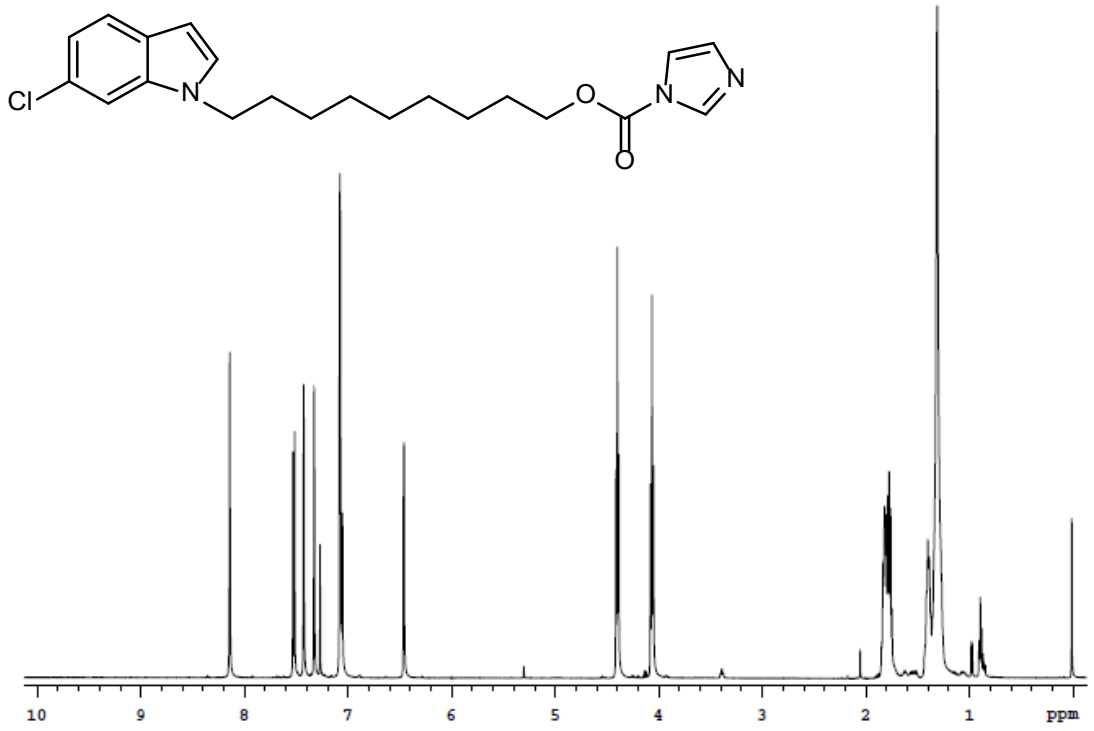

-(9-(6-chloro-1H-indol-1-yl)nonyl)-1H-imidazole-1-carboxamide, ^{1}H NMR

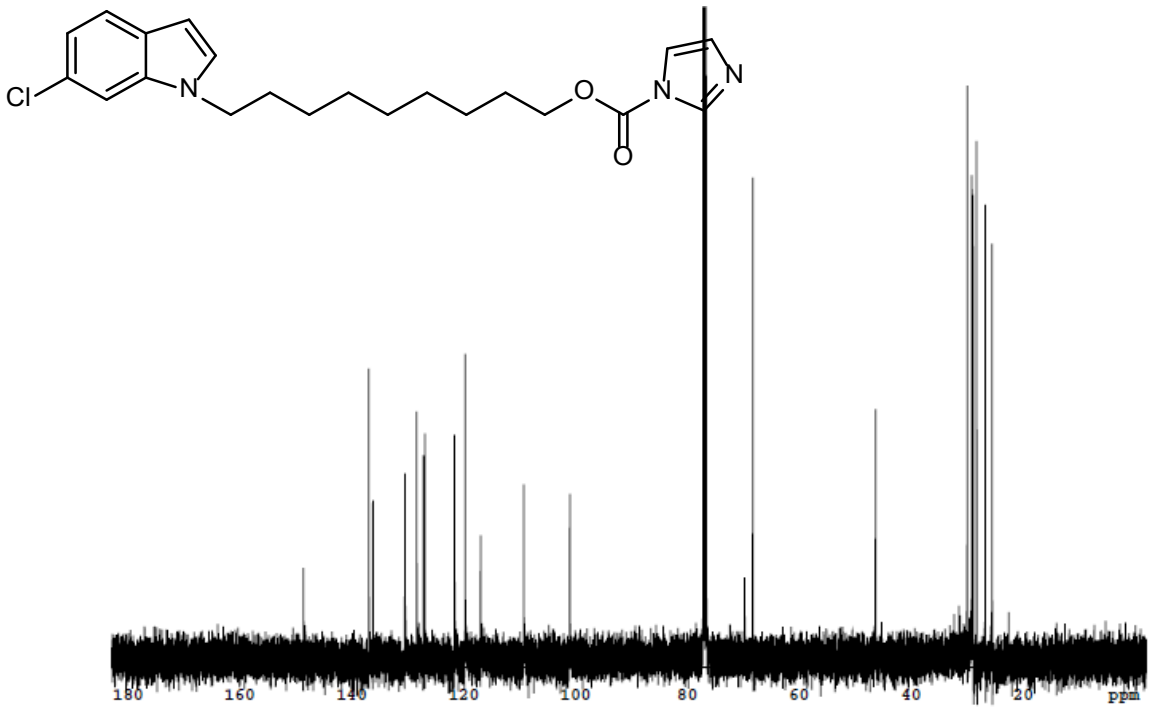

-(9-(6-chloro-1H-indol-1-yl)nonyl)-1H-imidazole-1-carboxamide, ^{13}C NMR

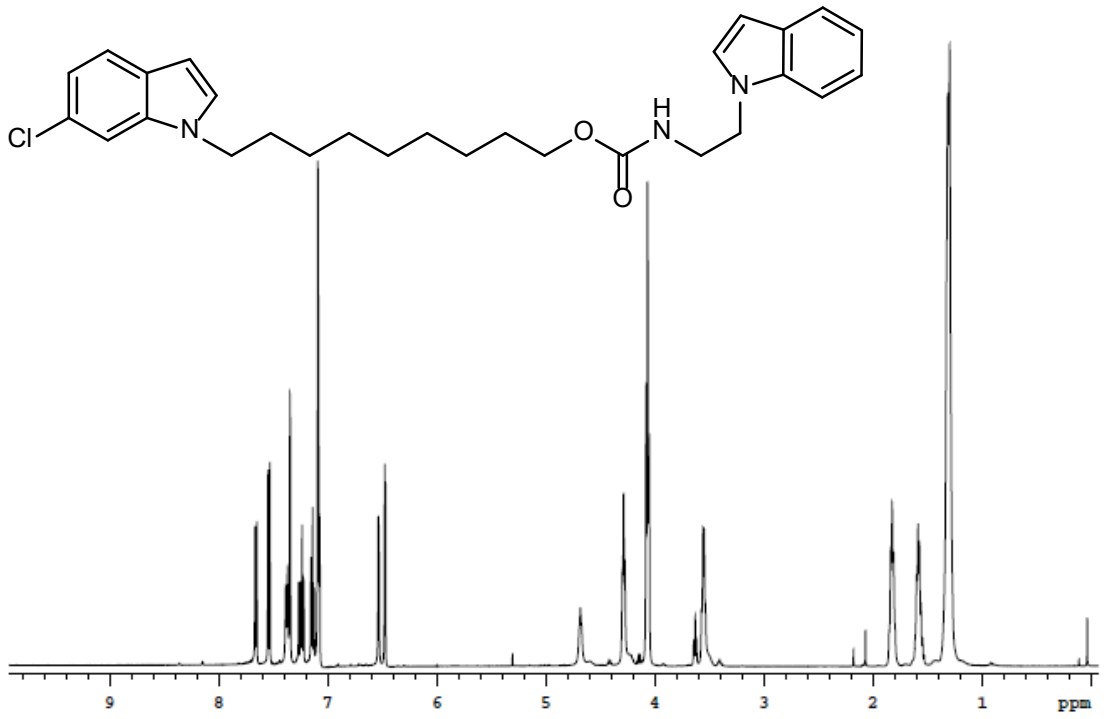

2-(1H-indol-1-yl)ethyl (9-(6-chloro-1H-indol-1-yl)nonyl)carbamate, ^{1}H NMR

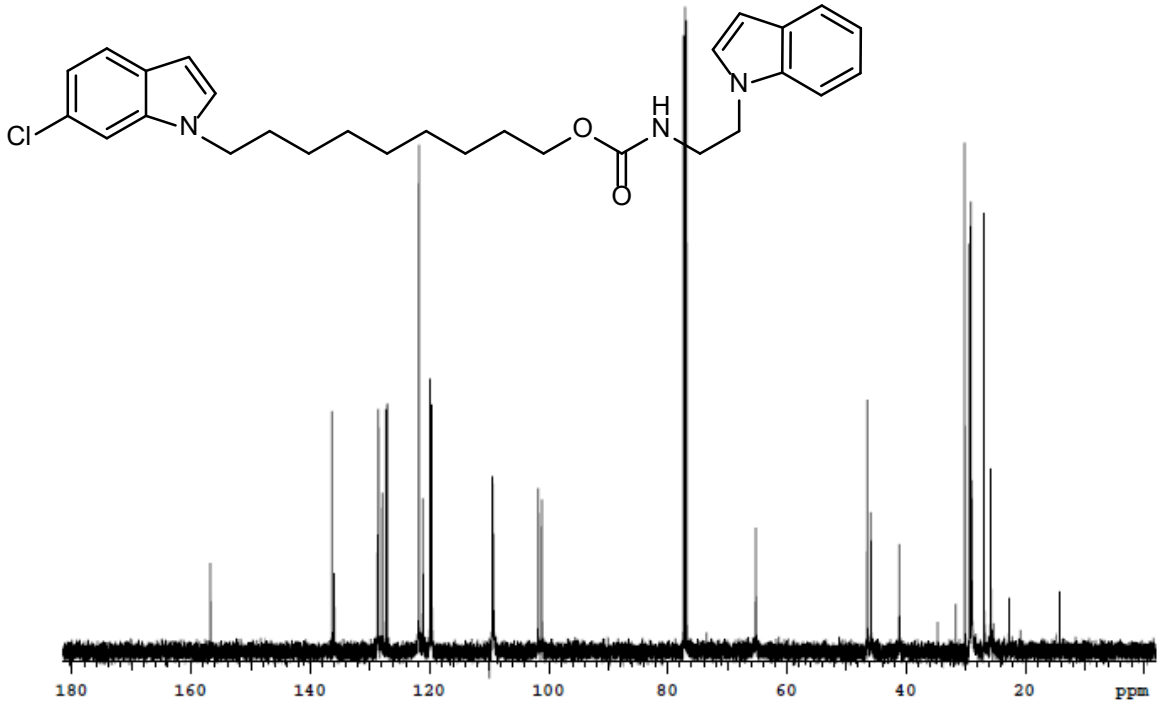

2-(1H-indol-1-yl)ethyl (9-(6-chloro-1H-indol-1-yl)nonyl)carbamate, ^{13}C NMR

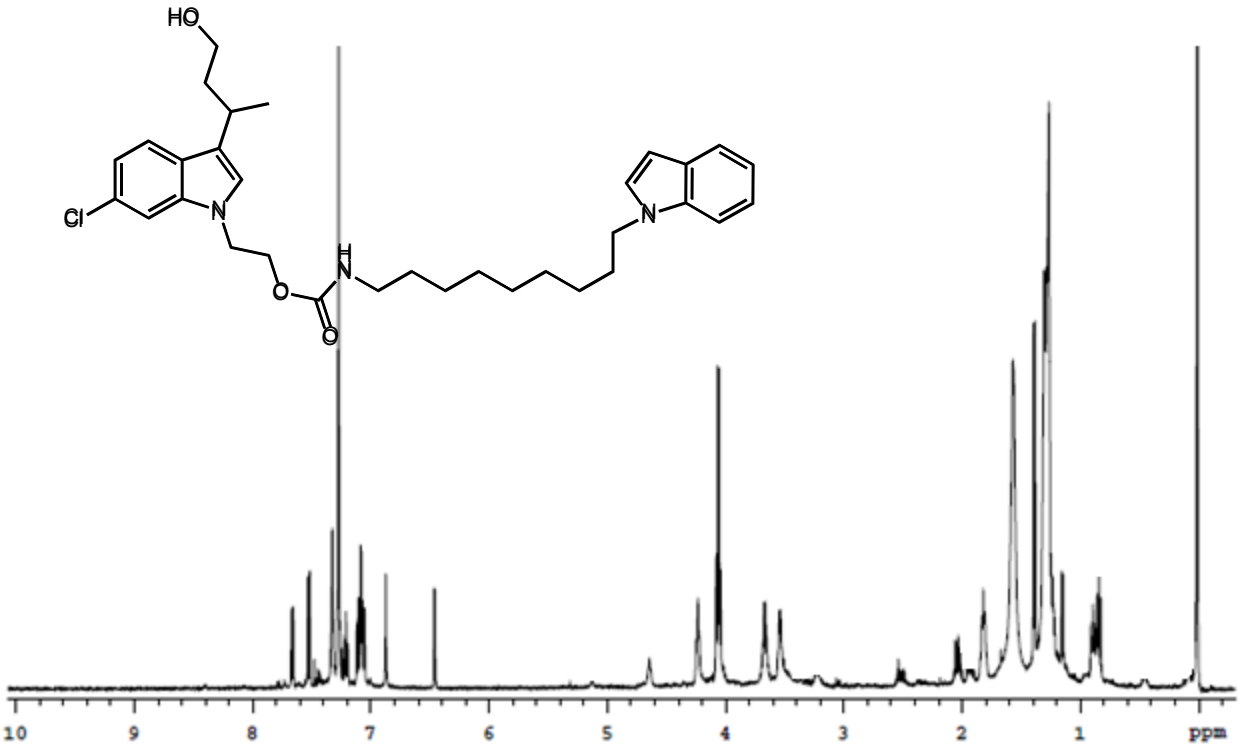

2-(6-chloro-3-(4-hydroxybutan-2-yl)-1H-indol-1-yl)ethyl (9-(1H-indol-1-yl)nonyl)carbamate, ^{1}H NMR

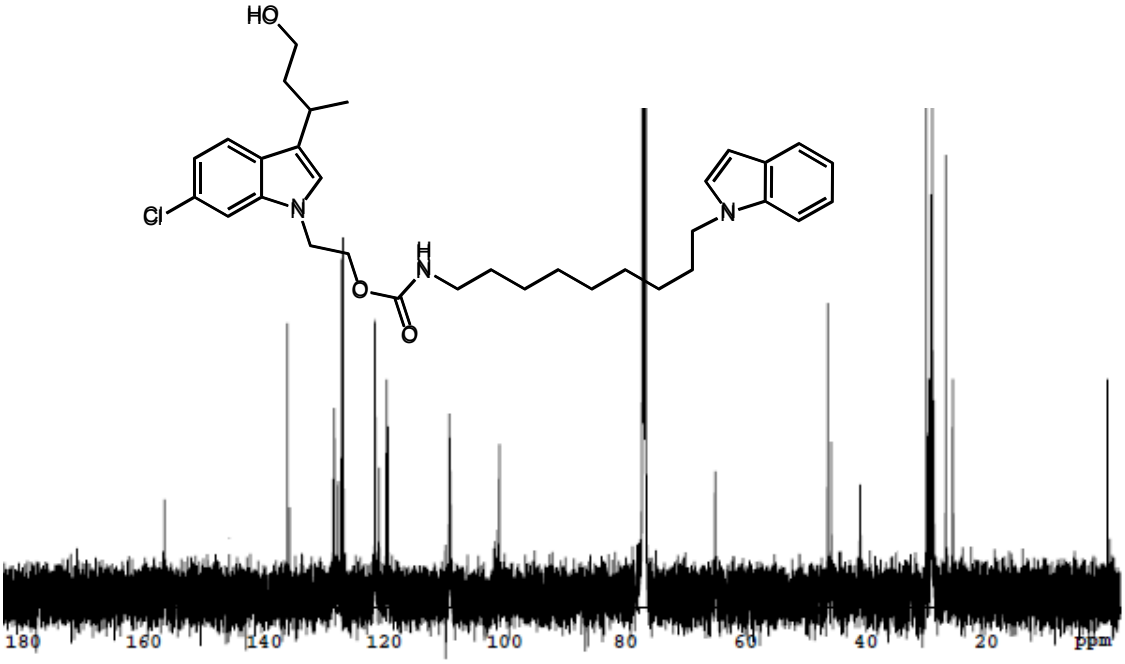

2-(6-chloro-3-(4-hydroxybutan-2-yl)-1H-indol-1-yl)ethyl (9-(1H-indol-1-yl)nonyl)carbamate, ^{13}C NMR

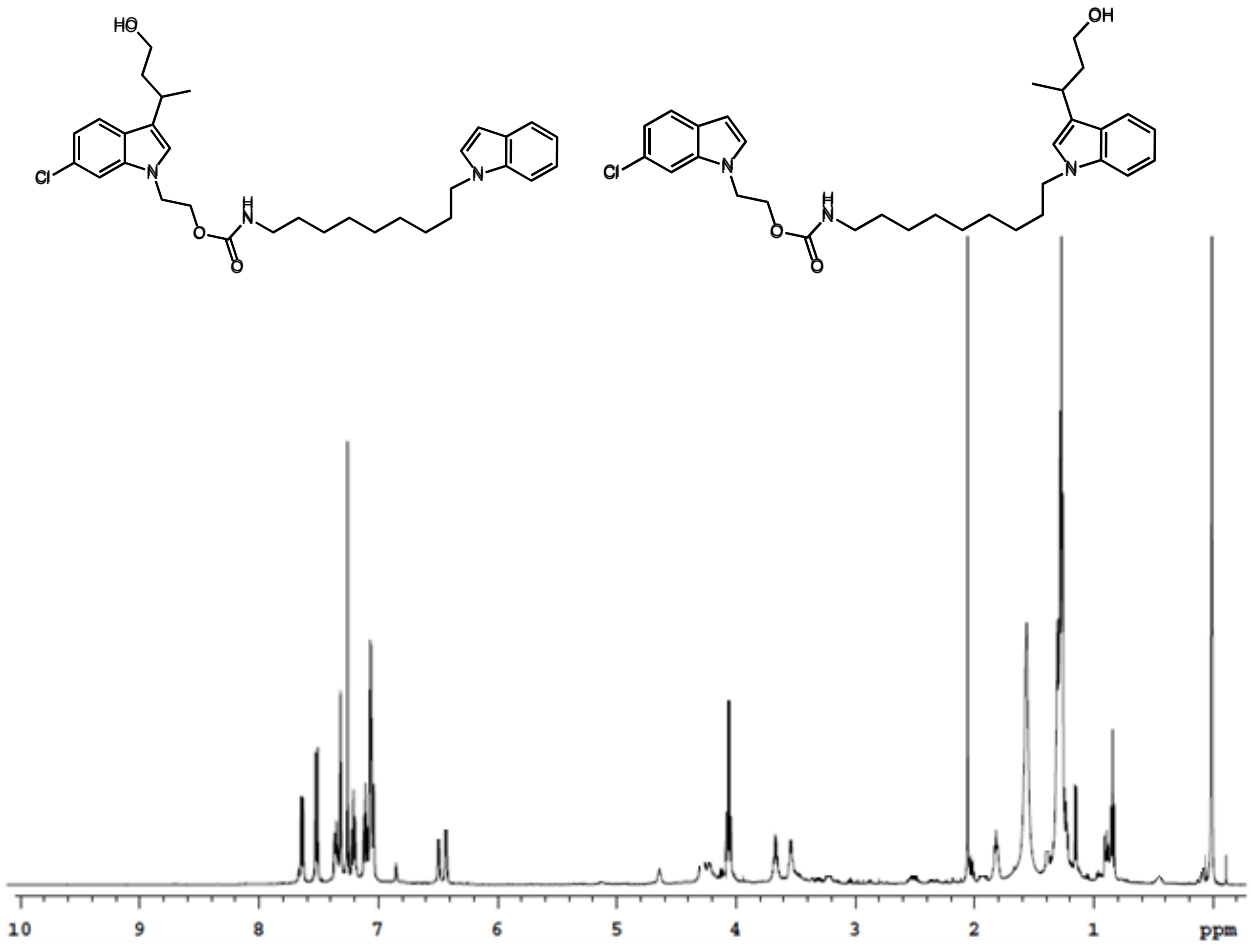

2-(6-chloro-3-(4-hydroxybutan-2-yl)-1H-indol-1-yl)ethyl (9-(1H-indol-1-yl)nonyl)carbamate and 2-(6-chloro-1H-indol-1-yl)ethyl (9-(3-(4-hydroxybutan-2-yl)-1H-indol-1-yl)nonyl)carbamate ^{1}H NMR

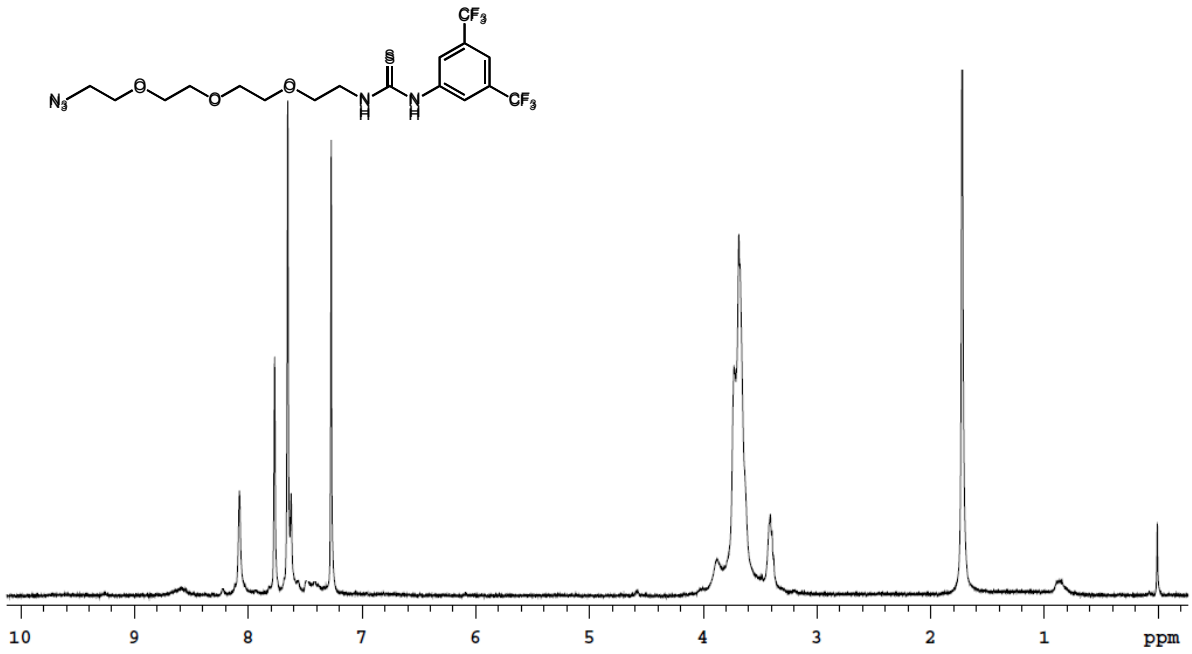

1-(2-(2-(2-(2-azidoethoxy)ethoxy)ethoxy)ethyl)-3-(3,5-bis(trifluoromethyl)phenyl)thioure
^{1}H NMR

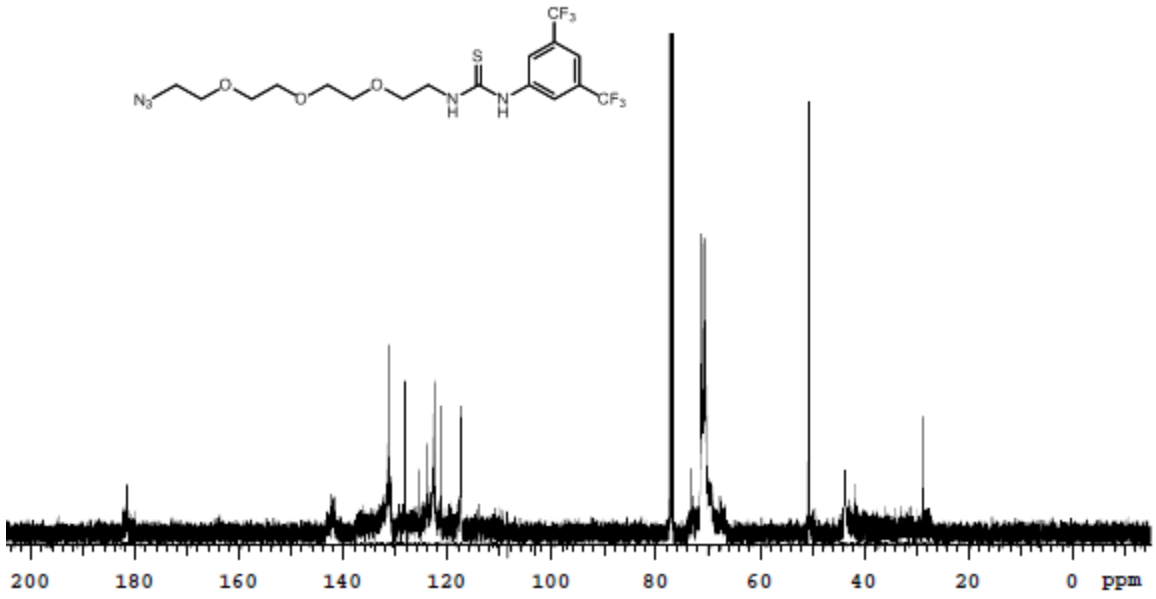

1-(2-(2-(2-(2-azidoethoxy)ethoxy)ethoxy)ethyl)-3-(3,5-bis(trifluoromethyl)phenyl)thioure
^{13}C NMR

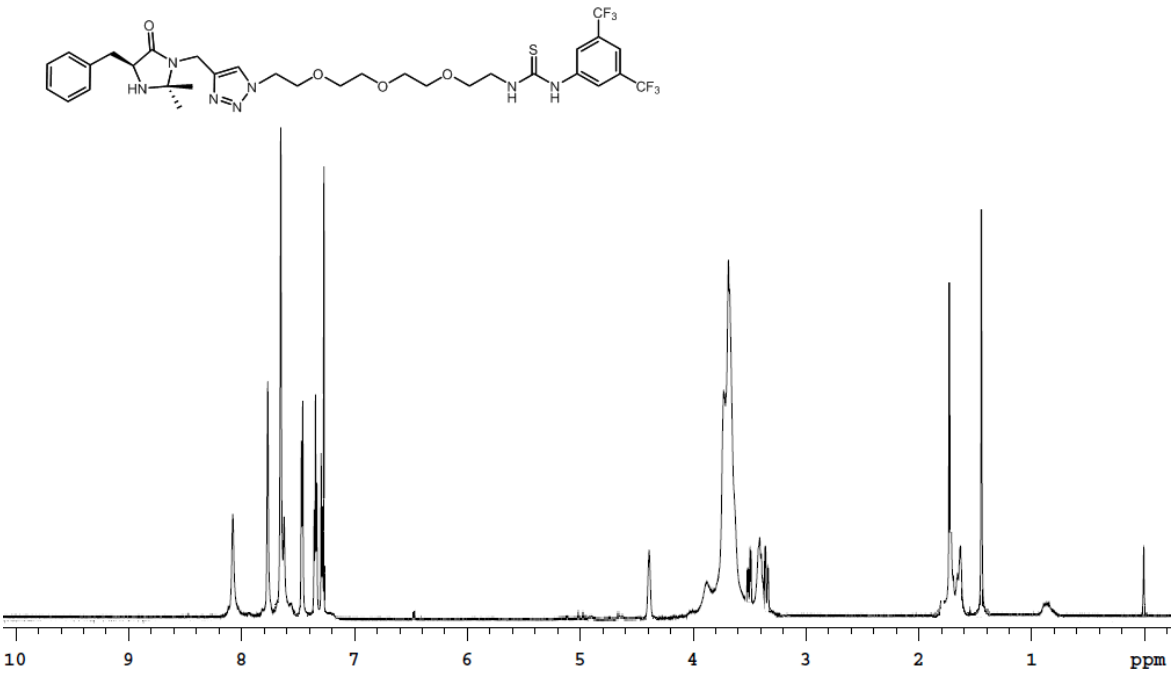

(S)-1-(2-(2-(2-(2-(4-((4-benzyl-2,2-dimethyl-5-oxoimidazolidin-1-yl)methyl)-1H-1,2,3-triazol-1-yl)ethoxy)ethoxy)ethoxy)ethyl)-3-(3,5-bis(trifluoromethyl)phenyl)thiourea ^{1}H NMR

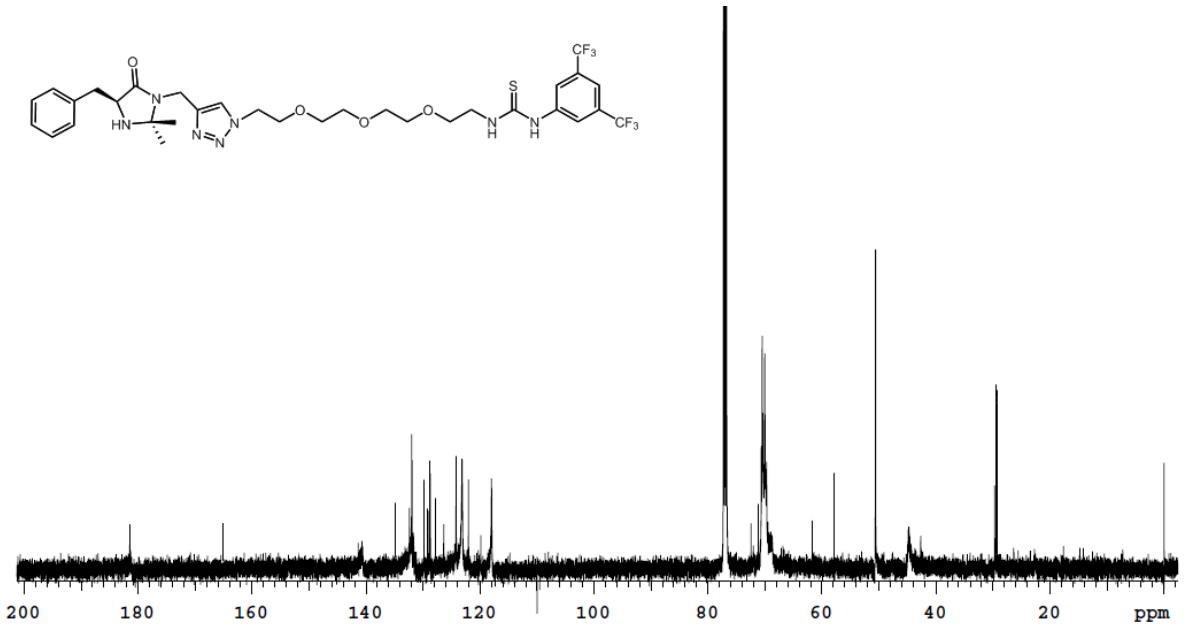

(S)-1-(2-(2-(2-(2-(4-((4-benzyl-2,2-dimethyl-5-oxoimidazolidin-1-yl)methyl)-1H-1,2,3-triazol-1-yl)ethoxy)ethoxy)ethoxy)ethyl)-3-(3,5-bis(trifluoromethyl)phenyl)thiourea ^{13}C NMR

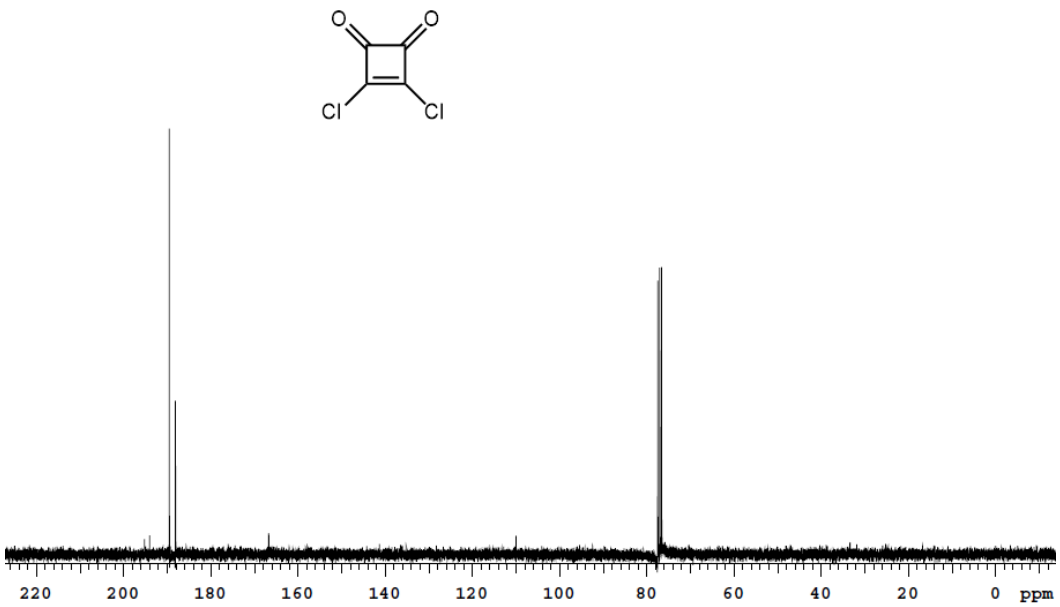

3,4-dichlorocyclobut-3-ene-1,2-dione (2) ^{13}C NMR